# Role of the exosome co-factor Rrp47 in RNA processing and surveillance

**A thesis submitted to the University of Sheffield for the degree of Doctor of Philosophy**

**By**

**Monika Feigenbutz**


**Department of Molecular Biology and Biotechnology**
**University of Sheffield**
**United Kingdom**

**December 2013**

# *Abstract*

*RNA surveillance by the exosome complex is remarkably conserved from yeast to humans and best studied in baker's yeast Saccharomyces cerevisiae. The multi-subunit RNA exosome is involved in the processing, maturation, quality control and general turnover of RNAs, as well as the degradation of harmful, aberrant or unwanted transcripts. To execute its distinct cytoplasmic and nuclear functions, the exosome requires compartment-specific co-factors like Rrp47, a protein directly associated with the nuclear exosome exoribonuclease Rrp6. The aim of this study was to investigate the role of Rrp47 in exosome-mediated processes based on the model that Rrp47 is an RNA binding protein that helps direct Rrp6 to its substrates. Mutational analysis of Rrp47 revealed that the Sas10 domain which Rrp47 shares with other proteins involved in RNA processing is critical for Rrp6 binding and for all in vivo Rrp47 functions. However, the less conserved C-terminus of Rrp47 functions in the final maturation of snoRNAs, and both C- and N-terminus cooperate in RNA binding in vitro. Protein and mRNA expression analyses demonstrate that the proteins critically influence each other's stability and expression levels whereby Rrp47 expression is drastically reduced when Rrp6 is absent. Studies into the assembly of Rrp47-Rrp6 suggest that the proteins are imported into the nucleus separately where Rrp47 is degraded if Rrp6 is not available for interaction. Rrp47 has less pronounced effects on Rrp6 stability and expression, yet defects in the processing of Nrd1 terminated transcripts were alleviated by Rrp6 overexpression in cells lacking Rrp47. Specifically, growth was restored by overexpressing Rrp6 in an otherwise synthetic lethal rex1Δ rrp47Δ strain, suggesting that Rrp47 is critical for maintaining adequate Rrp6 levels. Taken together this study has given crucial new insights into domains required for Rrp47 function, as well as assembly and interdependency of Rrp47 and its associated exonuclease Rrp6.*

# *Acknowledgements*

First and most of all, my thanks goes to Phil for giving me the opportunity to do a PhD in his lab, for sharing his incredible knowledge and skills, for listening and discussing my many weird and wonderful (and not so wonderful) ideas and for all his support.
Thanks so much for everything!

Many thanks also to all the Mitchell lab members past and present especially Jon, Joe and Becky for getting me back into lab shape, and Martin and Will for not only being great company, but also being extremely helpful on so many occasions and making the best ever competent cells!

I'd also like to thank everyone whose work has helped me in direct or indirect ways to carry out this PhD and particular thanks to those who helped me with certain aspects of my work, Stefan Millson (gel filtrations), Guillaume Hautbergue (qPCR), David Caballero-Lima and Darren Robinson (fluorescence imaging/ Delta Vision microscope).

Finally, as many apologies as 'thank yous' to my family for being incredibly patient and supportive, despite missing out on countless hot dinners while I was writing this. Let's hope it was worth it and will enable me to help Holly and Tim to realise their dreams! Love you lots!

# *Table of Contents*

# *Index of Figures*

# *Index of Tables*

# *Frequently used abbreviations and conventions*

| | |
|---|---|
| $A_{260}$ | Absorption at 260 nm wavelength |
| A , T, G, C | adenine, thymine, guanine, cytosine – base constitutents of DNA |
| AA | amino acid |
| ATP | adenosine triphosphate |
| b and bp | bases and base pairs |
| C-/CTD | C-terminus / C-terminal domain |
| cps | counts per second |
| CUT | cryptic unstable transcript |
| DEPC | diethylpyrocarbonate |
| DNA | deoxyribonucleic acid |
| *E. coli* | *Escherichia coli* |
| 5'ETS | 5 'external transcribed spacer of the 35S pre-rRNA |
| 5'FOA | fluoro-orotic acid |
| g | relative centrifugal force measured in units of gravity |
| GST | glutathione-S-transferase (fusion tag) |
| His | histidine |
| HRDC domain | helicase and RNase D C-terminal domain |
| IPTG | Isopropyl-β-D-thiogalactopyranoside |
| ITS1 and 2 | internal transcribed spacers 1 and 2 of 35S pre-rRNA |
| kDa | kilodalton |
| M | molar, µM micromolar, nM nanomolar |
| mRNA | messenger RNA |
| ncRNA | non-coding RNA |
| nt | nucleotide |
| OD | optical density |
| ORF | open reading frame |
| PAGE | polyacrylamide gel electrophoresis |
| PAP | peroxidase-anti-peroxidase |
| PCR | polymerase chain reaction |
| PMC2NT | N-terminal domain of Rrp6 which binds Rrp47 |
| PMSF | phenylmethylsulphonylfuoride – serine protease inhibitor |
| Poly(A) or pA | polyadenylation/polyadenylated |
| psi | pounds per square inch |
| RNAP | RNA polymerase |
| RNA / RNP | ribonucleic acid/ribonucleoprotein particle e.g. mRNP, snRNP |
| rRNA | ribosomal RNA |
| S | Svedberg units (in 5S or 5.8S rRNA), sedimentation coefficient |
| *S. cerevisiae* | *Saccharomyces cerevisiae* aka budding yeast aka baker's yeast |
| SDM | site-directed mutagenesis |
| sl | synthetic lethal |
| snRNA/snRNP | small nuclear spliceosomal RNAs/RNP particles |
| snoRNA/snoRNP | small nucleolar RNAs/RNP particles |
| TAP | tandem affinity purification (fusion tag) |
| tRNA | transfer RNA |
| ts | temperature sensitive |
| U | units of enzyme or uracil base constituent of RNA |
| UTR | untranslated region |
| zz- | fusion tag consisting of two copies of the z-domain of protein A from *Staphylococcus aureus* |

# Chapter One

# Introduction

**Figures 1.1 – 1.9**

# Chapter 1 - Introduction

## 1.1 DNA, RNA and gene expression

### 1.1.1 Gene expression and the importance of RNA surveillance

All organisms face the vital task of preserving the integrity of their genome, as well as ensuring the fidelity of gene expression, the correct transcription and translation of this genetic master plan into functional RNAs and proteins. The eukaryotic genome is made up of long chains of deoxyribonucleic acid (DNA). Herein, the genetic code is contained in the distinct sequence of four basic building blocks, called nucleotides, and safeguarded by their specific base-pairing (A-T, G-C) in a stable, double stranded DNA helix. The DNA is packaged with proteins into a dense structure called chromatin to form the chromosomes in the nucleus.

The genome is divided into genes, defined as regions of DNA that encode and generate functional RNAs and proteins in a highly regulated process termed gene expression. In the first stage single-stranded ribonucleic acid (RNA) copies of the DNA coding strand are produced. These primary transcripts are then further processed and modified to generate the mature functional RNAs assembled into RNA-protein-complexes; coding mRNAs are exported to the cytoplasm where ribosomes translate the code into amino acids to generate proteins. Gene expression is tightly controlled and diverse proof-reading and surveillance mechanisms monitor every step of the way from DNA to RNA and to protein (Richard and Manley 2009).

Cells make huge amounts of RNA and therefore efficient RNA regulation is imperative to ensure the right type of RNA is produced at the right time and in sufficient amount and quality. This requires a highly regulated but flexible system that allows for rapid changes of transcript amounts according to requirements. Faulty regulation of RNA levels has been implicated in many diseases, including cancer (Rougemaille and Libri 2010, Staals and Pruijn 2010). Moreover, the abundance and importance of regulatory RNA molecules discovered over the last decade have revolutionised the understanding of gene expression and regulation. Only recently it has come to light that yeast and human cells transcribe almost their entire genomes (Belostotsky 2009, Houseley and Tollervey 2009), a vast fraction thereof non-coding RNAs which have become apparent as regulators in gene expression. Most of these transcripts appear to be regulated and degraded by the RNA exosome, a key cellular RNA surveillance complex. Pervasive transcription of the genome and the ever expanding diversity of known non-coding RNAs raise fundamental questions over the purpose of these RNA molecules and put a new perspective on the importance of RNA surveillance by the RNA exosome and other ribonucleases in the “policing of the transcriptome” (Belostotsky 2009, Rougemaille and Libri 2010).

### 1.1.2 The vast world of RNAs – RNA diversity and versatility

RNA is an extremely versatile molecule which can encode information, allow sequence or structure specific interactions with DNA, proteins and other RNA molecules, assume stable secondary and tertiary structures and display catalytic activity (Sharp 2009). Most likely, cellular life originated with RNAs fulfilling both functions as information carriers and regulatory molecules. Many genes therefore not only encode one RNA molecule but in higher eukaryotes genes often constitute a complex system that can generate different RNA molecules from several, bi-directional promoters and through alternative co- and posttranscriptional processing mechanisms (Dinger *et al.* 2011, Tuck and Tollervey 2011).

The bona fide types of stable RNAs in the cell are messenger RNAs (mRNAs), transfer RNAs (tRNA) and ribosomal RNAs (rRNA); mRNAs are transcripts of protein-coding genes which are decoded with the help of tRNAs by translating nucleotide triplets (codons) into corresponding amino acids. These are assembled into proteins by ribosomes, cellular protein factories made up of rRNAs and proteins. Although best studied, mRNA constitutes less than 5 % of the total RNA in a typical cell. Other stable RNAs are small nucleolar RNAs (snoRNAs) which are required for rRNA processing and modification and small nuclear RNAs (snRNAs) required for mRNA splicing which involves the removal of non-coding intron sequences and joining of the coding exon sequences (Richard and Manley 2009, Kuehner *et al*. 2011). Catalytic RNAs were first discovered in the form of self-splicing introns contained in the pre-rRNA of Tetrahymena. Other RNAs with enzymatic functions include RNaseP involved in converting precursor tRNAs into active tRNAs and the rRNA in the large ribosome subunit ("ribozyme") which catalyses protein synthesis from amino acids. Moreover, some double-stranded RNAs were shown to inhibit gene expression via RNA interference pathways (RNAi) using microRNAs (miRNAs) and small interfering RNAs (siRNAs) to regulate mRNA transcription, translation and stability. Other small regulatory non-coding RNAs include piwi-interacting RNAs (piRNAs), repeat-associated small interfering RNAs (rasiRNAs) and transcription initiation RNA (tiny or tiRNA).

More recently, numerous new classes of non-coding RNAs (ncRNAs) have been discovered in yeast and other eukaryotes resulting from pervasive transcription by RNAPII such as cryptic unstable transcripts (CUTs) and stable unannotated transcripts (SUTs) in yeast (Marquardt *et al*. 2011, Xu *et al*. 2009, Neil *et al.* 2009, Davis and Ares 2006), promoter upstream transcripts (PROMPTs), promoter-associated and terminator-associated small RNAs (PASRs and TASRs) in mammals and upstream non-coding transcripts (UNTs) in *Arabidopsis* (Belostotsky 2009). The functions of these transcripts are poorly understood. Some of these ncRNAs function in locus-specific gene regulation and silencing, others might just represent transcriptional noise. PROMPTs have been found to influence DNA modification patterns in humans (Belostotsky 2009, Preker *et al*. 2008 and 2011).

## 1.2 RNA synthesis – The basics of transcription

### 1.2.1 RNA polymerases transcribe a specific set of RNAs

In most eukaryotes, three enzymes termed RNA polymerases (RNAP I, II and III) are responsible for the transcription of the DNA template into a specific subset of RNAs. Table 1 gives an overview of the transcripts of the three RNAPs (Richard and Manley 2009). Two further RNA polymerases have been characterised in plants, termed RNAP IV and V. They appear to specifically function in gene silencing; RNAP IV produces silencing RNA (siRNA) precursors and RNAP V generates non-coding RNA targets for the siRNAs (Wierzbicki *et al.* 2008).

Eukaryotic RNAPs are multi-subunit enzymes that share a high degree of sequence and structural similarities and they also share some subunits. However, the core catalytic activities are unique to each of the enzymes to carry out their specific task (Schneider 2011). Apart from the TATA-binding protein TBP which is required for transcription by all three enzymes, each of the three RNAPs has its own set of general transcription factors (Hahn and Young 2011).

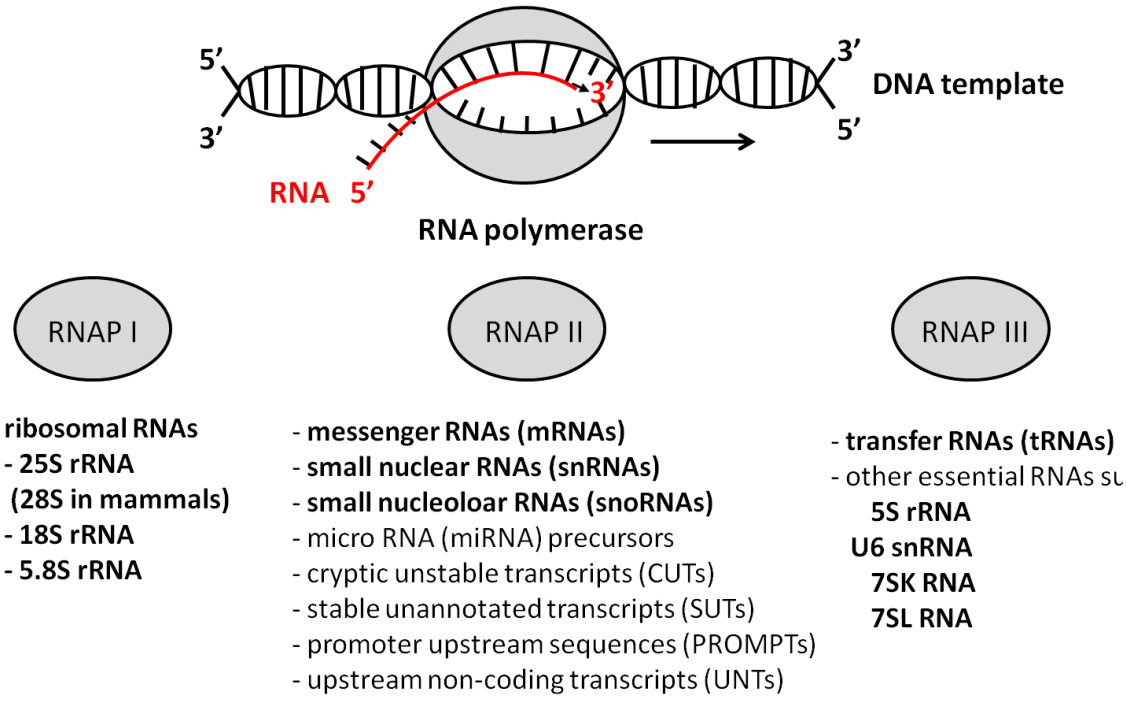


**Figure 1.1 RNA polymerases I, II and III transcribe a specific set of RNAs.**
Simplified schematic of transcription showing only the helical double stranded DNA template, the RNA polymerase (grey circle) and the nascent single stranded RNA in red. The arrow marks the direction of transcription from 5' to 3' denoting the free ends of the ribose backbone. Listed below are transcripts produced by each of the three eukaryotic RNA polymerases (RNAP I, II and III), stable RNAs are marked in bold.

The transcription process by the three RNAPs shares basic features, and although more complex, it has been best studied for RNAPII and a short overview of RNAPII transcription is given here. The three main stages of the transcription process are initiation, elongation and termination. Transcription involves complex interactions between RNAP, proteins, DNA and RNA and is a dynamic, yet highly regulated and coordinated process. Transcription is closely coupled to termination, processing and modification events which determine the fate and localisation of the transcript once matured into a fully functional ribonucleoprotein (RNP) particle (Richard and Manley 2009).

### 1.2.2 RNAPII transcription is coordinated by its C-terminal domain (CTD)

The C-terminal domain (CTD) of the largest RNAPII subunit Rpb1 is thought to have a unique function as an interaction platform for transcription, processing and termination factors (Egloff *et al.* 2008). The CTD contains multiple heptameric repeats of the peptide consensus sequence YSPTSPS. The number of repeats varies in different organisms (26 repeats in yeast and 52 in humans). The phosphorylation state of the CTD serine residues (Ser2P, Ser5P and Ser7P) during the transcription cycle determines which factors bind to the CTD and in which order, thus dynamically orchestrating the assembly of distinct factors to the CTD and coordinating events during the transcription cycle (Buratowski 2009). Ser5P correlates with transcription initiation and early elongation, Ser2P with advanced elongation and poly(A)dependent termination and Ser7 phosphorylation appears specifically associated with snRNA transcription (Egloff *et al.* 2010).

### 1.2.3 Transcription initiation

Transcription is initiated by the assembly of the RNA polymerase and a set of general transcription factors (GTFs) on the DNA template. The GTFs recognise and bind a regulatory upstream region of genes, called the promoter, and position the RNAP near the transcription start site. Next, the DNA double helix is unwound (11-15 base pairs) and the template strand enters the active site of the RNAP in an open complex (Luna *et al*. 2008, Sikorski and Buratowski 2009). RNAPII then scans the DNA for a suitable start site. Besides the GTFs, transcriptional activators and repressors are modulating and regulating transcription by binding to upstream activation or repression sequences (UAS and URS) and chromatin-modifying complexes. The pre-initiation complex (PIC), consisting of RNAP and a minimal set of transcrition factors, is not universal, but promoter-dependent; different subsets of transcription factors are utilised depending on promoter context. Several DNA sequence elements have been identified for basal promoter recognition, including the TATA element, downstream promoter elements (DPEs), TFIIB recognition elements (BREs) and the initiator element (INR). Any of these can be present at a promoter and associate with a distinct set of transcription factors to modulate transcription (Sikorski and Buratowski 2009).

### 1.2.4 Transcription elongation

When the transcript reaches a certain length (after the eighth nucleotide for RNAPII) the promoter is cleared, coinciding with start of the CTD phosphorylation cycle (Luna *et al*. 2008). At this critical stage, the PIC is partially disassembled; some GTFs are released from the transcription complex and other factors associate with the RNAP to coordinate subsequent events (Luna *et al.* 2008). As Ser2P levels increase and Ser5P levels drop, the RNAP enters full elongation mode producing 1-4 kilobases RNA per minute (Egloff and Murphy 2008). A RNA-DNA-hybrid of 8 nucleotides is maintained during elongation and disruption of this heteroduplex is thought to affect termination (Kuehner *et al*. 2011). The elongation stage coincides with the activation of splicing, moreover, "early export factors" such as Yra1 and Sub2 are recruited to the RNAPII CTD via the THO complex to prepare the export of the RNA to the cytoplasm (Rougemaille *et al*. 2008).

### 1.2.5 RNAPII has two transcription termination pathways

Transcription termination by all three polymerases occurs through specific termination signals and/or factors present at the 3' end of the nascent transcript or gene. Generally, termination follows shortly after endonucleolytic cleavage of the nascent transcript (Richard and Manley 2009). The polymerase ceases RNA synthesis and is released from the DNA template (Kuehner *et al*. 2011). Termination is best studied for RNAPII which uses two distinct termination pathways, the poly(A)-dependent pathway for transcripts > 1kb and the Nrd1-dependent pathway for shorter, mostly non-coding RNAs <1kb (Steinmetz *et al.* 2001 and 2006, Kuehner *et al*. 2011). The choice of termination pathway is influenced by the phosphorylation status of the RNAPII CTD subunit (Egloff and Murphy 2008, Gudipati *et al*. 2008); Ser2P has been shown to coincide with poly(A)-dependent termination, whereas Ser5P-CTD is linked to Nrd1-dependent termination (Vasiljeva *et al*. 2008). The two RNAPII transcription termination pathways share some features and it appears that they can provide "mutual fail-safe termination", for example to rescue RNAPs that fail to terminate at poly(A) sites (Kim *et al.* 2006, Kuehner *et al.* 2011).

***Poly(A) dependent termination***

Most mRNAs are cleaved downstream of a conserved termination and polyadenylation signal AAUAAA by the multi-subunit cleavage/polyadenylation complex, in yeast comprising the cleavage and polyadenylation factor (CPF) and cleavage factors CF1A and CF1B (Proudfoot 2011). Endonucleolytic cleavage is thought to create an entry point for the 5' exonuclease Rat1. This allows the exonuclease to chase the RNA polymerase and trigger transcription termination ("torpedo model") as well as polyadenylation of the free mRNA 3' end by the poly(A)polymerase Pap1 (Luna *et al.* 2008). The resulting poly(A) tail at the 3'OH end (app. 70-

90 residues in yeast and 250 residues in humans) is bound by poly(A) binding proteins (PABP) and thus protected from exonucleolytic degradation (Houseley and Tollervey 2009). Strikingly, more than 50 polypeptides within multiple subcomplexes are required for 3' end cleavage and polyadenylation (Proudfoot 2011) indicating the high complexity of this process.

***Nrd1-dependent termination***

In *S. cerevisiae*, an early, alternative RNAPII transcription termination pathway was discovered for small non-coding RNAs such as snRNAs, snoRNAs and CUTS (Steinmetz *et al.* 2006). Termination occurs within the first few hundred nucleotides of elongation and the short transcripts have no poly(A) tail in their mature form. Transcription termination of these RNAs depends on the Nrd1-complex consisting of the RNA binding proteins Nrd1 and Nab3 and the putative RNA/DNA helicase Sen1. Nrd1 directly interacts with Ser5P-CTD at the early stages of transcription (Vasiljeva *et al*. 2008a). Nrd1 and Nab3 form a heterodimer and both recognise and bind the nascent RNA at specific motifs, GUAA/G and UCUU, respectively (Carroll *et al*. 2004). Binding of the Nrd1-complex to both RNA and CTD is thought to trigger the release of the transcription machinery from the DNA template (Carroll *et al*. 2007).

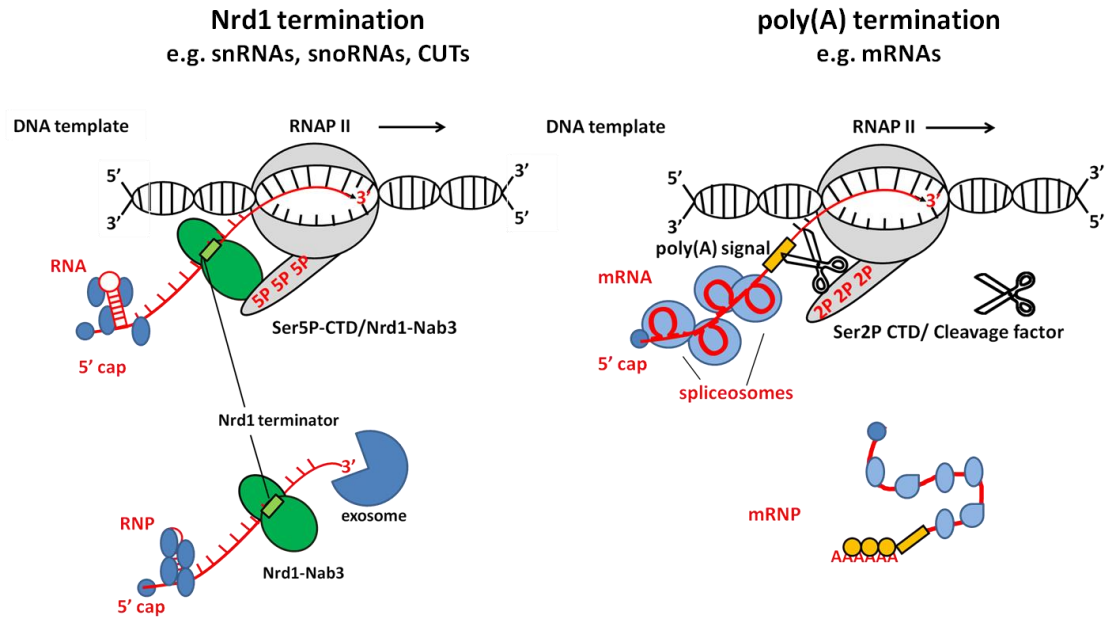


**Figure 1.2 RNAPII uses two transcription termination pathways.**
Depicted are the Nrd1-dependent termination of sn/snoRNAs and CUTs versus the poly(A)-dependent termination of mRNAs. The choice of termination pathway is directed by the phosphorylation state of the RNAPII C-terminal domain (CTD). Ser5P directly interacts with Nrd1-Nab3 and terminates RNAs with Nrd1 terminator sequences. The RNA is then 3' processed by the exosome for maturation or in the case of CUTs completely degraded due to the lack of protective features. In contrast, Ser2P interacts with the cleavage and polyadenylation complex of the poly(A) termination machinery and leads to termination and 3' end polyadenylation by Pap1. The nascent transcripts are co-transcriptionally processed and packaged into functional mature ribonucleoprotein particles (RNPs).

## 1.3 RNAs, their processing and maturation

### 1.3.1 Processing and maturation of primary transcripts (pre-RNAs)

Primary transcripts follow distinct processing and maturation pathways. Whilst mRNAs and snRNAs/snoRNAs are processed into RNP particles, RNA fragments and pervasive transcripts such as CUTs are immediately degraded (Schmid and Jensen 2008b). Stable RNAs are generally transcribed as long, heterogeneous nuclear RNAs (hnRNAs) or precursors (pre-RNAs). Many RNAs undergo 5' maturation by the addition of a 5' cap structure (all RNAPII transcripts). Further, spacer fragments (pre-rRNA) and introns (pre-mRNAs) are excised from primary transcripts and subsequently degraded or processed if the introns encode other RNA species. Finally, the processing of 3' ends, often involving precise trimming of 3' extended precursors, is required in the formation of functional RNAs of all known eukaryotic species. Transcription termination and pre-RNA processing are tightly coupled. The nascent RNA molecules associate with specific RNA-binding proteins which direct a series of modification and processing steps to allow proper folding and packaging of the RNAs with proteins to generate the functional “mature” RNAs, ready to be exported into the cytoplasm or to exert diverse nuclear functions.

Notably, most RNAs are functional as RNA-protein complexes, which require elaborate folding and assembly. The associated proteins protect the RNA from exonucleolytic degradation and coordinate or direct downstream events, localisation und functions of the mature ribonucleoprotein particles (RNPs). These maturation processes are thought to be continuously monitored by surveillance systems (Houseley *et al.* 2006, Luna *et al*. 2008). Tight coupling between transcription termination and 3’ end processing is essential because RNAs with free 3’ ends that lack protective or stabilising features are rapidly degraded by the exosome as demonstrated with CUTs (Rosonina *et al.* 2006, Rougemaille and Libri 2010). In yeast, these RNA processing and degradation activities also involve the 5'-3' exonucleases Rat1 in the nucleus and Xrn1 in the cytoplasm. Transcription and RNA processing are closely interlinked processes directed by cross-stimulatory interactions. Each stage provides a check-point and influences downstream events thus determining the fate of the transcript (Proudfoot 2011). There is also evidence for reverse coupling, as splicing has been shown to have a stimulatory effect on transcription initiation. Moreover, gene loops are formed by contacts between 5' and 3' ends of genes for rapid reinitiation of transcription thus allowing the recycling of RNAP and GTFs (Luna *et al.* 2008, Lykke-Andersen *et al.* 2011b).

### 1.3.2 mRNAs are matured into mRNPs for export to the cytoplasm

In order to produce a translatable mRNA, the nascent transcript undergoes 5'-capping, splicing, 3'-end processing and packaging with mRNP proteins and export factors for translocation to the cytoplasm. CTD-Ser5 phosphorylation attracts the capping enzymes. Capping at the emerging 5' end requires removal of the 5' phosphate, addition of GTP and methylation of guanine to generate the 7-methylguanosine (m7G)-cap. Pausing of RNAPII is thought to act as a checkpoint to ensure only correctly capped mRNAs are extended (Coppola *et al.* 1983). The newly formed cap is then bound by the nuclear cap binding complex (CBC) which not only protects the nascent RNA from 5' decay, but is critical for subsequent events including splicing, termination, export, mRNA decay and translation (Luna *et al.* 2008, Schmid and Jensen 2008b).

Protein-coding genes can not only generate one specific mRNA, however this is the norm for simpler eukaryotes like yeast. In contrast, higher eukaryotes often have larger and more complex genes with multiple expressed sequences (exons) and non-coding intervening regions (introns) which can encode multiple mRNAs with distinct coding and regulatory sequences (Licatalosi and Darnell 2010). Introns are removed from the pre-mRNA in a process termed splicing, and exons are then joined to generate the complete coding sequence (Patel and Bellini 2008). Alternative splicing, a key feature of gene regulation in mammals, allows multiple mRNA isoforms to be produced from a single gene or pre-mRNA precursor (Jurica and Moore 2003, Proudfoot 2011). This highly regulated process is mediated by the spliceosome formed by the U1, U2, U4, U5 and U6 snRNPs together with over 300 other splicing factors which assemble onto the pre-mRNA (Brody and Abelson 1985, Patel and Bellini 2008).

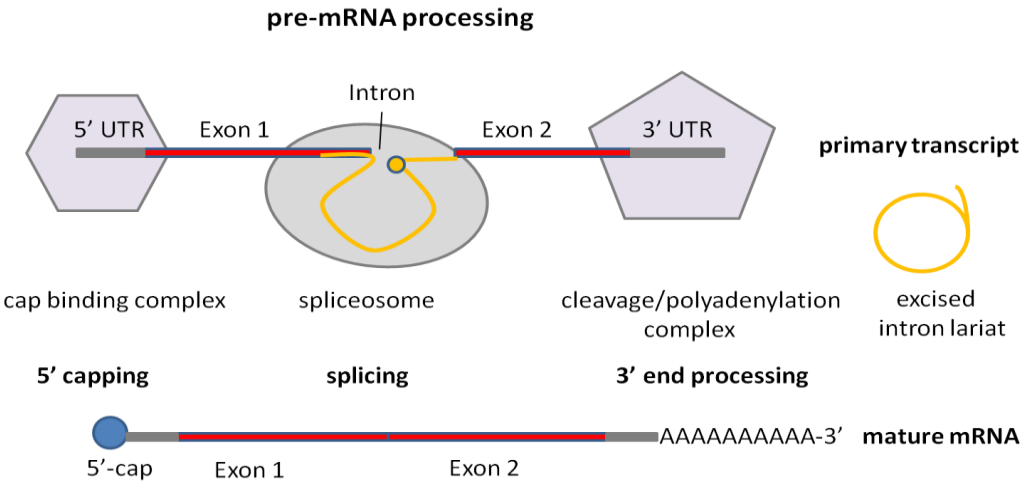


**Figure 1.3 Schematic of pre-mRNA processing.** The pre-mRNA contains coding sequences" Exons", as well as intronic non-coding sequences "Introns" and untranslated regions (UTRs) at both 5' and 3' ends. The pre-mRNA is capped at the 5' end, introns are removed by the spliceosome and exons are joined guided by snRNA base-pairing at exon and branch point (orange circle) junctions, the 3' end is cleaved and polyadenylated.

***mRNA 3' end processing and mRNP formation***

3' end formation is an essential step in the maturation of all mRNAs and is closely coupled to RNAPII termination (Buratowski 2005). The mature mRNA 3' end is not defined by the stop codon of the mRNA, but by a non-coding sequence called the 3' untranslated region (3'UTR) which contains the poly(A) signal (PAS) AAUAAA (Proudfoot 2011). An upstream and a GU-rich downstream sequence element (USE and DSE) were also shown to enhance 3' end formation. The DSE–AAUAAA-USE pattern is generally conserved across eukaryotes. In addition, the actual nucleotides at the site of 3' end cleavage can influence efficiency of 3' end formation. 3' UTRs can vary in length from 50 to several 1000 nucleotides with a 3' proximal PAS or close consensus. Alternative poly(A) signal (PAS) selection is another, more recently discovered source of mRNA variation and gene regulation. The resulting mRNA isoforms differ in the length of their 3' UTR which determines stability and translatability of the mRNA (Proudfoot 2011). In parallel to the processing events, the nascent transcript is also co-transcriptionally loaded with assembly factors and packaged into correctly assembled mRNP particles which are targeted to the nuclear pore complexes for export (Vinciguerra and Stutz 2004). In *S. cerevisiae* these factors include the THO complex, the RNA helicase Sub2, RNA binding protein Yra1, the mRNA export receptor Mex67:Mtr2 and hnRNPs (Rougemaille *et al.* 2007, Fasken and Corbett 2009).

### 1.3.3 snRNAs, snoRNA and CUTs

These RNAs are all 3' processed and/or degraded by the exosome. The Nrd1-termination complex recruits the exosome to its substrates coupling transcription termination tightly to 3' end processing (Vasiljeva *et al*. 2006). This leads to 3' trimming and maturation of snRNA and snoRNA precursors or immediate degradation of CUTs and aberrant RNAs. 5' and 3' end processing of sn- and snoRNAs also involves Rnt1, an RNAse III type endonuclease (Houseley *et al*. 2009).

***snRNAs***

The uridine-rich small nuclear spliceosomal snRNAs are non-polyadenylated ncRNAs which assemble with proteins into small nuclear ribonucleoprotein particles (snRNPs). U7 snRNP functions in histone pre-mRNA 3' processing, whereas all other snRNPs form the core of the spliceosome and function in the precise removal of introns from pre-mRNAs through base-pairing interactions at the exon-intron and branch point junctions. The Sm snRNAs (U1, U2, U4, U5, U7, U11, U12) are transcribed by a specialised form of RNAPII as 3' extended precursors (Matera *et al.* 2007, Patel and Bellini 2008). Like all RNAPII transcripts, they are co-transcriptionally capped at the 5' end and thought to be bound by the CBC like pre-mRNAs. Transcription is dependent on the snRNA-specific core promoter, a proximal sequence element

(PSE), and a conserved 3'-box element. Co-transcriptional 3' processing is dependent on factors which associate with the RNAPII CTD at the promoter, the Integrator complex in metazoans and the Nrd1 complex in conjunction with the exosome in yeast. Endonucleolytic cleavage occurs downstream from the 3'-box (Richard and Manley 2010). Recently, Ser7P was shown to be specifically required for the expression of Sm snRNAs and the recruitment of the integrator complex in mammalians (Egloff *et al*. 2010). The Lsm-class snRNA U6 is transcribed by RNAPIII and contains a cluster of uridines at the 3' end which forms the Lsm binding site and also constitutes the RNAPIII transcription terminator.

Lsm class snRNAs are solely nuclear whereas Sm class snRNAs are exported to the cytoplasm for maturation. The snRNA specific export complex comprises the export adaptor PHAX, the export receptor CRM1 (exportin-1) and the CBC. Assembly of the snRNAs with the heptameric Sm core on the consensus Sm site into stable snRNPs is performed by the survival motor neuron (SMN) complex and its associated factors known as Gemins (Matera *et al.* 2007). Hypermethylation of the 5' cap triggers reimport into the nucleus and final maturation of the snRNPs in the Cajal bodies which involves assembly with a unique set of snRNP-specific proteins and site-specific modifications.

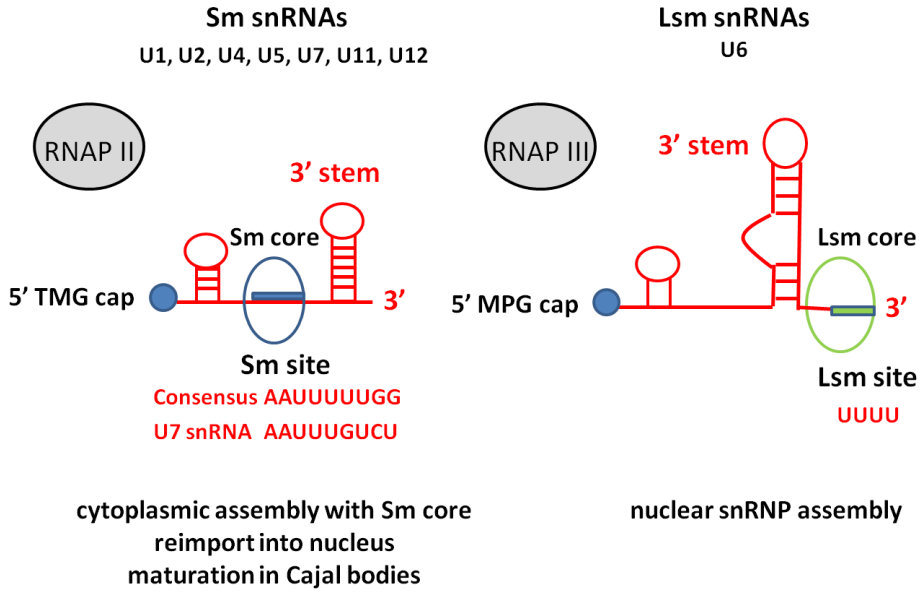


**Figure 1.4 Features of Sm- and Lsm- class snRNAs** (adapted from Matera *et al.* 2007).
Sm snRNAs are transcribed by RNAPII and contain a 5'-trimethylguanosine (TMG) cap, a consensus Sm site (except U7) and a 3' stem loop. Sm snRNAs are exported for 3' trimming and assembly with the ring-shaped heptameric Sm core before hypermethylation of the 5' cap which triggers reimport into the nucleus and targeting to Cajal bodies for snRNP maturation. Lsm RNAs are transcribed by RNAPIII and carry a 5' monomethylphosphate cap, a 3' stem loop and a 3' terminal stretch of uridines constituting the Lsm site for assembly with the heptameric Lsm core.

***snoRNAs***

snoRNAs can be divided into two structurally and functionally defined classes termed H/ACA snoRNAs and box C/D snoRNAs defined by conserved sequence elements and secondary structures. They are co-transcriptionally assembled into RNA-protein-complexes termed small nucleolar ribonucleoproteins (snoRNPs) and mainly direct nucleotide modifications in rRNA, however they also affect other target RNAs as shown for snRNAs in eukaryotes and tRNAs in archaea. Box C/D snoRNAs function as guide RNAs in the site-specific 2'*O*-ribose methylation of rRNAs and H/ACA snoRNAs direct the pseudouridinylation of rRNAs. Both classes of snoRNPs are essential for ribosome function. They target key rRNA regions within the ribosomes like the peptidyl transferase centre and the mRNA decoding centre through antisense elements. Telomerase RNA, also an H/ACA RNA, is required for telomere synthesis. In addition, there are numerous "orphan" snoRNAs with as yet unknown targets (Henras *et al.* 2004, Richard and Kiss 2006, Matera *et al.* 2007). Contrary to the small number of snRNA species (24 in yeast), eukaryotic cells contain more than 200 unique C/D and H/ACA snoRNA species. These abundant and functionally diverse trans-acting ncRNAs are essential for protein translation, mRNA splicing and genome stability; besides eukaryotes, they are also present in archaea (Matera *et al.* 2007). In yeast, most C/D and H/ACA snoRNAs are produced as independent RNAPII transcripts, however they can also be derived from polycistronic precursors containing several RNAs which are released through cleavage by the endonuclease Rnt1 (yeast RNAse III). In mammalians and plants, snoRNAs are generally encoded in introns of protein-coding genes and require release from the spliced host intron by the RNA lariat-debranching enzyme Dbr1 (Bernstein and Toth 2012). The nuclear exosome is critical for co-transcriptional quality control which leads to either correct exonucleolytic 3' end maturation of the snoRNP or complete degradation of aberrant RNAs.

***snoRNP assembly***

Co-transcriptional recruitment and association of a core set of snRNP proteins protects the nascent RNA from degradation and is required for snoRNA maturation, stability and nuclear localisation. Other proteins are necessary for specialised functions (Matera *et al.* 2007, Richard and Manley 2009). H/ACA snoRNP assembly occurs co-transcriptionally. Yeast nuclear-assembly factor Naf1 can interact with the RNAPII CTD and actively recruits Cbf5/dyskerin (pseudouridin-synthase) to the ACA box and the lower stem of the guide RNA where the antisense element is positioned close to the catalytic site. The other H/ACA snoRNP proteins Nop10, Nhp2 and Gar1 are recruited to intronic snoRNAs during pre-mRNA synthesis (Richard and Kiss 2006, Richard and Manley 2009). The assembled pre-RNPs are matured to functional RNPs in Cajal bodies where Naf1 is exchanged for Gar1 in H/ACA RNPs (Fig. 1.5).

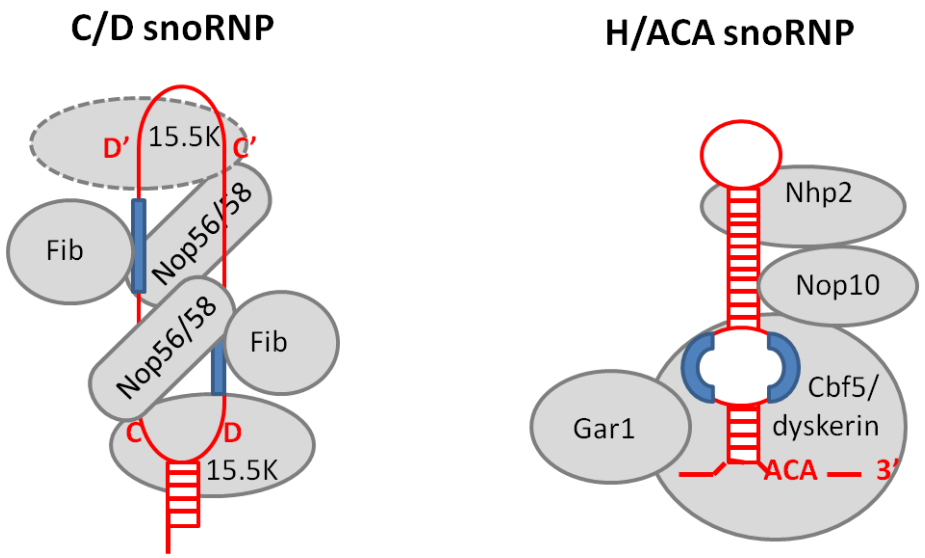


**Figure 1.5 Features of box C/D and H/ACA snoRNPs** (adapted from Matera *et al.* 2007).
The two classes of snoRNAs (depicted in red) are defined by conserved sequence elements (marked in blue) and secondary structures. To form functional snoRNPs, the snoRNAs interact with a core set of highly conserved proteins. Box C/D snoRNAs associate with the 2'-O-methyltransferase Fibrillarin/Nop1, Nop56-Nop58 and the 15.5K protein/snu13. H/ACA snoRNAs assemble with the pseudouridine synthase Cbf5/dyskerin, Gar1, Nhp2 and Nop10. Final maturation of the snoRNPs occurs in Cajal bodies.

Co-transcriptional box C/D snoRNP assembly is thought to be splicing-dependent. The majority of mammalian box C/D snoRNAs require an optimal distance of approximately 50 nucleotides upstream of the splicing branch point and are processed in a splicing dependent manner. The emerging transcript is first bound by the 15.5 kDa K-turn binding protein (Snu13 in yeast) followed by the ribose-2'O-methylase fibrillarin (Nop1 in yeast) and the two related nucleolar proteins Nop56 and Nop58. The C/D RNP exchange factor is most likely Bcd1 which also seems to interact with RNAPII CTD and is probably replaced by Nop56 when the snoRNP is finally matured in the Cajal bodies (Matera *et al*. 2007).

***CUTs and other non-coding RNAPII transcripts***

In yeast, cryptic unstable transcripts (CUTs) are only stabilised and therefore readily detectable in exosome/*rrp6Δ* mutants, whereas they are rapidly and efficiently degraded by the exosome in wild-type strains (Wyers *et al*. 2005, Thiebaut *et al*. 2006). CUTs are relatively short transcripts (200 to 600 nucleotides) from yeast intergenic regions with very short half-lives. They have a 5'-cap and heterogeneous 3' ends. Some CUTs appear to play a regulatory role in gene expression by controlling adjacent gene activity via transcriptional interference or gene silencing. Most commonly, CUTs are the result of bidirectional transcription where the actual gene and its antisense CUT compete for transcription (Xu *et al.* 2009, Neil *et al*. 2009, Belostotsky 2009). Efficient clearance of CUTs requires Nrd1-termination and Trf4-dependent

polyadenylation which stimulates degradation by the exosome. In contrast to stable snoRNAs and snRNAs, CUTs lack stabilising features at their 3' end and are therefore rapidly degraded by the exosome (Arigo *et al*. 2006a, Thiebaut *et al*. 2006, Rougemaille and Libri 2010).

Recently, stable unannotated transcripts (SUTs) and Xrn1 sensitive transcripts (XUTs) have been distinguished from CUTs due to their higher and more easily detectable levels in wild-type strains and their mode of termination and degradation (Marquardt *et al*. 2011). SUTs resemble mRNAs in some respects and have similar half-lives. They appear to escape degradation by the exosome and instead are exported to the cytoplasm and degraded by cytoplasmic RNA decay pathways including NMD (nonsense mediated decay), decapping enzymes and Xrn1-dependent 5' to 3' degradation (Mitchell *et al.* 2003b). Some of these ncRNAs are dependent on translation to initiate the NMD pathway. Depletion of the nuclear exosome subunit Rrp6 or Rrp47 leads to a marked increase in CUTs but only a partial accumulation of SUTs (Marquardt *et al.* 2011).

### 1.3.4 rRNA processing and ribosome biogenesis

RNAPI is specialised on rRNA synthesis and is responsible for more than half of total cellular RNAs in a growing cell (Warner 1999, Russell and Zomerdijk 2005). RNAPI produces three of the four ribosomal RNAs, termed 25S (28S in mammals), 18S and 5.8S according to their sedimentation properties, whereas 5S rRNA is synthesised by RNAPIII. In all eukaryotes the ribosomal DNA (rDNA) is arranged in multiple tandem repeats (150-200 copies in yeast, 400 copies in humans). The rDNA is transcribed as a single, large precursor (35S yeast/45S human) with a conserved layout that contains all three rRNA species (Venema and Tollervey 1999, Schneider 2011).

Only a portion of rDNA genes is actively transcribed. Downstream terminator elements (T, see Fig. 1.6) guide the termination of the 35S transcript and RNAse III/Rnt1 cleaves the precursor at the 3' end (Richard and Manley 2010, Kufel *et al*. 1999). Initially, the 5' external transcribed spacer region (5'ETS) is rapidly degraded by the 3' to 5' exo- and endonucleolytic activities of the exosome and TRAMP (Lebreton *et al*. 2008). Then the internal transcribed spacers (ITS1 and ITS2) are removed and degraded and the rRNA precursors are further processed at their 5' and 3' ends. The pre-rRNA undergoes a complex and highly coordinated sequence of endonuclease cleavages and exonuclease trimming, co-transcriptional and post-transcriptional processing, modification and folding steps to generate the mature 18S, 5.8S and 25/28S rRNA, respectively (Fig. 1.6).

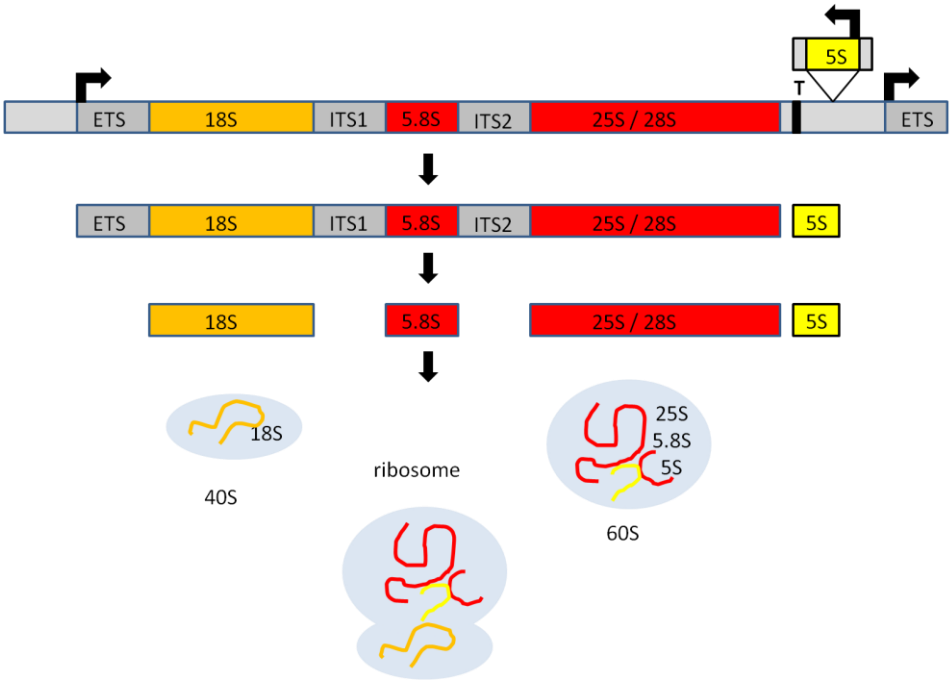


**Figure 1.6 Diagram of the 35S/45S ribosomal DNA repeat and ribosome assembly** (adapted from Schneider 2011). Bent arrows indicate RNAP promoters. Internal and External transcribed spacers (5'ETS, ITS1, ITS2) are excised from the primary transcript in a complex series of processing reactions to produce the mature 18S, 5.8S and 25S (28S in mammalians) and 5S rRNAs which assemble with ribosomal proteins into the pre-40S and pre-60S subunits to form the mature 80S ribosome.

The most abundant post-transcriptional rRNA modifications found in the rRNAs of all species are pseudouridine (ψ) and 2'*O*-methylribose (Schneider 2011). Yeast ribosomes have around 50 modified sites of each type. They cluster in key functional regions of the ribosome and are thought to aid folding and increase stability of the rRNA (Bernstein and Toth 2012). In eukaryotes the modifications are carried out by snoRNPs within the nucleolus where the rRNAs also assemble with ribosomal proteins to form the pre-40S and pre-60S subunits (Henras *et al*. 2008, Reichow *et al.* 2007). The pre-ribosomal subunits are then exported to the cytoplasm for final maturation and assembly into mature ribosomes, the protein factories of the cell. Ribosome biogenesis, a universal cellular process, involves more than 100 accessory proteins, about as many snoRNPs in addition to 60-80 ribosomal proteins (Peculis 2002). A growing yeast cell produces around 2000 rRNA precursors per minute equivalent to some 14 million nucleotides (Warner 1999, Houseley *et al.* 2006). Defective ribosomes are largely degraded by the TRAMP-exosome complex (Houseley and Tollervey 2009). This probably involves the large number of ATPases required for ribosome synthesis. It is not yet understood how defective ribosomes are identified and specifically targeted.

### 1.3.5 tRNAs and other RNAPIII transcripts

RNA polymerase III is highly specialised for the synthesis of tRNAs and also transcribes a variety of short (100-150 bp), essential non-coding RNAs (ncRNAs) such as 5S rRNA, U6 snRNA, 7SL RNA, 7SK RNA which regulates RNAPII activity, and others (White 2011). RNAPIII terminates efficiently at a simple T-rich 3' consensus sequence aided by an intrinsic cleavage activity without the need of other factors (Richard and Manley 2010). The processing of tRNAs involves 5' cleavage by RNaseP and addition of the nucleotides CCA by a dedicated polymerase after 3' processing. tRNAs also undergo a series of folding and modification reactions to aquire their canonical L-shaped tertiary structure, and some tRNAs also undergo splicing. The major surveillance pathway for hypomodified tRNAs is 5' degradation by the exonuclease Rat1, which implies nuclear import of defective tRNAs. The processing of other RNAPIII transcripts is fairly simple and 3' ends are produced by simple trimming. RNAPIII transcripts are also known to undergo nuclear surveillance which can be performed by the exosome-TRAMP complex, as suggested for 5S rRNA, U6 snRNA and pre-tRNAs (Houseley and Tollervey 2009).

## 1.4 Nuclear RNA quality control - RNA surveillance and degradation

All organisms have highly efficient systems to remove aberrant RNAs and recycle all other RNAs at the end of their useful life. The various RNA species have very distinct half-lives, shortest for RNA fragments and processing by-products like excised introns and spacers, carefully regulated for protein-coding mRNAs and longest for stable sn/snoRNAs and rRNAs in ribosomes. The degradation of pre-rRNA spacers (app. 3.3 x 106 nts per minute) probably constitutes a substantial fraction of total cellular RNA degradation (Bernstein and Toth 2012). In higher eukaryotes, intron removal also produces huge amounts of RNA and a special debranching activity is needed to further process the circularised intron lariats. In addition to efficient debris removal, RNA surveillance systems closely monitor all processing and maturation steps from primary transcript to mature RNA, identifying and rapidly degrading unwanted and faulty transcripts and RNPs (Schmid and Jensen 2008). Nuclear mRNA decay pathways specifically target splicing intermediates or unspliced RNAs and quality control mechanisms prevent the export of incorrectly or too slowly processed mRNAs. RNA surveillance ensures that only correctly processed RNAs reach their final destination and avoids potentially detrimental effects of rogue non-functional RNA fragments (Houseley and Tollervey 2009). All eukaryotic RNAs are thought to be subjected to surveillance, however it is unclear how the diverse RNA degradation substrates are identified and targeted.

Three major classes of cellular RNA degrading enzymes (RNases, ribonucleases) are distinguished according to how they access RNA molecules: endonucleases cut RNA internally, 5’ exonucleases degrade RNA from the 5’ end and 3’ exonucleases digest RNA from its 3’ end. RNases are highly abundant and often have multiple and/or overlapping functions and substrates (Houseley and Tollervey 2009). This redundancy greatly enhances the efficiency of RNA processing and degradation. In yeast, two major nuclear RNA processing and degradation activities function in processing and degradation of transcripts of all three RNAPs, the 5’-3’ exonuclease Rat1 (Xrn2 in humans) and the 3’-5’ exonuclease activities of the nuclear exosome (Rrp6 and Rrp44/Dis3). In addition, bacteria and eukaryotes harbour multiple other 3’ exonucleases involved in RNA processing and degradation, often with partially overlapping functions and substrates (Lykke-Andersen *et al*. 2009).

However, ribonuclease activities, especially endonucleases, have to be tightly controlled to restrict degradation to unwanted RNAs. Pre-RNAs are highly susceptible to 3-5’ decay, therefore RNA stability seems primarily determined by protective features acquired during processing and maturation of the RNAs (Bousquet-Antonelli *et al*. 2000, Kufel *et al*. 2004). For stable RNAs exonucleolytic trimming stops at secondary structures and/or bound proteins that protect these RNAs from degradation and thus becomes a processing and maturation step. Accordingly, 5’ caps protect all RNAPII transcripts from the 5’ end, and 5’ degradation requires initial decapping to make the 5’ end accessible. Likewise, poly(A)-binding proteins (PABPs) and sn/snoRNP proteins protect the 3’ tail of mRNAs and stable sn/snoRNAs from 3’-5’ decay. In contrast, non-coding RNAs like CUTs which lack protective features are rapidly degraded as are RNAs produced in mutants defective in 3’ or 5’ processing, like aberrant mRNAs that are not adenylated or not bound by PABP (Anderson 2005, Lykke-Andersen *et al*. 2009).

Yeast RNA degradation activities are universal in so far as the diverse substrates generated by the three RNA polymerases are all targeted by the exosome or Rat1, despite no obvious common substrate features (Houseley and Tollervey 2009). The substrate specificity is thought to derive from the association of the exonucleases with co-factors. Moreover, the dual role in maturation and degradation of the same transcripts suggests mechanisms which allow further differentiation. Kinetic proofreading in 3’ end formation seems to play a role in distinguishing aberrant from correctly processed RNAs. For snoRNAs it has been shown that several cycles of oligoadenylation by Trf4 and trimming by the exosome appear to allow a certain time for the correct processing and assembly of the snoRNP which is then released. Alternatively, if the snoRNA fails to form a correctly folded and packaged mature RNP within the time given, it is completely degraded by the exosome (Grzechnik and Kufel 2008). This implies controlled counteracting efficiencies of polyadenylation and RNA decay which allow coupling of RNA

processing, surveillance and degradation in the same process (Burkard and Butler 2000, Jensen *et al.* 2003, Milligan *et al.* 2005). Notably, oligoadenylation of RNA 3' ends by poly(A)polymerases is now widely believed to be a general mechanism of providing a single-stranded fuse for exonucleolytic digestion, since all exonucleases initiate degradation inefficiently on structured RNAs. Interestingly, the role of polyadenylation in marking nuclear RNAs for degradation by the exosome is conceptually very similar to the polyubiquitylation of proteins for degradation by the proteasome (Makino *et al.* 2013b, Lorentzen and Conti 2006). In addition to poly(A) polymerases, other important co-factors for RNA degradation are ATP-dependent RNA helicases like Sen1 and Mtr4, components of the Nrd1 and TRAMP complexes, respectively (Jammonak *et al.* 2011, Bernstein and Toth 2012). Helicases participate in almost all RNA processing and degradation pathways possibly unwinding secondary structures and dislocating bound proteins while moving along RNA molecules or recruiting other factors for RNA degradation. Mtr4 has recently been shown to control the activity of its associated poly(A) polymerase Trf4 in the TRAMP complex (Jia *et al.* 2011).

## 1.5 The RNA Exosome

### 1.5.1 Nuclear RNA processing, surveillance and degradation by the exosome

The RNA exosome is a critical nuclear RNA processing and degradation activity, highly conserved from yeast to humans, with related complexes also present in bacteria and archaea. The multi-subunit protein complex was initially discovered through its role in stable rRNA processing (Mitchell *et al*. 1997, Mitchell and Tollervey 2010). However, the RNA exosome is now established as the major 3' to 5' RNA surveillance and degradation complex in eukaryotes dealing with a multitude of RNA substrates (Schneider *et al*. 2012). As well as ensuring adequate RNA quantities and quality of transcripts produced by all three RNA polymerases, the exosome also plays key roles in gene regulation by controlling the abundance of non-coding RNA transcripts and in antiviral protection by destroying harmful RNAs (Schmid and Jensen 2008). Most, if not all RNA molecules are thought to encounter the exosome at some stage in their life cycle for processing, quality control, controlled turnover or for degradation (Chlebowski *et al.* 2013, Butler and Mitchell 2010, Lykke-Andersen *et al.* 2009).

### 1.5.2 Exosome structure and function is highly conserved

The exosome complex is highly conserved in structure and function in all eukaryotes studied to date and has striking similarities in its architecture to RNA degrading exosomes from archaea and polynucleotide phosphorylase (PNPase) found in bacteria, plants and vertebrate mitochondria (Januszyk and Lima 2010). In eukaryotes, nine subunits of the exosome core (Exo-9) assemble into a two-layered barrel-shaped structure to form a channel which can accommodate single-stranded RNA (Fig. 1.7). The central hexameric ring is formed by three distinct heterodimers of RNase PH-like proteins (Rrp41-Rrp45, Rrp46-Rrp43, Mtr3-Rrp42). Three further RNA-binding subunits (Rrp4, Csl4 and Rrp40) form a cap and stabilise the complex by holding neighbouring dimers together (Liu *et al*. 2006).

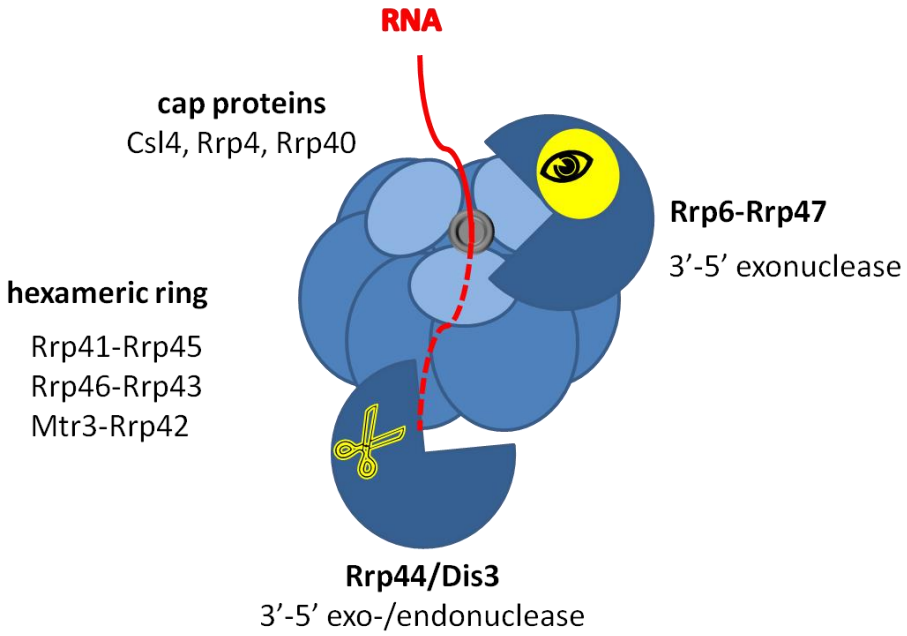


**Figure 1.7 Schematic representation of the structure of the eukaryotic exosome complex** indicating the spatial distribution of subunits, adapted from Lykke-Andersen *et al*. 2011a. The core of the exosome (Exo-10) is formed by the exo-/endonuclease Rrp44/Dis3 and 9 catalytically inactive subunits (Exo-9), six of which form a central channel which is capped by three RNA-binding proteins. In the nucleus, the Exo-10 associates with the 3'->5' exonuclease Rrp6 and its co-factor Rrp47 (depicted as yellow eye). The single-stranded RNA substrate (depicted in red) is channelled through the central tunnel to reach the active site of Rrp44/Dis3 (yellow scissors represent the endonucleolytic activity).

In comparison, the 9-subunit archaeal exosome is also made up of three dimers of the RNase PH like subunits Rrp41 and Rrp42 forming a hexameric ring, and the exosome cap is formed by Rrp4 and in some species Csl4. Whereas PNPase is a homotrimer of polypeptides with RNA binding domains and RNase PH like dimers similar to Rrp41-Rrp42 which also form a hexameric

ring with a central channel (Januszyk and Lima 2010). Whilst the architecture of these ancient RNA processing complexes is highly conserved with the same domain composition and spatial arrangement, the catalytic properties are very different. The prokaryotic complexes use the processive 3'-5' phosphorolytic ribonuclease activity within the Rrp41 RNase PH-like domains. In contrast, the core subunits of the eukaryotic exosome, although closely related to the bacterial phosphorolytic ribonuclease RNase PH, have lost their catalytic function and have evolved into inactive structural components (Januszyk and Lima 2010). However, through their residual RNA binding capabilities the core proteins have a critical function in channelling the substrate to the active site of Rrp44/Dis3 and seem to modulate substrate specificity and catalytic properties of all three associated hydrolytic ribonuclease activities provided by Rrp44/Dis3 and Rrp6 (Makino *et al*. 2013a, Chlebowski *et al.* 2013, Drazkowska *et al.* 2013).

### 1.5.3 The catalytic activity of the exosome core Dis3/Rrp44

The catalytic activity of the yeast exosome in both the nucleus and cytoplasm is supplied by the processive hydrolytic 3'-5' exonuclease Rrp44/Dis3 (Mitchell *et al*. 1997, Dziembowski *et al*. 2007). The essential protein degrades both circular and linear ssRNA substrates and is stably associated with the other nine exosome core subunits. Rrp44/Dis3 shares common features with bacterial RNase II (see Fig. 1.8) such as two cold-shock domains (CSD1, CSD2), an exonuclease domain (RNB) and a C-terminal RNA-binding domain (S1). However, it has an additional N-terminal PIN domain which adds an endonucleolytic activity and attaches Rrp44 to the core exosome (Lebreton *et al*. 2008, Lorentzen *et al.* 2008, Schaeffer *et al.* 2009, Schneider *et al*. 2009).

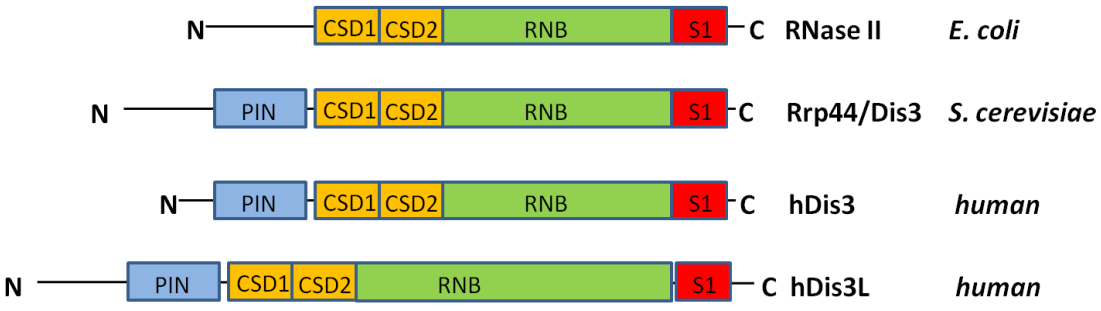


**Figure 1.8 Domain structure of Rrp44/Dis3 in yeast and humans vs. *E. coli* RNAse II** (adapted from Lykke-Andersen *et al.* 2011a). Comparison of architecture of Rrp44/Dis3 yeast and human homologues with RNAse II from *E. coli;* CSD= Cold shock domain, RNB= exonuclease domain, S1 = RNA binding domain, PIN= endonuclease domain.

How both endo- and exonucleolytic activities of Rrp44 modulate exosome functions is still poorly understood. Both activities appear to cooperate in the degradation of substrates and add versatility to the complex (Chlebowski *et al*. 2013, Lykke-Andersen *et al.* 2009). It has been proposed that RNAs designated for degradation thread through the central channel of the exosome core to the active Rrp44/Dis3 site which is tethered to the bottom of the exosome via direct interaction of its PIN-domain with Rrp41 (Bonneau *et al*. 2009, Schneider *et al.* 2009, Lykke-Andersen *et al.* 2011a). In agreement with this, blocking the exosome channel reduces both exo- and endonuclease activity of Rrp44 (Wasmuth and Lima 2012).

A recent crystal structure of the yeast Exo-10 with a trapped RNA substrate has given crucial insights into this channelling mechanism which is remarkably conserved from prokaryotes to eukaryotes (Makino *et al*. 2013a). The RNA binding path runs from the entrance pore at the cap to the Rrp44 active site and spans at least 25 unwound single-stranded nucleotides extending over 160 A°. All exosome subunits contribute to RNA binding via non-specific electrostatic interactions which allows the exosome to degrade such a wide variety of substrates. The mechanism of channelling RNA substrates through the exosome core for degradation is reminiscent of the mechanism by which polypeptides are threaded through a central channel to be degraded by the proteasome (Makino *et al*. 2013b).

### 1.5.4 Rrp6 adds a major 3’-5’ exonuclease activity to the nuclear yeast exosome

In yeast, Rrp44 is the only active exosome subunit in the cytoplasm, whereas in the nucleus Rrp6 contributes a major distributive hydrolytic 3'-5' exoribonuclease activity (Burkard and Butler 2000) which has also been shown to enhance the nuclear core Rrp44/Dis3 activities (Wasmuth and Lima 2012). Other eukaryotic Rrp6 homologues, like the human PM-Scl 100 kDa autoantigen, appear to be present in small quantities in the cytoplasm, however they are rarely associated with the cytoplasmic exosome (Lykke-Andersen *et al*. 2009, Chlebowski *et al*. 2013).

Whilst Rrp6 is not essential for growth, it is needed for optimal growth in yeast. Accordingly, Rrp6 deletion causes slow growth at 30 °C and a temperature-sensitive lethal phenotype at 37°C (Briggs *et al.* 1998). The exonuclease functions in nuclear RNA 3' maturation and degradation pathways of all known classes of RNAs. Rrp6 is also involved in regulating levels of specific mRNAs suggesting key functions in gene expression and regulation (Butler and Mitchell 2010, Januszyk *et al.* 2011). Cells lacking Rrp6 are defective in stable RNA processing and accumulate 3' extended precursors and processing intermediates (Allmang *et al.* 1999). Moreover, Rrp6 has unique functions in the final maturation of 5.8S rRNA, mRNA quality control near transcription sites and polyadenylation-dependent degradation of pervasive non-coding transcripts (Butler and Mitchell 2010).

Nuclear RNA processing defects can be seen in core exosome mutants or alternatively in mutants of Rrp6 and its co-factor Rrp47 (Allmang *et al.* 1999, Mitchell *et al.* 2003a). Although long used as a marker for nuclear exosome activity, there is increasing evidence for distinct functions and substrate specificities of Rrp6, Rrp44/Dis3 and core exosome subunits (Callahan and Butler 2008, Kiss and Andrulis 2010), as well as for core exosome-independent functions of Rrp6 as shown in cell cycle progression (Graham *et al.* 2009).

Despite its functions in RNA processing and surveillance, Rrp6 does not show stable RNA binding in vitro (Phillips and Butler 2003). Also, whilst purified Rrp6 degrades unstructured RNA efficiently, it is inhibited by stable RNA secondary structures such as stem loops *in vitro* which are known to be present in typical Rrp6 substrates e.g.the 5'ETS fragment (Liu *et al*. 2006, Burkard and Butler 2000). Rrp6 is therefore thought to be dependent on co-factors like Rrp47, TRAMP or the Nrd1 complex for substrate recognition, substrate specificity and the degradation of structured substrates (Butler and Mitchell 2010, Chlebowski *et al*. 2013).

***Rrp6 architecture***

Rrp6 belongs to the RNase D family of 3' to 5' exoribonucleases whose members typically contain an exonuclease domain consisting of four conserved acidic residues DEDD, in addition to one or more helicase and RNase D C-terminal (HRDC) domains (Callahan and Butler 2008, Butler and Mitchell 2010). Rrp6 homologues (see Fig. 1.9) have an additional N-terminal domain, termed PMC2NT domain (Staub *et al.* 2004).

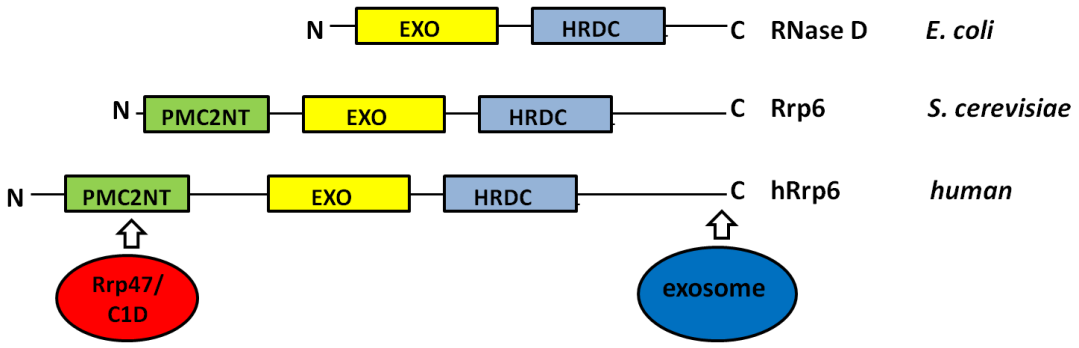


**Figure 1.9 Rrp6 and its eukaryotic homologues are considerably larger than their prokaryotic RNase D counterparts.** Comparison of DEDD exonucleases and Rrp6 domain structure, adapted from Lykke-Andersen *et al.* 2011a. HRDC= Helicase and RNase D C-terminal domain; EXO = catalytic exonuclease domain; PMC2NT=N-terminal domain required for interaction with co-factor Rrp47/C1D (red circle), C-terminal domain is required for binding to the exosome (blue circle).

The PMC2NT domain is required for Rrp6 binding to its co-factor Rrp47 (C1D in humans), but does not affect the interaction of Rrp6 with the core exosome (Stead *et al.* 2007). It has been suggested that this N-terminal region folds over the catalytic exo-domain of Rrp6 and could thus affect Rrp6 activity (Phillips and Butler 2003, Midtgaard *et al.* 2006). In contrast to Rrp6 deletion phenotypes, catalytically inactive Rrp6 mutants cause a loss of function and a cold-sensitive growth phenotype (Briggs *et al.* 1998). The C-terminal domain of Rrp6 appears to mediate Rrp6 and core exosome interactions. This is based on the observation that Rrp6 mutants with a C-terminal deletion fail to degrade rRNA intermediates that need cooperation between Rrp6 and Rrp44, whilst still processing the 3' ends of snoRNA and 5.8S rRNA precursors (Callahan and Butler 2008). The association of Rrp6 with the exosome does not seem to affect the catalytic activity of Rrp6, as opposed to exosome-bound Rrp44 whose enzymatic activity appears attenuated (Liu *et al*. 2006). At the very C-terminus, Rrp6 also contains a consensus bipartite nuclear localisation signal which if deleted mislocalises some Rrp6 to the cytoplasm (Briggs *et al.* 1998, Phillips and Butler 2003).

A recent crystal structure has further characterised the exosome-binding region of Rrp6 within its C-terminus (residues 518–693) and suggests that this region of Rrp6 wraps around the exosome cap structure and also contacts the RNase PH ring thereby stabilising the RNA binding path of the core exosome (Makino *et al.* 2013a). More specifically, residues 532–557 of Rrp6 form an α-helix that binds to Csl4 and Mtr3, and residues 565–619 contain an unstructured region followed by a small β-hairpin and α-helix that contact Mtr3, Rrp43 and approach Csl4 docking onto a conserved surface of Exo-9. The C-terminus of Rrp6 does not contact RNA directly but indirectly contributes to the long RNA-binding path by stabilising the exosome cap protein Csl4, thus ensuring an appropriate RNA-binding conformation. This could explain previous observations that Rrp6 binding to the core exosome increases Exo-10 exoribonuclease activity independently of Rrp6 catalytic activity (Wasmuth and Lima 2012, Makino *et al.* 2013a).

## 1.6 RNA Exosome functions

### 1.6.1 Stable RNA 3’ end processing and maturation

The exosome plays a critical role in stable RNA synthesis and specifically catalyses 3' end trimming and maturation of rRNA, snRNAs and snoRNA precursors (Allmang *et al*. 1999, Briggs *et al.* 1998). In 5.8S rRNA processing the exosome is required for the trimming of the 7S pre-rRNA to the mature 5.8S species (Allmang *et al.* 1999, Mitchell *et al*. 1997). The current understanding is that the core exosome exonuclease Rrp44 produces a 5.8S +30 rRNA

intermediate from the 7S pre-rRNA. Notably, the 30 nucleotide 3' tail matches the length required for an RNA substrate to thread through the exosome ring to the active Rrp44/Dis3 site. Further 3' end trimming to generate the 6S form is carried out by Rrp6 without the core exosome. However, efficient trimming of 3' extended 5.8S precursors by Rrp6 requires its co-factor Rrp47 in *S. cerevisiae* or its homologue C1D in humans (Butler and Mitchell 2010). Similarly, Rrp6 and Rrp47 are required for the final maturation of 3' extended snRNA and snoRNA precursors by removing the last few nucleotides which also requires the Nrd1 complex to recruit TRAMP and the exosome to the RNA substrates (van Hoof *et al.* 2000a; Grzechnik and Kufel 2008).

### 1.6.2 Nuclear quality control and degradation of aberrant RNAs

The exosome plays a crucial role in nuclear RNA surveillance and quality control by degrading aberrant processing intermediates such as snRNAs, snoRNAs, hypomodified tRNAs and pre-rRNAs, as well as processing by-products such as the 5' ETS and ITS excised spacer fragments from the 35S pre-rRNA precursor (Allmang *et al.* 1999 and 2000, Schmid and Jensen 2008a). Yeast *rrp6Δ* exosome mutants accumulate polyadenylated sn-/snoRNAs and pre-rRNAs as well as CUTs. Due to the huge amounts of rRNA produced in the cell, surveillance of pre-rRNAs and pre-ribosomes is highly active in yeast and degradation of defective precursors is largely mediated by TRAMP (see section 1.7) and exosome complexes (Fang *et al.* 2005, Kos and Tollervey 2010). Moreover, the same surveillance pathway is used for the degradation of non-coding pervasive transcripts by RNAPII such as CUTs (Butler and Mitchell 2010).

In yeast, the exosome is recruited via the Nrd1-termination complex co-transcriptionally (Vasiljeva and Buratowski 2006) for precise 3'-end processing and quality control of snRNA and snoRNAs, whereas unstable transcripts like CUTs and incorrectly processed RNAs are immediately degraded (Allmang *et al.* 2000, Wyers *et al.* 2005, Thiebaut *et al.* 2006). TRAMP-mediated polyadenylation of those substrates stimulates their degradation by Rrp6 (LaCava *et al.* 2005, Callahan and Butler 2010) which is contrary to the stabilising mRNA poly(A) tails in the cytoplasm. Like CUTS, many of the recently discovered non-coding RNAPII transcripts appear to be subject to exosome-TRAMP-mediated regulation and degradation, suggesting that the exosome is the guardian of the "dark matter" in the transcriptome (Belostotsky 2009, Vanacova and Stefl 2007). How TRAMP recognises substrates for degradation is still unclear. A kinetic proofreading model has been proposed which involves alternating cycles of polyadenylation of the 3’ end by TRAMP and trimming by the exosome to allow degradation of substrates that are processed too slowly. This implies that all RNAs are polyadenylated as part of their 3’ end processing and surveillance (Grzechnik and Kufel 2008).

### 1.6.3 Nuclear mRNA surveillance and regulation of mRNA levels

The nuclear exosome has critical functions in the surveillance of polyadenylated RNAs (van Hoof *et al*. 2002) and degradation of improperly spliced or processed mRNAs such as splicing intermediates and read-through transcripts (Anderson and Wang 2009, Milligan *et al.* 2005, Torchet *et al.* 2002). Exosome functions in mRNA surveillance have mainly been studied with Rrp6 deletion mutants which accumulate incompletely processed and polyadenylated mRNAs (Anderson 2005). Rrp6 also slows the conversion of pre-mRNAs to export-competent RNPs by retaining pre-mRNAs in nuclear foci at or close to their site of transcription (Hilleren *et al.* 2001). *S. cerevisiae* strains that lack Rrp6 fail to form nuclear foci and consequently aberrant transcripts exit the nucleus and reach the cytoplasm. Rrp6 also functions in the DRN pathway (degradation of mRNA in the nucleus) which degrades mRNAs that are exiting the nucleus too slowly (Butler and Mitchell 2010). Furthermore, some defects in the mRNA 3' end formation and polyadenylation pathways are suppressed in the absence of Rrp6 which leads to accumulation of aberrant mRNAs; examples are the temperature-sensitive *pap1-1* allele (Briggs *et al.* 1998) which produces non-polyadenylated mRNAs and the *rna14-1* mutant (Carneiro *et al*. 2008) which generates read-through transcripts that can generate functional mRNAs in the absence of Rrp6 (Butler and Mitchell 2010, Torchet *et al.* 2002).

Rrp6 also regulates levels of a number of mRNAs in simple feedback control pathways such as *NRD1* and *NAB2* mRNA in yeast (Arigo *et al.* 2006b, Roth *et al*. 2005) and also down-regulates histone mRNA levels at the end of the S-phase of the cell cycle. Strikingly, mRNA levels of the exosome co-factor Nrd1 are regulated on two levels, firstly the exosome is involved in premature termination and degradation of Nrd1 mRNA when Nrd1 is in excess and secondly, the exosome degrades the Nrd1 antisense CUT and thus allows Nrd1 expression (Arigo *et al.* 2006, Belostotsky 2009). The exosome is believed to have a general role in gene regulation by transcriptional attenuation, i.e. by controlling the switch between alternative transcription start sites (TSS) to produce either a functional mRNA or a CUT (Belostotsky 2009). Examples are the expression of the *IMD2* gene encoding the key enzyme of GMP biosynthesis and the yeast *URA2* gene which are regulated in response to GTP and uracil levels, respectively. It is still unclear how exactly Rrp6 is targeted to the substrates and how it distinguishes between degradation and maturation (Butler and Mitchell 2010).

### 1.6.4 Exosome functions in gene silencing

Silencing of genes and especially transposable elements and viral RNAs in eukaryotes is widely conserved and can be regulated through changes in chromatin structure, transcriptional and post-transcriptional repression as well as RNA stability (Belostotsky 2009). Most eukaryotes

utilise RNA interference (RNAi) pathways. These involve small interfering RNAs (siRNAs) produced from longer RNA precursors in the cytoplasm which target specific mRNAs by base-pairing interactions and thus promote their degradation or inhibit translation. Some organisms like *S. cerevisiae* lack RNAi machinery and silencing is mainly achieved via heterochromatin-inducing DNA and histone modifications e.g. by histone deacetylases Sir2 (Silent information Regulator) and by the exosome which degrades and down-regulates RNA species like antisense CUTs and other ncRNAs involved in gene silencing or chromatin remodelling, as well as harmful RNAs (Houseley and Tollervey 2008). In *S. cerevisiae*, the exosome contributes to heterochromatic silencing by directly degrading heterochromatic RNAPII transcripts from rDNA and telomeres, as well as cryptic transcripts. Moreover, the exosome-TRAMP (Trf4) mediated degradation of rDNA-CUTs helps to prevent loss of rDNA repeats via recombination (Houseley *et al.* 2007, Vasiljeva *et al.* 2008b, Wolin *et al.* 2012).

RNAi-independent pathways in other organisms also appear to rely on the exosome and its function in regulating the expression of ncRNAs and maintaining appropriate ncRNA levels a lot of which regulate gene silencing (Belostotsky 2009). The exosome is therefore believed to play a global role in regulating stability of antisense RNAs; examples are Ty1, GAL10 and PHO84 antisense RNAs which induce silencing of their respective sense genes and are stabilised in *rrp6Δ* mutants. However in wild-type cells, gene silencing and heterochromatin formation are antagonised by the degradation of the respective antisense CUTs by the exosome (Belostosky *et al.* 2009). In *S. pombe*, the exosome and TRAMP, or more specifically Rrp6, Rrp44 and Trf4, are involved in the silencing of telomeric, silent mating type and centromeric regions (Askree *et al*. 2004). In plants, aberrant RNAs enter RNAi pathways if not degraded by the exosome or Xrn1. Thus, in organisms which are equipped with RNAi systems, RNA species which are stabilised in exosome mutants can compete for RNAi biogenesis and interfere with heterochromatic silencing. There is accumulating evidence in mammalians for exosome-mediated ncRNA surveillance pathways with an even wider range of exosome co-factors than known in yeast (Wolin *et al*. 2012)

### 1.6.5 Cytoplasmic exosome functions

The yeast cytoplasmic exosome relies solely on Rrp44 for its ribonuclease activity and associates with four superkiller (Ski) proteins to degrade or process mRNAs that lack a stop codon or lack poly(A) tails following deadenylation. This also includes RNA fragments generated by endonucleolytic cleavage as well as viral RNAs which lack poly(A) tails (Schaeffer *et al.* 2009). The four Ski proteins, Ski2, Ski3, Ski7 and Ski8 are the only four co-factors required for all known cytoplasmic exosome functions (Mitchell and Tollervey 2003b). Ski2, Sk3 and two copies of Ski8 form a complex with a general helicase core provided by the DExH box RNA helicase Ski2 and protein-protein-interaction regions provided by Ski2, Ski3 and Ski8 (Synowsky

*et al.* 2009, Anderson and Parker 1998). Ski2 belongs like Mtr4 to the Ski2-like family of DExH helicases. The two helicases share great similarity, most notably an arch domain which is required for exosome-mediated RNA processing and only found in exosome-associated helicases (Jackson *et al.* 2010). The currrent understanding is that the Ski complex together with Ski7 recruits the exosome to its substrates. The Ski7 C-terminal region has an additional special function in nonstop mRNA decay. Ski7 recognizes stalled ribosomes on mRNAs and recruits the Ski complex along with the exosome for degradation interacting with both complexes via its N-terminus. The activity of the cytoplasmic exosome is not essential, which is in striking contrast to the vital role of the nuclear exosome. This is most likely due to overlapping functions of the cytoplasmic 5'-3' exonuclease Xrn1 which degrades mRNAs after decapping and provides the predominant pathway for mRNA degradation in the cytoplasm (Schaeffer *et al*. 2009).

## 1.7 Exosome substrates and cofactors

A wide variety of transcripts undergo exosome-mediated processing or decay, as has been proposed, most RNAs encounter the exosome at some point in their life cycle (Lykke-Andersen *et al.* 2009). With the dual role of the exosome in total RNA degradation and precise RNA processing in mind, the central question is how the exosome distinguishes between its numerous substrates for maturation or degradation. The versatility and processing mode of the exosome is believed to be achieved by the use of various distinct pathways and association with specific accessory factors which help to recognise and target its diverse substrates and avoid degradation of functional, mature RNAs (Butler and Mitchell 2010, Bernstein and Toth 2012, Chlebowski *et al*. 2013). In the cytoplasm the Ski proteins (see section 1.6.5) are the only known exosome co-factors for mRNA turnover and degradation of aberrant RNAs. In contrast, in the nucleus, a number of exosome co-factors have been identified such as the ATP dependent RNA helicase Mtr4 (Bernstein *et al.* 2008), the polyadenylation complex TRAMP (LaCava *et al*. 2005, Vanacova *et al.* 2005), the Nrd1-Nab3-Sen1 termination complex (see section 1.2.5), as well as the small nuclear proteins Rrp47 and Mpp6 (Mitchell *et al.* 2003a, Chen *et al*. 2001, Butler and Mitchell 2010).

### 1.7.1 The RNA helicase Mtr4 and TRAMP

TRAMP is a major co-factor of the exosome in the surveillance and degradation of stable RNAs, mRNAs and CUTs (LaCava *et al*. 2005., Vanacova *et al.* 2005) and has been shown to stimulate the exonuclease activity of the exosome and Rrp6 (Callahan and Butler 2010). TRAMP is a trimeric complex which contains the noncanonical poly(A)-polymerase Trf4 (or Trf5), the RNA-

binding protein Air1 (or Air2) and the RNA helicase Mtr4 linking TRAMP to the exosome (Houseley *et al.* 2006). TRAMP complexes are distinguished in TRAMP4 and TRAMP5 complexes depending on their constituent poly(A) polymerase Trf4 or Trf5 and have distinct surveillance and degradation activities (Egecioglu *et al.* 2006, , Houseley *et al.* 2007, Wery *et al.* 2009). The TRAMP complex is thought to mark its RNA substrates for degradation by adding short poly(A) tails which provide an unstructured "fuse" for rapid digestion by the exosome/Rrp6. This rationalises why many of the accumulated RNAs in *rrp6* mutants are oligo- or polyadenylated (Callahan and Butler 2010, Grzechnik and Kufel 2008). TRAMP requires a minimum 3' overhang of 3 nucleotides to initiate polyadenylation, however the precise mechanism by which TRAMP recognises its substrates is unknown. Callahan and Butler (2010) have shown that TRAMP enhances the rate of RNA degradation by recombinant Rrp6 around 10-fold. Experiments with reconstituted *S. cerevisiae* TRAMP have also shown that TRAMP inherently suppresses poly(A) addition after only 3 to 4 adenosines (Jia *et al.* 2011) as opposed to polyadenylation by the conventional poly(A) polymerase Pap1, which produces much longer poly(A) tails that stabilise mRNAs. This length restriction is controlled by Mtr4p which acts as a critical regulator of TRAMP polyadenylation in response to features in the RNA (Jia *et al.* 2011). Mtr4 is also thought to have TRAMP-independent functions (Bernstein *et al*. 2008, Bernstein and Toth 2012). TRAMP and the exosome are recruited co-transcriptionally to their substrates by the Nrd1 complex (Vasiljeva and Buratowski 2006, Honorine *et al.* 2011).

### 1.7.2 Mpp6

Mpp6 is a small, basic nuclear RNA-binding protein that was identified in association with exosome preparations that lack Rrp44/Dis3 but contain Rrp6 (Chen *et al.* 2001). Its role in exosome function is still unclear. Whilst Mpp6 shares certain similarities with Rrp47 (see 1.7.3), it shows different substrate specificities with a preference for pyrimidine-rich RNA (Milligan *et al.* 2008, Butler and Mitchell 2010). Lack of the human Mpp6 protein results in the accumulation of 5.8S rRNA precursors carrying a pyrimidine-rich sequence at their 3' ends (Schilders *et al.* 2005). It has been proposed that Mpp6 could target the exosome to a specific set of substrates and/or promote Rrp6-TRAMP interaction. Interactions between Mpp6 and the human Rrp6 homologue PM-Scl 100, as well as the TRAMP component hMtr4 have been shown by two-hybrid interaction and pull-down experiments (Schilders *et al.* 2007). Mpp6 is required for viability of cells lacking Rrp47 and/or Rrp6, thus Rrp47 and Mpp6 interactions with Rrp6 are not functionally redundant. Moreover, accumulation of the *NEL025c* model CUT is exacerbated when both Mpp6 and Rrp47 are depleted compared to the single deletion mutants (Milligan *et al.* 2008). This suggests an important function of these proteins in the regulation of CUTs which could explain the synthetic lethality of *rrp47Δ mpp6Δ* strains.

### 1.7.3 Rrp47 acts jointly with Rrp6 in RNA processing and surveillance pathways

Rrp47 in yeast (also known as Lrp1 or yC1D) and its human counterpart C1D are small basic proteins which interact directly with the nuclear exosome exonuclease Rrp6 in yeast and PM-Scl 100 in humans (Stead *et al.* 2007, Schilders *et al*. 2007). There is strong evidence for functional conservation of Rrp47/C1D (Mitchell 2010). Both, yeast Rrp47 and human C1D proteins have been implicated in DNA repair (Chen *et al.* 2004, Erdemir *et al*. 2002 a and b, Yavuzer *et al*. 1998) and are localised to the nucleus, consistent with roles in RNA surveillance and DNA repair (Kumar *et al*. 2002, Hieronymus *et al.* 2004). There is conclusive biochemical and genetic evidence that Rrp47 acts jointly with Rrp6 in the same final maturation step in stable RNA 3' processing, as well as in the surveillance of stable RNAs and degradation of non-coding RNAs like CUTs (Mitchell *et al*. 2003a, Peng *et al.* 2003, Arigo *et al.* 2006, Hieronymus *et al.* 2004, Butler and Mitchell 2010). The non-additive phenotype of *rrp47Δ rrp6Δ* double mutants also confirms that they act in the same pathway. However, the nature of the interaction of Rrp47 with Rrp6 and the precise function of Rrp47 in these pathways are still poorly understood.

Rrp47 has been shown to bind the N-terminal PMC2NT domain of Rrp6 and has no apparent effect on the Rrp6-exosome interaction (Mitchell *et al*. 2003a, Stead *et al*. 2007). Notably, the PMC2NT domain of Rrp6 is not only sufficient and necessary for Rrp47 binding, but also for normal Rrp47 expression in yeast since Rrp47 levels are drastically reduced in its absence (Stead *et al*. 2007). Rrp47 concomitantly binds Rrp6 and structured nucleic acids in vitro and can form a stable complex with structured nucleic acids and Rrp6 (Stead *et al*. 2007). Purified recombinant Rrp47 was found to bind to double-stranded (ds) DNA or structured RNA with comparable affinity, but showed no interaction with single-stranded (ss) nucleic acids. C1D has also been reported to bind to structured RNAs *in vitro* (Schilders *et al*. 2007). However, Rrp47 and C1D proteins do not share any sequence homology to previously characterised nucleic acid-binding proteins.

Based on the interactions of Rrp47 with Rrp6 and structured RNA, it has been suggested that Rrp47 might target Rrp6 to structured RNA substrates and facilitate the notoriously problematic 3’ exonucleolytic digestion of structured RNAs as Rrp6 is known to degrade structured RNAs poorly *in vitro* (Liu *et al*. 2006, Burkard and Butler 2000). Based on co-purification analyses of proteins from yeast cell extracts, the nuclear exosome appears to be the only protein complex with which yeast Rrp47 is stably associated (Peng *et al*. 2003). Rrp47 is known to play a role in Nrd1 termination and degradation of CUTs; the *rrp47Δ* mutation is synthetic lethal with the *nrd1-102* mutant which is defective in RNA binding (Arigo *et al.* 2006b) indicating a role for the RNA binding activity of Rrp47 in the recruitment of the exosome to termination regions.

## 1.8 Aims and objectives

The aim of this study was to elucidate the role of yeast Rrp47 in exosome-mediated RNA processing and degradation, specifically its function as a co-factor of the exoribonuclease Rrp6, one of the main nuclear RNA processing and surveillance factors. The conservation of the Rrp6 and Rrp47 interaction from yeast to humans indicates the importance of Rrp47 for its associated exoribonuclease and its role in RNA metabolism. However, as yet, it is not clear what the precise function of Rrp47 is and whether Rrp47 can function independently of Rrp6. Due to the lack of structural information, bioinformatics analyses of the Rrp47 protein sequence and site-directed mutagenesis were chosen as tools to reveal and map critical domains and residues within Rrp47 by creating and analysing loss of function mutants. As a co-factor of Rrp6, it was of particular interest to map sites or domains important for Rrp6 binding and/or RNA binding, to confirm the model that Rrp47 could target Rrp6 to its substrates or contribute to substrate recognition or binding. Furthermore, we were interested in the effects the proteins exert on each other, specifically the basis and implications of the conditional expression of Rrp47 in the presence of Rrp6. The main objectives of these investigations were to further characterise the interaction of Rrp6 with Rrp47 with respect to requirements within Rrp6 for interaction, assembly of Rrp6-Rrp47, nuclear import and localisation. These studies led to revisiting the effects of Rrp47 in maintaining Rrp6 stability, as well as gaining insights into the synthetic lethality of a joint deletion of Rrp47 and the yeast exonuclease Rex1.

# Chapter Two

# Materials and Methods

**Tables 2.1 – 2.13**

# Chapter Two

# Materials and Methods

## 2.1. Materials

### 2.1.1 General reagents, buffers and solutions

All reagents used were of molecular biology grade, purchased from Sigma-Aldrich (Sigma Aldrich Chemie GmbH, Munich, Germany) or Melford (Melford Laboratories Ltd., Ipswich, UK) and stored at room temperature unless stated otherwise. Solutions and their preparation are listed in Table 2.2 and Table 2.3. If required, solutions were sterilised by autoclaving at 121 psi for 20 min or by filtration through a 0.2 µM filter (Millipore, Bedford, USA) for sterilisation. Water was routinely Millipore-filtered and for RNA work also treated with Diethyl-pyrocarbonate (DEPC) and sterilised. Unless stated otherwise, enzymes were purchased from Promega (Promega Inc., Madison, USA), NEB (New England Biolabs., Massachusetts, USA) or Fermentas (Fermentas international Inc., Canada) and stored at -20 °C.

### 2.1.2 Bacterial strains, media and supplements

General cloning was carried out using the commercial *Escherichia coli* strains XL1-Blue (Stratagene, La Jolla, CA, USA) or DH5α™ (Invitrogen, Life Technologies Corporation, Paisley, UK). For protein expression the *E. coli* strain BL21(DE3) pLysS (Stratagene) was used (Table 2.1). All media and glassware for bacterial cultures were sterilised by autoclaving or filtration. Antibiotics (Table 2.4) were supplemented to media as required from 1000 x stocks (stored at -20 °C) after autoclaving/immediately before pouring the plates.

***Table 2.1 Bacterial media and supplements***

| | |
|---|---|
| **Luria Bertani (LB) medium** | 1 % bacto-tryptone, 0.5 % yeast extract, 1 % NaCl |
| **LB agar plates** | 2 % w/v bacto-agar added to LB broth |
| **Antibiotics**<br>- Ampicillin (Amp)<br>- Chloramphenicol (Cam)<br>- Kanamycin (Kan) | <br>100 µg/ml in 50 % ethanol<br>25 µg/ml in 100 % ethanol<br>50 µg/ml in 50 % ethanol |

***Table 2.2 Buffers and solutions for DNA and RNA expression, extraction and analysis***

| ***Buffers and solutions for*** | ***DNA and RNA expression, extraction and analysis*** |
|---|---|
| TfbI | 30 mM KAc, 100 mM $RbCl_2$, 10 mM $CaCl_2$, 50 mM $MnCl_2$, 15 % glycerol, pH adjusted to 5.8 with 0.2 M acetic acid |
| TfbII | 10 mM MOPS, 75 mM $CaCl_2$, 10 mM $RbCl_2$, 15 % glycerol, pH adjusted to 6.5 with 0.5 M KOH |
| TE (Tris-EDTA) buffer | 10 mM Tris-HCl (pH 8.0), 1 mM EDTA (pH 8.0) |
| Alkaline lysis solution I | 25 mM Tris-HCl (pH 8.0), 50 mM glucose, 10 mM EDTA (pH 8.0) |
| Alkaline lysis solution II | 0.2 M NaOH, 1 % SDS |
| Alkaline lysis solution III | 3 M potassium acetate, 11.5 % acetic acid |
| Phenol-Chloroform | 50 % phenol, 48 % chloroform, 2 % isoamylalcohol |
| 6 x DNA loading dye | 30 % glycerol , 0.25 % bromophenol blue, 0.25 % xylene cyanol |
| TBE | 90 mM Tris, 90 mM boric acid, 2 mM EDTA (pH 8.0) |
| 50 x Denhardt's solution | 0.04 % Ficoll, 0.04 % polyvinylpyrrolidone, 0.04 % BSA, -20°C |
| 20 x SSPE | 150 mM NaCl, 9 mM sodium di-hydrogen phosphate, 1 mM EDTA, adjusted to pH 7.4 with NaOH |
| Neutralisation buffer | 1.5 M NaCl, 0.5 M Tris, pH adjusted to 7.4 with HCl |
| DEPC-H2O | Millipore water treated with 0.1 % diethylpyrocarbonate (DEPC) |
| 2 x RNA loading dye | 95 % formamide, 20 mM EDTA, 0.05 % bromophenol blue, 0.05 % xylene cyanol |
| RNA glyoxal loading buffer | 50 % DMSO, 1 M glyoxal, 1 x MOPS, 10 % glycerol, 20 µg/ml ethidium bromide, 0.025 % (w/v) bromophenol blue, 0.025 % (w/v) xylene cyanol |
| 10 x MOPS | 200 mM MOPS (morpholinopropanesulfonic acid) pH 7.0, 50 mM NaAc, 10 mM EDTA |
| Na-Acetate mix | 10 mM Tris-HCl pH 8.0, 100 mM Na-Acetate pH 5.0, 1 mM EDTA pH 8.0 |
| GTC-mix | 6.1 M guanidine thiocyanate, 15 mM EDTA pH 8.0, 75 mM Tris-HCl pH 8.0, 3 % sarkosyl, 1.5 % β-mercaptoethanol |
| Oligohybridisation buffer | 6 x SSPE, 5 x Denhardt's, 0.2 % SDS |
| Stripping solution | 0.1 % SSPE, 0.1 % SDS |
| 1 x LiAc buffer | 10 mM Tris-HCl pH 8.0, 1 mM EDTA pH 8.0, 100 mM Lithium acetate pH 7.5 |
| Cell breaking buffer | 10 mM Tris-HCl pH 8.0, 1 mM EDTA pH 8.0, 100 mM NaCl, 1 % SDS, 2 % Triton X-100 |
| 10x HEPES binding buffer (UV-crosslinking buffer) | 200 mM HEPES pH 7.5, 1500 mM NaCl, 50 mM $MgCl_2$, 1 mM EDTA |
| RNA/DNA binding buffer | 10 mM Tris-HCl (pH 8.0), 2 mM $MgCl_2$, 0.1 mM EDTA, 10 % (v/v) glycerol, 150 mM NaCl |

***Table 2.3 Buffers and solutions for protein expression, purification and Aanalyses***

| ***Buffers and solutions for*** | ***protein expression, purification and analyses*** |
|---|---|
| H300 lysis buffer | 20 mM Hepes pH 7.4, 300 mM NaCl, 10 mM imidazole pH 7.6, 2 mM PMSF added prior to use |
| H300 wash buffer | As for H300 lysis buffer but with 20 mM imidazole |
| H300 elution buffer | As for H300 lysis buffer but with 250 mM imidazole |
| H150 lysis, wash buffers | As for H300 but with 150 mM NaCl instead of 300 mM |
| H500 elution buffer | As for H300 but with 500 mM NaCl instead of 300 mM |
| GST elution buffer | As for H300 lysis buffer but with 25 mM reduced glutathione |
| TMN-150 lysis buffer | 10 mM Tris-HCl pH 7.6, 5 mM $MgCl_2$, 150 mM NaCl |
| Alkaline lysis buffer | 0.2 NaOH, 0.2 % β-mercaptoethanol |
| 2 x Protein loading buffer | 160 mM Tris-HCl (pH 6.8), 10 % β-mercaptoethanol, 2 % SDS, 10 % glycerol |
| 5 x Protein loading buffer | 400 mM Tris-HCl pH 6.8, 25 % β-mercaptoethanol, 5 % SDS, 25 % glycerol |
| Tris-Glycine SDS running buffer (1 x TGS) | 25 mM Tris, 192 mM glycine, 0.1 % (w/v) sodium dodecyl sulphate |
| Coomassie Blue stain | 40 % ethanol, 10 % acetic acid, 0.1 % (w/v) Coomassie Brilliant Blue G250 |
| Destain solution | 20 % ethanol, 10 % acetic acid |
| Western transfer buffer | 0.5 x TGS, 20 % methanol, 0.1 % SDS |
| TBS (Tris-buffered saline) | 10 mM Tris-HCl (pH 7.4), 150 mM NaCl |
| Western blocking solution | 10 % (w/v) skimmed milk powder (sigma) dissolved in TBS |
| ECL solution I, 4°C | 100 mM Tris-HCl pH 8.7, 2.5 mM luminol, 400 µM p-coumaric acid |
| ECL solution 2, 4°C | 100 mM Tris-HCl pH 8.7, 5.4 mM $H_20_2$ |
| RNA binding buffer (filter binding) | 10 mM Tris-HCl pH 8, 150 mM NaCl, 10 % glycerol, 2 mM $MgCl_2$, 0.1 mM EDTA |

### 2.1.3 Yeast Strains, media and supplements

Media for cultivation of budding yeast *Saccharomyces cerevisiae* (Table 2.4) were prepared with Millipore water and autoclaved before use. Antibiotics were filter-sterilised and added to the cooled medium before pouring. For agar plates 2 % bacto-agar was added to the medium prior to autoclaving. *S. cerevisiae* strains were grown in suitable media shaking at 30 °C unless otherwise indicated. Strains were stored on slants at 4 °C for several months or supplemented with 25 % glycerol for long-term storage at -80 °C.

***Table 2.4 Yeast media and supplements***

| | |
|---|---|
| **YPD** | 2 % bacto-peptone, 1 % yeast extract, 2 % glucose |
| **YPGal** | 2 % bacto-peptone, 1 % yeast extract, 2 % galactose |
| **Minimal Synthetic Defined (SD) base** | 0.17 % yeast nitrogen base, 0.5 % ammonium sulphate,<br>2 % glucose or galactose or raffinose, amino acids were added as required from 100 x stocks (see below) |
| **YPD, YGal, SD agar** | 2 % (w/v) bacto-agar added to medium |
| **5'-FOA Agar** | 5'-Fluoro-orotic acid dissolved in DMSO was added to a final concentration of 1 mg/ml to autoclaved minimal SD base agar |

| **Amino Acids** (100 x stock in $H_2O$, -20 °C) | **mass per litre (g/l)** |
|---|---|
| Adenine hemisulfate, pH was neutralised with NaOH<br>Arginine monohydrochloride<br>Histidine monochloride<br>Methionine<br>Tryptophan<br>Uracil | 2 |
| Lysine monohydrochloride<br>Tyrosine, pH was neutralised with NaOH | 3 |
| Leucine | 6 |
| Phenyalanine | 5 |
| Threonine | 20 |

| **Antibiotics** | **Final concentration** |
|---|---|
| Geneticin (G418) | 200 µg/ml |
| Hygromycin B | 200 µg/ml |

***Table 2.5 Yeast strains used and generated in this study***

| ***Strain*** | ***Description/Genotype*** | ***Source/Reference*** |
|---|---|---|
| *BMA38* | *MATa/Matα ade2-1/ade2-1 his3-Δ200/his3-Δ200 leu2-3, 112/leu2-3, 112 trp1-1/trp1-1 ura3-1/ura3-1 can1-100/can1-100* | *Laboratory Stock, Baudin et al. 1993* |
| *P575* | *Haploid of BMA 38; Mata ade2-1 his3-Δ200 leu2-3,112 trp1-1 ura3-1 can1-100* | *Laboratory Stock* |
| *P364* | *Mata his3Δ1 leu2Δ0 met15Δ0 ura3Δ0, BY 4741 TAP-tagged strain background.* | *Open Biosystems, Mortimer and Johnston 1986* |
| | *Matα his3Δ1 leu2Δ0 lys2Δ0 ura3Δ0, BY 4742 TAP-tagged strain background.* | *Open Biosystems, Mortimer and Johnston 1986* |
| P158 | *rrp6Δ::TRP1* in P575 | *Laboratory Stock, Allmang et al. 1999* |
| P246 | *Mat**a** ade2-1 his3-11 leu2-3 trp1-1 ura3-52 rrp4Δ::HIS3* + pRS416[zzTEV-*rrp4*] | *Laboratory Stock, Mitchell et al. 2003* |
| P356 | *rrp47Δ::kanMX4* in P364 | *Euroscarf, University of Frankfurt* |
| P368 | *rrp47Δ::kanMX4* in P575 | *Laboratory Stock, Mitchell et al. 2003* |
| P369 | *rrp47Δ::kanMX4* in P246 + pRS416[zzTEV-*rrp4*] | *Laboratory Stock, Mitchell et al. 2003* |
| P414 | *rrp47-zz::HIS3$^{sp,}$* in P575 | *Laboratory Stock, Mitchell et al. 2003* |
| P439 | *rrp47-zz::HIS3$^{sp}$ rrp6Δ::TRP1$^{kl}$* in P575 | *Laboratory Stock, Mitchell et al. 2003* |
| P539 | *rrp6-TAP::HIS3$^{sp}$* in P364 | *Laboratory Stock, Open Biosystems* |
| P540 | *rrp6-TAP::HIS3$^{sp}$ rrp47Δ::kanMX4* in P364 | *Laboratory Stock* |
| P550 | *rex1Δ::kanMX4* in BY 4742 | *Laboratory Stock , Open Biosystems* |
| P589 | *rrp6Δ::TRP1$^{kl}$* in p246 + pRS415[zz-TEV-*rrp4*] | *Laboratory Stock* |
| P596 | plasmid shuffle strain; P368 x P550; *ade2 ade3 leu2 his3 trp1-1 ura3 can1-100 rex1Δ::kanMX4 rrp47Δ::kanMX4 + p265 (pRS416 [RRP47 URA3 ADE3])* | *Laboratory Stock, Costello et al. 2011* |
| P781 | *rrp6Δ::kanMX4* in P364 | *Euroscarf, University of Frankfurt* |
| P956 | *GAL10::rrp47* in P550 | *Laboratory Stock* |
| P957 | *GAL10::rrp47-TAP::TRP1$^{kl}$* in P575 | *R. Jones, Laboratory Stock* |
| 1095 | *erg6Δ::kanMX4* in P364 | *Euroscarf, University of Frankfurt* |

| | | |
|---|---|---|
| 1096 | *GAL10::rrp47-TAP::TRP1* $^{kl}$ *rrp6Δ::kanMX4* in P575 | *This study* |
| 1111 | *erg6Δ::kanMX4 rrp47-zz::HIS3*$^{sp}$ in P575 | *This study* |
| 1112 | *erg6Δ::kanMX4 rrp47-zz::HIS3*$^{sp}$ *rrp6Δ::TRP1* $^{kl}$ in P575 | *This study* |
| 1113 | *rrp47-GFP::kanMX4* in P575 | *This study* |
| 1114 | *rrp47-GFP::HIS5*$^{sp}$ in P575 | *This study* |
| 1115 | *rrp6Δ::TRP1 rrp47-GFP::HIS5*$^{sp}$ in P575 | *This study* |
| 1127 | *erg6Δ::hphMX4* in P364 | *This study* |
| 1160 | *rrp47-GFP::HIS5*$^{sp}$ in P364 | *This study* |
| 1161 | *rrp47-GFP::HIS5*$^{sp}$ *rrp6Δ::kanMX4* in P364 | *This study* |
| 1162 | *rrp47-GFP::HIS5*$^{sp}$ *rrp6Δ::kanMX4* in P364 | *This study* |
| 1163 | *rrp6-GFP::HIS3*$^{sp}$ in P364 | *Roche Diagnostics* |
| 1182 | *rrp6-GFP:::HIS3*$^{sp}$ *rrp47Δ::kanMX4* in P364 | *This study* |
| 1183 | *rrp6-GFP:::HIS3*$^{sp}$ *rrp47Δ::kanMX4* in P364 | *This study* |
| 1254 | *pep4Δ::kanMX4* in P364 | *Euroscarf, University of Frankfurt* |
| 1256 | *rrp47-zz::HIS3*$^{sp}$ *pep4Δ::kanMX4* in P575 *(pep4Δ* in P414*)* | *This study* |
| 1257 | *rrp6Δ::TRP1* $^{kl}$ *rrp47-zz::HIS3*$^{sp}$ *pep4Δ::kanMX4* in P575 *(pep4Δ/1* in P439*)* | *This study* |
| 1258 | *rrp6Δ::TRP1* $^{kl}$ *rrp47-zz::HIS3*$^{sp}$ *pep4Δ::kanMX4 in P575 (pep4Δ/2* in P439*)* | *This study* |
| 1259 | *rrp47Δ::hphMX4 rrp6Δ::kanMX4* in P575 | *This study* |
| 1528 | *rrp47Δ::hphMX4* in P364 | *This study* |
| 1599 | *rrp47Δ::hphMX4 rrp6Δ::kanMX4* in P364 | *This study* |

heterologous markers - His3 $^{Sp}$, His5$^{Sp}$= from *S. pombe* (Sp) and Trp1$^{Kl}$ from *K. Lactis* (kl),

drug resistance cassettes - hphMX4= resistance to hygromcin B, kanMX4= resistance to Geneticin (G418),

fusion peptides - GST (glutathione S-transferase) , His/His(6) (polyhistidine), GFP (green flurorescent protein),

zz-domain (double zinc-finger domain of protein A of *Staphylococcus aureus*), TAP – Calmodulin-bindng domain,

Tev protease site, Δ denotes a deletion or truncation

### 2.1.4 Plasmids used and constructed during this study

Plasmid backbones for this work are listed in Table 2.6. Laboratory stocks used and plasmids generated for this study are detailed in Table 2.7. and Table 2.8. For recombinant protein expression in *E. coli,* mutations were introduced into the *RRP47* genomic sequence in pRSETB (p238) and pRS314 (p262) by site-directed mutagenesis (SDM, see 2.2.10) using complementary oligonucleotide primers (e.g. o277/o278) carrying the desired mutations as listed in Tables 2.9. Point mutations were created by alanine substitutions e.g. E79A. C-terminal truncations were generated by introducing a stop codon (X) as desired e.g. I162X.

***Table 2.6 Plasmid backbones used for this study***

| **Plasmid** | **Description /Features** | **Manufacturer/ Reference** |
|---|---|---|
| **pRSET-B** *E. coli* expression vector | Allows high-level expression of proteins with an N-terminal polyhistidine tag (His6) from a bacteriophage T7 promoter in BL21(DE3) *E. coli.* | Invitrogen |
| **pGEX-6P1** *E. coli* GST fusion/ expression vector | Allows expression of proteins fused to 26 kDa glutathione S-transferase (GST) peptide with PreScission protease site. | Amersham |
| **pGEX-2T** *E. coli* GST fusion/ expression vector | Allows expression of proteins fused to 26 kDa glutathione S-transferase (GST) peptide with thrombin protease site. | GE Healthcare |
| **pBS1479** | For C-terminal TAP-tagging, Calmodulin-binding domain (CBD), TEV protease cleavage site, Protein A zz domain, ($Amp^r$, TRP1 marker *K. lactis)*. | Euroscarf/ Puig *et al.* 2001. |
| **pTL26** | For expression of genes under the inducible GAL promoter pGAL1-10 ($Amp^r$, HIS3 marker). | Euroscarf/ Lafontaine and Tollervey 1996. |
| **Yeast/E. coli shuttle vectors** | For cloning in *E. coli* and expression in yeast, selectable via specific amino acid markers and ampicillin resistance, T7 promoter, T3 promoter | Stratagene / Sikorski and Hieter 1989. |
| pRS314 | TRP1 marker, CEN6 single-copy vector | |
| pRS415 | LEU2 marker, CEN6 single-copy vector | |
| pRS416 | URA3 marker, CEN6 single-copy vector | |
| pRS425 | LEU2 selectable, 2µ multi-copy vector | |
| pRS426 | URA3 marker, 2µ multi-copy vector | |
| **For C-terminal GFP tagging** | | |
| p536 | pFA6a-GFP.S65T-kanMX6 | Longtine *et al.* 1998 |
| p537 | pFA6a-GFP.S65T-HIS3MX6 | Longtine *et al.* 1998 |

***Table 2.7 Plasmids for recombinant protein expression in E. coli used and generated in this study***

| No. | Name | Description / Construction | Source/ Reference |
|---|---|---|---|
| p238 | Rrp47-His | *RRP47* genomic sequence in pRSET-B | Stead *et al.* 2007 |
| p245 | GST-Rrp6NT | KpnI-StuI deletion of *RRP6 in* pGEX-2T, lacks residues 212-721 of Rrp6 | Stead *et al.* 2007 |
| p247 | Rrp47 ΔC1 | as p238 but with N121PGX Stop; truncation, lacks C-terminus of Rrp47 (121-184) | Costello *et al.* 2011 |
| p272 | Rrp47 ΔC2 | as p238 but with I162X Stop, truncation, lacks basic tail of Rrp47 (162-184) | J. Stead |
| p276 | Rrp47 E79A | as p238, but with E79A point mutation, SDM using o277/o278 | J. Stead |
| p313 | Rrp47 Y55A | as p238 but with Y55A point mutation, SDM using o296/o297 | This study |
| p311 | Rrp47 F62A | as p238 but with F62A point mutant, SDM using o298/o299 | This study |
| p305 | Rrp47 Y86A | as p238 but with Y86A point mutation, SDM using o300/o301 | This study |
| p302 | Rrp47 ΔC3 | as p238 but with G181X Stop, C-terminal truncation, SDM using o310/o311 | J. Costello |
| p323 | Rrp47 R82A | as p238 but with R82A point mutation, SDM using o349/o350 | This study |
| p325 | Rrp47 K84A | as p238 but with K84A point mutation, SDM using o351/o352 | This study |
| p327 | Rrp47 K89A | as p238 but with K89A point mutation, SDM using o353/o354 | This study |
| p331 | Rrp47 K92A | as p238 but with K92A point mutation, SDM using o355/o356 | This study |
| p329 | Rrp47 N113A | as p238 but with N113A point mutation, SDM using o357/o358 | This study |
| p348 | Rrp47 S100X | as p238 but with S100X Stop, C-terminal truncation, SDM using o373/o373 | This study |
| p382 | Rrp47 V70X | as p238 but with V70X Stop, C-terminal truncation truncation using o401/o402 | This study |
| p384 | Rrp47 L80X | as p238 but with L80X Stop, C-terminal truncation using o409/o410 | This study |
| p386 | Rrp47 mm | as p238 but with multiple mutations E79A, R82G, K84I, Y86S (mm) in p238 using o407/o408 | This study |
| p437 | Rrp47 G181X mm | as p238 but with G181X Stop and multiple mutations E79A, R82G, K84I, Y86S using o407/o408 on p302 | This study |
| p526 | Rrp47 G181X N* | as p238 but with 181X Stop and mutations E79A, R82G, K84I, Y86S, K89M, K91I using o537/o538 on p437 | This study |
| p528 | Rrp47 N* | as p238 but with multiple point mutations E79A, R82G, K84I, Y86S, K89M, K91I using o537/o538 on p386 | This study |

To generate yeast expression plasmids, standard molecular cloning techniques (see 2.2) were used including site-directed mutagenesis (SDM, see 2.2.10), PCR amplification of genomic or plasmid sequences (see 2.2.9) and cut-and-paste methods using restriction enzymes (see 2.25).

***Table 2.8 Yeast plasmids generated and used for this study***

| No | Name | Details/Construction | Source/ Reference |
|---|---|---|---|
| p44 | pRS416 with pRRP4, zz-tag | vector for expression of N-terminal zz-tagged fusion proteins from an *RRP4* promoter | P.Mitchell |
| p236 | Rrp47 wt in pRS416 | *RRP47* genomic wild-type allele from W303-1A | P. Mitchell |
| P248 | Rrp47 I162X in pRS416 | as p236 but with I162X Stop, lacks basic tail (162-184) of Rrp47 | J. Stead |
| p260 | zz-Rrp6ΔNT in p44 | as p263, but lacking *RRP6* N-terminus (Δ1-213) | P. Mitchell |
| p262 | Rrp47 wt in pRS314 | as p236, but *RRP47* gene in pRS314 (SacI-XhoI) | R. Jones. |
| p263 | zz-Rrp6 in p44 | *RRP6* wild-type genomic sequence in p44 (EcoRI-HinDIII) | Allmang *et al*. 1999 |
| p265 | Rrp47:: ADE3 in pRS416 | as p236 but with ADE3 gene (BamHI-XbaI) blunt end cloned into XhoI site of p236 | R. Jones |
| p274 | Rrp47 ΔC2 in pRS416 | as p236 but with I162X Stop, Rrp6 C-terminal truncation, SDM using o275/o276 | J. Stead |
| p285 | zz-Rrp6NT1 in p44 | as p263 but with P176X Stop,Rrp6 C-terminal truncation, SDM using o255/o256 | J. Stead |
| p287 | zz-Rrp6NT2 in p44 | as p263 but with L197X Stop,Rrp6 C-terminal truncation, SDM using o257/o258 | J. Stead |
| p289 | Rrp47 E79A in pRS314 | as p262 but with E79A point mutation, SDM using o277/o278 | J. Stead |
| p293 | Rrp47 ΔC1 in pRS314 | as p262 but with 121PGX Stop, lacks C-terminal region (121-184) of Rrp47, (from p274 XhoI-SacI) | This study |
| p295 | Rrp47 ΔC2 in pRS314 | as p262 but with I162X Stop, lacks basic tail (162-184) of Rrp47, (from p248 XhoI-SacI) | This study |
| p319 | Rrp47 Y55A in pRS314 | as p262 but with Y55A point mutation, SDM using o296 /o297 | This study |
| p317 | Rrp47 F62A in pRS314 | as p262 but with F62A point mutation, SDM using o298 /o299 | This study |
| p315 | Rrp47 Y86A in pRS314 | as p262 but with Y86A point mutation, SDM using o300 /o301 | This study |
| p322 | zz-*RRP6* in pRS426 | *zz-rrp6* allele with *RRP4* promoter (from p263 ClaI-SacI) | R. Jones |

| | | | |
|---|---|---|---|
| p338 | Rrp47 R82A in pRS314 | as p262 but with R82A point mutation, SDM using o349 /o350 | This study |
| p340 | Rrp47 K84A in pRS314 | as p262 but with K84A point mutation, SDM using o351/o352 | This study |
| p342 | Rrp47 K89A in pRS314 | as p262 but with K89A point mutation, SDM using o353/o354 | This study |
| p346 | Rrp47 K91A in pRS314 | as p262 but with K91A point mutation, SDM using o355/o356 | This study |
| p344 | Rrp47 N113A in pRS314 | as p262 but with N113A point mutation, SDM using o357/o358 | This study |
| p350 | Rrp47 S100X in pRS314 | as p262 but with S100X Stop, C-terminal truncation using o373/o374 | This study |
| p352 | Rrp47 F142A in pRS314 | as p262 but with K89A point mutation, SDM Rrp47 point mutation F142A in p262 using o332/333 | J. Costello |
| p354 | Rrp47 130X in pRS314 | as p262 but with I130X Stop, C-terminal truncation using o324/o325 | J. Costello |
| p356 | Rrp47 T140X in pRS314 | as p262 but with T140X Stop, C-terminal truncation using o326/327 | J. Costello |
| p358 | Rrp47 S150X in pRS314 | as p262 but with S150X Stop, C-terminal truncation using o328/329 | J. Costello |
| p362 | Rrp47 F135A in pRS314 | as p262 but with F135A point mutation, SDM using o330/331 | J. Costello |
| p376 | Rrp47 V70X in pRS314 | as p262 but with V70X Stop, C-terminal truncation, SDM using o401/402 | This study |
| p378 | Rrp47 L80X in pRS314 | as p262 but with L80X Stop, C-terminal truncation, SDM using o409/o410 | This study |
| p380 | Rrp47 mm in pRS314 | as p262 but with multiple mutations E79A, R82G, K84I, Y86S (mm), SDM using o407/o408 | This study |
| p389 | *zz-rrp6.1* in p44 | as p263 but with catalytically inactive *rrp6.1* allele (D238N), SDM using o366/o367 | P. Merothra |
| p390 | *pRRP4/RRP6* in pRS416 | as p263, but zz tag deleted, *RRP6* gene with *RRP4* promoter in pRS416 | P. Merothra |
| p409 | Rrp47 L60X in pRS314 | as p262 but with L60X Stop, C-terminal truncation, SDM using o429/430 | This study |
| p411 | Rrp47 I50X in pRS314 | as p262 but with I50X Stop, C-terminal truncation, SDM using o431/0432 | J. Costello |
| p413 | Rrp47 L40X in pRS314 | as p262 but with L40X Stop, C-terminal truncation, SDM using o433/0434 | J. Costello |
| p417 | Rrp47 NTΔ2-9 in pRS314 | as p262 but with N-terminal deletion of Rrp47 (Δ2-9) by two-step PCR using o437 /o158 and o439 | J. Costello |
| p419 | Rrp47 NTΔ2-19 in pRS314 | as p262 but with N-terminal deletion of Rrp47 (Δ2-19) by 2-step PCR using o438 /o158 and o439 | J. Costello |
| p427 | *zz-RRP6* in pRS314 | *zz-rrp6* allele with RRP4 promoter (XhoI-SacI from p263) | P. Merothra |
| p429 | *zz-rrp6.1* in pRS314 | as p427, but with catalytically inactive *zz-rrp6.1* allele (XhoI-SacI from p389) | P. Merothra |
| p436 | *RRP6* in pRS416ΔKpn1 | *RRP6* genomic sequence cloned Xba1-EcoR1 in pRS416 ΔKpn1 (Vent polymerase, o457/o458) | R. Jones |

| | | | |
|---|---|---|---|
| p448 | *rrp6.1* in pRS416ΔKpnI | as p436 but with catalytically inactive *rrp6.1* allele (D238N point mutation), SDM using o336/o337 | R. Jones |
| p449 | *rrp6ΔNT* in pRS416ΔKpn1 | as p436 but with *rrp6ΔNT* allele, lacks Rrp6 N-terminal region (1-213), deletes *RRP6* ORF to KpnI | R. Jones |
| p452 | Rrp47-N* in pRS314 | as p262 but with mutations E79A,R82G, K84I, Y86S, K89M, K91I, SDM on p380 using o537/o538 | R. Jones |
| p494 | *pRRP4/zz-RRP6* in pRS424 | *zz-rrp6* allele with RRP4 promoter in pRS424 (XhoI-SacI from p322) | M. Turner |
| p495 | *pRRP4/zz-rrp6.1* in pRS424 | as p494 but with *zz-rrp6.1* catalytically inactive allele (D238N), (XhoI-SacI from p389) | M. Turner |
| p496 | *rrp6ΔNT* in pRS424 | as p494 but lacks Rrp6 N-terminal region (Δ1-213), (XhoI-SacI from p449) | M. Turner |
| p503 | *RRP6* in pRS426 | *RRP6* wild-type sequence in multi-copy vector (CalI-SpeI from p390) | M. Turner |
| p513 | *rrp6ΔNT* in pRS314 | Rrp6 N-terminal deletion, (XhoI-SacI from p449) | M. Turner |
| p530 | *NEL025c* in pRS425 | PCR of NEL025c gene using o636/o637, cloned BamHI-SalI into pRS425 | This study |
| p532 | *NEL025c* in pRS426 | as p532 but cloned into pRS426 | This study |
| p538 | *rrp6NT* in pRS416ΔKpnI | Rrp6 truncation 197X Stop in p436 using o257/o258. | This study |
| p540 | pRRP4/zz-rrp6NT in pRS424 | Rrp6 truncation 197X Stop in p494, using o257/o258 | This study |
| p552 | *RRP6* in pRS314 | *RRP6* genomic clone (XhoI/SacI from p436) | M. Turner |
| p553 | *RRP6* in pRS424 | *RRP6* genomic clone (XhoI/SacI from p436) | M. Turner |
| p622 | *zz-RRP47* in p44 | *RRP47* genomic clone with N-terminal zz-tag and RRP4 promoter (using o818/o159) | P. Mitchell |
| p625 | *rrp6ΔC* in pRS416ΔKpnI | as p436 but with P523X Stop, Rrp6 C-terminal truncation, SDM using o812/o813 | This study |
| p627 | *zz-rrp6ΔC* in pRS416 | as p263 but with P523X Stop, Rrp6 C-terminal truncation, SDM using o812/o813 | This study |
| p631 | Rrp47 G181X mm in pRS314 | as p262 but with G181X Stop and mutations E79A, R82G, K84I, Y86S, SDM on p380 using o310/o311 | This study |
| p632 | Rrp47 G181X N* in pRS314 | as p262 but with mutations E79A, R82G, K84I,Y86S, K89M, K91I, SDM on p452 using o310/o311 | This study |
| p645 | *RRP6* in pRS416 ΔKpnI ΔCEN | *RRP6* genomic clone in PRS416 with CEN sequence deleted by two-step PCR on p436 using o839/o840 and o841/o842 to introduce Hpa1 sites 5' and 3' of CEN, digested Hpa1 and religated | This study |
| p651 | *rrp6.1* in p645 | as p645 but with cataytically inactive *rrp6.1* allele (D238N) (from p448 XhoI-SpeI) | This study |
| p652 | *rrp6ΔNT* in p645 | as p645 but with Rrp6 N-terminal deletion (Δ1-213) ( from p449 XhoI-SpeI) | This study |
| p653 | *rrp6NT1* in p645 | as p645 but with Rrp6 197X Stop, Rrp6 N-terminal truncation (from p538 XhoI-SpeI) | This study |
| p654 | *rrp6ΔC* in p645 | as p645 but with Rrp6 P523X Stop, Rrp6 C-terminal truncation (from p625 XhoI-SpeI) | This study |

### 2.1.5 Oligonucleotides

Purified and dephosphorylated oligonucleotides used for this for this work were obtained from Operon (Eurofins MWG Operon, Ebersberg, Germany). Oligonucleotides were diluted from 100 µM stocks to a working concentration of 5 µM in DEPC-$H_2O$ (or 2 µM for SDM) and stored at -20 °C. The sequences of oligonucleotides used in this study are listed in 5' to 3' direction in Tables 2.9 SDM primers, 2.10 PCR and qPCR primers and 2.11 primers for Southerns and northerns.

***Table 2.9 Oligonucleotide primer pairs designed and used for SDM***

| Mutation | No. | Sequence | Plasmid No. |
|---|---|---|---|
| Rrp6 P176X | o255_F<br>o256_R | ttgatgatgatgaaaataactagtgtcactacccccatccttatg<br>cataaggatgggggtagtgacactagttattttcatcatcatcaa | p285 |
| Rrp6 L197X | o257_F<br>o258_R | caagagtatagtccaggaatctagaaaattagagaggagattccc<br>gggaatctcctctctaattttctagattcctggactatactcttc | p287 |
| Rrp47 I162X | o275_F<br>o276_R | gacagtaccgatcactagtggaaagcaagtagtaag<br>cttactacttgctttccactagtgatcggtactgtc | p248, p272, p274, p295 |
| Rrp47 E79A | o277_F<br>o278_R | tgtctcctatactcggggccctgaaaagagta<br>tactcttttcagggccccgagtataggagaca | p276, p289 |
| Rrp47 Y55A | o296_F<br>o297_R | taatcgttacgcggctgtattgagctctctgatgtttg<br>caaacatcagagagctcaatacagccgcgtaacgatta | p313, p319 |
| Rrp47 F62A | o298_F<br>o299_R | cgtatgtattgagctctctgatggctgctaatatgaaag<br>ctttcatattagcagccatcagagagctcaatacatacg | p311, p317 |
| Rrp47 Y86A | o300_F<br>o301_R | aaaagagtaaaatcagccatggataaggctaaac<br>gtttagccttatccatggctgattttactctttt | p305, p315 |
| Rrp47 G181X | o310_F<br>o311_R | ataaagttggaaaaaagaaatgatatcagaagtagaggtcgacg<br>cgtcgacctctacttctgatatcatttctttttttccaactttat | p302, p631, p632 |
| Rrp47 I130X | o324_F<br>o325_R | caattcgagccctcttagagctcgagcaactttcaaggga<br>tcccttgaaagttgctcgagctctaagagggctcgaattg | p354 |
| Rrp47 T140X | o326_F<br>o327_R | tttcaagggaagcattagagctctgaaaacgatgaact<br>agttcatcgttttcagagctctaatgcttcccttgaaa | p356 |
| Rrp47 S150X | o328_F<br>o329_R | cgatgaactggcagagtagagctcgactaagattattga<br>tcaataatcttagtcgagctctactctgccagttcatcg | p358 |
| Rrp47 F135A | o330_F<br>o331_R | cctctataagcaggagtaatgcccaagggaagcatacga<br>tcgtatgcttcccttgggcattactcctgcttatagagg | p362 |
| Rrp47 F142A | o332_F<br>o333_R | agggaagcatacgaaggccgagaacgatgaactggcaga<br>tctgccagttcatcgttctcggccttcgtatgcttccct | p352 |
| Rrp47 R82A | o349_F<br>o350_R | ctcggcgaactgaaggccgtaaaatcatacatgg<br>ccatgtatgattttacggccttcagttcgccgag | p323, p338 |
| Rrp47 K84A | o351_F<br>o352_R | ggcgaactgaaaagggtcgcatcatacatggataagg<br>ccttatccatgtatgatgcgacccttttcagttcgcc | p325, p340 |
| Rrp47 K89A | o353_F<br>o354_R | aaatcatacatggacgccgccaaacaatacgataatag<br>ctattatcgtattgtttggcggcgtccatgtatga ttt | p327, p342 |
| Rrp47 K91A | o355_F<br>o356_R | catggataaggccgcgcaatacgataatagg<br>cctattatcgtattgcgcggccttatccatg | p331, p346 |
| Rrp47 N113A | o357_F<br>o358_R | agagcaagaaaaagcgaaggcgatcatttccaatgttttg<br>caaaacattggaaatgatcgccttcgctttttcttgctct | p329, p344 |

| | | | |
|---|---|---|---|
| Rrp47 S100X | o373_F<br>o374_R | aataggataaccaaatagatctaaaaatcgcaggcagagc<br>gctctgcctgcgatttttagatctatttggttatcctatt | p348, p350 |
| Rrp47 V70X | o401_F<br>o402_R | gaaagtcctaggctagcaagatatgtctcc<br>ggagacatatcttgctagcctaggactttc | p376, p382 |
| Rrp47 mm | o407_F<br>o408_R | cctatactcg gcgcactgaaaggagtaatatcatccatggataagg<br>ccttatccatggatgatattactcctttcagtgcgccgagtatagg | p380, p386, p437 |
| Rrp47 L80X | o409_F<br>o410_R | cctatactcggcgaatagatctgagtaaaatcatacatgg<br>ccatgtatgattttactcagatctattcgccgagtatagg | p378, p384 |
| Rrp47 L60X | o429_F<br>o430_R | cgcgtatgtattgagttcttagatctttgctaatatgaaagtcc<br>ggactttcatattagcaaagatctaagaactcaatacatacgcg | p409 |
| Rrp47 I50X | o431_F<br>o432_R | gagggctaaattagaactctagaatcgttacgcgtatgta<br>tacatacgcgtaacgattctagagttctaatttagccctc | p411 |
| Rrp47 L40X | o433_F<br>o434_R | ggatgaacagctgttgctctagactgatgagagggctaaa<br>tttagccctctcatcagtctagagcaacagctgttcatcc | p413 |
| Rrp47 N* | o537_F<br>o538_R | agtaatatcatcgatggatatggctatacaatacgataatagg<br>cctattatcgtattgtatagccatatccatcgatgatattact | p452, p526, p528 |
| Rrp6ΔC P523X | o812_F<br>o813_R | ggaagctactcccatttgagctcccgagaccaaagcagacg<br>cgtctgctttggtctcgggagctcaaatgggagtacgttcc | p625, p627, P654 |
| CEN 5' Hpa | o839_F<br>o840_R | gttggcgatccccctagagtcgttaacatcttcggaaaacaaaaactat<br>atagtttttgttttccgaagatgttaacgactctagggggatcgccaac | p645 |
| CEN 3' Hpa | o841_F<br>o842_R | aattatttttatagcacgtgatgttaacgacccaggtggcacttttcgg<br>ccgaaaagtgccacctgggtcgttaacatcacgtgctataaaaataatt | p645 |

***Table 2.10 Oligonucleotide PCR and qPCR primers used in this study***

| Name | No. | Sequence | Use/ used to generate |
|---|---|---|---|
| Rrp47_F<br>Rrp47_R | o158<br>o159 | cacgaattctcgtgcagt<br>gttaagcttgaagggttt | p417/p419 |
| Rrp47_5' Xho1_F<br>Rrp47_3' SacI_R | o191<br>o192 | aaactcgaggaactgactactga<br>aaagagctcaaactttcgctgg | Screening of Rrp47 mutants |
| Rrp47[2-9]_F | o437 | ttgaaaaactcctaacgtacattactgatctaatact | p417 |
| Rrp47[2-20]_F | o438 | tatttctggtttcagctccattactgatctaatact | p419 |
| Rrp47_R | o439 | tacgtcgacctctactt | p417, 419 |
| Rrp6_F<br>Rrp6_R | o457<br>o458 | cagtctagacttcgagatgagcttg<br>gctgggcccacctcagtattacagc | P1161, P1599 |
| KANMX4/HYG_F<br><br>KANMX4/HYG_R | o506<br><br>o507 | cgtacgctgcaggtcgacggatccccgggttaattaaggcgcg cgaagcttcgtacgctg<br>atcgatgaattcgagctcgttttcgacactggatggcggcgtat catcgatgaattcgag | P1528, P1599 |
| KANMX4_F<br>KANMX4_R | o508<br>o509 | cgtacgctgcaggtcgac<br>atcgatgaattcgagctcg | P1528, P1599 |
| RRP47 GFP_F<br><br>RRP47 GFP_R | o518<br><br>o519 | gattggataaagttggaaaaaagaaaggagggaagaagcgg atccccgggttaattaa<br>aaccctataagcatttttgcatttgtgctctcacatcaccgaattc gagctcgtttaaac | P1113, P1114, P1115 |
| NEL025c_5'BamH1<br>NEL025c_3'SalI | o636<br>o637 | catggatccatatgctgtctttaagcc<br>catgtcgacgaacgtaacgacttttcc | PCR NEL025c p530, p532 |
| RRP6_F<br>RRP6_R | o650<br>o651 | tggcttcagcgagatttagg<br>gcggtcttatacgccagtca | qPCR |

| | | | |
|---|---|---|---|
| SCR1_F<br>SCR1_R | o654<br>o655 | gagagtccgttctgaagtgtcc<br>cctaaggacccagaactaccttg | qPCR |
| ERG6 +500_F<br>ERG6 -500_R | o664<br>o665 | gatcagcaaaatttaggg<br>ttgaaaagcacatgccg | P1111/P1112 |
| ERG6 +1 kb_F<br>ERG6 -1 kb_R | o668<br>o669 | gccatcacgtgtacca<br>gtaacagtacatgggga | Screening |
| RRP47_F<br>RRP47_R | o701<br>o702 | ctcctatactcggcgaactgaa<br>tcccttgaaagttgctcctg | qPCR |
| ALG9_F<br>ALG9_R | o744<br>o745 | gtttaatccgggctggttc<br>cccagtggacagatagcgtag | qPCR |
| TCF1_F<br>TCF1_R | o748<br>o749 | ctgatagcgacggatccaag<br>tgaccgactcatctctgaagg | qPCR |
| PEP4_F<br>PEP4_R | o782<br>o783 | cttgagctcctcaattgtat<br>acgatgaagttgatcgtaca | P1256, 1257, 1258 |

***Table 2.11 Oligonucleotide probes used in this study (Southerns and northerns)***

| Name | No. | Sequence | Use |
|---|---|---|---|
| 5.8S | o221 | gcgttgttcatcgatgc | Northern probe for 5.8S rRNA |
| ITS2-5' | o222 | tgagaaggaaatgacgct | Northern probe for 5.8S+30, 7S |
| 5.8S | o236 | gcgttgttcatcgatgc | Northern probe for 5.8S |
| ITS2 | o237 | tgagaaggaaatgacgct | Northern probe for 5.8S+30, 7S |
| U14 | o238 | tcactcagacatcctagg | Northern probe for U14 |
| U18 | o239 | atatattatctgtctcctc | Northern probe for U18 |
| snR13 | o240 | caccgttactgatttggc | Northern probe for snR13 |
| SCR1 | o242 | aaggacccagaactaccttg | Northern probe for SCR1 |
| snR44 | o241 | catgggattaaatatcccgg | Northern probe for snR44 |
| U24 | o270 | tcagagatcttggtgataat | Northern probe for U24 |
| snR38 | o272 | gagaggttacctattattacccattcag acagggataactg | Northern probe for snR38-3' |
| 5'ETS | o274 | cgctgctcaccaatgg | Northern probe for 5'ETS |
| 5S | 5S | ctactcggtcaggctc | Northern probe for 5S |
| snR52 | o318 | gtatcagagattgttcacgctaatg | Northern probe for snR52 |
| pre-tRNA-Arg3 | o339 | agaaacaaagcactcacgat | Northern probe |
| 18S | o405 | catggcttaatctttgagac | Northern probe |
| 25S | o406 | ctccgcttattgatatgc | Northern probe |
| U3 | o443 | ttcggtttctcactctggggtac | Northern probe |
| snR30 | o444 | gaagcgccatctagatg | Northern probe |
| snR50 | o494 | ctgctgcaaattgctacctc | Northern probe |
| U6 | o517 | atctctgtattgtttcaaattgaccaa | Northern probe |
| NEL025c | o809 | ggcttctacagaacaagttgtatcgaa atgattgttggcgac | Northern probe |
| P523X probe | o814 | cccatttgagctcccgag | Southern probe |
| CEN6Δ seq | o843 | ttcttaggacggatcgcttg | Southern probe |
| R82A_F | o359 | aactgaaggccgtaaaa t | Southern probe |
| K84A_F | o360 | aaaagggtcgcatcatac a | Southern probe |
| K89A_F | o361 | ggacgccgccaaac | Southern probe |
| K91A_F | o362 | taaggccgcgcaatac | Southern probe |
| N113A_F | o363 | agcgaaggcgatcatt t | Southern probe |

### 2.1.6 Antibodies

Antibodies, their working dilutions in TBS and suppliers are listed in Table 2.12. Incubation was typically 2 hours for primary antibodies, followed by 1 hour for secondary antibodies at room temperature with gentle agitation on an orbital shaker. Antibodies were aliquoted and stored according to manufacturers' instructions. The abbreviations in brackets are frequently used in the text.

***Table 2.12 Antibodies used in this study***

| Name | Dilution in TBS | Supplier/ Source | 2nd antibody |
|---|---|---|---|
| ***Primary antibodies*** | | | |
| Mouse anti-penta-his (α-His) | 1:10.000 | Qiagen | RAMPO |
| Rabbit anti-Glutathione-S-Transferase (α-GST) | 1:10.000 | Sigma | GARPO |
| Peroxidase/anti-peroxidase (α-PAP) | 1:10.000 | Sigma | -- |
| α-PGK1 | 1:10.000 | Invitrogen | GAM |
| α-GFP Mouse IgG1K | 1:3.000 | Roche Diagnostics | GAM |
| α-NRD1 rabbit polyclonal antibody | 1:2.000 | Gift from D. Brow | GARPO |
| α-Rrp47 rabbit polyclonal antibody | 1:5.000 | Laboratory stock | GARPO |
| α-Importin-α (yD-18) α-SRP1 | 1:500 | Santa Cruz Biotch. Inc. | GAM |
| α-Rrp6NT rabbit polyclonal antibody | 1:5.000 | Gift from D.Tollervey | GARPO |
| | | | |
| ***Secondary antibodies*** | | | |
| Goat Anti Rabbit Peroxidase (GARPO) | 1:10.000 | Sigma | |
| Rabbit Anti Mouse Peroxidase (RAMPO) | 1:20.000 | Sigma | |
| Goat Anti Mouse (GAM) | 1:5.000 | Bio-Rad | |
| Mouse Anti Goat (MAG) | 1:5.000 | Santa Cruz Biotch. Inc. | |
| Donkey Anti-Goat (DAG) | 1:5.000 | Santa Cruz Biotch. Inc. | |

# Methods

## 2.2 *E. coli* growth and recombinant DNA techniques

### 2.2.1 Bacterial strains and growth

*E. coli* cultures were grown in LB medium at 37 °C shaking with good aeration unless otherwise stated. Antibiotics to select for plasmid carrying strains were supplemented to media from 1000 x stocks (stored at -20 °C). For long term storage, saturated cultures of transformed *E. coli* strains were supplemented to a final concentration of 17 % glycerol and stored at -80 °C.

### 2.2.2 Generating competent cells

The rubidium chloride method was used to generate "competent" *E. coli* cells to introduce plasmid DNA. A freshly grown colony of *E. coli* XL1-blue or DH5-α cells was grown in 5 ml LB over night at 37 ˚C. The overnight culture was diluted 100-fold into pre-warmed LB and grown shaking at 37 ˚C to an $OD_{595}$ of 0.48. Cells were harvested by centrifugation at 3.200 x *g* for 5 min at 4 ˚C and subsequently resuspended and incubated in 40 ml chilled Tfb1 buffer for 10 min. Cells were pelleted as before, resuspended and incubated in 5 ml TfbII buffer for 15 min. 100 µl aliquots were snap-frozen in liquid nitrogen and stored at -80°C.

### 2.2.3 Transformation of competent *E. coli*

Plasmids containing the desired DNA fragments for expression were introduced into competent *E. coli* cells by transformation. A 100 µl aliquot of competent cells was thawed on ice for 15 minutes and then incubated with 20 to 100 ng of plasmid DNA on ice for 30 minutes. Cells were then heat-shocked at 42 °C for up to 2 minutes and immediately transferred to ice again for 2 minutes. 800 µl LB was added to allow transformants to recover for 60 min at 37 °C before pelleting and plating the cells resuspended in 100 µl LB on selective medium. Plates were incubated over night at 37 °C.

### 2.2.4 Isolation of plasmid DNA from *E. coli* – "plasmid miniprep"

Single colonies of plasmid containing strains were grown in 5 ml LB broth with suitable selective antibiotic at 37 °C overnight shaking. Cells were pelleted by centrifugation at 15.000 x *g* for 1 min and the supernatant was discarded. Plasmids for SDM were purified with spin miniprep kits (DNEAZY miniprep kit I from omega bio-tek, Norcross, GA, USA) according to manufacturers' instructions. For the screening of transformants, plasmid DNA was extracted

using the alkaline lysis method (Birnboim and Doly, 1979). Cell pellets from 1.5 ml saturated overnight culture were resuspended in 100 µl alkaline lysis solution I, then 200 µl alkaline lysis solution II was added, mixed by inversion and incubated for 2 min. 150 µl cold alkaline lysis solution III was added, immediately mixed by inversion and incubated on ice for 5 min. Following centrifugation at 15.000 x *g* for 10 min, the supernatant was transferred to a new tube, mixed with an equal volume of phenol/chloroform pH 7.4 and centrifuged for 5 min at 15.000 x *g*. The aqueous phase was transferred to a new tube and DNA precipitated with 2 volumes of chilled 100 % ethanol. DNA was pelleted by centrifugation at 15.000 x *g* for 10 min and the pellet was washed twice in chilled 70 % ethanol. Pellets were air-dried, resuspended in 50 µl $H_2O$ or TE buffer and incubated with 1 µl of 1 mg/ml RNase A for 30 minutes at room temperature. Plasmid minipreps (10 % of prep) were routinely checked by restriction digest (see 2.2.5) and agarose gel electrophoresis (section 2.2.6). Plasmid DNA for laboratory stocks from sequenced plasmids was prepared from 15 ml cultures using the omega bio-tek miniprep kit II providing 100 µl stocks for storage at -80 ˚C.

### 2.2.5 DNA restriction digests

Restriction digests were performed according to enzyme manufacturer's instructions, generally in 20 to 50 µl reaction volume using < 1 µg plasmid DNA for miniprep screening or up to several micrograms of plasmid DNA for preparative digests. Products were analysed by agarose gel electrophoresis (see 2.2.6) and purified from gels (2.2.7) for cloning as required.

### 2.2.6 DNA agarose gel electrophoresis

DNA was analysed by agarose gel electrophoresis. Gels were prepared by dissolving 0.5 to 2 % agarose in 0.5 x TBE adding 1 µl of 10 mg/ml ethidium bromide solution per 100 ml of agarose. Samples were prepared with 6 x DNA loading buffer. The 1 kb ladder (Fermentas) was routinely used as a molecular weight marker. Gels were run in 0.5 x TBE running buffer at 75 volts in a Mini-Sub Cell GT Agarose Electrophoresis system (Bio-Rad, Munich, Germany). The DNA was visualised using a UV transilluminator.

### 2.2.7 Purification of DNA from agarose gels

Following electrophoresis, DNA fragments were excised from agarose gels under UV light and recovered using a gel extraction kit (omega bio-tek) according to manufacturer's instructions. DNA was eluted in 30 µl of the provided elution buffer or in $H_2O$ for sequencing. 10 % of the purified DNA was routinely checked on a 1 % agarose gel (see Section 2.2.6.).

### 2.2.8 DNA dephosphorylation and ligation

Digested vector DNA was dephosphorylated using shrimp alkaline phosphatase (SAP) to prevent re-ligation. Typically, 1 µl (1U) of SAP was added to a 50 µl restriction digest, incubated at 37 °C for 60 min and subsequently inactivated by heat denaturation at 80 °C for 15 min. The digested and dephosphorylated vector and insert DNA were run out on an agarose gel and purified after electrophoresis as described above in 2.2.7. The insert DNA was used for ligation with approximately 3 molar excess compared to the vector.

**Typical ligation reaction:**

~200 ng dephosphorylated vector DNA
insert DNA
2 µl 10 x T4 ligase buffer
1 µl T4 DNA ligase (1 U, Promega)
$H_2O$ to final volume of 20 µl

The ligation reaction was incubated over night at 4 °C. Another 1 µl of T4 DNA ligase was added to the ligation mix and incubated at room temperature for a further 4 hours. 10 µl of the ligation reaction was transformed into competent *E. coli* XL-1 or DH5α cells (see 2.2.3).

### 2.2.9 Polymerase chain reaction (PCR)

DNA sequences for cloning and screening of mutants were routinely amplified by polymerase chain reaction (PCR) using Taq polymerase (GoTaq®, Promega). Primers were diluted from 100 µM stocks to 5 µM working dilutions before use.

**Typical PCR reaction:**

| | |
|---|---|
| 26.5 µl | $ddH_20$ |
| 10 µl | 5 x GoTaq® buffer |
| 5 µl | 2 mM dNTP mix |
| 5 µl | 25 mM$MgCl_2$ |
| 1 µl | forward primer |
| 1 µl | reverse primer |
| 1 µl | (10 ng) of template DNA |
| 0.5 µl | GoTaq® polymerase (2.5 U) |

**Typical thermo-cycler settings:**

| | | | |
|---|---|---|---|
| Initial: | 98 °C | 2 min | |
| Denaturing: | 98 °C | 30 s | x 30 |
| Annealing: | 45-55 °C | 1 min | |
| Extension: | 68-72 °C | 1 min/kb | |
| Final: | 68-72 °C | 10 min | |

The amplified DNA products were analysed on agarose gels and if required, excised and purified as described in section 2.2.7 or using a PCR clean up kit (omega bio-tek) according to manufacturer's instructions.

### 2.2.10 Site-directed mutagenesis (SDM)

In order to generate specific mutations, amino acid substitutions or protein truncations, the Quikchange™ Site Directed Mutagenesis Kit (Stratagene/Agilent Technologies) was used according to manufacturer's instructions (Papworth *et al.* 1996). SDM of Rrp47 was mainly performed on two plasmids containing the ORF of Rrp47, the protein expression vector p238 and the *E. coli*/yeast shuttle vector p262 (see table 2.7 and table 2.8). For SDM on Rrp6, plasmids containing full-length Rrp6 (p436) and TAP-tagged Rrp6 (p263) were used. For each mutant two complementary oligonucleotide primers were designed which contained the desired mutations encoding amino acid substitutions or introducing a stop codon to generate truncations at the required position. For ease of screening candidates, restriction sites were introduced downstream of the new stop codons. SDM reactions were performed in 25 µl rather than 50 µl volume as specified by the manufacturer.

**Reaction mix: (25 µl)**

15 µl $H_2O$
2.5 µl 10 x reaction buffer
1.5 µl plasmid DNA (50-100 ng)
2.5 µl forward primer (2 µM stock)
2.5 µl reverse primer (2 µM stock)
0.5 µl dNTP mix
0.5 µl *Pfu* Turbo DNA polymerase (2.5 U / µl)

**Thermocycler parameters:**

| | | |
|---|---|---|
| 95 °C | 30 s | |
| 95 °C | 30 s | x 18 |
| 55 °C | 1 min | |
| 68 °C | 12 min | |
| 68 °C | 10 min (final extension) | |

Following amplification, the SDM reaction was incubated with 1 µl *Dpn*I (10 U) for 1 hour at 37 °C to digest the parental plasmid. 10 to 15 µl of the reaction mix were transformed into competent *E. coli* cells as described in section 2.2.3, except the heat-shock at 42 °C was reduced to 90 seconds. Transformants were screened by restriction digest or Southern blotting (see 2.2.11) with a complementary radio-labelled oligonucleotide probe. Positive candidates were confirmed by sequencing using appropriate primers (Source Bioscience, Nottingham, UK).

### 2.2.11 Southern blotting

In order to analyse electrophoretically separated DNA with specific probes, the DNA was transferred from the gel to Hybond N+-membrane (GE Healthcare Life Sciences, Bucks., UK) using the 'turboblot' procedure (Southern 1975). Gels were first soaked in 0.4 M NaOH for 15 min with gentle agitation for denaturing of the DNA, followed by 15 min in neutralisation buffer and a further 15 min wash in 10 x SSPE transfer buffer. The gel was then placed on a Hybond-N+ membrane pre-soaked in 10 x SSPE on a stack of paper towels. A wick connected to the elevated transfer buffer tank was placed on top of the gel and weighted for transfer over night in 10 x SSPE. After transfer, the DNA was cross-linked to the membrane using 1200 joules/$cm^2$ UV light at a distance of 10 cm. The Southern blot was then pre-hybridised immediately or stored saran-wrapped at -20 °C.

### 2.2.12 Labelling of short oligonucleotides (Maniatis *et al.* 1982)

For the detection of specific DNA or RNA sequences on Southern and northern blots, short complementary oligonucleotides were designed (5 µM working dilutions) and radio-labelled at their 5' hydroxyl group with γ[$^{32}$P]-ATP (Perkin Elmer, Mass., USA) using polynucleotide kinase (invitrogen).

**Typical 5' end labelling reaction**:

14 µl DEPC-$H_2O$
1 µl oligonucleotide (5 pmoles/µl)
2 µl Kinase buffer
1 µl Polynucleotide Kinase (PNK 10 U/ml))
2 µl [γ -$^{32}$P]ATP (~6 pmol total)

Reactions were incubated at 37 °C for 30 min, heat-inactivated at 65 °C for 5 min and mixed with 1 ml hybridisation buffer before passing through a 0.2 µM filter into 50 ml hybridisation buffer. Probes were stored after heat-inactivation or dilution in hybridisation buffer at -20 °C for re-use.

### 2.2.13 Southern/northern hybridisation with radio-labelled oligonucleotide probes

For analyses of membranes from Southern (DNA) and northern (RNA) transfers with 5' end labelled probes, the cross-linked membranes were pre-hybridised for 1 hour at 37 °C in hybridisation buffer with gentle agitation. The diluted 5' end labelled oligonucleotide probe (see above) was then filtered into the hybridisation buffer and incubated overnight at 37 °C with gentle agitation. The filter was then washed three times for 1 minute in 6 x SSPE and a fourth wash was left gently shaking at 37 °C for 15 minutes to remove all non-specifically bound material. Filters were dried and saran-wrapped for visualisation by autoradiography using MS film (Kodak, Kodak Ltd., Herts., UK) or phopshor imaging using phosphor storage screens (Kodak) and a Personal Molecular Imager FX (Bio-Rad). Exposure time to screen or film was adjusted according to the strength of the signal, typically between 4 and 16 hours at room temperature. Phosphor imaging screens were bleached under white light for 20 min before use. Non-saturated images were analysed using the ImageJ64 software (NIH). Oligonucleotide probes used for Southern and northern hybridisations are listed in Table 2.11.

## 2.3 Expression of recombinant proteins in *E. coli*, purification and analyses

### 2.3.1 Expression of recombinant proteins in *E. coli*

Recombinant proteins were over-expressed in *E. coli* strain BL21(DE3)pLysS cells transformed with plasmids containing the required gene to produce the desired protein or peptide. Single colonies of successful transformants selected on LB agar plates supplemented with the appropriate antibiotics (typically LBAC) were used to inoculate 5-10 ml LB starter cultures and grown over night to saturation. The starter cultures were diluted 100-fold into 0.5-1 litre pre-warmed medium and grown at 37 °C with agitation to 0.5 $OD_{600}$ before induction with IPTG at a final concentration of 0.5 mM. Cells were grown for a further 4 hours at 37 °C and harvested by centrifugation at 4.200 x *g* for 15 min. Cell pellets were lysed or frozen for storage at -80 °C.

### 2.3.2 Preparation of *E. coli* cell extracts

Cell pellets from *E. coli* expression cultures were thawed on ice if used from frozen and completely resuspended in chilled H300 lysis buffer (5-10 ml / litre cell culture). Cells were lysed by sonication with a MSE Soniprep 150 Sonicator (MSE Ltd, London, UK) using 10 cycles of 15 seconds sonication at 10 µm with 45 seconds pauses on ice. Cell lysates were clarified by centrifugation at 15.000 x *g* for 30 min at 4 °C and stored at -20 °C.

### 2.3.3 Two-step purification of His-tagged Rrp47 constructs from *E. coli* cell lysates

Recombinant His-tagged Rrp47 protein was purified from *E. coli* cell lysates in a two-step procedure, first by immobilised metal affinity chromatography (IMAC) using nickel-nitriloacetic acid agarose beads (Ni-NTA agarose, QIAGEN, protocol according to manufacturers' instructions) and then further purification of the protein via ion exchange chromatography (IEC) using SP sepharose (Amersham, Amersham Biosciences, New Jersey, USA). Disposable poly-prep columns (Bio-Rad) were loaded with 0.5 ml of resuspended Ni-NTA agarose and equilibrated with 10 ml of H300 lysis buffer. 5-10 ml clarified cell lysate from 1 litre expression culture was filtered (0.2 µm) onto the column and the flow-through was reloaded twice before washing 3 x with 10 ml H300 wash buffer. Bound protein was eluted using 1 ml H300 elution buffer containing 250 mM imidazole. For the subsequent IEC the eluate was diluted 10-fold into H300 lysis buffer to reduce the imidazole concentration and allow binding to SP sepharose beads. 0.25 ml of SP sepharose beads were equilibrated in H300 lysis buffer in a poly-prep column and the diluted eluate was passed three times through the column before washing 3 x in 10 ml H300 wash buffer to remove non-bound material. Bound proteins were eluted by

resuspending the SP sepharose beads in 0.5 ml H600 for 5 min before collecting the eluate. The purity and yield of protein were checked by Bradford assay (see 2.3.5), SDS-PAGE (described in 2.3.6) and western analysis (see 2.3.7). The purified protein could be stored at -80 °C for several weeks.

Rrp47 truncation mutants were purified by IMAC using Ni-NTA beads as described above, but dialysed into H150 buffer over night for IEC, rather than diluted with H300 buffer. Truncations which shorten the protein to less than 120 amino acid residues and remove most of the positive charge could not be bound to SP sepharose and were therefore only passed over the SP sepharose column after dialysis and collected as flow-through with some impurities removed.

### 2.3.4 Purification of GST-tagged recombinant proteins from *E. coli* cell lysates

GST-tagged proteins were purified from *E. coli* lysates, essentially as described in Smith and Johnson 1988. 10 ml clarified lysate was mixed with 0.5 ml glutathione sepharose 4B beads (GE Healthcare) pre-equilibrated in H150 lysis buffer for 2 hours with agitation. Non-bound material was removed by successive washes in 10 ml H150 wash buffer followed by centrifugation at 1.500 x *g* for 5 min. To elute bound material, 0.5 ml H150 GST elution buffer containing 25 mM glutathione was added and mixed for 15 min before collecting the supernatant.

### 2.3.5 Determination of protein concentration

The total protein concentration of a sample was routinely determined using either direct absorption at 280 nm or the Bradford assay (Bradford 1976). The Bradford assay was used to estimate protein concentrations by comparison with a BSA standard curve generated using known concentrations of BSA from 0.1 to 5 µg. 1 ml of Bradford assay solution (Bio-Rad) was mixed with 5 µl of protein solution and left for 1 min to develop, followed by measurement of absorption at 595 nm in a spectrophotometer. Alternatively, the concentration of purified protein samples was determined by direct UV absorption at 280 nm. For purified protein the concentration was calculated using the protein specific extinction coefficient ($E_{280}$) (Edelhoch 1967; Pace *et al.* 1995) using the formula:

$E_{280}$ ($M^{-1}$ $cm^{-1}$) = (#Tryptophan residues*5500) + (#Tyrosine residues*1490) + (#Cysteine residues*125)

The $E_{280}$ of recombinant Rrp47-His with 6 Tryosine residues was estimated to be 8940 $M^{-1}$ $cm^{-1}$. The protein concentration in mg/ml is then calculated as [Protein] (mg/ml) = $A_{280}/(E_{280}$(cuvette path length in cm)).

### 2.3.6 SDS-polyacrylamide gel electrophoresis (SDS-PAGE) of proteins

Proteins were routinely resolved and analysed by SDS-PAGE (Shapiro *et al.* 1967) using gels with acrylamide (37:1) concentrations ranging from 8 to 16 %. Prior to loading, samples were denatured in protein loading buffer at 90 °C for 5 min. Gels were run in 1 x TGS buffer using the Mini-Protean® Cell electrophoresis system (Bio-Rad) at 75 volts, increasing to 125 volts once the dye-front reached the resolving gel. The Precision Plus *Protein All Blue standard* (Bio-Rad) was routinely used as molecular weight marker (10-250 kDa). To visualise proteins after SDS-PAGE, gels were stained using Coomassie brilliant blue stain (Neuhoff *et al.* 1988) followed by de-staining as required or Instant Blue Coomassie colloidal stain (Expedeon, Harston, Cambridgeshire). Alternatively, the resolved proteins were transferred onto membranes for western analysis using protein-specific antibodies (2.3.7).

### 2.3.7 Western blotting

Following SDS-PAGE, proteins were transferred from gels to Hybond-C nitrocellulose membrane (GE Healthcare) over night at 15 volts in western transfer buffer using a HSI, TE Series Transphor Electrophoresis Unit (HSI, Hoefer Scientific Instruments, San Francisco, USA). After transfer, membranes were washed in TBS, stained in Ponceau S solution for 5 min to visualise the protein, photographed or labelled as required; blots were washed in TBS again and then blocked in 10 % skimmed milk powder in TBS for 1 hour. Membranes were washed again three times for 5 min in TBS before adding the primary antibody diluted in TBS at the required concentration for 2 hours. Membranes were then washed with TBS three times for 5 min and if required, incubated with the appropriate secondary antibody coupled to horseradish peroxidase (HRP) for 1 hour. After another final three washes in TBS, equal volumes of ECL solutions 1 and 2 were mixed and applied to the membrane for 1 min. Membranes were then wrapped in saran wrap for exposure to chemiluminescent film (Kodak) and film processing using a Compact X4 Developer (XOgraph, XOgraph Imaging Systems Inc., Gloucs., UK). Alternatively, ECL membranes were analysed using a G:Box iChemi XL system (Syngene). Details of antibodies and concentrations used are detailed in Table 2.12.

### 2.3.8 RNA-protein filter binding assays (slot blot assay)

RNA binding by recombinant proteins was analysed using a modified double-filter binding assay (Wong and Lohman 1993) using a MiniFold® II slot-blot apparatus (Schleicher & Schuell Inc., NH, USA). Strips of Hybond-N+ and Hybond-C were pre-soaked in 1 x RNA binding buffer. In a vacuum chamber, the Hybond-C membrane which retains protein and protein-bound RNA was placed on top of the Hybond-N+ membrane which retains all unbound RNA. Purified recombinant proteins were two-fold serially diluted in RNA-binding buffer generally starting at 20 µM protein. Triplicate 20 µl aliquots were mixed with 5 µl of $^{32}$P-labelled RNA substrate (50 cps, final concentration, 10 nM). After 15 min incubation on ice, the reaction mixtures were applied to the slots and vacuum-filtered through the double membranes. Slots were washed 3 times with 0.5 ml RNA binding buffer and left to dry before dismantling the apparatus and analysing the filters by autoradiography or using a phosphor imager (see 2.2.13) to allow quantification. Exposure times for the membranes were estimated using a Geiger counter, typically 16 hours overnight. Screens were scanned at a resolution of 100 µm and then analysed using ImageQuant v2.0 software (GE Healthcare). For quantification, background was deducted using a suitable reference point on the membrane. Bands were measured and the mean of the triplicate samples was calculated. Background binding of radio-labelled substrate to Hybond-C was taken into account by subtracting the mean count for the RNA-only control from the other experimental values. Values were then plotted as the percentage of signal detected on Hybond-C (protein-bound RNA) with respect to the total count on both membranes relative to the total protein concentration of the incubation mixture.

Uniformly $^{32}$P-labelled SLAU RNA (ggguuuccuucucaaacauucuguuugguagugaguaauuaaaaa ugaauu) was kindly provided by J. Stead generated by *in vitro* transcription from an EcoRI-linearised plasmid using T7 RNA polymerase. Yeast tRNAPhe (Sigma) was dephosphorylated and 5'-labelled as described (2.4.8).

### 2.3.9 UV cross-linking of RNA and protein

Two step-purified Rrp47 protein (10 µM, app. 5 µg) was incubated in 1 x Hepes binding buffer with app. 5 ng dephosphorylated 5' $^{32}$P-labelled tRNAPhe (sigma) or *in vitro* transcribed SLAU RNA (see above) in 20 µl reaction volume. Samples were irradiated with UV light on ice at 254 nm with 400 mJ/cm$^2$ four times at a distance of 10 cm with agitation in between. Following irradiation, 1 µg of RNase A was added and samples were incubated for 20 minutes at 37 ˚C. Reaction products, as well as irradiated protein-only controls, were supplemented with an equal volume of 2 x SDS loading buffer and resolved by 10 % SDS-PAGE. Gels were fixed in acetic acid and stained with Coomassie Blue to visualise relative levels of protein input; gels were then dried and RNA-protein cross-linked complexes, as well as non-bound $^{32}$P-RNA were analysed by autoradiography.

## 2.4 Yeast molecular biology techniques

### 2.4.1 Yeast growth, growth curves and spot growth plates

For growth rate analyses, pre-cultures were diluted into 50 ml pre-warmed medium to a starting $OD_{600}$ of 0.1 or above. OD was measured every 2 h or as appropriate and plotted on a logarithmic scale (log10) against time. For spot growth assays, serial 10-fold dilutions in $H_2O$ were prepared from freshly grown cultures with adjusted/equalised starting $OD_{600}$ and 4 µl of each dilution were spotted onto the appropriate solid medium plates and grown for 2 to 5 days at the required temperature.

### 2.4.2 Yeast transformation

Yeast transformations were performed using either a colony transformation protocol for plasmid DNA or a high efficiency protocol for chromosomal integration of PCR fragments (Gietz *et al.* 1992). For plasmid transformations, freshly growing colonies of the recipient strain were harvested and washed in 1 ml sterile TE buffer. Cells were pelleted by centrifugation at 13.000 x *g* for 15 s and resuspended in 1 ml LiT buffer before pelleting again. Cells were resuspended in 50 µl LiT buffer per transformation and mixed with 1 µl of the required plasmid DNA (~1 µg) and 5 µg of herring sperm carrier DNA (10 mg/ml, Roche). After 15 min at room temperature, 100 µl of sterile-filtered, freshly made 40 % PEG-4000 in LiT buffer was added and the mixture was incubated at room temperature for 30 min. Then, 15 µl of DMSO was added prior to a heat-shock at 42 °C for 15 min. Cells were then pelleted by centrifugation for 30 s, washed with 1 ml 1 x TE buffer, pelleted again and resuspended in 100 µl TE buffer and plated on appropriate selective medium.

For genomic integration of DNA fragments by homologous recombination, a high efficiency transformation protocol was used, harvesting cells in early log phase of growth. 50 ml cultures of the recipient strain were grown in appropriate medium to an $OD_{600}$ of 0.5 to 1.0 and harvested by centrifugation at 3.200 x *g*. Cells were successively washed in 5 ml TE buffer and 5 ml LiT buffer and then resuspended in 0.5 ml LiT buffer. For each transformation 100 µl cell suspension was used and mixed with 100 ng of DNA fragment (e.g. gel purified PCR product) and 5 µg of herring sperm DNA. After 15 min at room temperature, 300 µl of sterile-filtered, freshly made 40 % PEG-4000 in LiT buffer was added and the mixture was incubated at room temperature for 30 min. As before, 50 µl of DMSO was added prior to a heat-shock at 42 °C for 15 min. Cells were then pelleted by centrifugation for 30 s, washed with 1 ml 1 x TE buffer, pelleted and resuspended in 100 µl TE buffer and plated on appropriate selective medium. Where selecting for a G418 or hygromycin resistance, cells were initially plated and grown up on YPD for 2 to 3 days to allow expression of the resistance gene before replica plating on YPD plates containing G418 or hygromycin.

### 2.4.3 Genomic DNA extraction from yeast

Yeast genomic DNA for PCR analysis and amplification of DNA fragments was extracted using a method adapted from Cryer *et al*. 1975. 10 ml of yeast culture grown to saturation in appropriate medium was harvested by centrifugation at 3.200 x *g* for 5 min. Pellets were washed in 0.5 ml sterile water, transferred to a 1.5 ml microfuge tube and pelleted again before resuspension in 200 µl cell breaking buffer. 200 µl glass beads and 200 µl phenol/chloroform pH 7.4 were added and cells were vortexed for 5 min. 200 µl TE buffer was added, vortexed briefly and cell remnants were pelleted via centrifugation at 15.000 x *g* for 5 min. The supernatant was transferred to a new 1.5 ml microfuge tube and DNA was precipitated with 2 volumes cold 100 % ethanol for 15 min before centrifugation at 15.000 x *g* for 15 min. The supernatant was discarded and the pellet dissolved in 400 µl TE buffer. The prep was then incubated with 30 µl RNase A (1 mg/ml) at 37 °C for 30 min to remove RNA and DNA and was re-extracted with an equal volume of phenol-chloroform. The supernatant was precipitated by adding 135 µl 7.5 M $NH_4Ac$, and an equal volume of isopropanol at room temperature. The DNA was pelleted at 15.000 x *g* for 5 min, the supernatant was discarded, the pellet resuspended in 100 µl TE buffer. The isopropanol precipitation was repeated three times. The pellet was finally washed with 70 % ethanol, allowed to air-dry and resuspended in 50 µl TE buffer. The yeast genomic DNA (1 µl) was routinely analysed on an agarose gel.

### 2.4.4 RNA extraction from yeast

Total RNA was extracted from yeast cells using an adapted protocol of the hot phenol method (Maniatis *et al.* 1982, Tollervey and Mattaj 1987). 50 ml of yeast culture was grown in appropriate medium to 0.5 $OD_{600}$. Cells were harvested by centrifugation at 3.200 x *g* for 10 min at 4 °C. Pellets were either frozen for storage at -80 °C or lysed immediately by vortexing for 5 minutes with 1 ml sterile DEPC-treated glass beads, 0.5 ml of GTC mix and 0.5 ml of phenol pH 4.5. Another 1.5 ml of GTC mix and 1.5 ml of phenol were added, briefly vortexed, heated to 65 °C for 10 min and cooled on ice. 2 ml chloroform and 1 ml NaAc mix were added and mixed. Following centrifugation at 3.200 x *g* for 5 min at 4 °C, the aqueous phase was transferred to a new tube and re-extracted with an equal volume of phenol/chloroform at 3.200 x *g* for 5 min at 4 °C. The RNA contained in the aqueous phase was precipitated with 2 volumes of 100 % ethanol at -80 °C for 1 to 16 hours and then pelleted by centrifugation at 3.200 x *g* for 30 min at 4 °C. Pellets were washed twice in 70 % ethanol, air-dried for 10 minutes, resuspended in 100 µl DEPC-treated $H_2O$ and stored at -80 °C.

RNA concentration was determined by diluting 5 µl of the sample into 800 µl DEPC-treated water and measuring the absorbance at 260 nm and 280 nm. RNA concentration was calculated assuming a specific absorbance of 1 $A_{260}$ / 40 µg. An $A_{260}/A_{280}$ ratio of > 1.7 was taken as being of efficient purity. Values for $A_{260}$ were multiplied with a conversion factor of 6.4 to obtain the concentration of the RNA in µg/µl and the RNA was routinely analysed on denaturing polyacrylamide gels (5 µg) or on agarose gels (10 µg RNA samples) depending on size.

### 2.4.5 RNA polyacrylamide and agarose gel electrophoresis

Depending on type and size of the RNA of interest, total RNA was resolved on 6 to 15 % denaturing acrylamide gels to detect smaller RNA species and on 0.8 - 2 % agarose gels to visualise larger RNAs like mRNAs or RNAs > 15 S. Polyacrylamide gel solutions were prepared with 50 % (w/v) urea and 19:1 acrylamide: bisacrylamide in 0.5 x TBE. Samples were routinely prepared containing 5 µg of RNA in DEPC-$H_2O$ with 2 x RNA loading buffer in 8 µl final sample volume and denatured at 65 °C for 10 min prior to loading. Gels were run over night at 90 to 160 V in 0.5 x TBE and then stained in 100 ml 0.5 x TBE containing 2 µl of a 10 mg/ml ethidium bromide solution for 10 min to visualise the main RNA species on a UV transilluminator before proceeding to northern blot transfer as required. Agarose gels were prepared using 1 to 2 % agarose in 1 x MOPS buffer. Samples were prepared containing 10 µg of RNA in DEPC-$H_2O$ in 3 x RNA glyoxal loading buffer containing ethidium bromide and run in 1 x MOPS buffer at 30 V for 6 hours.

### 2.4.6 Transfer of RNA onto nitrocellulose filters (northern blotting)

For further analyses, RNA separated by gel electrophoresis was transferred onto nitrocellulose filters (Hybond-N+, GE Healthcare) by northern blotting (Alwine *et al.* 1977). For polyacrylamide gels, transfer was performed overnight at 15 volts in 0.5 x TBE buffer. RNA agarose gels were soaked in 75 mM NaOH for 15 min followed by 15 minutes in neutralisation buffer and 15 minutes in 2 x SSPE with gentle agitation. RNA from agarose gels was then transferred using the turboblot method as described in Southern blotting (section 2.2.11) but using 2 x SSPE for the transfer. After transfer, membranes were cross-linked using 1200 joules UV light at a distance of ~ 10 cm and pre-hybridised as described for Southerns or saran-wrapped and stored at -20 C.

### 2.4.7 Radio-labelling probes and northern hybridisation

For northern analyses, labelling reactions and hybridisations were performed as described for Southerns in 2.2.11 and 2.2.12. For successive hybridisations of the same membrane with different probes, blots were stripped by incubating in 100 ml boiling stripping solution for 30 min before adding the new probe. Oligonucleotide probes used for northern hybridisation to detect specific RNA species are listed in 5' to 3' direction in Table 2.11.

### 2.4.8 Dephosphorylating and radiolabelling tRNA

For use in filter binding assays, 50 µg tRNA-Phe (sigma, 1mg/ml) was treated with 10 U Alkaline Phosphatase (AP, Roche) for 1 hour at 50 °C. RNA was recovered by phenol-chloroform extraction and ethanol precipitation. The RNA was fractionated on a 10 % polyacrylamide urea gel, excised and extracted by soaking the gel slice over night shaking in extraction buffer (10 mM Tris pH 7.6, 1 mM EDTA pH 8, 100 mM NaCl, 0.1 % SDS). After centrifugation at 3.200 x *g* the aqueous phase was transferred to a new tube, RNA extracted with phenol-chloroform and precipitated with 100 % ethanol. The pellet was taken up in 50 µl DEPC $H_2O$ and RNA (5 µg/ml) was diluted 4-fold to 5 pmol/µl for 5'-end labelling as described in 2.4.7. After a final phenol-chloroform extraction, 1 µl glycogen was added for ethanol precipitation over night at -20 °C. The RNA was pelleted at 15.000 x *g*, air dried and diluted as required for filter binding to approximately 50 cps.

### 2.4.9 Real-Time quantitative PCR (RT-qPCR)

For quantitative analyses of steady state mRNA levels, yeast strains were grown in 50 ml appropriate medium to 0.5 $OD_{600}$. Total RNA was extracted using the hot-phenol GTC method as described (2.4.4) and 100 µg RNA was purified using the RNeasy miniprep kit (Qiagen) following the manufacturer's RNA clean up protocol. To test the integrity of the RNA, 5 µg samples were resolved through a 1 % agarose gel, stained with ethidium bromide and visualised by UV. 10 µg RNA were treated with 1 µl DNase I (Roche) in a 20 µl reaction volume for 30 minutes at 25 °C, followed by heat inactivation of the enzyme for 10 minutes at 65 °C. Reverse transcription (cDNA synthesis) was performed in triplicate on 2 µg DNase I treated RNA (cDNA synthesis kit, Bioline Reagents Ltd, UK) using random hexamer primers, according to the manufacturer's protocol. qPCR primers were designed with a Tm of 60 °C using the qPCR settings of the Primer3Plus server (http://www.bioinformatics.nl/cgi-bin/primer3plus, Untergasser *et al.* 2007) and checked for specificity by BLAST search (Lopez *et al.* 2003). Primer specificity was further confirmed in a test PCR run with the appropriate cDNAs.

The best of at least three primer pairs designed and analysed per gene was used for RT-qPCR. cDNAs were diluted 10-fold in RNase free $H_2O$ and 4 µl were added to 6 µl of a master-mix containing the appropriate primers and 5 µl 2 x SensiMix™ SYBR kit (Bioline Ltd., UK) according to manufacturer's instructions. RT-qPCR was performed in triplicate 10 µl reaction mixtures in a Corbett Rotor-Gene cycler (RotorGene™, Qiagen) using a '3-Step with Melt' protocol: initial polymerase activation for 10 minutes at 95 °C followed by 45 cycles of 15 s denaturation at 95 °C, 15 s annealing at 60 °C and 25 s extension at 72 °C. RT-PCR reactions were analysed with the associated RotorGene 6000 software v1.7 using comparative quantitation analysis (comparative CT method*,* Schmittgen *et al.* 2008*)* to normalise *RRP47* and *RRP6* mRNA levels against the reference gene *SCR1* and two validated qPCR reference genes *TCF1/ALG1* (Teste *et al.* 2009). Data from at least three replicate experiments were pooled and displayed in bar graphs with error bars representing the positive and negative ranges of the standard error of the means from at least three independent experiments.

## 2.5 Expression and purification of recombinant yeast proteins

### 2.5.1 Preparation of yeast cell lysates

Native yeast cell extracts were prepared as described in Mitchell *et al.* 1996. Strains were grown in appropriate media to an $OD_{600}$ 1-2 and harvested by centrifugation at 4.200 x *g* for 5 min. Cell pellets were either washed in TMN-150 and stored at -80 °C or resuspended in an equal volume TMN-150 and PMSF was added to 1 mM. An equal volume of sterile glass beads (Sigma) was added and the cells were lysed by vortexing 10 times for 30 s with 1 min pauses on ice. Lysates were then clarified by centrifugation at 15.000 x *g* for 30 min and transferred to a new tube. Lysates were either used immediately or were mixed with glycerol to a final glycerol concentration of 8.6 % and stored for several weeks at -80 °C.

For quantitative western analyses, cell lysates were prepared under strictly denaturing conditions using an alkaline lysis protocol (Motley *et al*. 2012). 10 OD freshly grown cells were harvested (10 ml at 1 $OD_{600}$) by centrifugation at 3.200 x *g* for 5 min. Pellets were either frozen for storage at -80 ˚C or immediately lysed on ice by complete resuspension in 500 µl ice-cold NaOH/SDS lysis buffer and incubation for 10 minutes on ice. Protein was then precipitated by adding 40 % trichloracetic acid (TCA, final 10 %) and incubating for 10 minutes on ice followed by centrifugation at 15.000 x *g* for 5 min. Pellets were then resuspended in 10 µl Tris pH 9.4 and 90 µl of 2 x SDS loading buffer were added. Samples were denatured for 5 min at 90 ˚C and centrifuged for 1 min at 15.000 x *g* before loading 10 µl (equivalent to 1 OD harvested sample) on an SDS-PAGE gel.

For quantification, generally three independent experiments were performed with triplicate samples resolved by SDS-PAGE and analysed by western blotting using an appropriate antibody and an internal control (Pgk1). For ECL imaging a G:Box iChemi XL system (Syngene) was used and bands were quantified using the associated GeneTools software. Values were adjusted against the internal control Pgk1 and relative values were plotted onto a graph using Microsoft Excel. Error bars were added to represent the positive and negative ranges of the standard errors of the means from at least two independent experiments.

### 2.5.2 Purification of TAP-tagged proteins expressed in yeast

Native yeast cell extracts from strains expressing TAP-tagged proteins were prepared as described in section 2.5.1. The purification protocol was adapted from Rigaut *et al.* 1999 and Puig *et al*. 2001. 1 ml of lysate was mixed with 50 µl of IgG Sepharose (GE Healthcare) equilibrated in TMN-150 buffer and bound for 2 hours at 4 °C with gentle agitation. Flow through was collected and the beads were washed extensively in TMN-150 buffer. Bound Proteins were eluted with 50 µl 0.5 M acetic acid and eluates were subsequently lyophilised.

### 2.5.3 Co-immunoprecipitation of TAP-tagged yeast proteins using IgG-Sepharose

Yeast strains expressing TAP-tagged protein were grown to 1 $OD_{600}$ in 500 ml appropriate medium and harvested by centrifugation at 3.200 x *g* for 10 minutes at 4 ˚C. Yeast native cell lysates were prepared as described (2.5.1) with 2 x 500 µl extractions using lysis buffer supplemented with the serine protease inhibitor phenylmethylsulfonyl fluoride (PMSF, final concentration 1 mM) and the protein concentration was then determined through direct UV absorption at $A_{280}$. Extracts from a 500 ml culture were pooled and loaded onto a polyprep column (Bio-Rad) charged with 250 µl IgG Sepharose beads equilibrated with TMN-150 lysis buffer and bound for 2 hours rotating at 4 ˚C. The flow-through fraction was collected and columns were washed 5 times with 10 ml lysis buffer. Bound proteins were eluted twice for 5 minutes with 500 µl 0.5 M acetic acid. Samples were lyophilised, resuspended in 1 ml $H_2O$ and lyophilised again to remove traces of acetic acid. Samples were finally taken up in 90 µl $H_2O$ and 10 µl 2 x SDS-PAGE loading buffer, denatured for 5 minutes at 90 ˚C and analysed by western blotting using appropriate antibodies (see Table 2.12).

### 2.5.4 Pull-down of TAP-tagged yeast proteins on recombinant Rrp47-His

Polyhistidine-tagged recombinant Rrp47 was purified on Ni-NTA agarose beads (20-50 µl), as described (first step in section 2.3.3). The beads were then washed successively in 10 ml of H300 wash buffer, followed by 10 ml H300 wash buffer with 0.1 % NP-40, and 10 ml TMN-150 binding buffer. Beads were then mixed with 0.5 ml lysate from a yeast strain expressing the TAP-tagged protein of interest and 0.5 ml TMN-150 binding buffer and left to bind for 2 hours at 4 °C with gentle agitation. After binding the supernatant was removed and the beads were washed five times with 1 ml TMN-150 buffer containing 0.1 % NP-40 for 10 minutes. As required, beads were incubated with DNase I, micrococcal nuclease or RNase A (Sigma) in lysis buffer appropriately supplemented with $CaCl_2$ (50 µl incubation volume) and then rewashed. Bound proteins were then eluted by adding 50 µl H300 elution buffer containing 250 mM imidazole and incubating the mixtures on ice for 15 minutes. Eluates were mixed with 50 µl 2 x SDS loading buffer and heat-denatured at 90 °C. Samples were resolved by SDS-PAGE followed by western blotting using the peroxidase/antiperoxidase (PAP) antibody (Sigma).

### 2.5.5 Translation shut-off assay / protein stability assay

Protein stability was assessed in translation shut-off experiments using the protein synthesis inhibitor cycloheximide (Sigma). Strains were grown in appropriate medium to an $OD_{600}$ of 0.5 in 300 ml cultures at 30 ˚C. 10 OD cells (20 ml) were harvested by centrifugation at 3.200 x *g* for 5 min marking the zero time point and cycloheximide was added to 100 µg/ml final concentration from a 10 mg/ml stock in 50 % ethanol. 10 OD cells were then harvested at 10 minute intervals after cycloheximide addition over a period of 80 minutes. Samples were prepared by alkaline lysis (2.5.1), 1 OD was resolved by SDS-PAGE and analysed by western blotting with a protein- or tag-specific antibody, followed by anti-Pgk1 as internal control.

### 2.5.6 Localisation of GFP-tagged proteins by fluorescence microscopy

Strains expressing GFP-tagged proteins or the wild-type control (P364) were grown on minimal medium to an $OD_{600}$ below 1.0. A 1 ml aliquot was collected and DNA was stained with 1 µl DAPI (4'-6-diamidino-2-phenylindole, 1 µg/ml) in $H_2O$ to reveal localisation of the cell nuclei. 5 µl of the cell suspension was then mounted on a microscopy slide and coverslipped for live-imaging using a Delta Vision RT microscope running Softworx™ version 3.2.2 (Applied Precision Instruments, Washington, USA) with a 100 x Olympus objective. Stacks of micrographs of each strain were taken with identical exposure settings using standard FITC and DAPI channels. Images were cropped, and stack projections and merged images were created using the ImageJ MacBiophotonics software package (Rasband, W.S., ImageJ, National Institutes of Health, Bethesda, Maryland, USA (http://rsb.info.nih.gov/ij/).

### 2.5.7 Glycerol gradient ultracentrifugation

In order to investigate the size distribution of proteins, yeast cell lysates expressing TAP-tagged proteins were subjected to glycerol gradient ultracentrifugation. 12 ml 10-30 % glycerol gradients were prepared in TMN-150 buffer by under-laying, using a Beckman Model 385 Gradient former (Beckman-Coulter, Beckman-Coulter (UK), Ltd, Bucks, UK). A 30 % glycerol /TMN-150 solution in the outer chamber was mixed with a 10 % glycerol/TMN-150 solution in the outlet chamber and poured into 12 ml SW41 Beckman ultracentrifugation tubes (Beckman-Coulter). Depending on protein concentration, 100 to 500 µl native cell lysate were loaded onto the top of the gradient. Ultracentrifugation was performed using a SW41 rotor at 100.000 x *g* for 36 hours at 4 °C using a Beckman-Optimer™, LE-80X, Ultracentrifuge (Beckman-Coulter). Fractions of 650 µl were taken successively from the top of the gradient and 50 µl aliquots were analysed on SDS-PAGE gels by Coomassie staining and by western blotting using an appropriate antibody. In addition to the cell lysates, a solution of 1 mg/ml of proteins of known sedimentation coefficients were similarly fractionated and resolved in parallel by SDS-PAGE to be used as size markers after visualisation by Coomassie staining. The molecular weight and S-values of each of the protein standards are shown in Table 2.13 below.

***Table 2.13 Molecular weight markers used in glycerol gradient ultracentrifugation***

| **Protein Name** | **S-value** | **MW (kDa)** | **Elution volume (ml)** | **Reference** |
|---|---|---|---|---|
| Catalase (bovine liver) | 11.3S | 250 | 9 | Rowe and Khan 1972 |
| BSA | 4.3S | 66 | 4 | Rowe and Khan 1972 |
| Ovalbumin | 3.4S | 43 | 3 | Svedberg 1934 |

### 2.5.8 Bioinformatics

Yeast gene and protein sequences were obtained from the Saccharomyces Genome Database (SGD) (http://yeastgenome.org). Rrp47 homologous protein sequences were acquired using BLAST searches (Altschul *et al.* 1990, Lopez *et al.* 2003) and alignments obtained using ClustalW (Larkin *et al.* 2007) and displayed using Jalview (Waterhouse *et al.* 2009). Protein structural prediction information was obtained from the web server Phyre2 (Kelley and Sternberg 2009). Prediction of RNA and DNA binding was obtained from the BindN web server (Wang and Brown 2006). The Pfam database was used to identify protein families and shared domains of proteins (Finn *et al.* 2008). The Mfold web server (Zuker 2003) was used to predict folding of RNA sequences, e.g. the SLAU RNA used in filter binding assays.

# Chapter Three

# Mutational analysis of the exosome co-factor Rrp47

**Tables 3.1 – 3.2**

**Figures 3.1 – 3.30**

# Chapter 3

# Mutational analysis of the exosome co-factor Rrp47

## 3.1 Introduction

The small nuclear protein Rrp47, and its human homologue C1D, have been implied in various nuclear processes such as RNA surveillance, RNA processing and degradation (Mitchell *et al*. 2003a, Peng *et al*. 2003), DNA repair (Erdemir *et al*. 2002a and b, Hieronymus *et al*. 2004) and telomere maintenance (Askree *et al*. 2004). Rrp47 co-purifies with the nuclear exosome exonuclease Rrp6 and associated yeast exosome complexes (Mitchell *et al.* 2003a), and like other exosome factors, Rrp47 is conserved throughout eukaryotes. Its human counterpart C1D also functions with the human Rrp6 homologue PM/Scl-100 in stable RNA processing pathways and both proteins have RNA- and DNA-binding activity (Stead *et al*. 2007, Schilders *et al*. 2007).

Rrp47 interacts directly with the Rrp6 N-terminal PMC2NT domain (residues 13-102) (Stead *et al*. 2007). The Rrp47-Rrp6 interaction is independent of RNA and is very stable (in salt concentrations up to at least 2 M NaCl). Rrp47 is not essential for cell viability, but strains lacking Rrp47 display similar, albeit less pronounced defects in growth and RNA processing to strains lacking Rrp6 (Mitchell *et al*. 2003a, Peng *et al*. 2003). Loss of Rrp47 in yeast strains leads to an accumulation of 3' extended RNA processing intermediates which in the presence of Rrp47 are processed to mature RNAs or degraded and therefore not detectable. These include 5.8S rRNA, snoRNAs and snRNAs, 5' ETS and ITS2 (5' external and internal transcribed spacers) and cryptic unstable transcripts CUTs (Wyers *et al*. 2005, Arigo *et al*. 2006, Milligan *et al*. 2008). However, *rrp47Δ* has a weaker, less pronounced effect on stable RNA processing compared to *rrp6Δ* and also a more moderate non-conditional growth defect compared to the temperature sensitive-lethal phenotype of *rrp6Δ s*trains (Mitchell *et al*. 2003). This indicates that Rrp6 function for optimal growth is independent of Rrp47. Mutants with deletions of both *RRP6* and *RRP47* appear like an *rrp6Δ* mutant, they do not display any additive or synergistic effects. This indicates related or cooperative functions for the two proteins in the same pathway.

Due to its association with the RNA exonuclease Rrp6, a related function for Rrp47 in RNA processing or degradation is assumed. Notably, binding of nucleic acids occurs concomitantly with Rrp6 (Stead *et al.* 2007). However, Rrp47 has no similarity to known ribonucleases and purified recombinant Rrp47 did not show exoribonuclease activity when tested on a variety of RNA substrates *in vitro* (J. Stead, unpublished data). Yet, recombinant Rrp47 has been shown to bind both RNA and DNA *in vitro* with preference for double-stranded or structured nucleic acids like tRNA or polyA-polyU stem loops over linear substrates e.g. polyA. Also, dsRNA is a

competitor to DNA binding by Rrp47 (Stead *et al.* 2007), indicating that binding is mutually exclusive, most likely because RNA and DNA compete for the same site. However, unlike characterised RNA binding proteins, Rrp47 has no known RNA binding or recognition motif and no obvious RNA sequence specificity (Butler and Mitchell 2010).

Initially, Rrp47 was thought to aid the digestion of structured RNA by increasing the retention time of Rrp6 on its substrates or by positioning the RNA 3' end close to the catalytic centre of Rrp6 (Mitchell *et al*. 2003, Butler and Mitchell 2010). However, *in vitro* RNA degradation assays have failed to show stimulation of Rrp6 activity by Rrp47 (unpublished data/communication, J. Stead and C. Lima). The data so far suggest a function for Rrp47 as a co-factor of Rrp6 in the recognition or recruitment of structured substrates, sensing RNA secondary structures rather than sequence motifs. This is supported by the observation that Rrp6 has been shown to degrade structured RNA substrates poorly *in vitro (*Liu *et al.* 2006*)*, yet the majority of known Rrp6 substrates *in vivo* are in fact structured RNAs. The 3' ends of 5.8S rRNA and snoRNA precursors which accumulate in *rrp6Δ and rrp47Δ* mutants are predicted to form imperfect double-stranded structures (Villa *et al.* 2000, Yeh *et al*. 1990). Thus the RNA binding activity of Rrp47 could be of key importance to its function as an exosome co-factor.

The aim of this study was to elucidate Rrp47 function and investigate which parts of the protein are relevant for its interactions with Rrp6 and RNA. Loss of function mutants created by *in vitro* mutagenesis were used to map critical residues and domains within Rrp47. Due to the lack of a Rrp47 3D-structure, bioinformatics analyses were employed to gain information and predictions about conservation, secondary structure and RNA binding to identify potentially critical target residues and domains for mutagenesis. Subsequently, the chosen targets were subjected to site-directed mutagenesis creating single amino acid exchanges, multiple point mutations and C-terminal truncations. The Rrp47 mutants were expressed as recombinant proteins in *E. coli* and assessed for Rrp6 and RNA binding *in vitro,* as well as expressed in yeast and tested for growth, *rrp47Δ* complementation and RNA processing defects *in vivo*. The here described mutational analysis of Rrp47 has revealed and mapped regions required for Rrp6 interaction, stable expression, normal growth, RNA binding and snoRNA processing. This study reveals that the N-terminal Sas10 domain of Rrp47 is critical for fitness and Rrp6 binding, whereas the C-terminal region specifically contributes to snoRNA processing. RNA binding assays and UV cross-linking of recombinant protein to RNA showed that both C- and N-terminus of Rrp47 contribute to RNA binding *in vitro*. Results of this study are published in Costello *et al*. 2011 and led to an ongoing cooperation with Elena Conti's laboratory (MPI, Tuebingen, Germany) where recently a 3D structure of the Rrp47ΔC-Rrp6NT complex was obtained. This complex is currently being further characterised by mutagenesis for interactions of Rrp47 and Rrp6 with other proteins.

## 3.2 Results

### 3.2.1 Bioinformatics analyses reveal functional residues and domains within Rrp47

Lacking any structural information on Rrp47, sequence analysis and bioinformatics tools were used to reveal potentially critical features and regions of interest within Rrp47 to choose as targets for mutagenesis. Information about conservation, homologies, predicted protein folding patterns and potential RNA binding sites was collected and analysed. In parallel, efforts to crystallise the protein in order to obtain an atomic resolution structure in cooperation with other labs were underway, as well as a project by another lab member to generate a library of Rrp47 mutants by error-prone PCR.

***Rrp47 has a C-terminus rich in basic residues***

Rrp47 is a small, 21 kDa protein consisting of 184 amino acids. A striking feature is the high number of basic amino acid residues within Rrp47, and particularly the highly basic C-terminus (basic residues are highlighted red in Figure 3.5A) which results in a fairly high isoelectric point of 10.39. Half of the 24 C-terminal residues (160-184) are basic amino acids, including 10 lysines (K) and 2 arginines (R). Such highly basic K/R clusters can be found in a number of proteins from bacteria and viruses involved in RNA recognition such as the tat and rev gene expression regulators (Chen and Varani 2005) or proteins involved in DNA/RNA binding as well as nucleolar localisation as documented for ribosomal proteins L22 and L7 (Houmani *et al*. 2009, Hemmerich *et al*. 1997).

***The N-terminus of Rrp47 is well conserved across species***

By directly comparing the amino acid sequences of Rrp47 homologues across different species (Fig.3.1), conserved features and domains within the protein can be identified. To generate sequence alignments, Rrp47 homologous sequences were identified by BLAST searches of the EMBL non-redundant database using WU-BLAST2 (http://dove.embl-heidelberg.de/Blast2/) (Altschul *et al*. 1990, Lopez *et al.* 2003). Alignments of the obtained sequences were created using ClustalW2 (http://www.ebi.ac.uk/clustalw/index.html) (Larkin *et al.* 2007) and displayed with Jalview (Waterhouse *et al.* 2009, Clamp *et al.* 2004). The sequence alignments indicate consensus, quality and conservation of amino acid residues across the various species. The comparison shows that the N-terminus of Rrp47, residues 1-120, contains the majority of conserved residues, many of them basic or charged.

In contrast, the C-terminus (121-184) shows less conservation or consensus across species apart from the basic cluster with a high content of lysine (K) and arginine (R) residues which is a conserved feature across species. The region 130-144 contains a number of residues conserved in yeast species but not in other eukaryotes.

Table 3.1 shows an overview of the best conserved residues within the alignment (score >5) and alternative amino acids in those positions in other species. Notably, most of the conserved residues in the very N-terminus (1-80) have hydrophobic side chains (A, I, L, M, F, Y, V), whereas most other highly conserved residues between 82-113 are basic (K, R).

| 7 | 11 | 14 | 18 | 21 | 25 | 47 | 48 | 54 | 55 | 70 | 76 | 79 | 80 | 82 | 83 | 84 | 86 | 87 | 89 | 91 | 111 | 113 |
|---|---|---|---|---|---|---|---|---|---|---|---|---|---|---|---|---|---|---|---|---|---|---|
| I<br>L<br>V | V<br>L<br>M | F<br>L<br>M | L<br>V<br>I | L<br>V<br>M | I<br>L<br>L | L<br>A<br>A | E<br>K<br>K | A<br>T | Y | V | I<br>V | E | L | R | V<br>I | K<br>R | Y | M<br>F<br>M | K<br>R | K<br>R | A | N<br>R |

**Table 3.1 Highly conserved Rrp47 residues (score >5).**
Residues of Rrp47 with their position in *S. cerevisiae* and amino acids in one letter code found in this position in other species in the alignment (in Fig. 3.1). I=Isoleucine, L=Leucine, V= valine, M=methionine, F=phenylalanine, A=alanine, E=glutamic acid, K=lysine, T=threonine, Y=tyrosine, R=arginine, N= asparagine.

**Figure 3.1 The N-terminus of Rrp47 is highly conserved across species *(See next page).***
Multiple sequence alignment of Rrp47 homologues across a range of species using BLAST to search for homologous sequences (Altschul *et al.* 1990), aligning sequences with ClustalW (Larkin *et al.* 2007) and using Jalview (Lopez *et al.* 2003, Waterhouse *et al.* 2009) for display. The *S. cerevisiae* sequence is at the bottom of the alignment with rankings (0 lowest to 9 highest) for conservation, quality and consensus of the residues given below. Conserved amino acids are depicted using the default ClustalW/Jalview colour scheme:

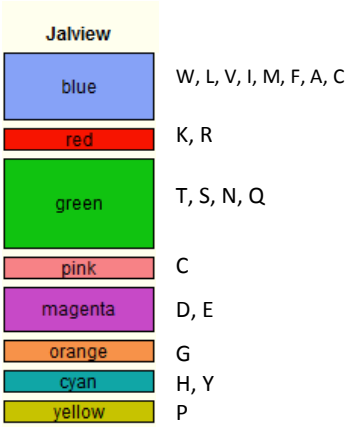

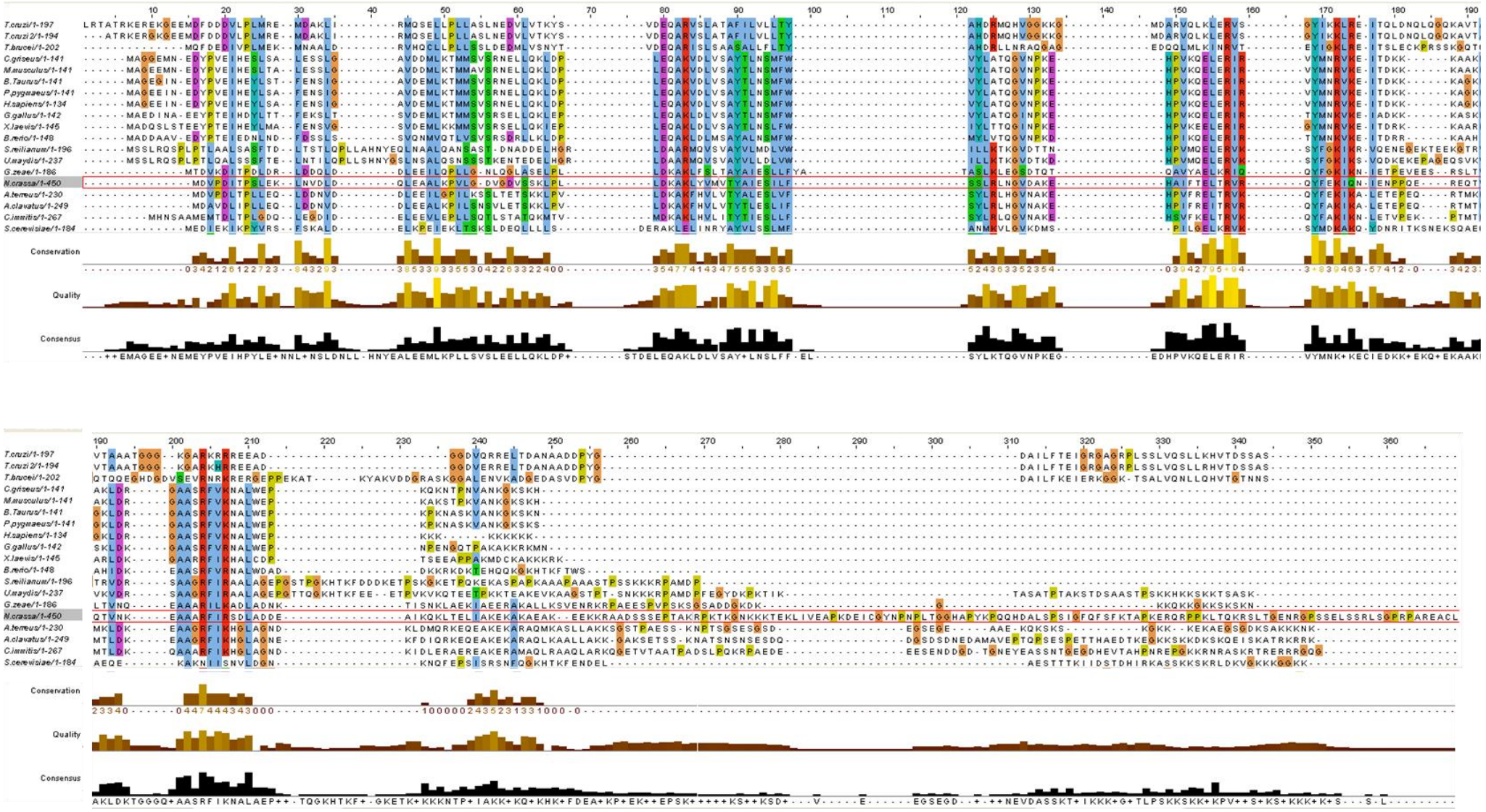


**Figure 3.1 The N-terminus of Rrp47 is highly conserved across species.**

***Rrp47 belongs to the Sas10/C1D family***

A search for Rrp47 homologues in the Pfam database (protein families database of alignments and hidden markov models; http://pfam.sanger.ac.uk/) revealed that Rrp47 belongs to the Sas10/C1D family with Pfam reference accession number PF04000 (Finn *et al.* 2008, Mitchell 2010). The so-called Sas10 domain is common to all members of this family, which include Rrp47, its human homologue C1D, as well as the Sas10/Utp3 and Lcp5 proteins required for 18S rRNA synthesis (Kamakaka *et al*. 1998, Wiederkehr *et al.* 1998, Dragon *et al.* 2002), and the mammalian protein neuroguidin, an eukaryotic initiation factor (eIF4E) binding protein (Jung *et al.* 2006). The Sas10 domain shares around 22 % average identity among its members according to Pfam. The function of this domain is as yet unknown, however, all members in this family are known to associate with RNA; the nature of this interaction, whether direct or indirect, has yet to be established (Fig. 3.2 Sas10 / C1D family). The Sas10 domain spans residues 10-89 in yeast Rrp47 and 17-96 in its human counterpart C1D. Notably, C1D which has also been shown to bind RNA and DNA is a much smaller protein with a basic C-terminus but lacking the extended C-terminal tail present in Rrp47.

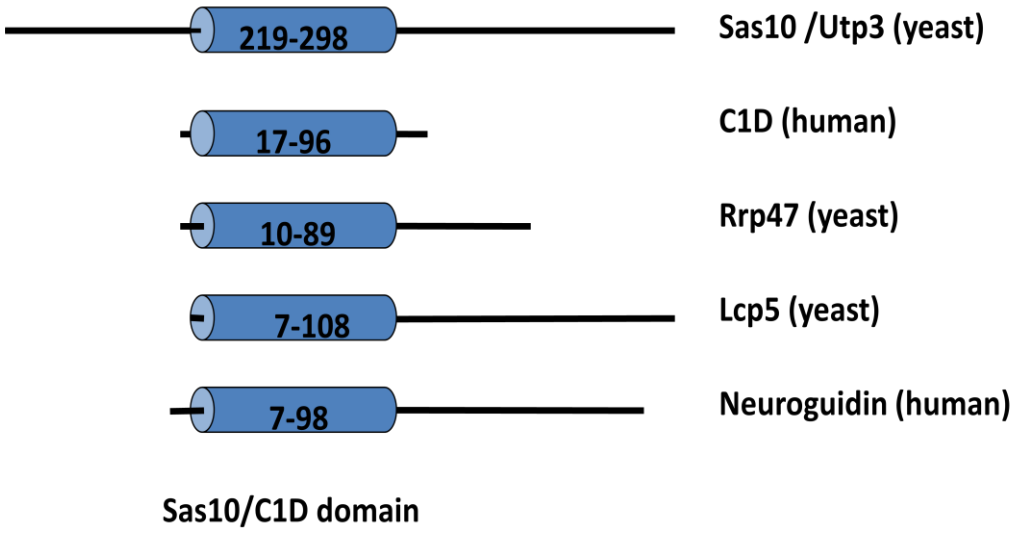


**Figure 3.2 Rrp47 belongs to the Sas10/C1D family of proteins.**
Schematic of proteins of the Sas10/C1D family and location of the Sas10/C1D homology domain in blue with amino acid residues within the protein given. The domain corresponds to Rrp47 region 10-89 and is also found in Sas10 (residues 219-298 in *S. cerevisiae* and 229-310 in humans), the human Rrp47 homologue C1D (residues 17-96), Lcp5 (residues 7-108), and neuroguidin (7-98).

***The Rrp47 N-terminus is predicted alpha-helical, the C-terminus unstructured***

Due to the lack of structural data, the Rrp47 primary amino acid sequence was entered into the 3D fold recognition server Phyre2 (http://www.sbg.bio.ic.ac.uk/phyre2; Kelley and Sternberg 2009). Although no good fit to resoled structures could be obtained, the programme provided a consensus a secondary structure prediction (Fig. 3.3). Around half (52 %) of the Rrp47 sequence is predicted to be disordered including the C-terminus (residues 120-184) with very little structural organisation. For disordered regions a secondary structure cannot be meaningfully predicted. Accordingly, the confidence for short potential helices in the C-terminus is very low. However, the prediction proposes with high confidence (cut-off value of 7) four putative alpha-helices spanning residues 4-29, 43-67, 75-91 and 108-117 at the N-terminus of Rrp47. In context, the Sas10/C1D homology domain corresponds to Rrp47 region 10-89 and contains the predicted helices 1, 2 and most of helix 3. Interestingly, in the first helix hydrophobic and hydrophilic residues alternate every 3 to 4 residues (L18, L21, K22, I25, K27, L28, K30). This amphipathic helix organisation has been implicated in functions including DNA binding and protein dimerisation (Patel and Sen 1998).


**Figure 3.3 Rrp47 contains four putative α-helices at its N-terminus.**
Rrp47 secondary structure prediction using the web server Phyre2 (Kelley and Sternberg 2009). The top row gives the *S. cerevisiae* amino acid sequence in one letter code and sequence position annotated above. The predicted secondary structure and confidence of prediction is indicated colour-coded (see key below) below. Likewise, the disorder prediction and confidence is annotated at the very bottom. A key is given for confidence, disorder and structure annotations.

***Rrp47 is predicted to bind RNA and DNA***

Similarly, to address RNA and DNA binding, the amino acid sequence of Rrp47 was entered into the BindN web-based tool for efficient prediction of DNA and RNA binding sites in amino acid sequences (Wang and Brown 2006, http://bioinfo.ggc.org/cgi-bin/bindn/bindn.pl). BindN predicts 54 residues that potentially interact with RNA at a user-defined specificity of 90 %. Notably, three clusters of RNA binding sites could be identified spanning residues 80-112, 131-141 and 162-184 of Rrp47 with high confidence (6 or higher out of 10) which could indicate RNA binding domains. 14 of the predicted binding sites lie within the Sas10 homology domain, most of them in the 80-112 cluster. Very similar results are obtained for DNA binding with an additional small cluster at the N-terminus of Rrp47 spanning residues 10-16.

```
Sequence:  MEDIEKIKPYVRSFSKALDELKPEIEKLTSKSLDEQLLLLSDERAKLELINRYAYVLSSL
Prediction:-------+---+--------------+--++------------+----------------
Confidence:998972863146242168568265746416726767998847366163574247278249

Sequence:  MFANMKVLGVKDMSPILGELKRVKSYMDKAKQYDNRITKSNEKSQAEQEKAKNIISNVLD
Prediction:--------------------++-+++--+-+-+-+--+-++++-+++-++-+-+--------
Confidence:858593777836736966376837683283726117468771878367266628724862

Sequence:  GNKNQFEPSISRSNFQGKHTKFENDELAESTTTKIIDSTDHIRKASSKKSKRLDKVGKKK
Prediction:--+-------++++-+++--+------------+--------++-+++++++-++--+++
Confidence:41611323256967286811755486763311174642243388199998993791189 9

Sequence:  GGKK
Prediction:++++
Confidence:8898
```

**Figure 3.4 Rrp47 is predicted to bind RNA.**
The Rrp47 amino acid sequence was entered into the BindN server for RNA binding prediction (Wang and Brown 2006) with a user-defined specificity of 90 %. Predicted RNA binding residues are highlighted in pink labelled with a "+", non-binding residues in green labelled with "-". The confidence for the prediction is given below from level 0 (lowest) to level 9 (highest).

***Conclusions from bioinformatics analyses for Rrp47 mutagenesis***

The combined results of the bioinformatics analyses are presented in Fig. 3.5. In summary, the Rrp47 sequence analyses indicate that the predicted α-helical N-terminus of Rrp47 (Sas10 domain, residues 10-89) is highly conserved from yeast to humans. The N-terminal domain is arranged into four putative α-helices, three of which are part of the Sas10 domain. The additional fourth helix predicted from position 108-116 and a number of highly conserved residues between helix 3 and helix 4 are indicative of a putative RNA binding domain.

The C-terminal portion of Rrp47 is less structured and poorly conserved among Rrp47 homologues, except for the cluster of basic amino acids (K/R) at the very end of the C-terminus (162-182). This is a conserved feature between species potentially mediating nucleic acid binding, recognition or nucleolar localisation.

**A**

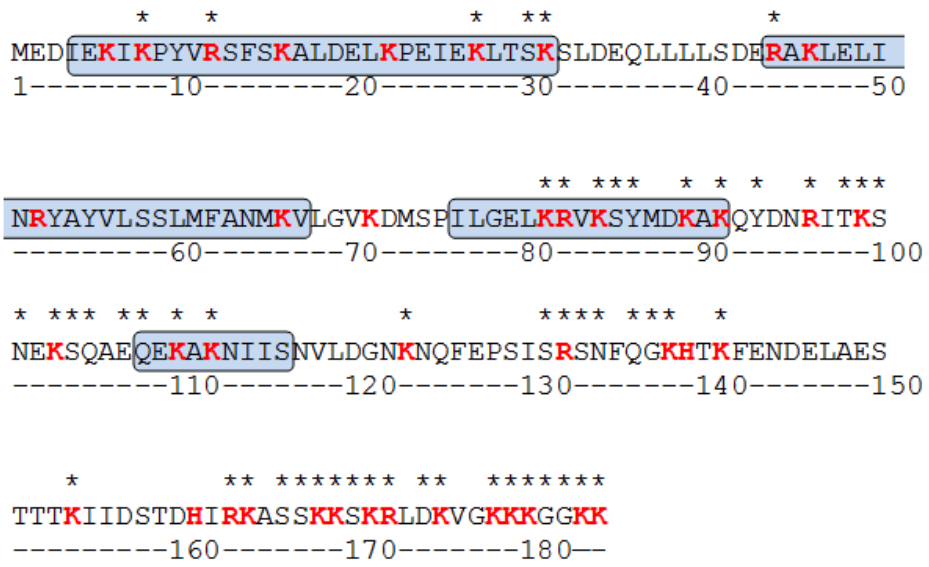


**B**

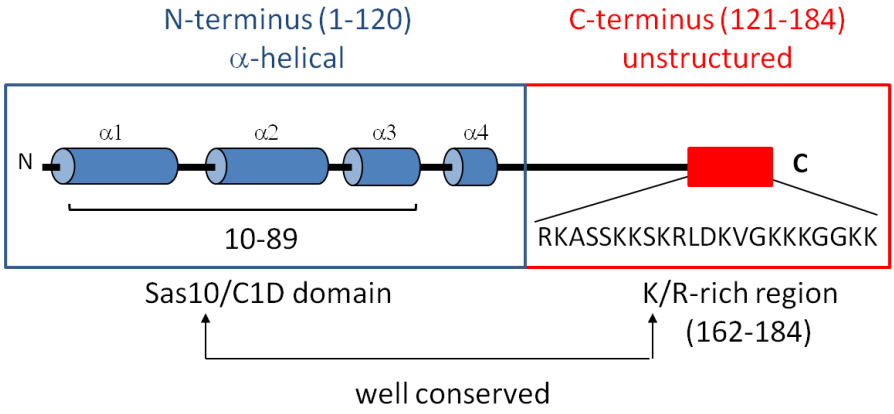


**Figure 3.5 Bioinformatics summary and schematic of Rrp47 architecture.**
(A) Annotated Rrp47 amino acid sequence in one-letter code. Basic residues are displayed bold in red and predicted RNA binding residues (BindN) are marked with an asterisk above letters; putative α-helices are marked as boxes around the letter sequence with the numbering of the amino acid residues below. (B) Rrp47 architecture based on amino acid sequence analysis using bioinformatics tools. The mainly α-helical N-terminus is well-conserved and includes the Sas10/C1D homology domain (residues 10 to 89). The four predicted α-helices are depicted in blue (α1 –α4). The C-terminus is poorly conserved except for a stretch of basic residues, the K/R rich region (depicted as a red box).

### 3.2.2 Generating and analysing Rrp47 mutants

***Alanine substitution of highly conserved residues within the N-terminus of Rrp47***

Amino acids that occur with a high consensus at the same position throughout a range of species are most likely to be critical for protein function and characteristics. Such highly conserved residues (E79, N113), as well as bulky aromatic residues (Y55, F62 and Y86), and charged basic amino acids (R82, K84, K89, K91) were selected as targets for mutagenesis (Fig. 3.6). The chosen residues lie within the Sas10 domain and putative RNA binding region within helices 2, 3 and 4. Point mutations were created by converting the chosen residues into alanine residues by base exchanges using site-directed mutagenesis (SDM, Papworth *et al.* 1996). Where possible, a restriction site was introduced for screening, or alternatively, mutants were screened by Southern blotting with mutant-specific oligonucleotide probes. All mutations were confirmed by sequence analysis. SDM was performed in parallel on an *Escherichia coli* protein expression vector (based on pRSETb) containing a His(6)-tagged *RRP47* wild-type allele (p238) and in a yeast/*E. coli* shuttle vector (based on pRS314) containing the wild-type *RRP47* sequence (p262).

**Figure 3.6 Mutations of highly conserved residues of Rrp47 (*see next page*).**
Highly conserved residues within Rrp47 were identified by sequence alignment of Rrp47 homologues using BLAST, ClustalW and Jalview. The *Saccharomyces cerevisiae* sequence is framed by a black box and mutated residues are annotated with arrows pointing to their position in the *S. cerevisiae* sequence sequence alignment of the conserved Rrp47 N-terminus below (120 residues of *S. cerevisiae* Rrp47) and a schematic of the position of the putative α-helices (above).

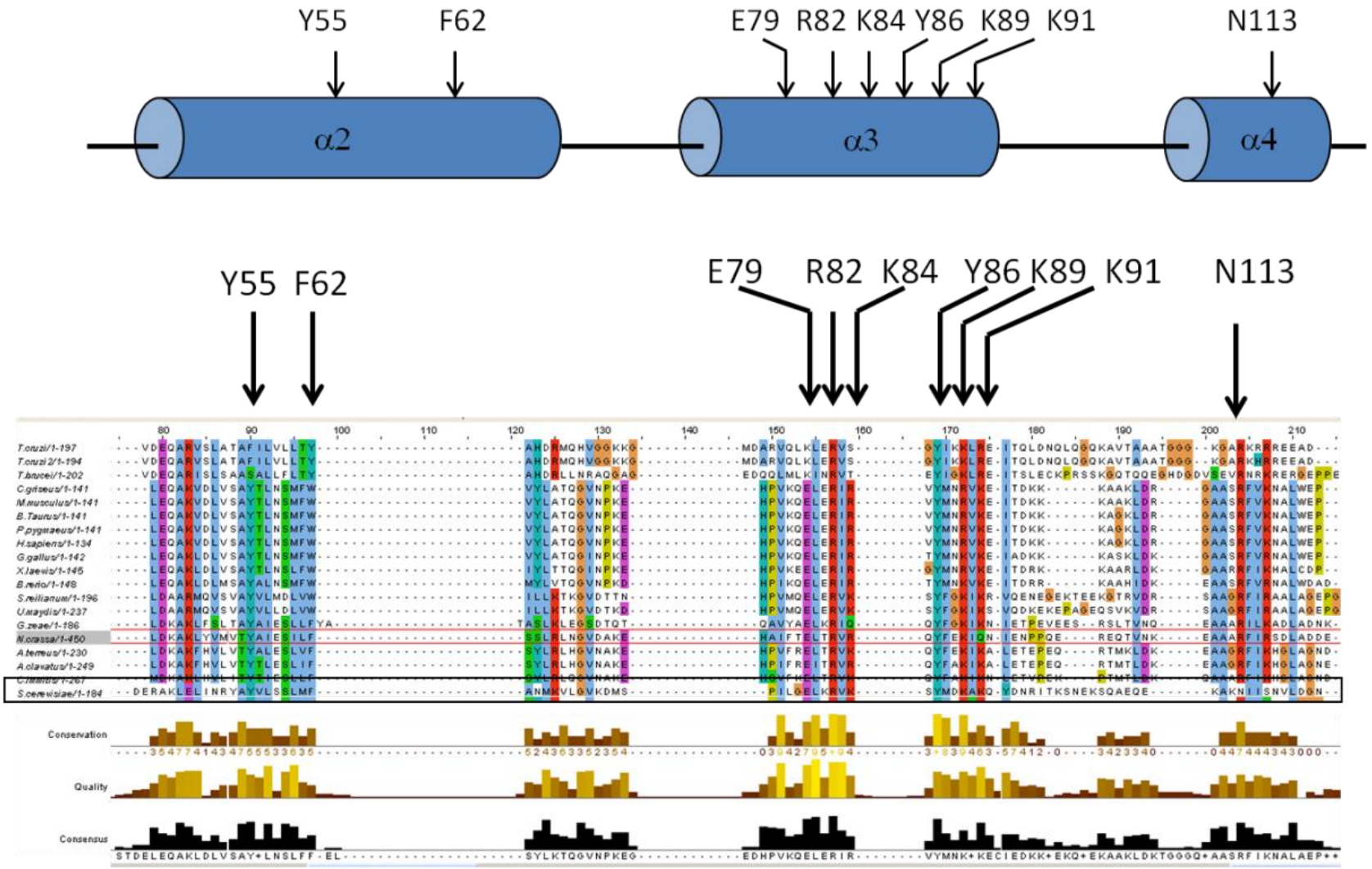
Y55
F62
E79
R82
K84
Y86
K89
K91
N113
α2
α3
α4
Y55
F62
E79
R82
K84
Y86
K89
K91
N113
80
90
100
110
120
130
140
150
160
170
180
190
200
210
T.cruzi/1-197
T.cruzi 2/1-194
T.brucei/1-202
C.griseus/1-141
M.musculus/1-141
B.Taurus/1-141
P.pygmaeus/1-141
H.sapiens/1-134
G.gallus/1-142
X.laevis/1-145
B.rerio/1-148
S.reilianum/1-196
U.maydis/1-237
G.zeae/1-186
N.crassa/1-450
A.terreus/1-230
A.clavatus/1-249
C.immitis/1-267
S.cerevisiae/1-184
Conservation
Quality
Consensus

***Overview of assays to analyse Rrp47 mutants***

A number of *in vitro* and *in vivo* assays were performed to analyse the Rrp47 mutants carrying single amino acid substitutions for the loss of critical functions as summarised in Table 3.2. Recombinant His-tagged proteins of Rrp47 mutants were expressed in *E. coli* and analysed for binding to the Rrp6 N-terminal domain (GST-Rrp6NT), as well as binding to RNA *in vitro* in filter binding and UV cross-linking assays. Yeast strains with mutant *rrp47 alleles* were assayed *in vivo* for complementation of the *rrp47Δ* slow growth phenotype, as well as for functionality in a synthetic lethal (sl) *rex1Δ rrp47Δ* double mutant. The mutated strains were also assessed for Rrp47-specific RNA processing phenotypes, specifically accumulation of 3' extended processing intermediates of 5.8S rRNA and various sn/snoRNAs, as well as accumulation of the 5' external transcribed spacer (5'ETS). The table shows the phenotypes of *RRP47* wild-type (column 1) vs. *rrp47Δ* deletion mutant (column 2) and point mutants analysed in this study (column 3 Rrp47* point mutants are Y55A, F62A, E79A, R82A, K84A, Y86A, K89A, K91A, N113A).

| Analyses of Rrp47 point mutants | Rrp47 | *rrp47Δ* | Rrp47*mutants |
|---|---|---|---|
| *Recombinant Protein assays* | | | |
| - Pull-down by GST-Rrp6NT | + | n.a. | + |
| - UV crosslinking to RNA | + | n.a. | + |
| - Filter binding to RNA | + | n.a. | + |
| | *RRP47* | *rrp47Δ* | *rrp47** |
| *Growth /Complementation assays* | | | |
| - complementation of *rrp47Δ* | + | - | + |
| - slow growth phenotype | - | + | - |
| - complementation of sl *rex1Δ rrp47Δ* double mutant | + | - | + |
| *RNA processing phenotypes* | | | |
| - 5.8S +30 rRNA / ITS2 | - | + | - |
| - 5'ETS | - | + | - |
| - snR38 and other snoRNAs | - | + | - |

**Table 3.2 Overview of analyses of Rrp47 mutants.**
Recombinant His-tagged proteins of Rrp47 point mutants were expressed in *E. coli* and analysed for binding to Rrp6 (GST-Rrp6NT) and binding to RNA *in vitro*. Yeast strains with mutant *rrp47 alleles* were assayed for complementation of the *rrp47Δ* slow growth phenotype, as well as complementation of synthetic lethality (sl) of *rex1Δ rrp47Δ* (Peng *et al*. 2003) *in vivo.*

### 3.2.3 Rrp47 point mutants behave like wild-type protein with respect to expression levels, Rrp6 and RNA binding

***All Rrp47 point mutants can be expressed and purified similarly to wild-type protein***

Using standard procedures, the recombinant His-tagged Rrp47 proteins Y55A, F62A, E79A, R82A, K84A, Y86A, K89A, K91A, N113A were expressed in *E. coli* cells and purified using a two-step protocol established for Rrp47 in the lab (Stead *et al.* 2007). A typical purification is shown in Figure 3.7 (A and B). Competent *E. coli* BL21(DE3)pLysS cells were transformed with protein expression plasmids containing the Rrp47-His wild-type and mutant sequences. Typically 0.5 to 1 litre LBA expression cultures were grown up at 37 ˚C to an $OD_{600}$ of 0.5 and protein expression was induced by adding IPTG. Cultures were grown for another 4 hours before harvesting by centrifugation. Cells were lysed by sonication and extracts clarified by centrifugation. The obtained lysates (A, B lane 1) were then sequentially purified over NiNTA metal-affinity chromatography followed by ion exchange chromatography using SP Sepharose. Samples were resolved by 12.5 % SDS PAGE and stained with Coomassie Blue (A) or analysed by western blotting (B) using an anti-His antibody. The eluate fractions (A, lane 4 and lanes 8-10 and B, lanes 3 and 5) show the enriched purified protein with a size of 25 kilo Dalton. Up to 5 mg protein could be obtained from 1 litre *E. coli* expression culture.

All Rrp47 point mutants carrying an amino acid substitution were expressed and purified with the same method. Proteins eluted from NiNTA (E1) and further purified SP Sepharose eluates (E2) are shown in Figure 3.7 (C). The mutant proteins showed no significant differences in protein yield or stability compared to the wild-type protein and could be stored for several weeks at -20 ˚C. The purified proteins were used in pull-down-assays to determine binding to Rrp6 (see Fig. 3.8) and in filter binding and UV cross-linking assays to analyse RNA binding (see Fig. 3.9 and 3.10).

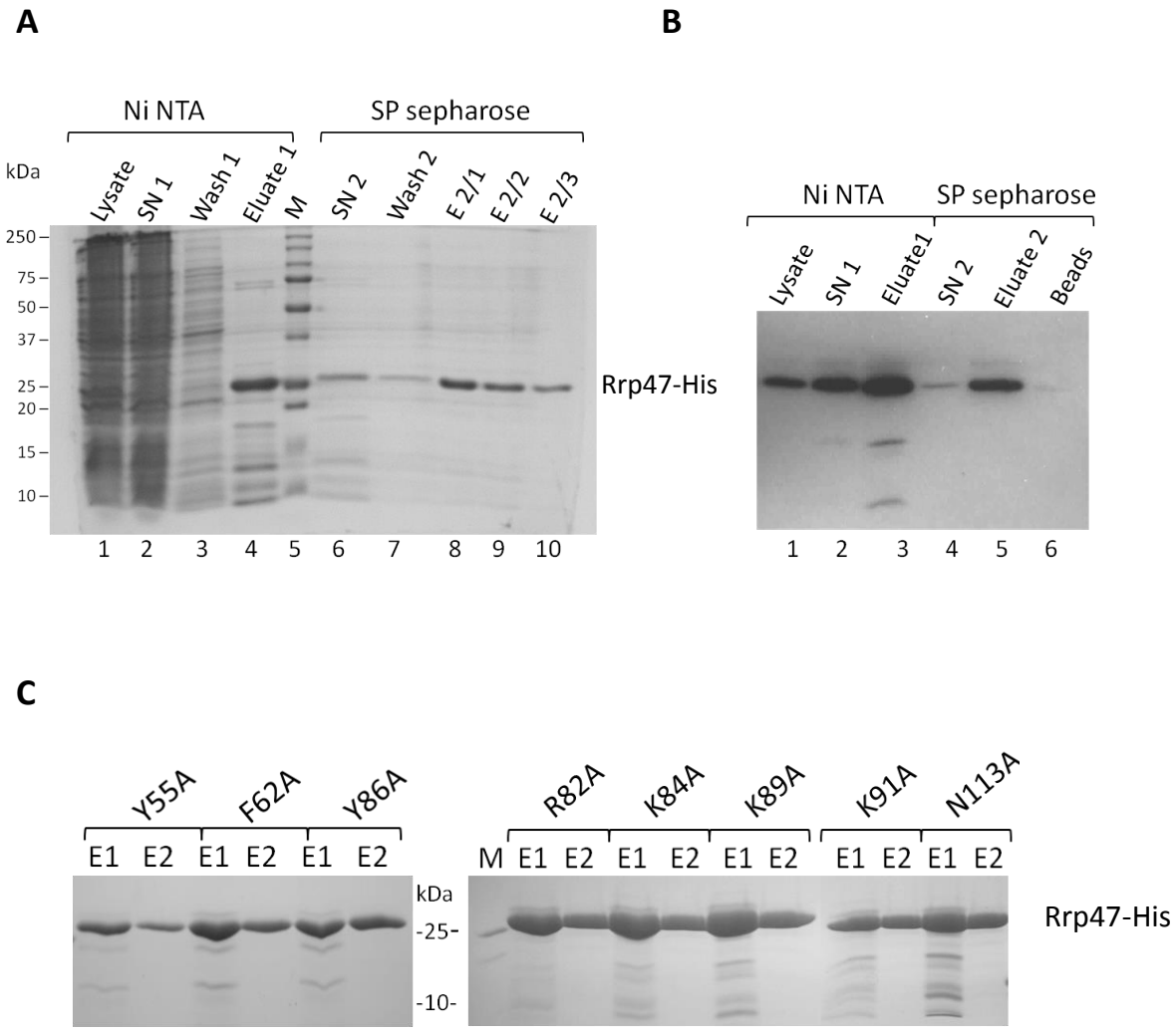


**Figure 3.7 Two-step purification of recombinant Rrp47 mutant proteins.**
Two-step purification of recombinant His-tagged Rrp47 (p238) over NiNTA and SP sepharose. Equivalent amounts (0.1 %) of lysate, supernatant (SN) and wash fractions, as well as 0.1 % of eluate fractions E1 (app. 5 µg) and E2 (app. 2.5 µg) were resolved through 12.5 % SDS-PAGE and (A) stained with Coomassie-Blue or (B) analysed by western blotting using a His antibody. (C) Coomassie stain of NiNTA (E1) and SP Sepharose eluates (E2) of purified mutated Rrp47 proteins resolved by 12.5 % SDS-PAGE as indicated (Y55 p313, F62A p311, Y86A p305, R82A p323, K84A p325, K89A p327, K91A p331, N113A p329).

***The single point mutations introduced into Rrp47 do not affect binding to Rrp6***

Binding of Rrp47 to its co-factor Rrp6 has previously been assessed in the lab in a pull-down assay using as bait a GST-tagged Rrp6 protein truncated to its N-terminal domain required for Rrp47 interaction (Stead *et al*. 2007). The same assay was used to determine whether the single point mutations introduced into Rrp47 affect Rrp6 binding. GST-Rrp6NT and the GST-tag control were expressed in *E. coli* cells and lysates were mixed with glutathione sepharose resin to allow binding of GST-Rrp6NT and GST, respectively. After several washes, equal amounts of purified Rrp47 proteins were incubated with the glutathione sepharose beads pre-charged with GST or Rrp6-GST fusion protein. After binding for 1 hour at 4 ˚C, the beads were washed extensively with lysis buffer and bound proteins were boiled off the resin with SDS loading buffer. GST and Rrp6-GST eluates were resolved side by side through 12.5 % SDS-PAGE and analysed by western blotting with antibodies directed against the His or the GST tag (Fig. 3.8 upper and lower panel). All Rrp47 point mutants tested were captured by GST-Rrp6NT (even numbered lanes) with similar efficiency. No Rrp47 protein could be detected in the GST-control (odd numbered lanes). In conclusion, Rrp6 binding is not clearly affected by any of the single point mutations in Rrp47 tested in this pull-down assay.

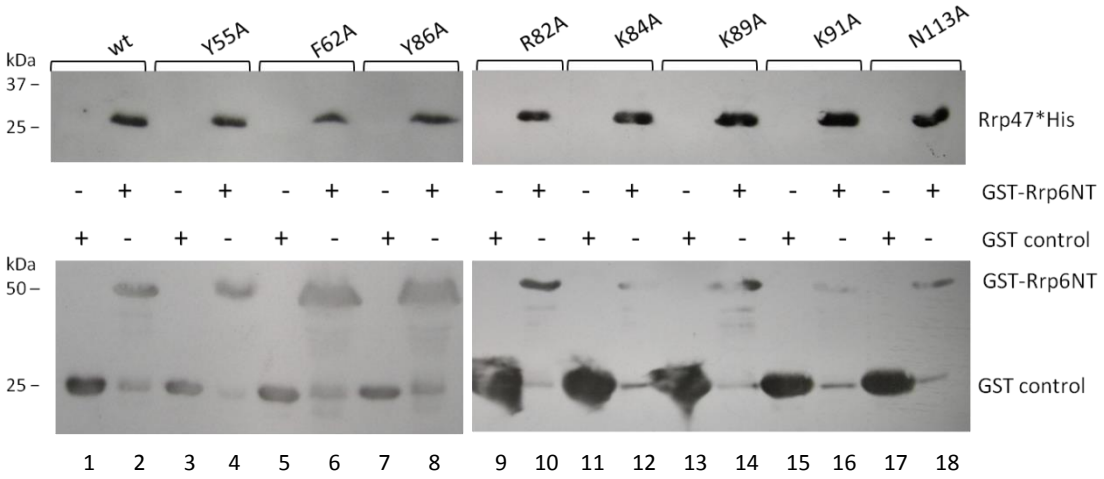


**Figure 3.8 All Rrp47 mutant proteins bind GST-Rrp6NT *in vitro*.**
Western analysis of pull-down-assays of Rrp47 mutants on GST-Rrp6NT (p245). Purified recombinant Rrp47 proteins (50 µg each) were incubated for 1 hour with equal amounts of GST-Rrp6NT (even numbered lanes) or GST-control (odd numbered lanes) bound to glutathione sepharose beads. Beads were eluted with SDS loading buffer, resolved through 12.5 % SDS PAGE and analysed by western blotting with antibodies against the His(6)-tag to detect bound Rrp47 proteins (upper panel) and anti-GST to detect the input of the bait proteins GST-Rrp6NT and the GST control (lower panel).

***Mutant Rrp47 proteins bind structured RNA in a concentration-dependent manner***

Next, binding of recombinant Rrp47 proteins to RNA was assessed with a modified double filter binding assay as previously described (Stead *et al.* 2007). Structured RNA substrates were used that have shown to be bound by Rrp47 in a concentration-dependent manner, i.e. yeast tRNA-Phe and a model RNA based on the ITS2 rRNA fragment which accumulates in *rrp47Δ* mutants. The model RNA generated by *in vitro* transcription contains a 5' stem loop linked to a 3' A/U rich sequence (SLAU RNA) and was kindly provided by J. Stead. A schematic of the filter binding assay is shown (Fig. 3.9). The purified Rrp47 proteins were dialysed overnight into RNA binding buffer. Triplicates of serially diluted protein were mixed with $P^{32}$-labelled RNA and incubated for 15 minutes on ice (A). Samples were then loaded onto a slot blot apparatus fitted with layered membranes to capture either protein/protein-bound RNA (C filter, top) or non-bound RNA (N filter, bottom) upon vacuum filtration (B). After washing and drying, the blots were arranged side by side and analysed using either X-ray film or phosphor imaging.

A typical slot blot for Rrp47 wild-type protein is shown with triplicate samples (Fig. 3.9 C). The amount of non-bound RNA retained on the N-filter visibly decreases with rising Rrp47 protein concentration, and the signal of Rrp47-bound RNA appears on the C-blot. The bands were quantified as percentage of ligand bound to protein and the average values of the triplicates were plotted against the protein concentration to obtain an RNA binding saturation curve as shown here for Rrp47 and tRNA-Phe (D). Rrp47 binds RNA in a concentration-dependent manner with a dissociation constant (Kd) of approximately 1 µM indicating the protein concentration where 50 % of the ligand is bound. Above a protein concentration of 1 µM RNA binding increases sharply and at 20 µM effectively all of the RNA substrate is bound to protein.

The mutated Rrp47 proteins were tested for RNA binding using the slot blot assay and the primary data is shown in Figure 3.10 for mutated aromatic residues (A) and for mutants with substitutions in basic residues and the highly conserved N113 site (B). None of the point mutants showed a significant loss or decrease in RNA binding compared to the wild type protein (A, top and B, first panel). The mutants K89A and N113A (B, bottom row) appeared to start binding RNA at a slightly higher protein concentration (see C filters). However, the signal was overall weaker and subsequent quantification of the bands and the resulting binding curves (Fig. 3.10 C) showed a very similar profile for the K89A and N113A mutants and the wild type protein or the R82A mutant (Fig. 3.10). In conclusion, the Rrp47 point mutants tested here do not show any significant effects on RNA binding in these *in vitro* assays.

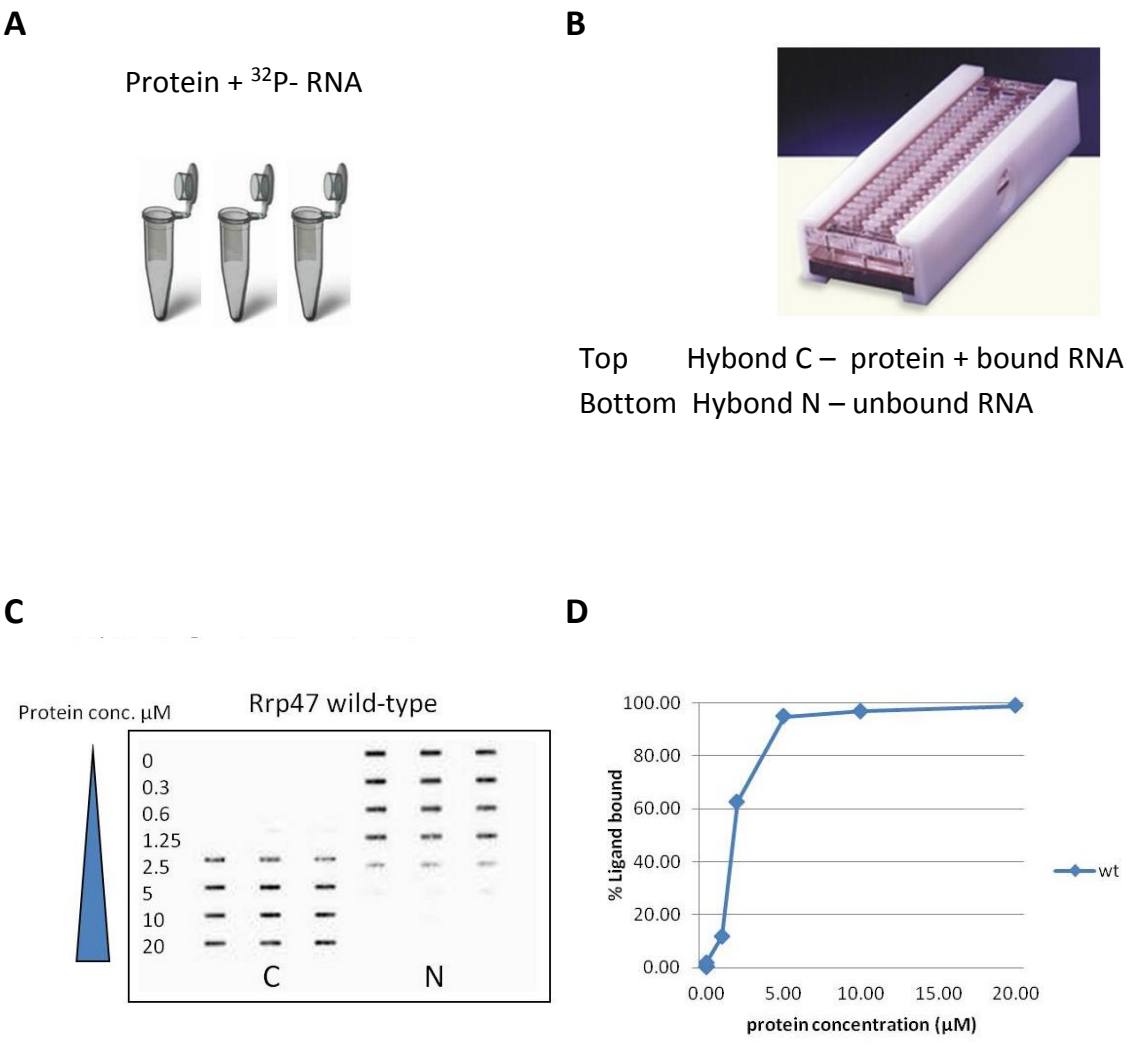


**Figure 3.9 The double filter binding assay to analyse RNA binding by Rrp47 mutants.**
(A) Triplicate samples of serially diluted, purified protein were incubated with 5' $^{32}$P-labelled RNA substrate for 15 minutes on ice. (B) Pre-soaked Hybond C (on top) and Hybond N (below) membranes were assembled into the slot blot apparatus (photo: Schleicher). Samples were loaded in rows of triplicates and adsorbed by applying vacuum. After washing and drying, the C- and N-filter were exposed side by side to a phosphor imager screen or X-ray film (C). Bands were quantified using ImageQuant software and the average of the triplicate data was plotted as the percentage of bound ligand against the protein concentration. (D) RNA binding saturation curve for wild-type Rrp47 and SLAU-RNA (see text).

A

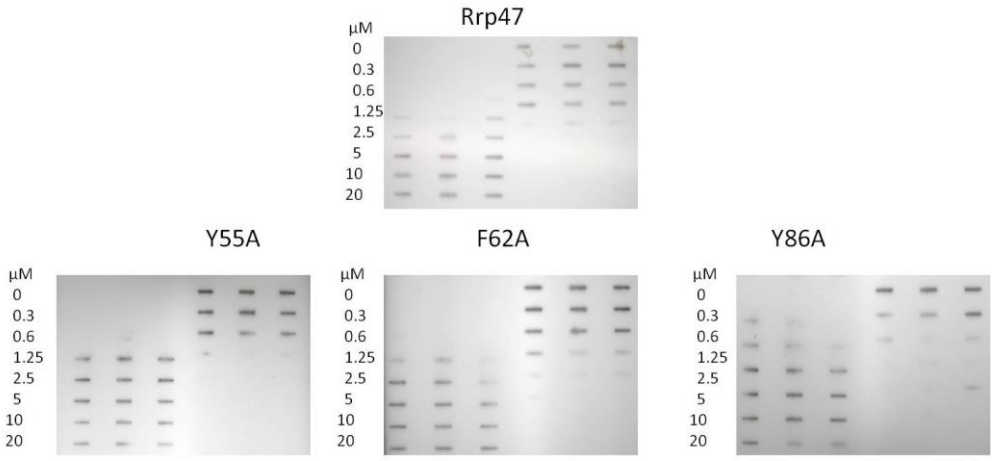


B

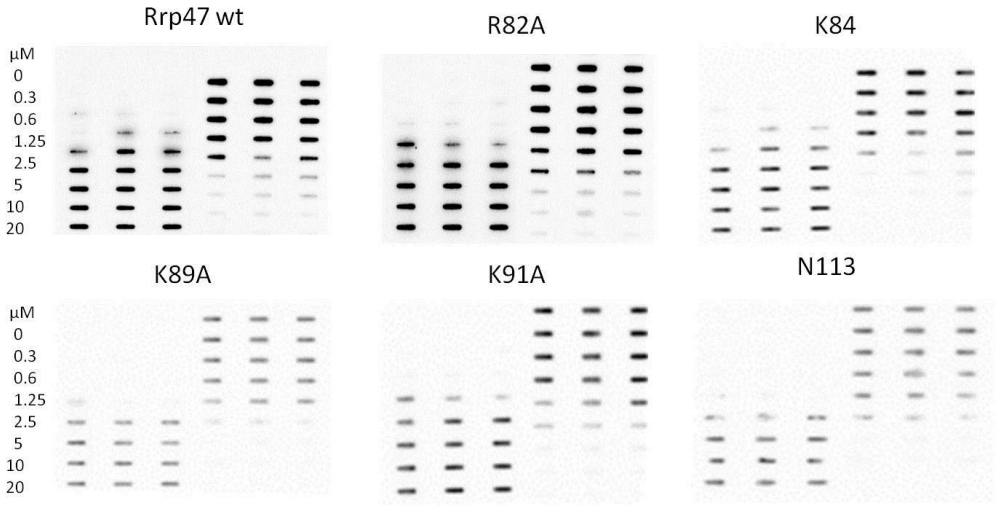


C

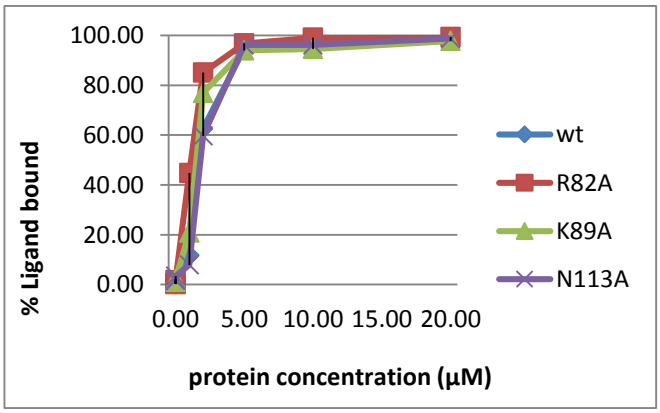


**Figure 3.10 Rrp47 point mutants bind RNA with similar efficiency to wild-type.**
Slot blot assays (A+B). Shown are the C- and N- slot blot filters of RNA binding assays side by side for the Rrp47 point mutants as indicated above the panels binding to SLAU RNA (Stead *et al*. 2007). The C filter on the left shows triplicate samples of the RNA bound to protein with increasing protein concentration from 0 to 20 µM, whereas the N-filter on the right shows the unbound RNA. (C) Filter binding saturation curves obtained from the average of the triplicate primary slot blot data for the K89A, N113A and R82A mutants and wild-type Rrp47 showing percentage of ligand bound.

### 3.2.4 Rrp47 point mutants complement *rrp47Δ* growth and RNA processing defects

Strains lacking Rrp47 have a moderate slow growth phenotype at 25 ˚C, 30 ˚C and 37 ˚C (Mitchell *et al*. 2003a). To assess the effect of the mutations on growth, plasmids carrying the mutated Rrp47 sequences and a selectable marker were transformed into an *rrp47Δ* strain *(rrp47Δ::kanMX4* allele in BMA38*).* Serial dilutions of freshly grown cultures with equal starting cell densities were spotted onto plates containing selective medium and left to grow for 3 days at 30 ˚C. Plates were generally done in duplicate and two independent transformants of each mutant strain were tested as shown for Y55A, F62A and Y86A. The *rrp47Δ* strain transformed with the vector control showed the characteristic slow growth defect (Fig. 3.11 A top row) which could be alleviated with the introduction of a wild type gene (pRS314::*RRP47,* second row). Strains transformed with the mutated alleles also showed complementation of the slow growth phenotype seen in the vector control and recovered growth similar to the wild-type gene as seen on the spot growth plates. Thus, none of the mutations notably affected growth.

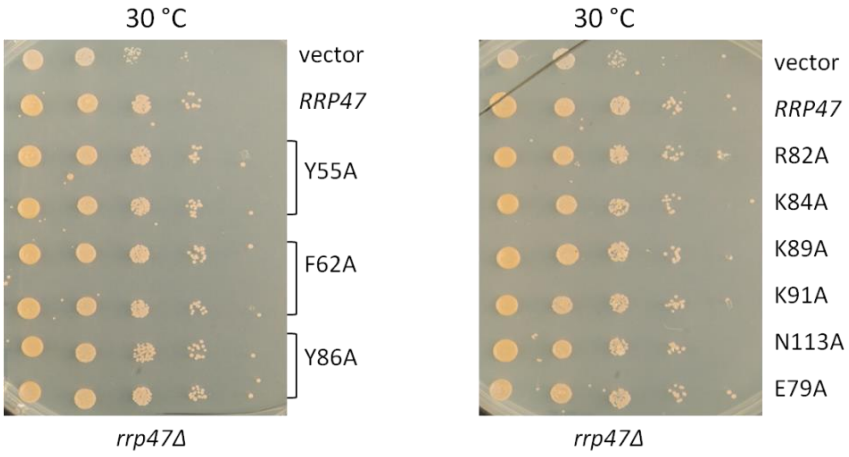


**Figure 3.11 Rrp47 point mutants complement slow growth of *rrp47Δ.***
Spot growth assays. Rrp47 point mutants, a vector control (pRS314) and an *RRP47* wild type allele (p262) were transformed into an *rrp47Δ* strain *(*P368*)*. Serial 10-fold dilutions of freshly grown cultures with equal starting $OD_{600}$ were spotted onto plates containing selective medium (SD-trp) and grown up for three days at 30 °C. The *rrp47Δ* vector control is shown at the top of each plate with strains complemented with *RRP47* wild type and mutant alleles below as indicated to the right (Y55 p319, F62A p317, Y86A p315, R82A p338, K84A p340, K89A p342, K91A p346, N113A p344).

***Rrp47 point mutants do not show typical RNA processing defects of rrp47Δ strains***

Another characteristic of strains lacking Rrp47 or Rrp6 are defects in RNA processing which affect early steps in pre-rRNA processing, as well as the final 3' maturation of 5.8S rRNA and snoRNAs. As a result, these mutants accumulate degradation and processing intermediates (Mitchell *et al.* 1996 and Mitchell *et al.* 2003). One of these accumulated species is the 5' external transcribed spacer (5'ETS) which is generated by the initial cleavage of the 35S precursor rRNA (Fig 3.12 A) and which is rapidly degraded by the exosome and Rrp6-Rrp47 in wild-type cells. 35S pre-rRNA processing requires a complex series of processing reactions involving numerous endo- and exonucleases. Exosome mutants and *rrp47Δ* and *rrp6Δ* strains show distinct defects in the synthesis of 5.8 S rRNA. The core exosome is involved in processing a 3' extended 7S precursor containing roughly 140 nucleotides of the internal transcribed spacer (ITS2), whereas *rrp47Δ* and *rrp6Δ* strains accumulate a 30 nucleotide 3' extended species (5.8S+30, 188 nt). Similarly, *rrp47Δ* and *rrp6Δ* mutants accumulate box C/D snoRNAs with distinct 3' extensions of 3 nucleotides indicating a defect in the final 3' processing step. Again, core exosome mutants accumulate longer 3' extended species of snoRNAs with 3' extensions of variable length.

**A**

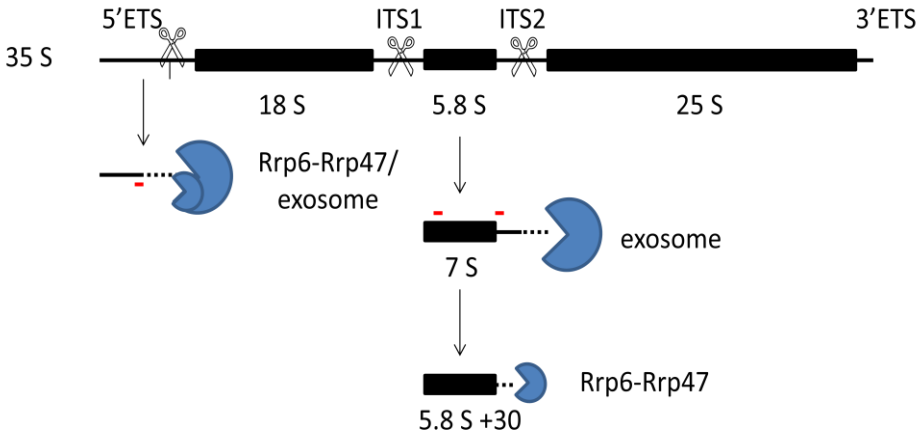


**Figure 3.12 A Schematic of Rrp47 function in pre-rRNA processing.**
Schematic of 35S pre-rRNA processing with focus on the first processing step which produces the 5'ETS fragment that is degraded by the exosome and Rrp6-Rrp47 and the 3' processing of 5.8S rRNA which involves processing of a 3' extended 7S precursor by the exosome to produce a 5.8S+30 RNA species which is then processed by Rrp6-Rrp47. rRNA coding regions are denoted as bars, transcribed spacer regions as lines, scissors represent cleavages. The position of northern probes to detect these RNA species is marked with red bars.

To assess RNA processing defects of Rrp47 point mutants, total RNA isolated from these strains was resolved through 8 % denaturing polyacrylamide gels. Due to the predominance of rRNA in total cellular RNA, the 5S and 5.8S/5.8S+30 species can easily be seen on ethidium stained gels (Fig. 3.12 B lane 1, bottom panel). For less abundant species, the resolved RNAs, once transferred to a membrane, can be detected with 5' $^{32}$P-labelled transcript-specific oligonucleotide probes, a method termed northern hybridisation, as shown here for 5'ETS and the snR38 species (Fig. 3.12 B upper panels). Whilst the *rrp47Δ* mutant showed the typical accumulation of 5'ETS, snR38 and 5.8S+30 species (lane 1), the single point mutations had no effect on the RNAs analysed. There was no accumulation of the 5'ETS fragment, the 5.8S+30 processing intermediate or the 3' extended snR38 +3 species seen in strains expressing the mutated proteins. All mutants displayed RNA processing phenotypes similar to the strain containing wild-type *RRP47* (lane 2).

**B**

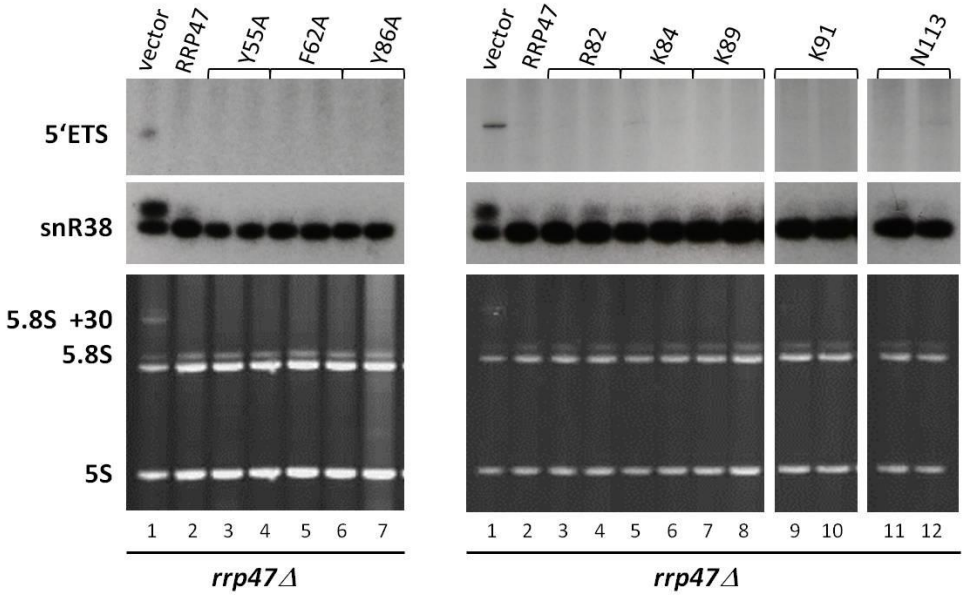


**Figure 3.12 B Rrp47 point mutants complement *rrp47Δ* RNA processing defects.**
Analysis of RNA from strains expressing *rrp47* point mutations. Cells were grown to just below 0.5 $OD_{600}$, total RNA was extracted and 5 µg resolved through an 8 % polyacrylamide gel followed by northern hybridisation with probes complementary to the 5' ETS and snR38 RNA species (upper panels) as indicated to the left. The 5.8 S/5.8 S+30 and 5S rRNA bands are shown on the ethidium bromide stained gel (lower panel). Lane 1 shows the *rrp47Δ* vector control, lane 2 the *RRP47* complemented mutant, lane 3-7 and lane 3-12, respectively, show two independent transformants of the point mutants as indicated above the panels.

### 3.2.5 All point mutants complement a synthetic-lethal *rex1Δ rrp47Δ* double mutant

Yeast strains lacking Rrp47 or Rrp6 and the 3' to 5' exonuclease Rex1 (RNA exonuclease 1) are synthetic-lethal (Peng *et al*. 2003). The reason for the synthetic lethality is not established, however Rex1 has been shown to be involved in 5S processing (van Hoof *et al.* 2000, Piper *et al.* 1983) and it is believed that Rrp6 and Rex1 have redundant functions and thus the loss of both exonucleases is lethal. Rrp47 point mutants were assessed for their ability to complement *rex1Δ rrp47Δ* synthetic lethality in a plasmid shuffle assay (Fig. 3.13 A schematic). The point mutants were transformed into a double mutant test strain (P596) that carries a plasmid with a wild-type *RRP47* allele for viability and an *ADE3* allele resulting in red coloured colonies which allows visualisation of strains harbouring this plasmid. Complementing Rrp47 mutants (*rrp47**) allow stochastic loss of this original plasmid during cell division resulting in red/white colony sectoring. In contrast, if only the vector control is transformed, the essential *RRP47* allele and the *ADE3* allele on the plasmid are retained and solid red colonies develop (*ade2* phenotype) as seen in the first panel for the vector control (Fig. 3.13 B). Like the wild-type *RRP47* allele and the E79A mutant shown here, all point mutants in this study allowed colony sectoring and therefore expressed functional proteins (C). Moreover, the white *rex1Δ rrp47** subpopulation was isolated from sectoring strains and the loss of the original *RRP47* allele was confirmed by loss of growth on SD-ura. Mutant *rex1Δ rrp47** strains were analysed for fitness at 30 °C in a spot growth assay (D), as well as for possible RNA processing defects, but the *rex1Δ rrp47** double mutants showed no considerable differences to the wild-type allele in these analyses and also showed no RNA processing defects (Fig. 3.13 D and data not shown).

**A**

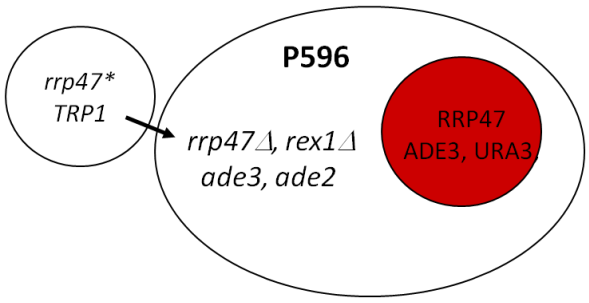


**B**


*rex1Δ rrp47Δ [RRP47 ADE3 URA3]*

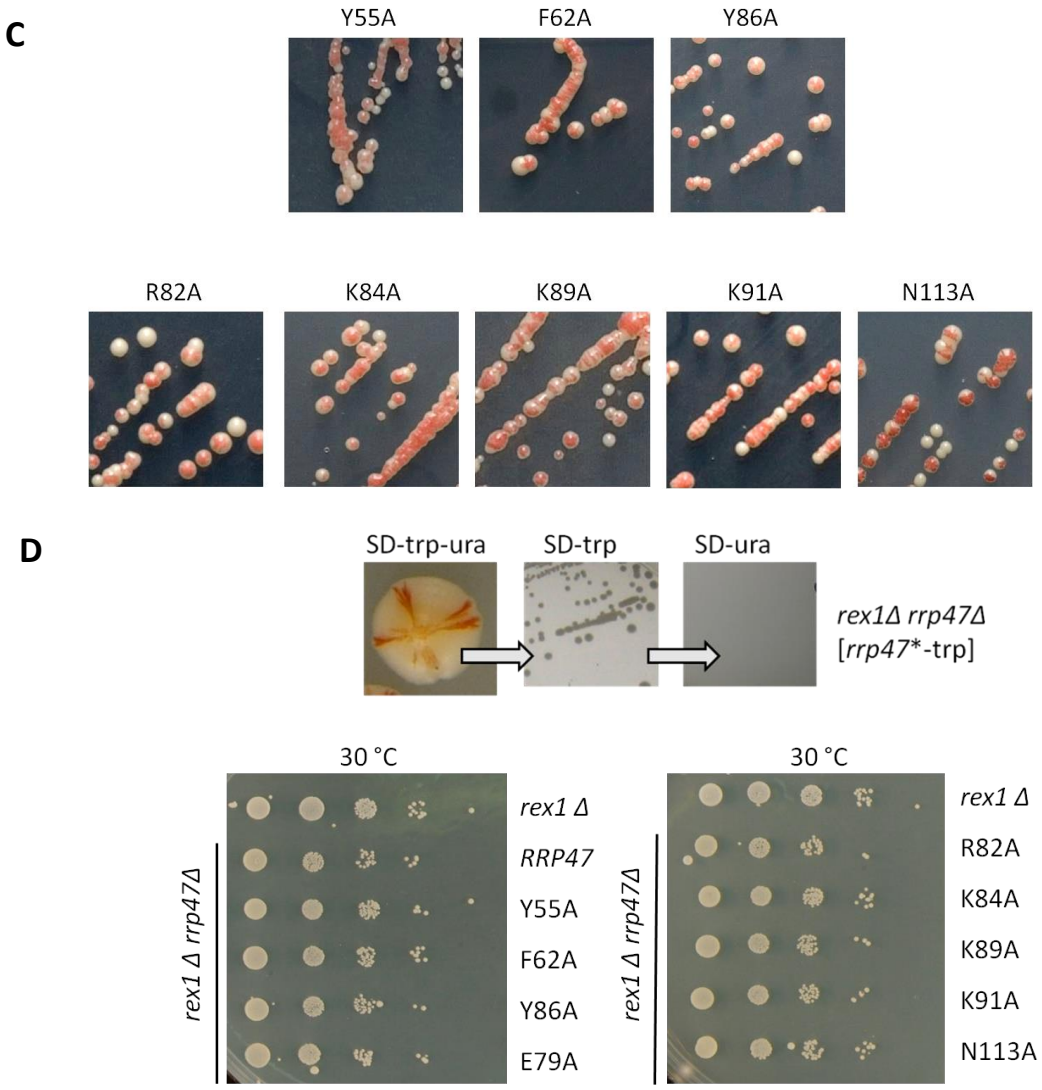


**Figure 3.13 All point mutants complement a synthetic-lethal *rex1Δ-rrp47Δ* mutant.**
(A) Schematic of the plasmid shuffle assay (Kranz and Holm 1990). Plasmid-encoded Rrp47 mutants (depicted as circle, *rrp47*TRP*) were transformed into a synthetic-lethal *rex1Δ rrp47Δ* plasmid shuffle strain (depicted as big oval, P596) carrying a copy of the *RRP47* wild-type, *URA3* and *ADE3* alleles on a plasmid (red circle). (B) Colony sectoring results for vector control, *RRP47* wild-type and *E79A* mutant allele transformed into the *rex1Δ rrp47Δ [RRP4] strain* (P596*).* (C) Sectoring results for Rrp47 point mutants. (D) Isolation of *rex1Δ rrp47** double mutants (white sector) on SD-trp, confirming lack of growth on SD-ura and spot growth assay on SD-trp for 3 days at 30 ˚C along with *rex1Δ* single mutant (top row).

In summary, the Rrp47 single point mutants behaved in all respects like wild-type Rrp47 in these assays. They had no clear adverse effect on growth, protein function or RNA processing *in vivo* and no effect on Rrp6 and RNA binding *in vitro* (Summary in Table 3.1 Rrp47*). Taken together, these results indicate that despite the high conservation of the residues chosen for mutagenesis, the single point mutations in the Rrp47 sequence tested here are still producing and replacing a functional wild-type Rrp47 protein.

### 3.2.6 Analysis of Rrp47 C-terminal truncations and multiple mutations

In addition to the point mutants, Rrp47 truncations were generated to elucidate the functions of the basic C-terminus and effects caused by its partial or whole deletion. Initially, two truncations were investigated, the C-terminal deletions ΔC1 (residues 120-184) removing the whole disordered C-terminus and ΔC2 (residues 162-184) removing the conserved C-terminal K/R cluster (Fig. 3.14). Recombinant ΔC1 and ΔC2 truncated proteins had already been investigated in the lab for Rrp6 and RNA binding, however no *in vivo* data had been produced to assess genetic and RNA processing phenotypes in yeast. The C-terminal truncation ΔC1 (also referred to as N121PGX) was created by subcloning from a construct previously generated in the lab by deletion of the C-terminus and insertion of linker oligos before the stop codon (Stead *et al*. 2007). At later stages additional truncations were created by SDM that terminate at residue 100, 80, 70 and 60 by introducing a stop codon (X) at the required site and a restriction site for screening. An overview of Rrp47 truncations is shown in Figure 3.14. The truncation mutant G181X, as well as two N-terminal deletions ΔN2-9 and ΔN 2-19 analysed in this study were generated by Joe Costello (detailed in Costello *et al*. 2011).

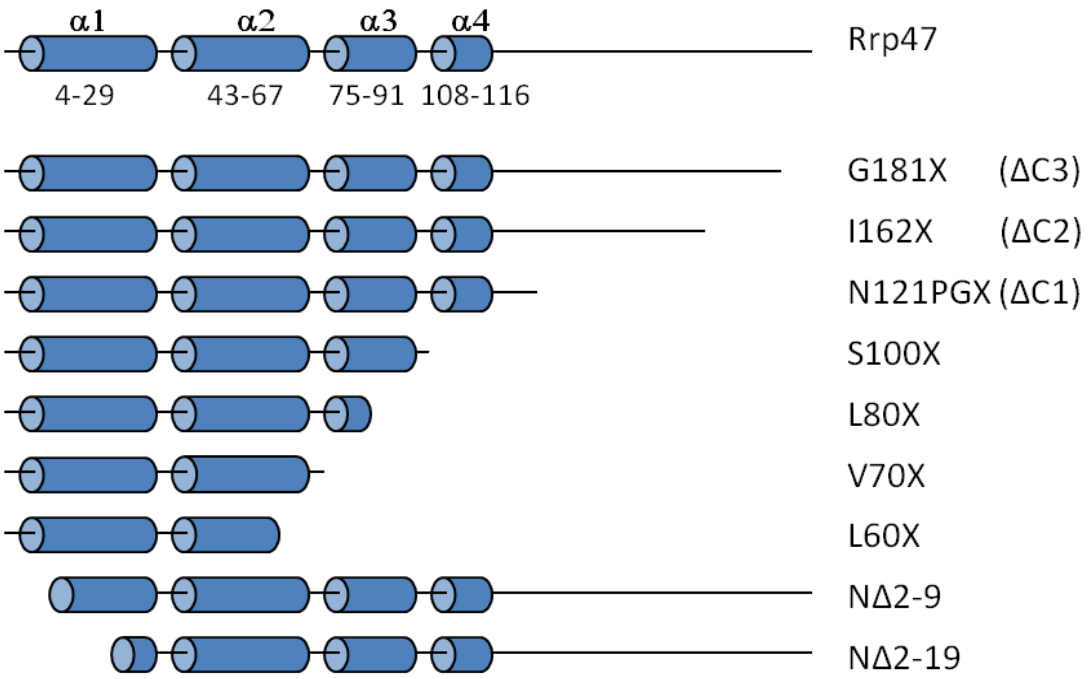


**Figure 3.14 Schematic of Rrp47 truncation mutants analysed in this study.**
Schematic of Rrp47 C-terminal truncations ending with an X denoting the Stop codon at the indicated position and N-terminal deletions depicted in relation to the predicted α-helices (α1-α4, depicted as blue cylinders) in the N-terminus of Rrp47 (full length 184 residues).

Moreover, due to the lack of phenotypes in the single point mutants, multiple mutations were combined within the putative N-terminal RNA binding domain in helix 3 to create the quadruple mutant “mm” which combines point mutations E79A, R82G (to glycine), K84I (to isoleucine) and Y86S (to serine). Instead of changing the amino acids to alanine as before, amino acid substitutions were chosen which altered charge or size of the amino acid residue.

### 3.2.7 Protein yield and stability decreases for larger Rrp47 truncations

Recombinant proteins of the Rrp47 truncations ΔC1, ΔC2 ΔC3, 100X, 80X, 70X and the multi-mutant (mm) were expressed and purified using a similar procedure as for the point mutants before. Due to the loss of the basic tail and positive charge, the C-terminal truncations are less stable in high salt and bind to SP sepharose only very inefficiently. Therefore, the purification protocol for truncated proteins was modified to include dialysis of the NiNTA purified protein into lower salt Hepes buffer containing 150 mM NaCl over night before loading onto the SP Sepharose beads for further purification. The amounts of purified protein recovered were similar for the wild-type and the multiple mutant (mm, Fig 3.15 lane 12 vs. lane 18). However, expression and/or protein stability decreased the more of the C-terminus was removed. The ΔC1, ΔC2, ΔC3 and 100X truncations could be produced in similar, albeit slightly reduced amounts compared to the wild type protein (left panel). Strikingly, recombinant protein recovered for the truncations 80X (lane 16) and 70X (lane 14) was considerably reduced and further truncations (60X, 50X) could not be expressed/purified as recombinant proteins at all.

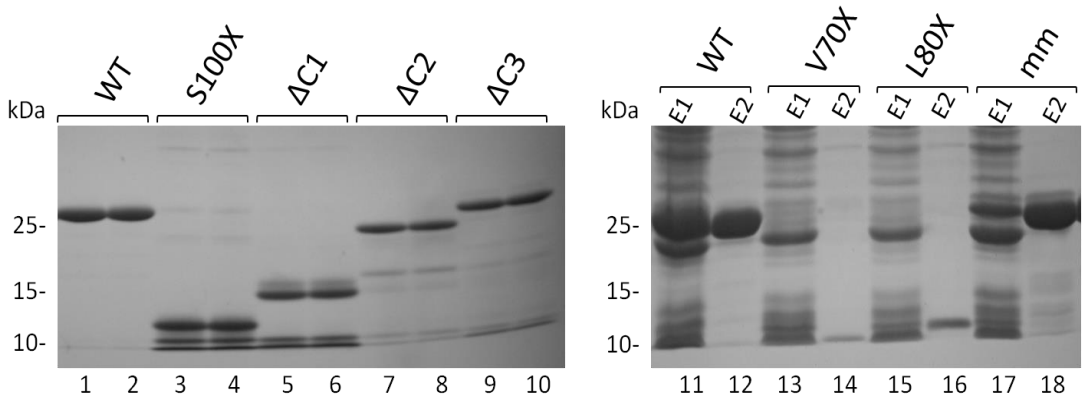


**Figure 3.15 Expression levels and stability decreases for truncated Rrp47 proteins.**
Coomassie stains of 10 % (left) and 12.5 % (right) SDS-PAGE gels with purified truncated Rrp47 proteins expressed in *E. coli* as recombinant His-tagged proteins. Lanes 1 to 10 display duplicate samples of purified S100X (p348), ΔC1 (N121 PGX p247), ΔC2 (I162X p272) and ΔC3 (G181X p302) proteins (app. 5 µg). Lane 11 to 18 shows 1 % of the NiNTA (E1) and SP Sepharose eluate (E2) resolved side by side (app. 10 µg of wild-type protein) of full length Rrp47 (p238), V70X (p382), L80X (p384) and mm (p386).

***Truncations that affect the Sas10 domain reduce protein stability and Rrp6 binding***

To assess Rrp6 binding, the C-terminal truncations and the multi-mutant were incubated with GST-Rrp6NT fusion or GST control bound to glutathione sepharose as described before. The C-terminal truncations S00X, ΔC1 and the multi-mutant (mm) were captured by the Rrp6 interaction domain with equal efficiency to the wild-type protein (Fig. 3.16 lanes 3, 5, 7, 9, 11), but not by the GST control (lanes 2, 4, 6, 8, 10) or the vector control (lane 1). In contrast, the amount of bound protein was markedly decreased for the 80X truncation and reduced to an even greater extent for the 70X mutant in pull-downs using purified protein. Since expression and purification of these truncations was much less efficient (see Coomassie stain above Fig. 3.15), the loss of binding could be due to weaker expression and lack of protein stability, rather than lack of binding sites. The experiment was repeated using cell lysates instead of purified Rrp47 protein to ensure an excess of 80X and 70X protein input, however with the same result as observed for purified protein before; hardly any 70X was detectable bound to GST-Rrp6NT and the amount of 80X was greatly reduced (Fig. 3.16 lanes 13 and 15) compared to wild type and multi-mutant (lanes 9 and 11). None of the Rrp47 proteins could be detected with the GST control (even numbered lanes). In conclusion, C-terminal Rrp47 truncations which shorten the protein below 100 residues cutting into the Sas10 domain were pulled down much less efficiently than 100X, ΔC1, mm or full-length Rrp47 which were pulled down with similar efficiency by GST-Rrp6NT (odd numbered lanes).

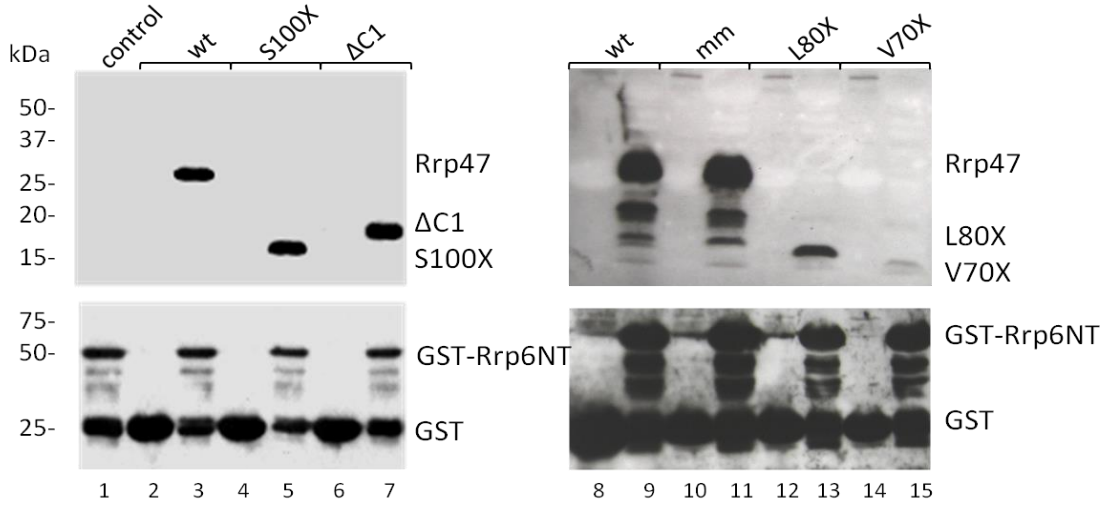


**Figure 3.16 Rrp6 binding is diminished for truncations within the Sas10 domain.**
Pull-down-assays on GST-Rrp6NT with vector (pRSETb) and wild-type control (p238), truncation mutants S100X and ΔC1, as well as the multi-mutant (E79A, R82G, K84I, Y86S) and truncations L80X and V70X. Purified proteins were incubated with GST-Rrp6NT fusion or GST control bound to glutathione sepharose. Eluates were resolved by 12 % SDS-PAGE and analysed by western blotting with antibodies against the His(6)-epitope (upper panel) to show bound protein and GST-tag (lower panel) to show bait input, respectively.

### 3.2.8 Removal of the Rrp47 C-terminus (120-184) abolishes RNA binding *in vitro*

As previously shown in our lab, even short C-terminal truncations (181X) of Rrp47 can decrease RNA binding (Costello *et al*. 2011) and RNA-binding is lost for the ΔC1 truncation in filter binding assays, but can still be observed in UV cross-linking assays (J. Stead unpublished data). Accordingly, the S100X mutant was assessed for RNA binding in a filter binding assay (Fig. 3.17 A) and alongside the 80X and 70X truncations in a UV-cross-linking assay (below Fig. 3.17 B). As before, $^{32}$P-labelled SLAU RNA was used as a binding substrate and incubated on ice with triplicate serial dilutions of purified wild-type Rrp47 and 100X proteins for filter binding. The Rrp47 wild-type protein bound the SLAU-RNA in a concentration-dependent manner, as seen before, with a dissociation constant of approximately 1 µM calculated based on the concentration of the monomeric protein. The slot blot for the 100X truncation (Fig. 3.17 A) showed no protein-bound RNA (right panel) even at a protein concentration of 40 µM as seen by the lack of signal on the C filter; the labelled RNA is solely captured by the N-filter.

Less stable protein-RNA interactions can still be detected by cross-linking of pre-formed complexes. Therefore, RNA binding of the 100X, 80X and 70X truncations was further assessed by UV cross-linking. Purified protein and radio-labelled SLAU-RNA (Stead *et al*. 2007) diluted to 50 counts per second as used for filter binding assays were mixed and incubated on ice alongside protein-only controls. Samples were irradiated on ice with UV light (total 420 mJ/cm$^2$), resolved through 10 % SDS-PAGE including a non-irradiated RNA control and visualised using X-ray film (Fig. 3.17 B upper panel). The wild-type Rrp47 protein (lane 6) and the multi-mutant (lane 14) showed distinct cross-links in the presence of RNA of 50 kDa size as expected, since both the His-tagged full length Rrp47 protein and SLAU-RNA run at 25 kDa. In contrast, no cross-links were observed for the 100X, 80X and 70X truncations *(B*, lane 8, 10, 12). Cross-linked products were also not observed for the GST controls or the RNA irradiated and non-irradiated controls. Notably, protein levels assayed were lower for the 80X and 70X truncations as seen from the Coomassie stain of the protein input (lower panel). However, UV cross-links could be obtained for equally low levels of Rrp47ΔC1 with two different RNA substrates (J. Stead unpublished data).

In summary, the more extensive C-terminal truncations S100X, 80X and 70X did not bind RNA in either the filter binding (A) or the UV cross-linking assay (B). In conclusion, RNA binding is not observed for Rrp47 truncations that shorten the protein to its N-terminal 100 amino acids or less and lie within the Sas10 domain, respectively.

**A**

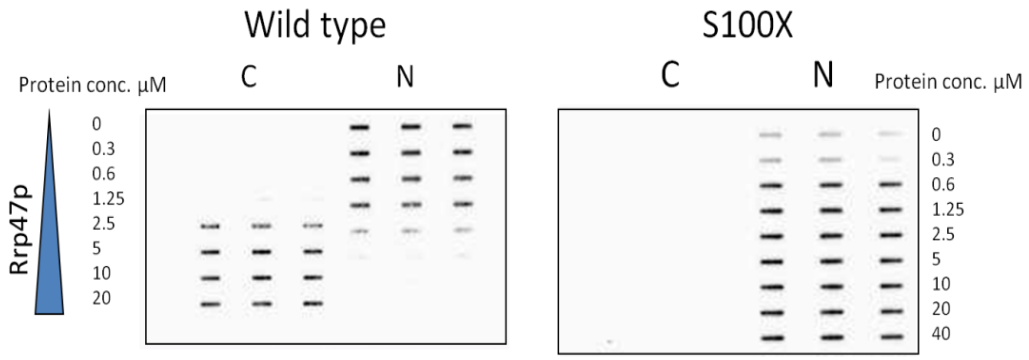


**B**

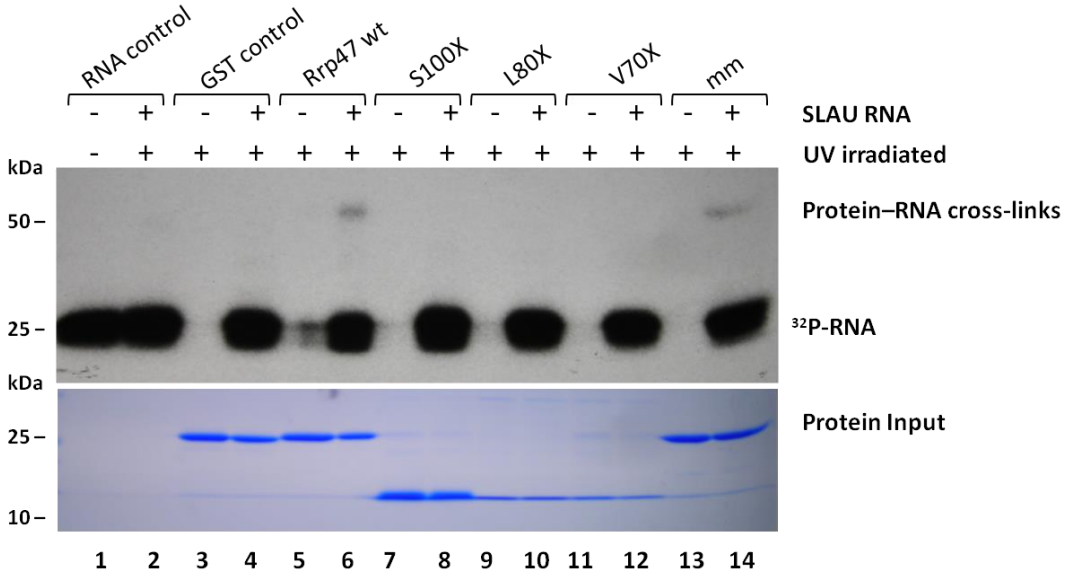


**Figure 3.17 RNA binding is not observed for mutants shorter than 100 residues.**
RNA binding of Rrp47 truncations. (A) Slot blot assay for purified recombinant Rrp47 wild-type protein (left) and S100X truncation (right) binding to $^{32}$P -labelled stem loop AU-rich (SLAU) RNA. Triplicate samples of serially diluted protein starting at 20 µM were incubated for 15 minutes with equal amounts of RNA and loaded onto a slot blot. The filters were visualised side by side using a phosphor imager with the C filter showing protein-bound RNA and the N-filter retained non-bound RNA. (B) UV cross-linking assays. Purified Rrp47 proteins were incubated with $^{32}$P-labelled SLAU-RNA and irradiated four times with UV light at 254 nm (420 mj/cm$^2$) and then incubated with RNase A. Reaction products, as well as irradiated protein-only controls, were resolved by 10 % SDS-PAGE. RNA-protein cross-links, as well as non-bound $^{32}$P-RNA were visualised by autoradiography (upper panel). The Coomassie-Blue stain (lower panel) shows the relative input levels of protein.

### 3.2.9 The Rrp47 truncations complement growth in an *rrp47Δ* strain, but ΔC1 has a specific snoRNA processing phenotype

***Rrp47 ΔC truncations complement growth in an rrp47Δ strain***

To assess the truncations for complementation of an *RRP47* deletion, the Rrp47 ΔC1, ΔC2 and S100X alleles were transformed into the *rrp47Δ* strain (P368) alongside wild-type and vector controls. Two transformants of each mutant were tested in a spot growth assay as shown in Figure 3.18. Despite the *in vitro* observed loss of RNA binding, all truncations complemented the *rrp47* null allele *in vivo* and displayed similar growth to the *RRP47* wild-type allele.

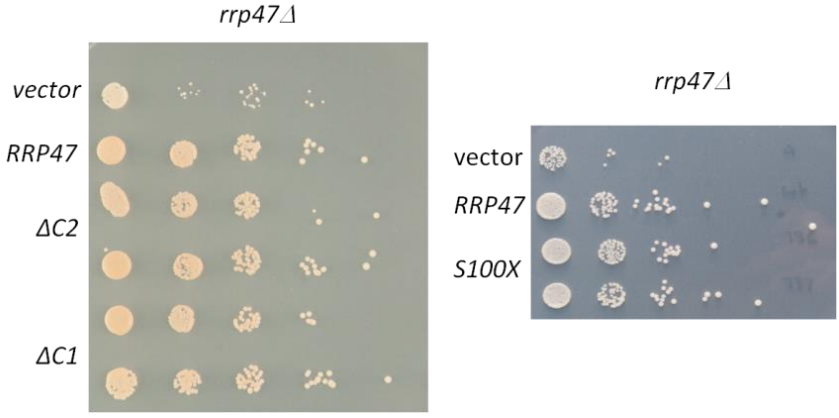


**Figure 3.18 Rrp47 truncations complement the *rrp47Δ* slow growth defect.**
Spot growth assays. Truncation mutants ΔC1 (p293), ΔC2 (p295) and S100X (p350) were transformed into an *rrp47Δ* strain (P368). 10-fold serially diluted, freshly grown cultures were spotted onto SD-trp plates and grown for 3 days at 30 ˚C. The vector control (pRS314) and wild type (p262) complemented strain are shown at the top along with two transformants each carrying the ΔC2 (1162X), ΔC1 (N121PGX) and S100X alleles (right panel).

***Rrp47ΔC truncations do not affect rRNA processing***

Next, the *rrp47Δ* strains carrying the truncations were analysed for the complementation of RNA processing defects observed in strains lacking Rrp47 (Fig. 3.19). Initial northern blot analyses were performed for the ΔC1 (121PGX) and ΔC2 (162X) mutants and the E79A point mutant which had been made by J. Stead but had not yet been analysed. Total RNA was extracted from the strains and resolved through 8 % denaturing polyacrylamide gels for northern hybridisation as before. The 5.8S and 5S species were visualised by ethidium bromide staining of the gel (Fig. 3.19 A). As seen previously, the *rrp47Δ* strain (lane 2) showed accumulation of the distinct 5.8S +30 species, however, the defect was complemented by the

truncations, the E79A point mutant and the wild-type protein. The rRNA processing phenotypes were investigated more specifically by northern hybridisation. Figure 3.19 B shows typical defects of the *rrp47Δ* strain in rRNA processing. The 5'ETS probe (B1) detects cleaved, but undegraded 5'ETS fragments from the pre-rRNA which were only present in the *rrp47Δ* vector control strain (lane 2). The ITS2 probe (B2) targets sequences at the 5.8S-ITS2 boundary and gives a strong 5.8S +30 signal for the *rrp47Δ* strain carrying the vector control, but not for the Rrp47 wild-type (lane 1) or mutants (lane 3-8). The probe specific for mature 5.8S rRNA (B3 and B4) also showed the distinct 5.8S +30 species, as well as the longer 7S precursor for longer exposure times (B4) only for the vector control (lane 2). In summary, neither the truncation mutants, nor the E79A mutant showed any defects in rRNA processing observed in the absence of a functional *RRP47* allele.

***Rrp47ΔC1 has a specific snoRNA processing phenotype***

Rrp47 is also required for snoRNA maturation (Mitchell *et al.* 2003) and probes complementary to a number of snoRNAs (Fig. 3.19 C and D) revealed the typical 3 nucleotide extended snoRNAs, as well as longer, polyadenylated and more heterogenous precursors of various length in the *rrp47Δ* strain shown here for snR38-3' (C1) and U14-3' I-pA and II-pA (D3) which represent polydenylated (pA) transcripts from two snoRNA termination sites I and II (Grzechnik and Kufel 2008). Strikingly, the *rrp47ΔC1* mutant, but not the *rrp47ΔC2 or E79A* mutant, retained discrete 3' extensions of 3 nucleotides of the box C/D snoRNAs snR38, snR52 and U24 (Fig.3.19 C2, C3, D2, lanes 5 and 6) along with reduced levels of mature snoRNA (D1, D2). This indicates that the C-terminal domain (120-184) of Rrp47 has an effect on snoRNA synthesis, albeit not as pronounced as the *rrp47Δ* deletion (C and D, lane 2). The *rrp47ΔC1* mutant only affects the final +3 step in the 3' end maturation, whereas the *rrp47Δ* mutant has a more comprehensive 3'-maturation defect with longer 3'-extended precursors as seen for snR38 (C1, lane 2) and U14 (D3, lane 2).

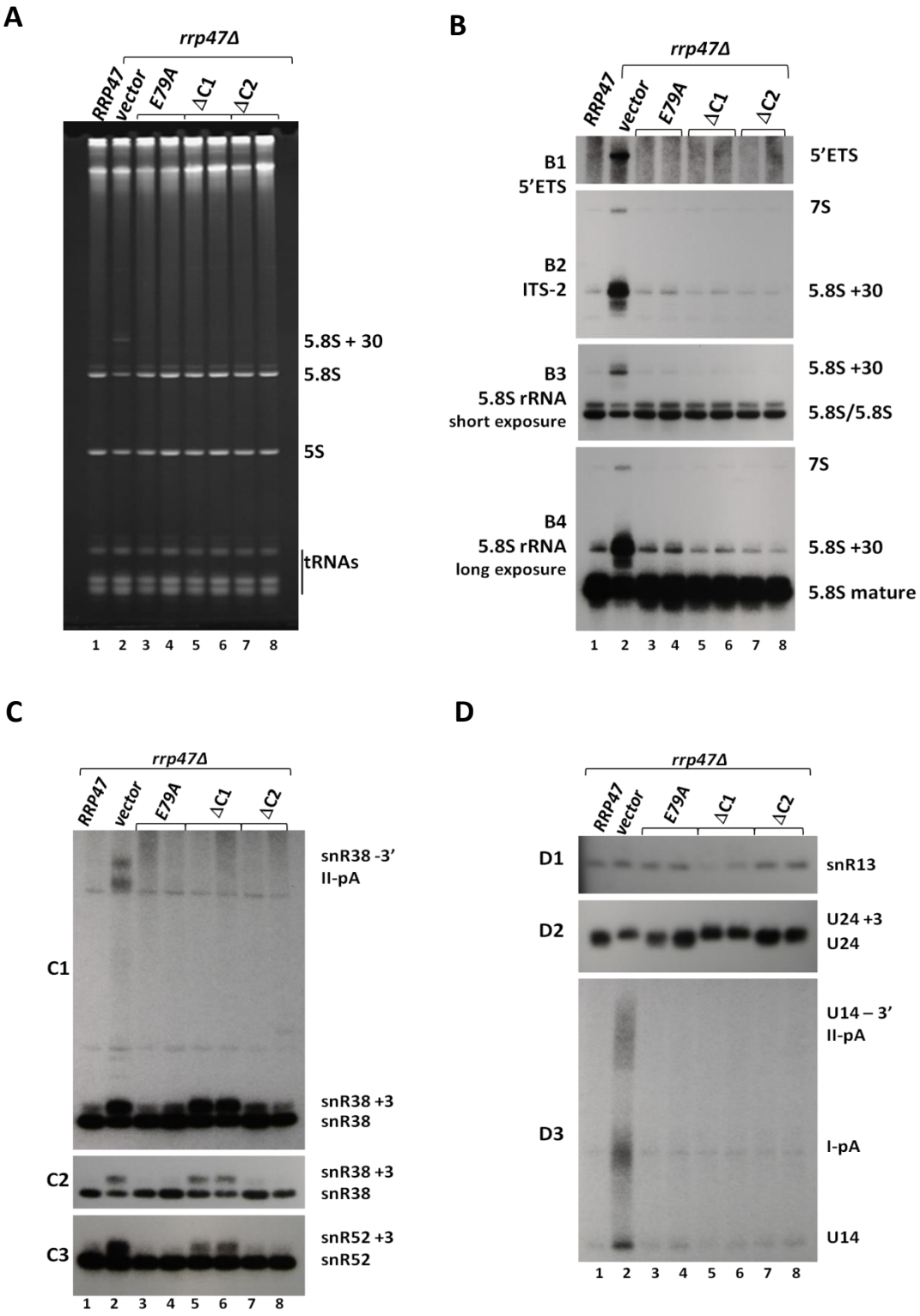


**Figure 3.19 The *rrp47ΔC1* truncation has a specific snoRNA processing phenotype.**
Total RNA analyses of *rrp47Δ* strains complemented with Rrp47 mutants *E79A, ΔC1* and *ΔC2* along with wild-type and vector controls. (A) Ethidium bromide stain of 5 µg RNA of each strain resolved through an 8 % denaturing polyacrylamide gel. (B-D) Northern analyses. Blots were hybridised with 5' radio-labelled probes complementary to discrete RNA species as denoted to the right of the panels. For snR38 (C) and 5.8S rRNA (B3, B4) two different exposures are shown to visualise either the longer 3' extended precursors (C1, II-pA) or the +3 RNA species (C2) and the 7S (B4) or the 5.8S+30 species (B3), respectively.

### 3.2.10 C-terminal domain mutants complement *rex1Δ rrp47Δ* synthetic lethality, but Rrp47ΔC1 has a specific defect in snoRNA processing.

Mutants lacking the C-terminal domain were further assessed for complementation of the synthetic lethal *rex1Δ rrp47Δ* strain (P596) using the previously detailed plasmid shuffle assay (compare Fig. 3.13). Colony sectoring which results from loss of the *RRP47* wild-type allele in the presence of another functional Rrp47 protein was observed for E79A, both the ΔC1 and ΔC2 mutants and the wild-type (Fig. 3.20 A). In contrast, the vector control which does not express a functional Rrp47 protein retains the shuffle plasmid with the *RRP47* wild-type allele and develops solid red colonies. Double *rex1Δ rrp47ΔC* mutants were then isolated from the white sections of the colonies and the so obtained *rex1Δ rrp47** mutant strains were tested for growth defects in a spot assay. Two independent transformants each are shown. No difference in growth was observed for the C-terminal truncations ΔC1, ΔC2 and E79A compared to the *RRP47* wild-type allele (B).

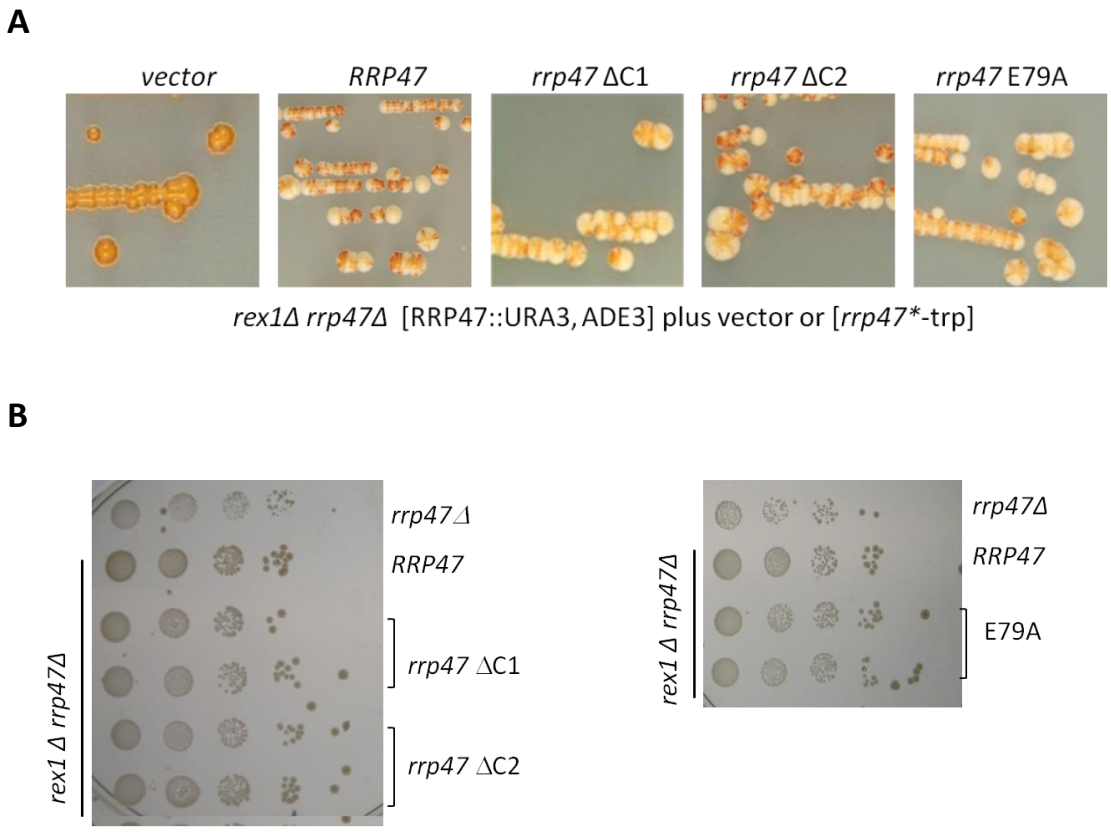


**Figure 3.20 The Rrp47 truncation mutants and E79A produce functional proteins.** (A) Colony sectoring assay**.** Complementation of a *rex1Δ rrp47Δ* synthetic lethal double mutant with vector control, wild-type Rrp47, and mutated Rrp47 proteins ΔC1, ΔC2 and E79A (*rrp47*-trp*) in a plasmid shuffle strain (P596). (B) Spot growth assays of the *rrp47Δ* strain compared to the *rex1Δ rrp47Δ* strains complemented with the *RRP47* wild-type allele, as well as two separate transformants of the ΔC1, ΔC2 truncations and the E79A mutant.

***Rrp47ΔC1 shows a specific snoRNA processing defect in the rex1Δ background***

In addition to RNA species accumulating in *rrp47Δ* mutants, RNA analyses of the *rex1Δ rrp47** double mutants included probing for tRNA-Arg3 and 5S rRNA (Fig. 3.21 A). Processing of both species is known to be affected by the absence of Rex1 (v. Hoof *et al*. 2000, Piper *et al.* 1983). tRNA-Arg3 is the only yeast tRNA that can contain two tRNA-Arg3 genes (two cistrons) in one transcription unit, whereas all other yeast tRNAs are produced as monomeric transcripts. The dicistronic precursors (A1, marked with an asterisk) are processed into two monomeric intermediates, however, due to the lack of 3' termination signals the 5' cistron requires further processing by Rex1. 5S rRNA is transcribed by RNAPIII as a 3' extended pre-rRNA with 7 to 13 nucleotide extensions which require trimming. Rex1 is thought to process the final step in 5S rRNA maturation since *rex1Δ* strains accumulate 5S rRNA species which are 3 nucleotides longer (5S +3) than wild-type 5S rRNA at the 3' end. Total RNA analyses of the *rex1Δ rrp47** mutant strains with the ΔC1, ΔC2 and E79A mutations showed no discernible effects on 5S, 5.8S and tRNA-Arg3 processing (Fig. 3.21 A) when compared to the double mutant complemented with wild-type *RRP47*.

Rex1 mutants also accumulate 1 to 4 nucleotide extended snoRNA species (v. Hoof *et al.* 2000). Interestingly, the *rex1Δ rrp47 rrp47ΔC1* double mutant showed a more exacerbated snoRNA processing defect than the *rex1Δ* single mutant (Fig. 3.21 A, compare lane 4, 5 with lane 2) or *rrp47Δ* single mutant complemented with *rrp47ΔC1* (Fig. 3.19 C lane 2). Instead of the discrete +3 bands observed for ΔC1 in the *rrp47Δ* strain, a more diffuse signal with 3' extensions of variable lengths is detected for snR52, snR38 and U24 (A, lanes 4, 5 asterisk) in the *rex1Δ rrp47 ΔC1* double mutant, along with a clear depletion of the mature snoRNA as seen for U24 and to some extent for snR38. Termination of snoRNAs occurs either via an Nrd1/Nab3/Sen1-dependent pathway (at site I) or via a fail-safe terminator further downstream using the mRNA 3' end formation machinery (site II). Precursors of snoRNAs terminating at both sites are thought to be polyadenylated by default by Pap1 and Trf4 as an essential step for snoRNA processing and quality control by the exosome and other exonucleases (Grzechnik and Kufel 2008). The heterogeneous 3' extended species in the combined *rex1Δ rrp47ΔC1* mutant are indicative of polyadenylated snoRNA precursors or processing intermediates terminated at site I which require Rex1 and/or the C-terminal portion of Rrp47 for proper maturation. The ΔC2 mutant showed a similar phenotype to the Rrp47 wild-type allele (lane 6, 7 compared to lane 2) with short 1 to 4 nucleotide extensions as described for the *rex1Δ* single mutant. Interestingly, the E79A mutant (lane 3) appears to suppress the *rex1Δ* phenotype and looks similar to wild-type strain (lane 1).

Taken together the deletion of the Rrp47 C-terminus (121-182) does not complement a *rex1Δ rrp47Δ* double mutant to the same degree as wild-type *RRP47* with respect to snoRNA processing. Notably, the effect on snoRNA processing observed in the *rex1Δ rrp47Δ rrp47Δ*C1 mutant is the first synergistic defect observed in a conditional double mutant and points to redundant functions for Rrp47 and Rex1 in snoRNA processing as a possible reason for synthetic lethality of the *rex1Δ rrp47Δ* double mutant.

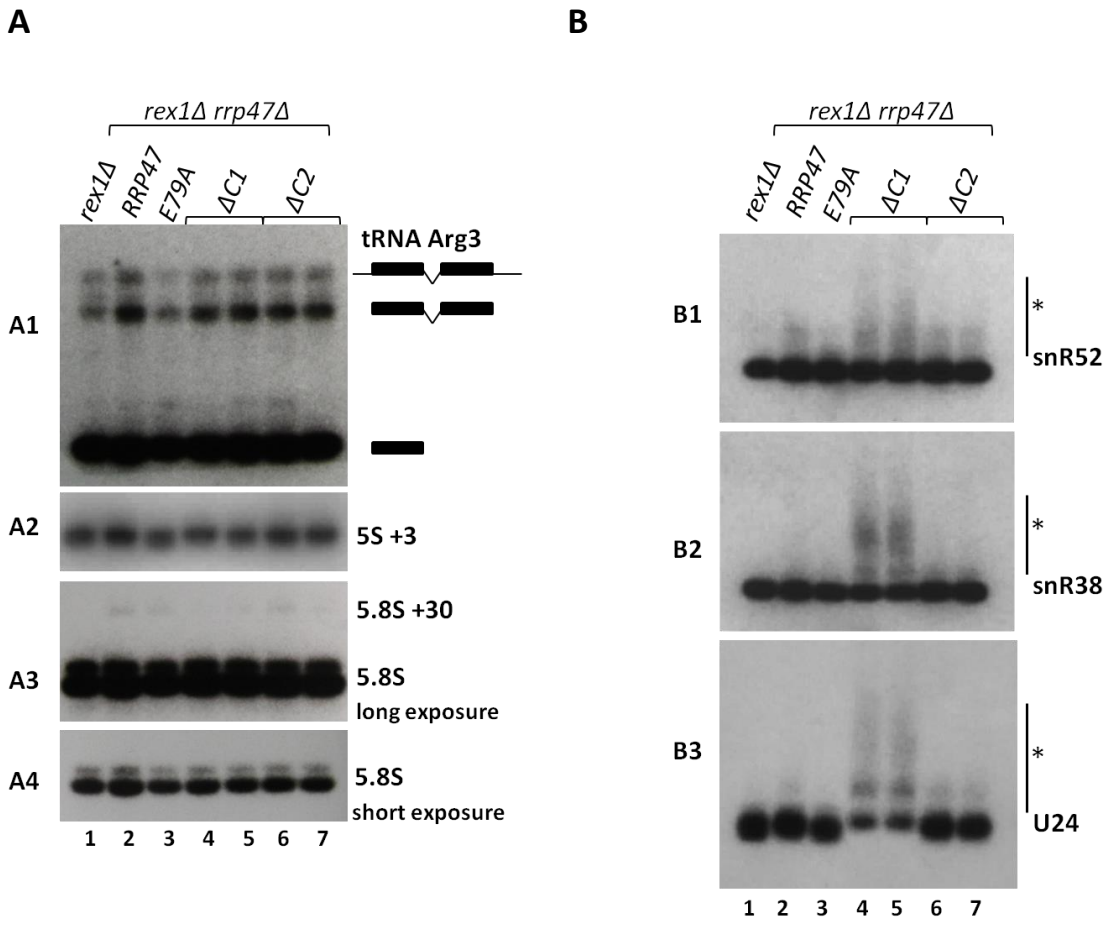


**Figure 3.21 Rrp47 truncations show snoRNA processing defect in *rex1Δ* background.**
Northern analysis of *rex1Δ rrp47Δ rrp47** strains carrying the mutant *rrp47* ΔC1, ΔC2 and E79A alleles versus the *rex1Δ* single mutant (lane 1). Total RNA was resolved through an 8 % denaturing RNA gel and analysed by northern hybridisation with probes complementary to the RNA species indicated to the right of the panels (A) tRNA-Arg3 (schematics of unprocessed and processed dicistronic precursors and mature tRNA Arg3 are shown (A1), 5S (A2) and 5.8S rRNA long (A3) and short (A4) exposure (B) snR52, snR38 and U24. The heterogeneous 3'-extended snoRNA precursors are marked with a bar and an asterisk.

### 3.2.11 The Sas10 domain is critical for fitness and Rrp6 binding

For a direct comparison, the most interesting Rrp47 truncation mutants produced in the lab, were assayed together for complementation of the slow growth phenotype of the *rrp47Δ* strain (Fig 3.22 A and B). Due to the rather moderate effect on growth, differences were not very pronounced in the spot growth assay (Fig. 3.22 A), therefore growth rates were determined in liquid cultures over a period of 9 hours (Fig. 3.22 B). Data was plotted on a logarithmic scale as the ratio of the optical density (OD) at the time point taken divided by the OD at time point zero as a function of time. A combined graph of all mutants assessed is shown in B1 and subsets of mutants are shown in separate graphs B2, B3 and B4 for better resolution of the data. The C-terminal 100X truncation and all lesser C-terminal truncations (130X to 181X not shown here) which contain the full Sas10 domain displayed a growth rate similar to the wild-type (B2). In contrast, the 80X and 70X truncations which lie within the Sas10 domain grew significantly slower and the 60X mutant showed a growth rate similar to the *rrp47Δ* strain (B3). Furthermore, growth rates obtained for the N-terminal truncations removing 10 and 20 residues, respectively, showed that while deletion of the first 9 N–terminal amino acids has no discernible effect, the loss of the first 19 N-terminal residues reaching into the Sas10 domain results in slow growth and loss of *rrp47Δ* complementation (B4).

Moreover, Rrp47 truncations were assessed for complementation of the synthetic lethal *rex1Δ rrp47Δ* strain. The plasmid shuffle strain (P596) described in Figure 3.13 was transformed with plasmids encoding the mutant *rrp47* alleles and grown on 5'FOA (fluoro-orotic acid) to detect non-complementing *rrp47* alleles by counter-selecting for the *URA3*$^{+}$ marker. Due to toxicity of 5'FOA for cells expressing Ura3, complementing mutants lose the original plasmid with the *URA3* gene (Fig. 3.23). Mutants were grown in parallel on minimal medium (SD-trp) as control and on 5' FOA to check for complementation of the mutated alleles. Consistent with observations in the *rrp47Δ* strain, the plasmid shuffle assay showed that the Δ2-9N, 100X and lesser C-terminal deletions (ΔC1, ΔC2) produced a functional protein and thus grew on 5'FOA, whereas the Δ2-19N, 60X and 80X mutants did not and the 70X mutant allowed partial complementation (right panel). Additional Rrp47 mutants used for this analysis were generated by J. Costello (N-terminal truncations N2-9, N10-19, and the C-terminal truncations 130X, 140X, 150X, 181X, as well as point mutations F135A, F142A (Costello *et al*. 2011).

In summary, *rrp47* mutants which encode a complete Sas10 domain showed normal growth rates and produced functional proteins. The growth rate analysis strongly suggests that the N-terminal Sas10 domain of Rrp47 is necessary and sufficient for growth, as well as for the complementation of an *rrp47Δ* strain and a synthetic lethal *rrp47Δ rex1Δ* double mutant.

**A**

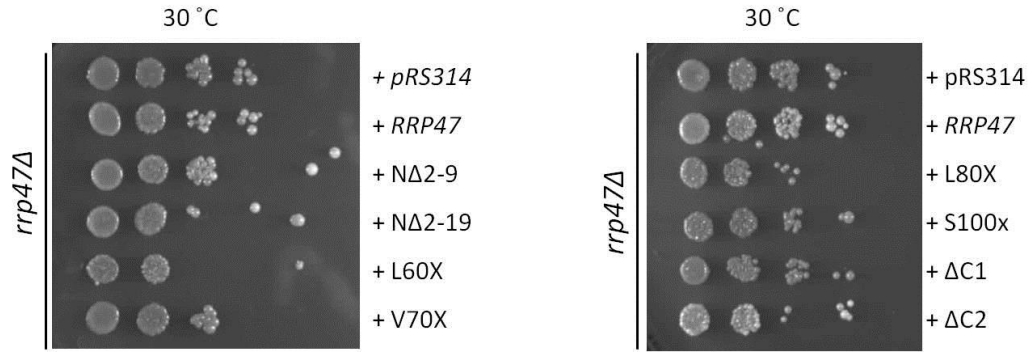


**B**

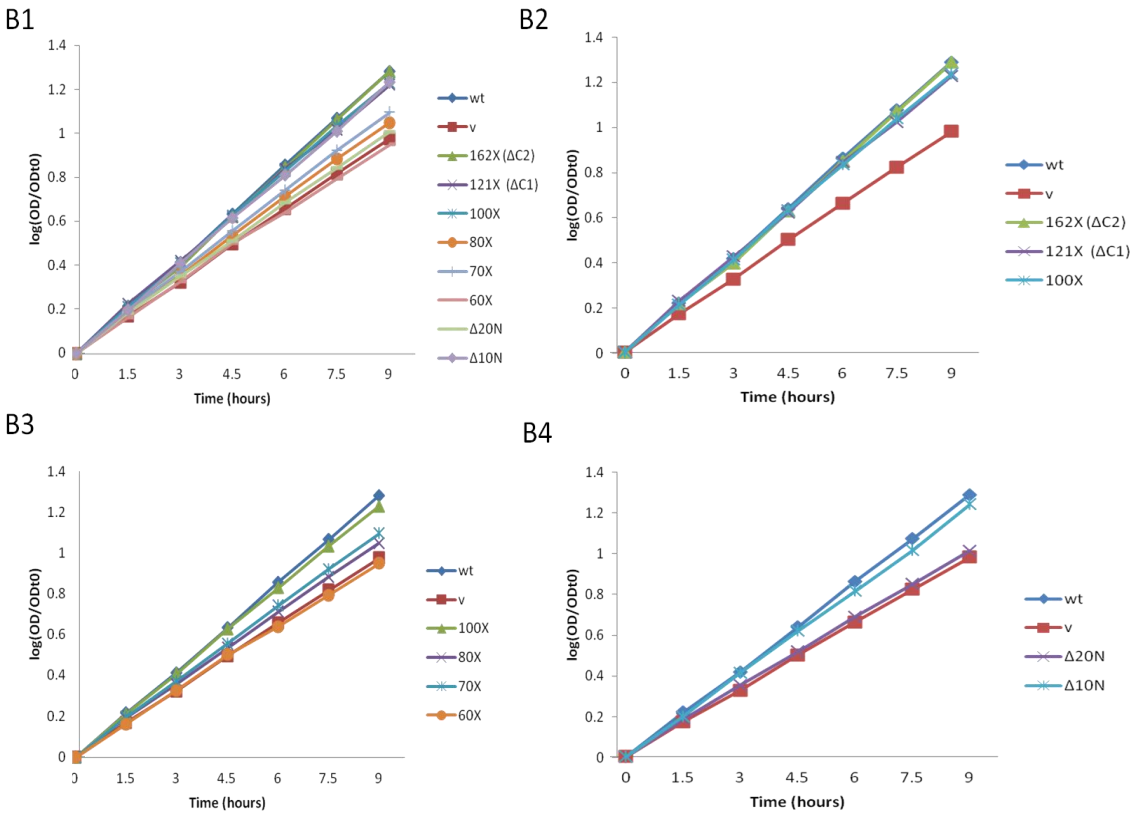


**Figure 3.22 The Sas10 domain is necessary and sufficient for normal growth.**
Complementation and growth analysis of Rrp47 truncations. (A) Spot growth assay of Rrp47 mutants transformed into an *rrp47Δ* strain. Strains were grown up on minimal medium at 30 ˚C for 3 days. (B) Growth rate analysis in liquid minimal medium cultures measured over 9 hours. Log10 values of the ratios of $OD_{600}$ readings at the given time points to OD at time zero (OD/ODt0) were plotted against time in hours. B1 shows combined data for all mutants B2-B4 show subsets of mutants as indicated in the legends to the right of the graphs for better comparison.

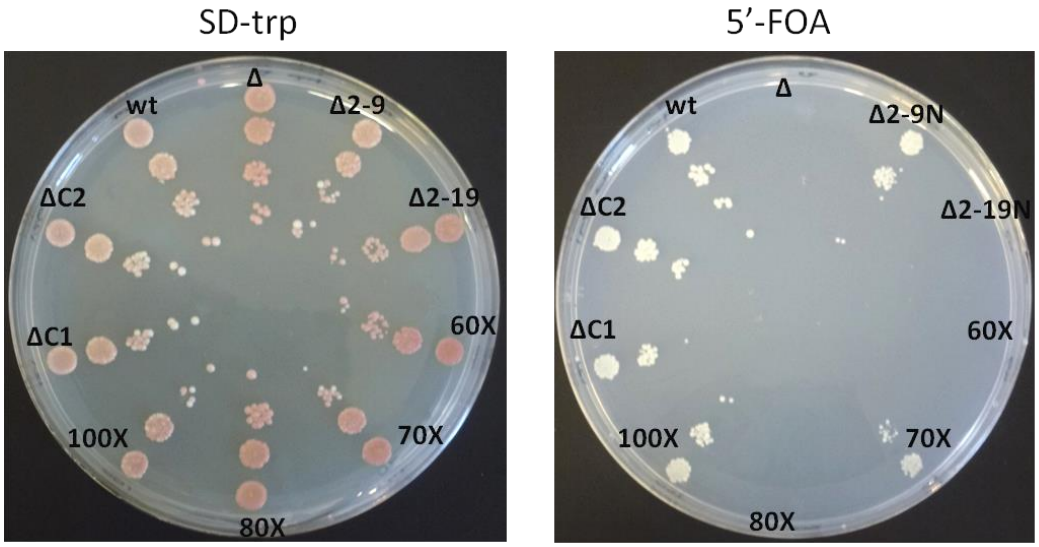


**Figure 3.23 Truncations within the Sas10 domain do not produce functional proteins.**
Complementation and growth analyses of Rrp47 truncation mutants. Rrp47 truncation mutants were assayed for complementation of a synthetic lethal *rex1Δ rrp47Δ* double mutant in a plasmid shuffle strain containing a plasmid with an *RRP47*, *ADE3* and *URA3* alleles (as detailed in Fig. 3.13). This strain was transformed with plasmids encoding the mutant *rrp47* alleles and mutants were grown on SD-trp control (left) and 5'FOA (fluoro-orotic acid) for 3 days to detect non-complementing *rrp47* alleles by counter-selecting for the *URA3*$^{+}$ marker (right). Due to the toxicity of 5'FOA for cells expressing Ura3, complementing mutants lose the original plasmid with the *URA3* gene.

### 3.2.12 Rrp47 truncations affecting the Sas10 domain show *rrp47Δ* phenotypes

The complete set of Rrp47 truncation mutants was then analysed for characteristic *rrp47Δ* RNA processing phenotypes (Fig. 3.24). As already seen above, yeast *rrp47Δ* strains accumulate 3'-extended processing intermediates of 5.8S rRNA and box C/D snoRNAs, as well as the 5'ETS (external transcribed spacer) excised from the 35S pre-rRNA (Figure 3.24 compare lane 3 to wild-type and complemented wild-type lane 1,2). All truncations that lie within the Sas10/C1D domain from amino acids 10 to 89 in *S. cerevisiae* (Δ2-19, 50X, 60X, 70X, 80X, lanes 5-10) caused the characteristic rRNA processing defects of an *rrp47Δ* allele (lane 3) with accumulation of 5.8S+30 rRNA (A) precursors and 5'ETS fragments (B). Also 3 nucleotide extended snoRNA species were observed for snoRNAs snR38 (D), snR50 (E), snR52 (F), as well as longer 3' extended precursors shown here for snR38 (C 3' II-pA) which were also seen for other snoRNAs. The U6 snRNA showed more diffuse 3' extended oligoadenylated precursors and the accumulation of a degradation intermediate in Sas10 domain mutants typically seen in *rrp47Δ* mutants (G). This indicates that the Sas10 domain is critical for Rrp47 function in RNA processing.

Interestingly, mutants 100X to 140X showed an accumulation of snoRNA+3 precursors (D-F) but not the longer extended forms of snR38 (lanes 11-14), indicating an effect on the final step of snoRNA maturation. In contrast, strains with the Δ2-9 mutation (lane 4) and shorter C-terminal truncations (150X, ΔC2 162X, ΔC3 181X, lanes 15-17) showed no significant accumulation of extended or aberrant forms of any of the RNA species tested. Two point mutations of highly conserved residues, F135A and F142A (lanes 18 and 19), confirmed the relevance of these residues for snoRNA maturation. Particularly the F142 mutant showed a strong accumulation of the 3 nucleotide extended snoRNAs (C-E lane 19) comparable to the ΔC1 mutant lacking residues 121-184 of full length Rrp47. Subsequent protein capture assays could demonstrate that Rrp47 can interact directly and independently of RNA with the snoRNP proteins Nop56 and Nop58 (Costello *et al*. 2011) strongly indicating a role for the C-terminus of Rrp47 in snoRNP assembly.

In summary, while the Sas10 domain of Rrp47 is critical for processing of all RNA species tested here, the C-terminus of Rrp47 has a role in the final maturation of snoRNAs involving the removal of the last 3 nucleotides.

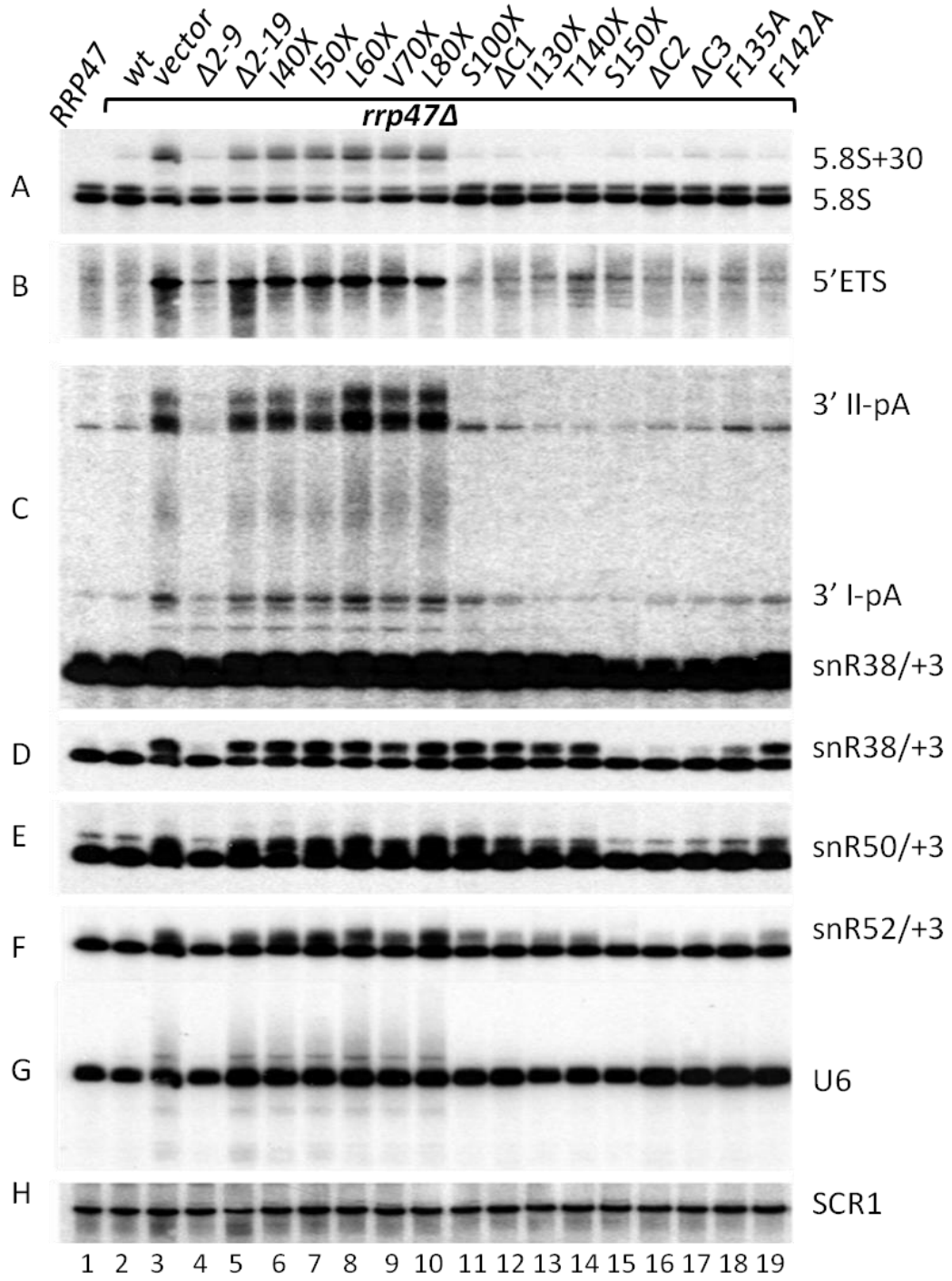


**Figure 3.24 Sas10-domain mutants have an *rrp47Δ* RNA processing phenotype.**
Northern analyses of *rrp47* mutant strains. Total RNA was resolved through an 8 % denaturing polyacrylamide gel and analysed by northern hybridisation using probes complementary to various stable RNAs as indicated on the right of the autoradiographs A-H. 3'I-pA and 3' II-pA (C) indicate 3' extended polyadenylated snoRNA precursors terminated at site I or II respectively and "+3" indicates the 3 nucleotide extended species seen above the mature snoRNA (C-F). *SCR1* RNA serves as a loading control. Lane 1 shows RNA from the wild-type strain and lanes 2-19 from the *rrp47Δ* strains carrying plasmids encoding the Rrp47 wild-type, vector or mutant *rrp47* alleles as indicated at the top.

### 3.2.13 N-terminus and C-terminus of Rrp47 cooperate in RNA binding.

As observed by J. Costello, even short C-terminal Rrp47 truncations decrease RNA binding in filter binding assays. The G181X mutant only lacks the last three C-terminal residues of Rrp47 and shows a significant decrease in RNA binding compared to full length Rrp47 in filter binding assays; RNA binding is not detectable for more extensive C-terminal truncations such as ΔC1 and S100X. To assess whether the C-terminus and the putative RNA binding domain in helix 3 (residues 75-91) cooperate in RNA binding, a sextuple mutant (N*) was created with the point mutations E79A, R82G, K84I, Y86S, K89M, and K91I, as well as a combination of the sextuple mutant with a short C-terminal truncation (G181X N*). The short C-terminal truncation G181X and additional mutations K89M and K91I were introduced by SDM into the quadruple mutant "mm" E79A, R82G, K84I and Y86S. A schematic of the mutations is shown in Figure 3.25 A.

The G181X truncation, N* multiple mutant and combined G181X N* mutants were expressed in *E. coli* and purified using the two-step protocol as before. The proteins were expressed with similar efficiency compared to the wild-type protein (Fig. 3.25 B). Pull-down-assays on GST-Rrp6NT were performed as previously described to confirm interaction with GST-Rrp6NT (Fig. 3.25 C) before using the proteins in the RNA-binding assays. The mutant proteins were pulled down by the GST-Rrp6NT fusion protein (C, lanes 2, 4, 6, and 8) to a comparable extent, but not by the GST control (lanes 1, 3, 5, and 7).

Parallel filter binding assays of the G181*X* and the G181*X* N*mutant were performed and slot blots are shown in Figure 3.26 A. The sextuple mutant (N*) bound RNA slightly less efficiently than the wild-type protein. However, the mutations within the Sas10 domain combined with the G181X truncation had a much greater effect on RNA binding than the G181X truncation or the multiple mutant (N*) on its own. Protein-bound RNA on the C-filter is greatly reduced in the combined N- and C-terminal mutants. Earlier experiments comparing binding of the G181X mm and the G181X mutants using SLAU RNA (stem loop from the ITS2 spacer with an AU-rich tail) showed a similar pattern with the RNA binding of the combined mutant considerably decreased (3.16 A right). Notably, binding of G181X to the SLAU substrate was clearly reduced compared to wild-type Rrp47 which was also seen for G181X in experiments done by J. Costello with other RNA substrates (unpublished data). The filter binding saturation curves for wild-type or mutant Rrp47 proteins for the $tRNA^{Phe}$ substrate showed considerably decreased RNA binding for the G181X N* mutant whereas RNA binding by the sextuple N* or G181X mutant alone is only slightly affected compared to the wild-type protein (Fig. 3.26 B). This confirms that both the C-terminus and the N-terminal domain of Rp47 are required for and cooperate in stable RNA binding.

**A**

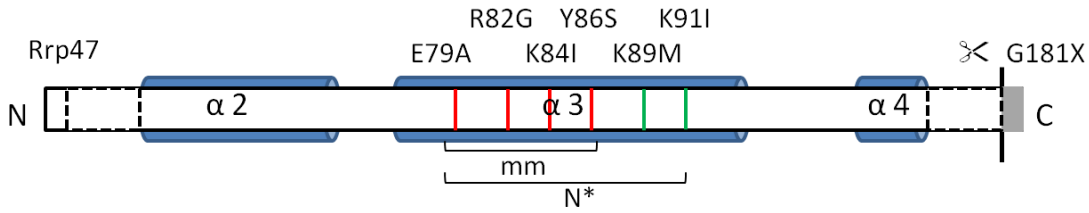


**B**

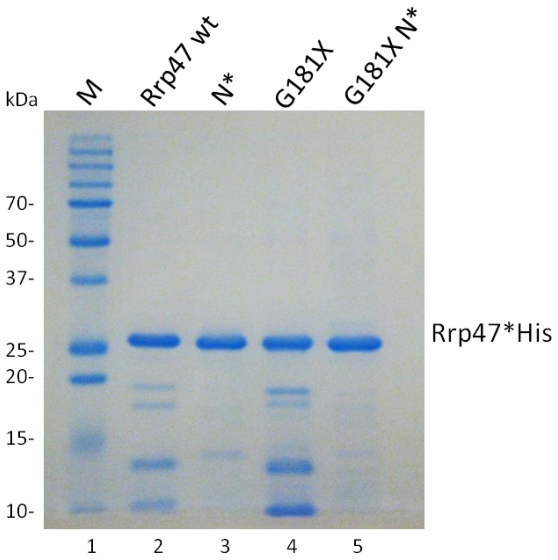


**C**

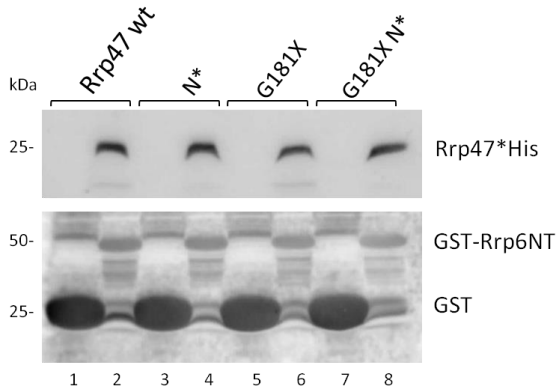


**Figure 3.25 Architecture, protein expression and Rrp6 binding of multiple point and C-terminal mutations.** (A) Schematic of Rrp47 mutants combining multiple mutations within the putative N-terminal RNA binding domain in combination with the short C-terminal truncation G181X (p302). Mutants were generated by SDM on the previously tested quadruple mutant "mm" (p386) E79A, R82G (to glycine), K84I (to isoleucine) and Y86S (to serine). The sextuple mutant N* (p528) has two additional mutations in positions K89M (to methionine) and K91I (to isoleucine). Combinations of these multiple mutations with the 181X C-terminal deletion were generated, "G181X mm" (p437) and "G181X N*" (p526). (B) Coomassie Blue-stain of the purified recombinant Rrp47 mutants resolved by 12.5 % SDS PAGE. (C) Pull-down-assays of the mutant Rrp47 proteins (upper panel) on the GST-Rrp6NT fusion protein or GST control (lower panel) were performed as described in before in Fig. 3.8 and 3.16.

**A**

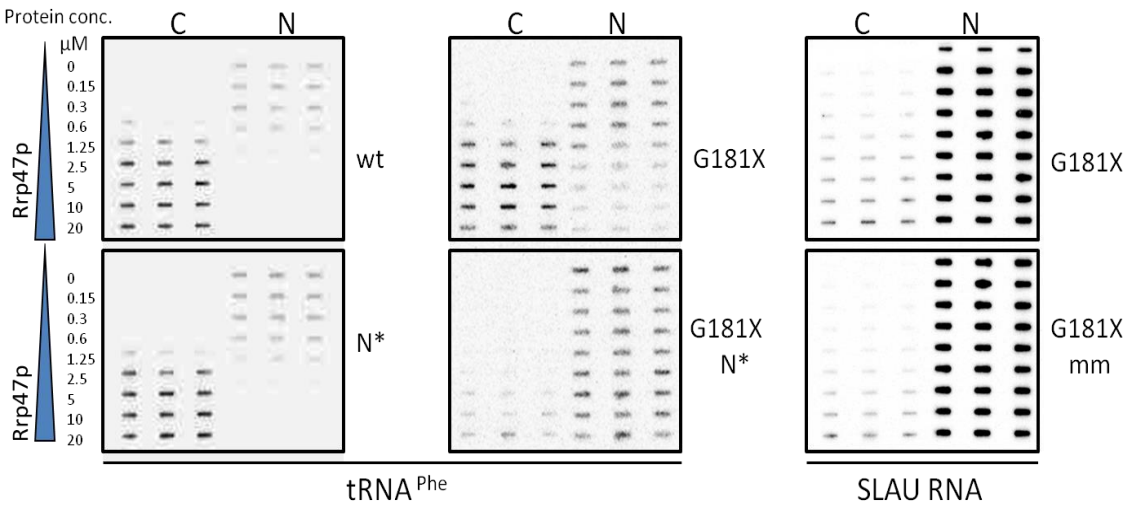


**B**

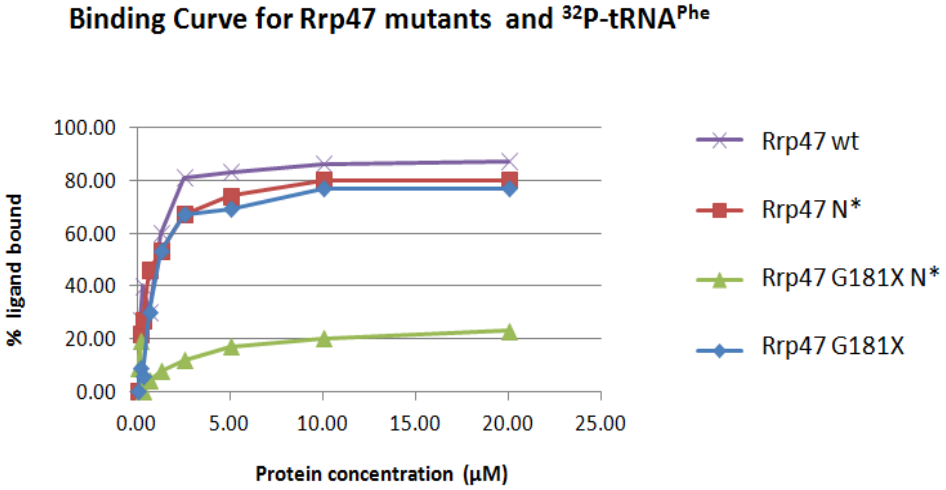


**Figure 3.26 N-terminus and C-terminus of Rrp47 cooperate in RNA binding.**
RNA binding assays of Rrp47 mutants combining N- and C-terminal mutations. (A) Slot blots of N- and C-terminal Rrp47 mutants with radio-labelled $tRNA^{Phe}$ and SLAU RNA substrates. Filter binding assays were performed as described before. Results were visualised using a phosphor imager. (B) Filter binding saturation curves for wild-type and mutant Rrp47 proteins with tRNA-Phe. Slot blot data was quantified using ImageQuant software. The amount of protein-bound radio-labelled tRNA was plotted against the concentration of Rrp47 protein.

Combined G181X truncation and mutiple N-terminal mutations were generated by SDM in the yeast shuffle plasmid carrying the *RRP47* wild-type allele (p262) and transformed into the *rrp47Δ* strain (P368). The vector control (lane 1) showed the typical accumulation of the 5'ETS fragment (A), the 5.8S +30 species (B and C) and 3' extended snoRNAs U3 (E), snR38 (F) and snR13 (H) and snRNA U6 (G), as well as degradation intermediates for U3, U6 and snR13. In contrast, the G181X mutant, the multiple mutants Rrp47 mm and Rrp47 N* and the combined C- and N-terminal mutants did not display any RNA processing defects seen in the *rrp47Δ* mutant (vector control). Only a very mild accumulation of the 5.8S +30 RNA could be observed for the multiple mutations mm and N*, as well as for the combined mutants G181X mm and G181X N* using the ITS2-probe (C) which is complementary to the 5.8S-ITS2 boundary. Thus, despite the loss of RNA binding in the G181X mm and G181X N* mutants in filter binding assays, RNA analyses of the mutants showed no discernible effect of the combined mutations on RNA processing *in vivo*.

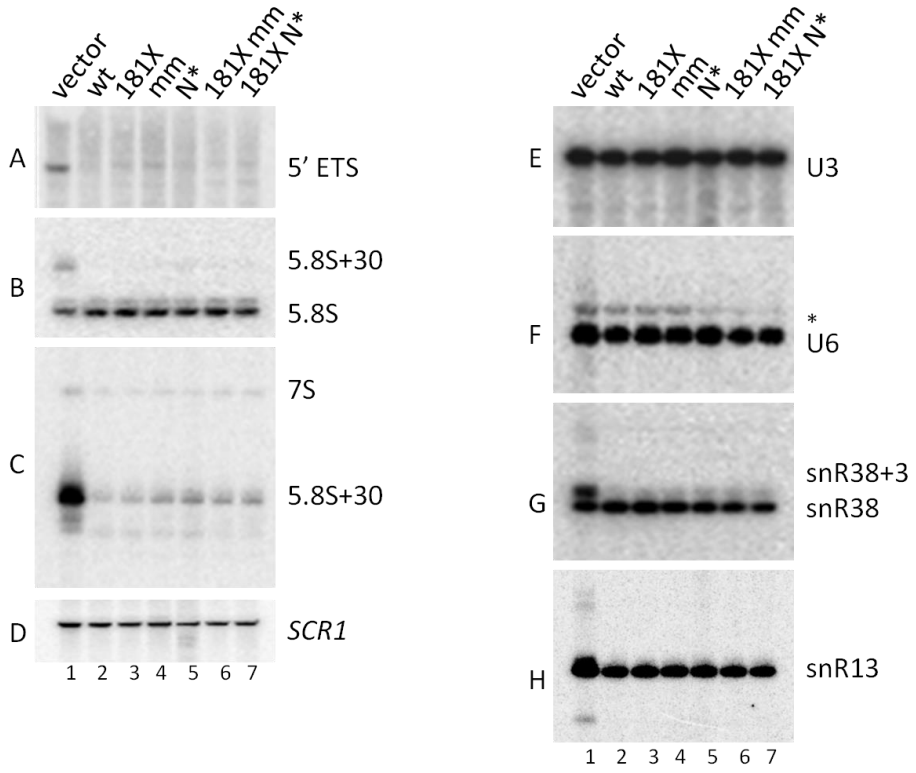


**Figure 3.27 RNA processing in the combined G181X N* mutant is not affected.**
Northern analyses of *rrp47Δ* strains (P368) carrying the Rrp47 mutants G181X , the multiple mutants mm (p380) and N* (p452), G181X mm (631), G181X N* (p632) mutants, wild-type RRP47 (p262) or vector control (pRS314). Total RNA of these strains was extracted and resolved through an 8 % denaturing polyacrylamide gel followed by successive northern hybridisations using probes complementary to various stable RNAs as indicated on the right of the autoradiographs A-H. SCR1 RNA (D) serves as a loading control. The band above U6 snRNA is a retained signal from a previous hybridisation (marked with an asterisk).

The G181X and N-terminal combination and single mutants were then transformed into the *rex1Δ rrp47Δ* plasmid shuffle strain to test for complementation of the synthetic lethal growth phenotype. Colony sectoring relies on the expression of a functional Rrp47 protein and was observed for all the mutants tested, but not for the vector control which does not carry an *RRP47* allele (Fig. 3.28 A). Consistent with the colony sectoring, all the mutants tested grew on 5'FOA which counter-selects against the shuffle plasmid with the wild-type *RRP47* and *URA3* alleles. This allows the observation of growth depending on complementation of the synthetic lethal *rex1Δ rrp47Δ* strain with the plasmid carrying the *rrp47* mutant allele only. In contrast, the vector control showed no growth on 5'FOA.

**A**

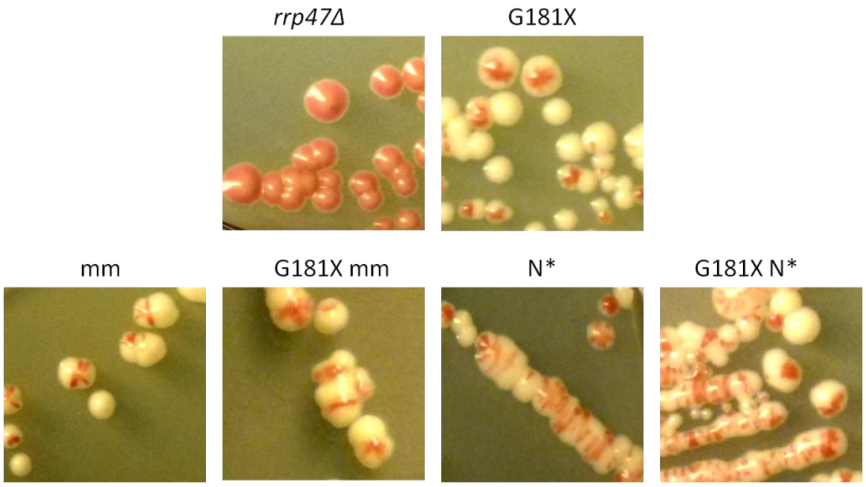


**B**

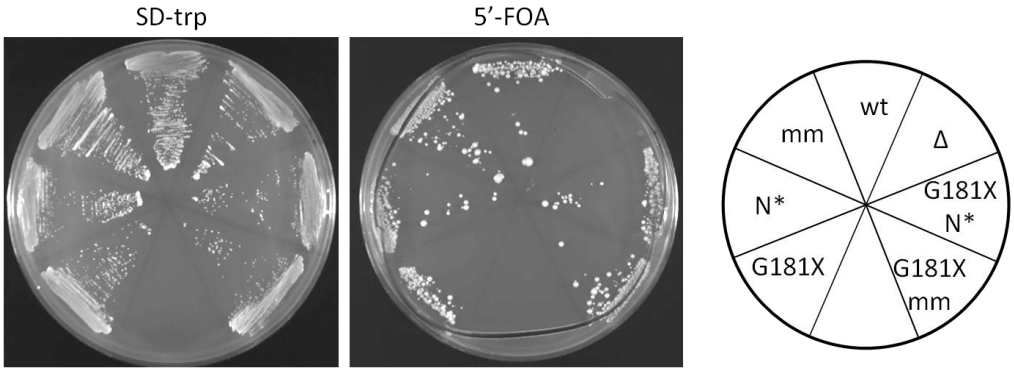


**Figure 3.28 Combined C- and N-terminal mutants complement *rex1Δ rrp47Δ* synthetic lethality.** (A) Colony sectoring of the Rrp47 mutants compared to the vector control using the plasmid shuffle assay (compare Fig. 3.13). (B) Growth assay of Rrp47 mutants shown on SD-trp versus 5'FOA. The schematic shows the arrangement of the strains carrying the *RRP47* wild-type and mutant alleles.

Taken together the data gathered for the combined N- and C-terminal mutants, both the putative RNA binding region (75-91) and the basic C-terminus of the protein clearly showed cooperation in RNA binding *in vitro*. However, growth and complementation of the *rrp47Δ* strain or the synthetic lethal *rex1Δ rrp47Δ* strain were not affected, neither was the processing of RNA species that are typically affected in the absence of Rrp47. The combined mutations therefore still produce a functional Rrp47 protein *in vivo* in terms of growth and complementation of *rrp47Δ* mutants.

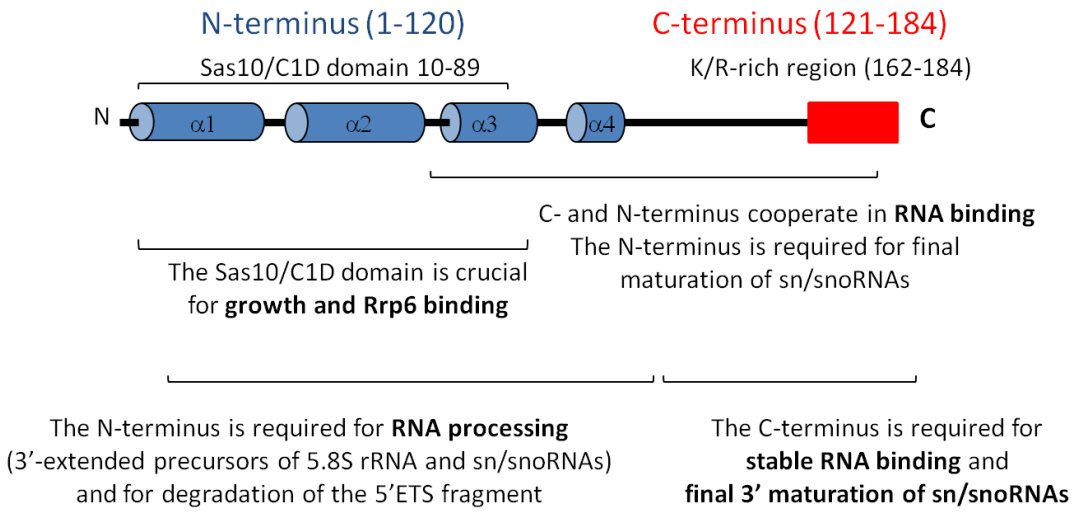


**Figure 3.29 Summary of results of mutational analysis of Rrp47.**
Schematic of Rrp47 annotated with domains and features revealed by the mutational analyses. The N-terminus of Rrp47 containing the Sas10 domain is crucial for Rrp6 binding. Mutations in this region affect growth and RNA processing similar to an *RRP47* deletion. The less conserved basic C-terminus is not required for growth or RNA processing *in vivo*, however mutants lacking the C-terminal domain showed a specific defect in snoRNA 3' maturation and loss of stable RNA binding *in vitro*. Combining mutations in the putative RNA binding region encompassing helix 3 (75-91) with the short C-terminal truncation G181X also led to a loss in stable RNA binding *in vitro* and indicate that both regions of the protein cooperate in RNA binding.

## 3.3 Discussion

Rrp47 is an evolutionarily conserved eukaryotic co-factor of the nuclear exosome exonuclease Rrp6. The precise function of the protein is as yet unknown. The purpose of this mutational analysis was to identify conserved features and map regions and residues within Rrp47 critical for its function in exosome-mediated RNA processing. Bioinformatics analyses suggest a role for Rrp47 in nucleic acid binding. This is consistent with *in vitro* RNA and DNA binding studies (Stead *et al.* 2007) and reports that the human Rrp47 homologue C1D also binds to DNA and structured RNA (Nehls *et al*. 1998, Schilders *et al.* 2007). However, Rrp47 has no sequence homology to any characterised DNA or RNA binding protein, no known RNA recognition motif (RRM) or specific DNA/RNA target sequences suggesting that Rrp47 recognises 3D RNA-structures or RNA-protein conformations rather than one-dimensional RNA sequences. As such, Rrp47 may represent a novel class of RNA binding protein with structural motif and mode for RNA recognition still to be identified. Rrp47 preferentially binds to structured as opposed to single-stranded RNA or DNA *in vitro* and Rrp47 binds to RNA and Rrp6 concomitantly (Stead *et al.* 2007). Since Rrp6 has been shown to process structured RNAs poorly *in vitro (*Liu *et al.* 2006, Burkard and Butler 2000), Rrp47 is thought to aid Rrp6 in the processing of structured RNA substrates either by modulating Rrp6 activity *in vivo* or by recruitment and stable binding of structured RNA substrates.

Multiple sequence alignments of Rrp47 homologues across a wide range of species revealed that the N-terminus of the protein is highly conserved and predicted to fold into 4 putative α-helices. Many of the conserved residues are either positively charged (17 % lysines) or hydrophobic (25 % leucines) (Mitchell 2010). Hydrophobic amino acids are known to play a role in protein interactions and dimerisation, whereas basic amino acids like lysines and arginines, many of them clustered in the highly basic tail of Rrp47, again point to nucleic acid binding consistent with the prediction of three putative RNA/DNA binding regions; an amphipathic helix at the N-terminus of Rrp47 further points to DNA binding or dimerisation. Consistent with this, the lab has recently shown that Rrp47 is expressed as a homodimer and forms a heterodimer with Rrp6 (Feigenbutz *et al*. 2013).

The N-terminus of Rrp47 contains a homology-domain identified by bioinformatics which is also found in its human counterpart C1D and other proteins like Sas10/Utp3 and Lcp5 which are involved in 18S rRNA processing. This so-called Sas10/C1D domain spans the first three putative α-helices predicted for Rrp47 (residues 10-89). Against expectations, single mutations of well conserved charged or aromatic residues within the Rrp47 N-terminal region identified by multiple sequence alignment did not show any effect on growth, Rrp6-binding, RNA processing or *in vitro* RNA binding; even multiple mutations targeting a cluster of well conserved amino acid residues within the putative RNA binding domain in helix 3 (75-91),

namely Glu-79, Arg-82, Lys-84, Tyr-86, Lys-89 and Lys-91, showed no discernible effect. However, further analysis of Rrp47 truncations revealed that the well conserved N-terminal domain of Rrp47 (residues 10-100) is critical and sufficient for Rrp6 binding and, more generally, critical for Rrp47 function and normal growth. The ability of Rrp47 to interact with Rrp6 therefore appears to be key to its function. Rrp47 truncations that do not include the complete Sas10/C1D domain (Δ2–19, L40*X*, I50*X*, L60*X*, V70*X*, L80*X*) displayed RNA-processing defects characteristic for *rrp47*Δ and *rrp6Δ* mutants and could not be stably expressed as proteins**.** The conserved Sas10/C1D homology domain could therefore represent an Rrp6 binding domain. However, Sas10/Utp3 or Lcp5 have not been found to bind to Rrp6 (M. Turner, unpublished data), yet an interaction with PMC2NT-like domains of other proteins is a possibility.

Alternatively (or in addition), the Sas10/C1D family of proteins could function in RNA binding in a similar manner to Rrp47. Notably, Sas10/Utp3 and Lcp5 associate with U3 snoRNA, whereas neuroguidin associates with proteins found in mRNP particles. Moreover, all three proteins have basic clusters at their C-terminus (Kamakaka *et al.* 1998, Wiederkehr *et al*. 1998, Jung *et al*. 2006) and basic residues (lysine or arginine) are conserved across the Sas10/C1D domain family at positions equivalent to K84 and K89 of Rrp47. It remains to be seen whether these proteins have a common mode of action, especially in view of their functional links. Rrp6 is required for the turnover of aberrant 23S pre-rRNA processing intermediates that accumulate in the absence of Sas10/Utp3 or Lcp5 (Lafontaine and Tollervey 1999). And more strikingly, overexpression of Sas10 or loss of Rrp6 blocks heterochromatin silencing (Lafontaine andTollervey 2000, Reinisch *et al.* 2007, Doma and Parker 2007).

In contrast, the C-terminal region of Rrp47 is poorly conserved and truncating the protein to its 100 N-terminal residues did not affect Rrp6 binding or growth. Even though the C-terminus contains the most potential RNA binding sites and is required for stable RNA binding *in vitro*. RNA binding assays in this study have demonstrated that N- and C-terminus cooperate in RNA binding *in vitro* and that binding considerably decreases when mutations in the putative RNA binding region and the C-terminus of Rrp47 are combined. This strongly suggests that for efficient and stable RNA binding *in vitro* residues in both the C-terminus and N-terminus are required. However, short C-terminal truncations that diminished stable RNA binding *in vitro* (*e.g.* the I162*X* mutant) did not significantly affect RNA-processing *in vivo and neither did the combined C- and N-terminal mutations (G181X mm, G181X N*).* The basic C-terminus therefore is dispensable for the main RNA-processing functions *in vivo*. The human counterpart C1D is also characterised as a DNA and RNA binding protein with a basic C-terminus, however it does not possess an extended C-terminal region like Rrp47. Taken together, this suggests that RNA-binding of Rrp47 might not be critical for its function in stable

RNA-processing, perhaps due to redundancy with other RNA-binding proteins or due to interactions with other proteins that also mediate stable RNA-binding.

Interestingly, deletion of the C-terminal region of Rrp47 (ΔC1) resulted in a specific defect in snoRNA maturation with the accumulation of a short extended precursor (+3 nucleotides). This defect in the final step of snoRNA maturation was exacerbated in the absence of the exonuclease Rex1, where the Rrp47ΔC1 mutant accumulated longer, more heterogeneous 3' extensions and the production of mature snoRNA was reduced. This indicates that producing the '+3' intermediate or mature snoRNA in the absence of Rrp47-Rrp6 requires the activity of Rex1, suggesting that this redundant function in snoRNA processing and related pathways (CUTs, snRNAs, Nrd1 terminated transcripts) could be the reason for the synthetic lethality of the *rex1Δ rrp47Δ* double mutant.

Short snoRNA 3' extensions have also been reported in strains expressing mutant alleles of the box C/D snoRNP proteins Nop1 and Nop58 (Lafontaine and Tollervey 2000, Gautier *et al.* 1997). The +3 extensions on snoRNAs have been shown not to be encoded but to be added by the TRAMP poly(A) polymerase Trf4 after Nrd1 termination (Grzechnik and Kufel 2008). The oligoadenylation by TRAMP is now thought to be an intrinsic part of 3' end processing of snoRNAs which involves several rounds of oligoadenylation and trimming by the exosome. This is seen as part of a kinetic process which allows time for maturation of properly assembled snoRNPs and results in degradation of stalled or misassembled snoRNP. Further studies by J. Costello have determined the critical residues F142 and F135 in the C-terminus of Rrp47 required for the final step in the 3' maturation of box C/D snoRNAs and revealed that the C-terminal domain of Rrp47 interacts with Nop56 and Nop58 in an RNA/DNA independent manner. This strongly indicates a role for Rrp47 in snoRNP assembly (Costello *et al*. 2011). Nop56/58 are finalising the assembly into the mature snoRNP and an interaction with Rrp47 could serve to protect and differentiate properly matured snoRNPs from improperly assembled snoRNAs which are rapidly degraded by Rrp6 due to the lack of protective structures or protein interactions (Fig. 3.30). Rrp47 could have a function in sensing correctly assembled mature snoRNPs and trigger their release upon contact with the snoRNP proteins, thus preventing degradation by Rrp6.

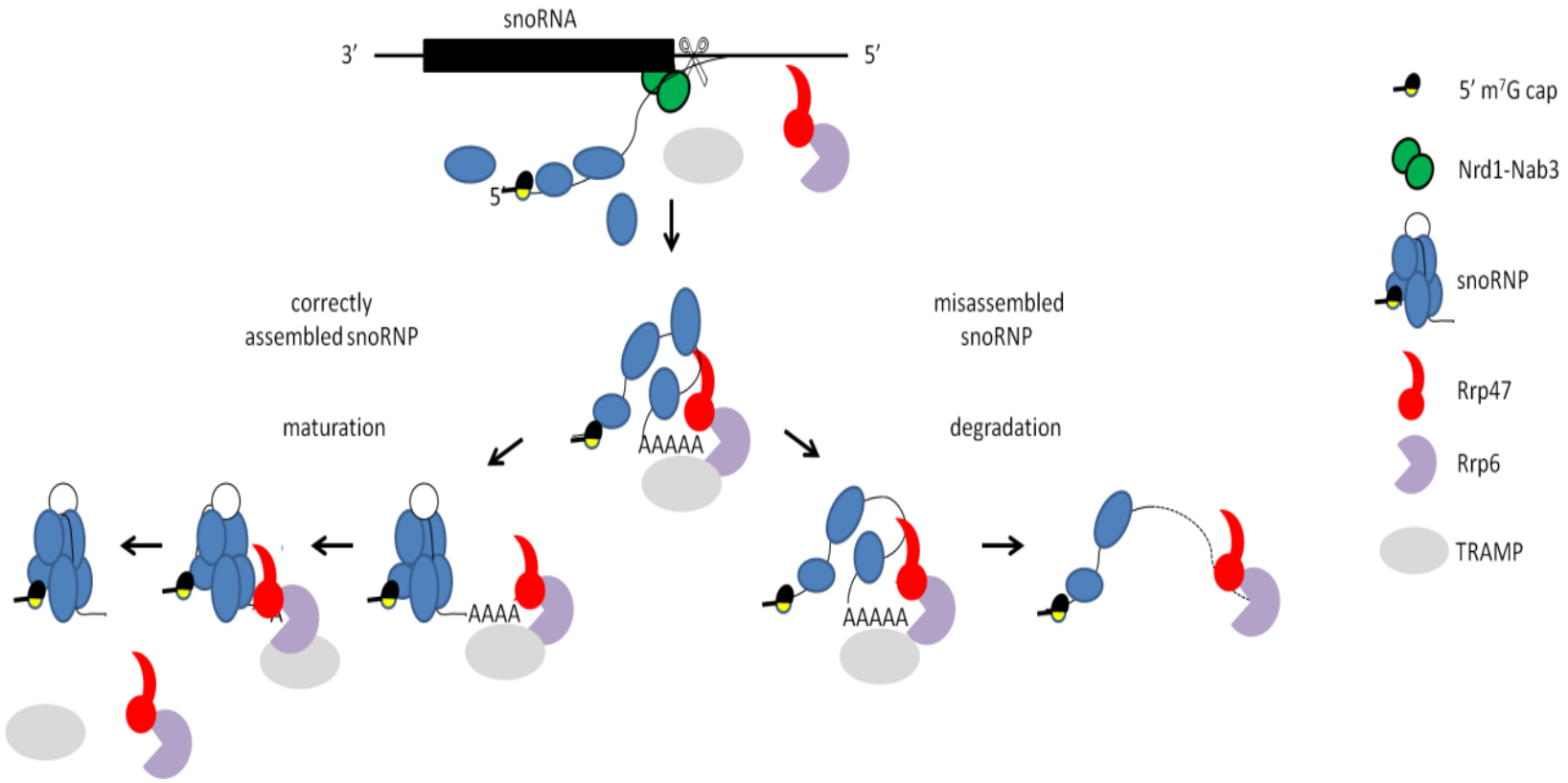


**Figure 3.30 Model for Rrp47 function in snoRNA processing and snRNP assembly**. The nascent snoRNA is terminated via the Nrd1-Nab3 pathway and oligoadenylated by the TRAMP polyA polymerase Trf4 which leads to recruitment of Rrp6-Rrp47 and/or the exosome. Rrp47 could make the initial contact with the substrate enabling Rrp6 processing. If the snoRNP is correctly assembled, the contact of Rrp47 with the Nop56/58 proteins leads to the release of Rrp6-Rrp47 from the substrate. In contrast, when the snoRNP is incorrectly assembled or assembly takes too long, Rrp6 proceeds to degrade the RNA which lacks protection from snoRNP proteins.

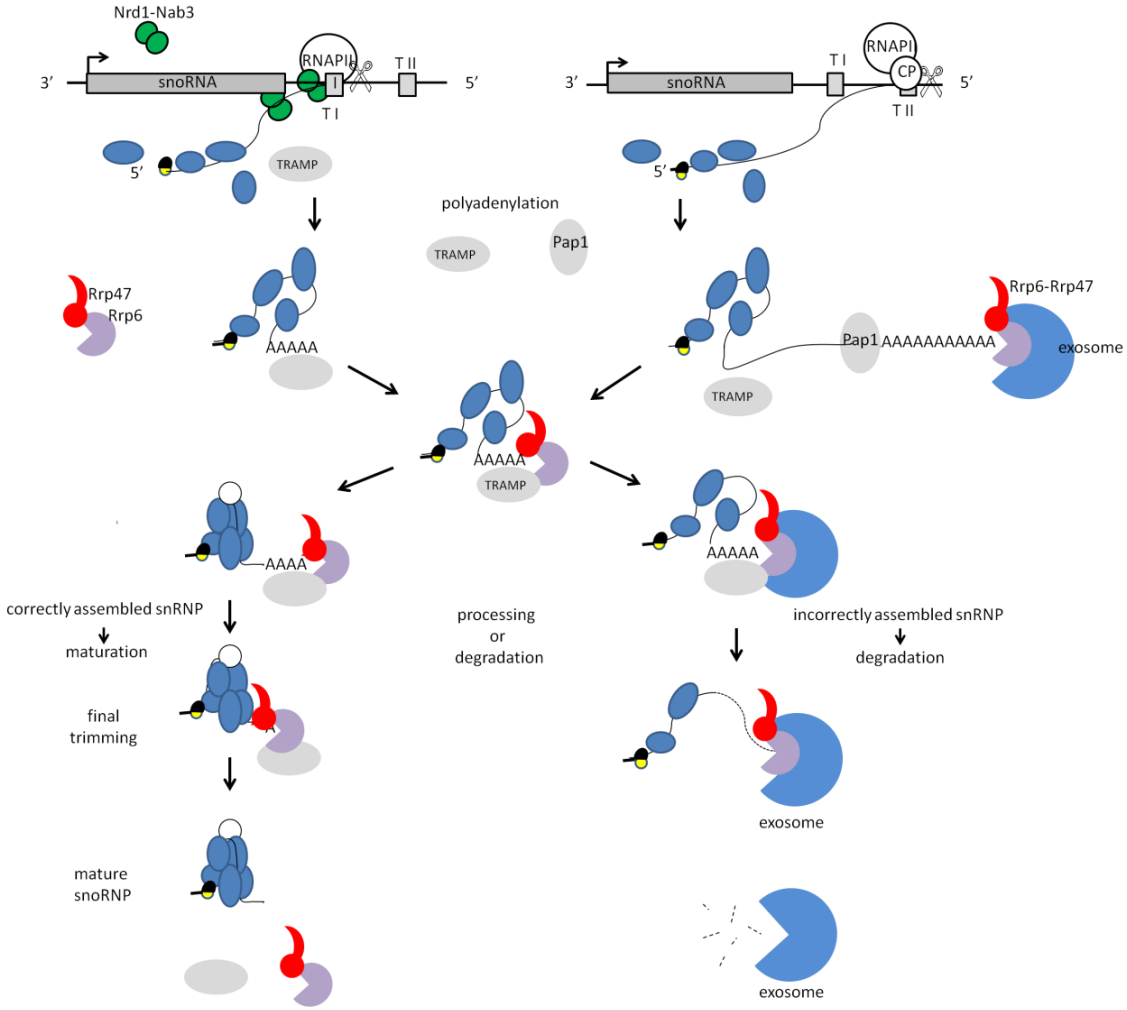


**Figure 3.31 Extended Model for Rrp47-Rrp6 function in snoRNA processing.**
The two modes of snoRNA termination are depicted at the top of the schematic. Nrd1-dependent termination (left) uses an early terminator (site TI) and Nrd1-Nab3 heterodimers bind to the nascent RNA which is oligoadenylated by the TRAMP polyA polymerase Trf4 which leads to recruitment of Rrp6-Rrp47 and/or the exosome. Fail-safe termination at site II uses the polyadenylation-dependent pathway where termination and polyadenylation by Pap1 are driven by the canonical mRNA 3'end processing machinery. Transcripts from both termination sites are processed by Rrp6/exosome and TRAMP complexes. Rrp47 could make the initial contact with the substrate enabling Rrp6 processing. If the snoRNP is correctly assembled, the contact of Rrp47 with the Nop56/58 proteins leads to the release of Rrp6-Rrp47 from the substrate. In contrast, when the snoRNP is incorrectly assembled or assembly takes too long, Rrp6 proceeds to degrade the RNA which lacks protection from snoRNP proteins.

# Chapter Four

# Investigating the Assembly of the Rrp47-Rrp6 complex

**Tables 4.1- 4.2**

**Figures 4.1 – 4.26**

# Chapter 4

# Investigating the Assembly of the Rrp47-Rrp6 complex

## 4.1 Introduction

Assembly pathways of exosome complexes and their associated ribonuclease activities and co-factors are as yet poorly understood. Yeast Rrp47 and Rrp6 are restricted to the nucleus and herein are found in the nucleoplasm and the nucleolus, a region specialised on rRNA transcription, processing and assembly of pre-ribosomal subunits (Allmang *et al*. 1999, Burkard and Butler 2000). However, minor amounts of cytoplasmic Rrp6 have been reported in *Drosophila melanogaster*, *Arabidopsis thaliana*, *Trypanosoma brucei* and humans (Lejeune *et al.* 2003, Graham *et al.* 2006, Haile *et al.* 2007, Lange *et al.* 2008). Whilst Rrp6 has widely been presumed as the main nuclear exosome activity and used as a marker for nuclear exosome activity, there is mounting evidence for exosome independent functions of Rrp6 and Rrp6-specific substrates (Callahan and Butler 2008). The loss of Rrp6 interaction with the core exosome does not interfere with RNA 3' end processing, but inhibits degradation of rRNA substrates that require both Rrp6 and the core exosome. Since *rrp47Δ* and *rrp6Δ* strains show the same RNA processing phenotypes, Rrp47 is thought to be required for both exosome core-dependent and core-independent functions of Rrp6 such as the degradation of the 5' ETS fragment derived from initial cleavage of the 35S pre-rRNA and the 3' maturation of 5.8S rRNA and snoRNAs, respectively.

A key biochemical activity of Rrp47 is its ability to directly interact with Rrp6 as shown by affinity capture analyses of protein complexes in yeast (Mitchell *et al.* 2003, Synowsky *et al*. 2006) and by *in vitro* reconstitution studies (Stead *et al*. 2007, Costello *et al*. 2011). Notably, deletion of the PMC2NT interaction domain results in similar phenotypes to the loss of Rrp47 and led to the discovery that the interaction with Rrp6 is required for normal expression levels of Rrp47 (Stead *et al.* 2007). More recent hydrodynamic and protein cross-linking studies could establish that recombinant Rrp47 assumes a non-globular structure and is expressed as a homodimer (Feigenbutz *et al*. 2013a). Yet, analysis of the Rrp47-Rrp6 complex revealed a stable Rrp47-Rrp6 heterodimer with a 1:1 stoichiometry. This implies that Rrp47 requires structural remodelling from homodimer to heterodimer either before or through interaction with Rrp6. These observations strongly suggest that nuclear localisation and assembly of the Rrp6-Rrp47 complex are important steps to ensure proper functional competence of Rrp6 and Rrp47 heterodimers, as well as exosome complexes. The following work has set out to answer how Rrp47 expression is controlled by Rrp6 and to give insights into how and where Rrp47-Rrp6 assembly occurs.

Described here are studies on Rrp47 stability, localisation and the assembly with its partner Rrp6, which in concert with the exosome plays a pivotal role in the processing, quality control and degradation of RNAs. The data presented here shows that rapid Rrp47 depletion in the absence of Rrp6 is due to protein instability and establishes Rrp47 as a substrate of proteasome-dependent protein degradation. Consistent with this, Rrp47 could be shielded from degradation in the absence of Rrp6 by tagging its N-terminus which determines protein stability according to the N-end rule (Varshavsky 1996 and 2011). Analysis of Rrp6 mutants further revealed that the N-terminal Rrp6 heterodimerisation domain (Rrp6NT) is sufficient to recover Rrp47 expression in an *rrp6Δ* mutant. Moreover, Rrp47 can be titrated out of Rrp6 heterodimers by exogenous overexpression of the Rrp6NT domain providing a useful tool to study Rrp47 functions independently of Rrp6. Further, pull-down-assays on cell extracts confirmed that Rrp47 cannot be found associated with the Rrp6-Srp1 (importin-α) import complex, and GFP fusions of Rrp6 or Rrp47 localise to the cell nucleus separately and in the absence of one another. Moreover, in the absence of Rrp6, Rrp47-GFP accumulates as a proteolytic degradation intermediate in the nucleus. This indicates that localisation of Rrp47 is independent of Rrp6 and that Rrp6-Rrp47 assembly occurs after independent nuclear import of both proteins to the nucleus where a proteasome-dependent mechanism prevents Rrp47 expression in the absence of Rrp6. The major results presented in this chapter were published in Feigenbutz *et al*. 2013a and Garland *et al.* 2013.

## 4.2 Results

### 4.2.1 Rrp47 levels are reduced more than 15-fold in the absence of Rrp6

The lab has reported previously that Rrp47 expression levels are effectively depleted in the absence of Rrp6 or in yeast strains expressing an Rrp6NT mutant lacking the N-terminal PMC2NT domain required for Rrp47 interaction (Stead *et al.* 2007). To readdress and quantify this observation, steady state levels of Rrp47 protein of an *rrp6Δ* and an isogenic *RRP6* strain from denatured cell extracts were resolved by 12 % SDS-PAGE and analysed by western blotting (Fig 4.1 A). Rrp47 bands were quantified and adjusted against the internal control Pgk1. Data from five independent experiments was averaged. Rrp47 protein was reduced more than 15-fold in the *rrp6Δ* mutant compared to the wild-type strain (6.1%, SE=2.1%, n=5). Parallel experiments were performed for Rrp6-TAP expression in dependence of Rrp47 (Fig. 4.1 B), however Rrp6 protein levels were only slightly decreased in the absence of Rrp47 to approximately 70 per cent of the wild-type strain (Rrp6 protein 73.11 %, SE= 7.5, n=6). Figure 4.1 shows representative western data for both proteins.

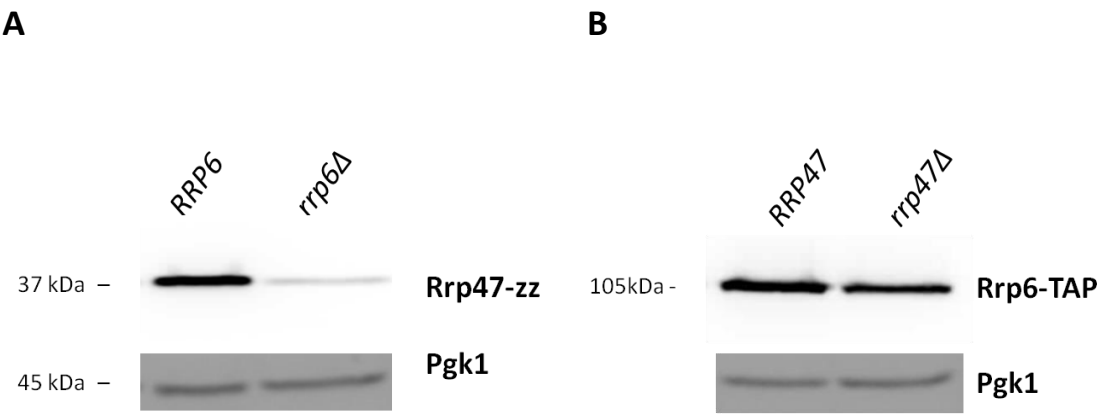


**Figure 4.1 Rrp47 protein is depleted in the absence of Rrp6.**
Representative images are shown for western analyses of Rrp47 and Rrp6 expression levels in the presence and absence of their respective partner. Denatured cell extracts of wild-type *RRP47*-zz (P414) and *RRP6*-TAP (P539) strains, as well as the isogenic deletion strains *RRP6 rrp47Δ* (P540) and *RRP47 rrp6Δ* (P439) were resolved by 12 % SDS-PAGE and analysed by western blotting with peroxidase-anti-peroxidase (PAP) antibody to detect Rrp47-zz and Rrp6-TAP followed by anti-Pgk1 antibody as loading control. (A) Rrp47-zz expression levels in wt *RRP6* and *rrp6Δ* strain. (B) Rrp6-TAP expression levels in the wild-type *RRP47* and *rrp47Δ* strain.

### 4.2.2 Depletion of Rrp47 levels in *rrp6Δ* strains is due to protein instability

As concluded from the western analysis, Rrp47 expression is clearly dependent on Rrp6. In order to investigate this dependency and determine whether Rrp47 depletion in the absence of Rrp6 is due to protein instability or a decrease in mRNA expression levels (or turnover), steady state levels of *RRP47* mRNA transcripts were determined by real-time quantitative PCR (RT-qPCR). Total RNA was extracted from strains expressing *RRP47*-zz and *RRP6*-TAP along with their isogenic deletion strains *RRP47-zz rrp6Δ* and *RRP6*-TAP *rrp47Δ* grown at 30 ˚C and column purified for use in RT-PCR. RNAs were DNAse I treated and cDNAs were prepared in triplicates for the qPCR analysis. Controls in preparation for RT-qPCR are shown in Figure 4.2. RNAs were resolved through a 1.5 % agarose gel to show they are intact (A). RNAs were also resolved through an 8 % polyacrylamide gel and analysed by northern blotting with a probe complementary to snR38 snoRNA (B). The RNA analyses showed the strain-specific phenotypes, mature snR38 species in the wild-type, the characteristic 3 nucleotide extended 'snR38+3' species in the *rrp6Δ* mutant and an intermediate phenotype with both mature and '+3' species in the *rrp47Δ* mutant.

Primers were shown to be specific for the appropriate gene product in a test PCR using qPCR conditions (C) showing that only the cDNAs (+RT) produce a PCR product of the expected size but not the “no enzyme” (-RT) and water controls. Melt curves for the used qPCR primers were shown to be uniform as required (D). *SCR1* is commonly used as internal control in northern blot analyses and its suitability as internal standard was confirmed using the *ALG1* mRNA and *TCF1* mRNA as comparison (E) which have been shown to be suitable internal standards for use in qPCR for a wide range of conditions (Teste *et al*. 2009). Parallel qPCR results for *RRP6* mRNA levels for *SCR1, TCF1* and *ALG9* are shown in Figure 4.2 (E) testing triplicate samples of cDNAs in an *RRP47* and *rrp47Δ* strain. The results of all three internal standards are in very good agreement and confirm *SCR1* as a suitable internal control for the qPCR analyses.

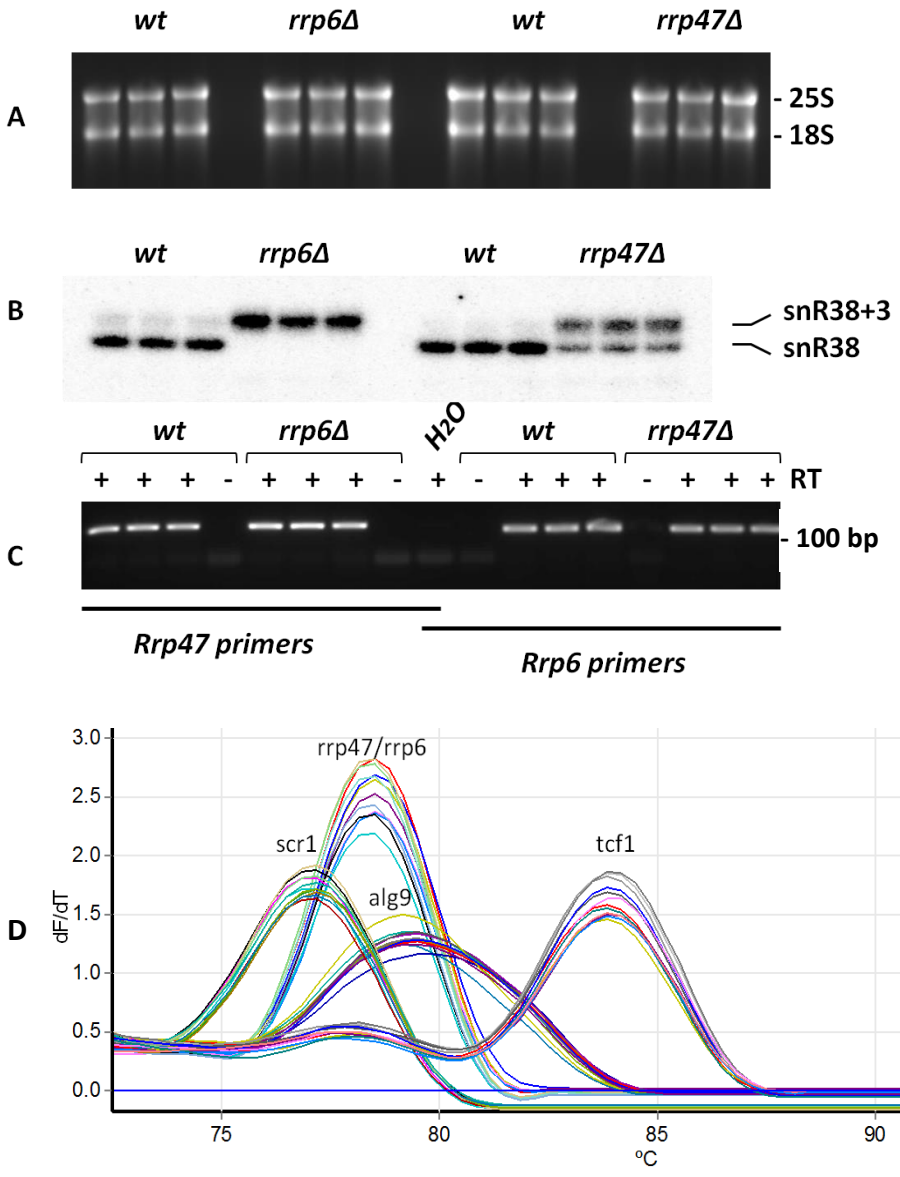

E

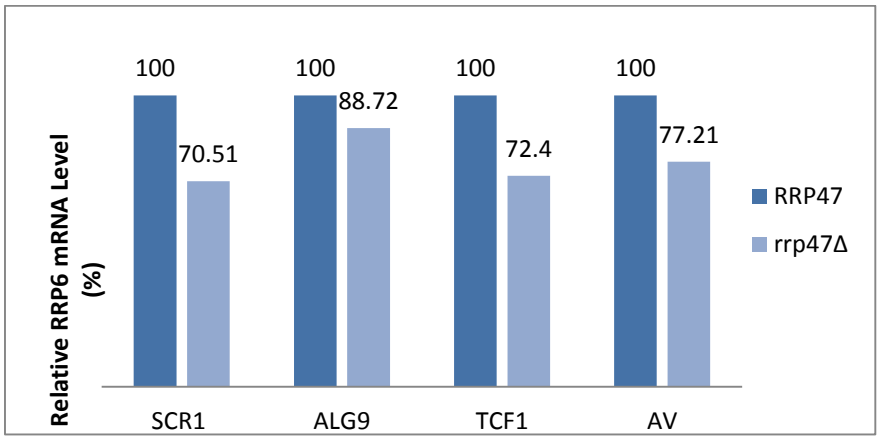


**Figure 4.2 Controls for Real-Time quantitative PCR (RT-qPCR).**
Total RNA preparations of three independent biological samples of each strain (P414 *RRP47-zz*, P439 *RRP47-zz rrp6Δ,* P539 *RRP6-TAP*, P540 *RRP6-TAP rrp47Δ)* were checked for quality and integrity (A) 10 µg RNA resolved through a 1 % agarose gel and (B) 5 µg resolved through an 8 % PAA gel followed by northern hybridisation with a snR38 probe (o272). (C) A control PCR was performed with triplicate cDNAs, as well as no enzyme (-RT) and water controls to check the specificity of the chosen qPCR primers, samples were resolved through 2 % agarose. (D) Melt curve analysis of the qPCR primers *ALG9* (o744/o745), *RRP6* (o650/o651), *RRP47* (o701/o702), *TCF1* (o749/o748), SCR1 (o654/o655). (E) *RRP6* mRNA levels determined by RT-qPCR on the tested RNAs using three different internal controls *SCR1, ALG9* and *TCF1* for comparative quantitation ($\Delta\Delta C_T$ method).

Having performed the necessary controls on cDNAs and primers, *RRP47* and *RRP6* mRNA levels were determined by RT-qPCR using *SCR1* as internal standard for comparative quantitation. Results of quantitative western and RT-qPCR analyses are combined in graphs in Figure 4.3. *RRP47* transcript levels were only slightly lower (70.7 %, SE=8.6 %, n=6) in *rrp6Δ* compared to the wild-type strain and thus cannot account for the drastic reduction in Rrp47 protein. Rrp6 mRNA transcript levels were slightly decreased in the absence of Rrp47 to approximately 70 per cent of the wild-type strain, consistent with the mildly reduced steady state protein levels (Rrp6 protein 73.11 %, SE=3.4, n=6, RRP6 mRNA 70.5 %, SE=7.0, n=6). Taken together, the absence of Rrp6 has a drastic effect on Rrp47 protein but not on *RRP47* mRNA transcript levels, whereas Rrp6 mRNA and protein levels are only mildly affected by the absence of Rrp47.

A

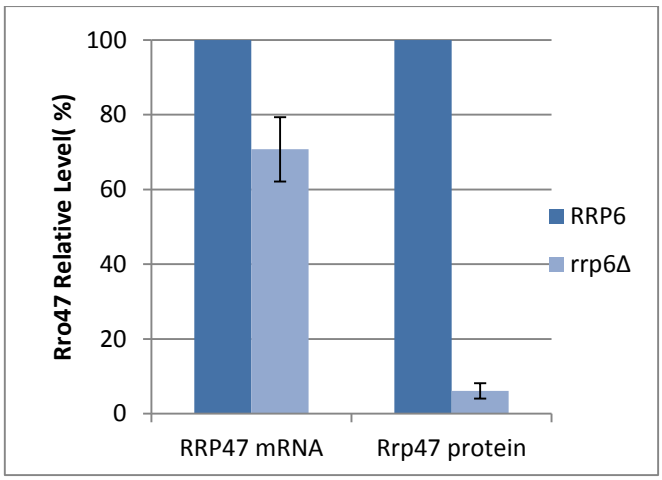


B

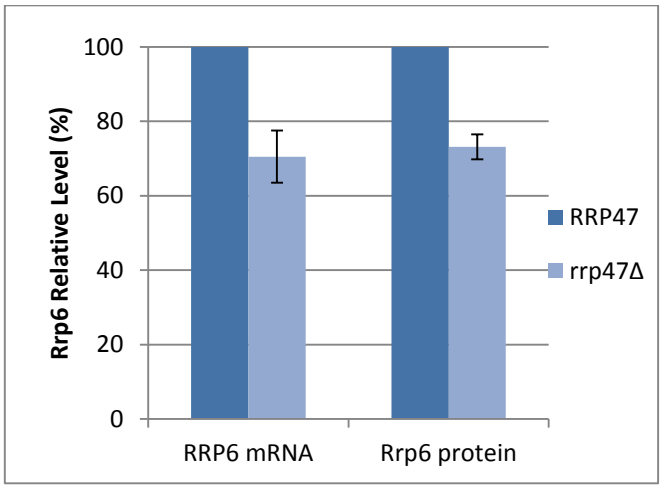


**Figure 4.3 Rrp47 protein but not mRNA is depleted in the absence of Rrp6.**
Quantitative RT-PCR and western analyses of relative Rrp47 and Rrp6 mRNA and protein expression levels observed in *RRP6* and *RRP47* wild-type strains and the respective isogenic *rrp6Δ* or *rrp47Δ* strains. *RRP6 and RRP47* mRNA levels were determined by RT-qPCR in 6 triplicate assays and standardised to *SCR1* levels. Western analyses were performed on alkaline lysed cells from 5 biological replicates resolved through 12 % SDS PAGE and probed with PAP and anti-Pgk1 antibodies. Western bands were quantified and standardised to Pgk1 levels. Error bars indicate the positive and negative ranges of the standard error of the mean values. (A) *RRP47* mRNA and protein expression levels in dependence of Rrp6. (B) *RRP6* mRNA and protein expression levels in dependence of Rrp47.

***Rrp47 protein is unstable in the absence of Rrp6***

To further determine the effect of Rrp6 on Rrp47 protein stability, a translational shut-off experiment (Fig 4.4) was conducted by Phil Mitchell and is included here for its centrality to this study. To ensure "normal" Rrp47 expression levels in the absence of Rrp6, an *rrp6Δ* strain was created by PCR mediated integration of the *rrp6Δ::kanMX4* cassette into a strain which expresses the Rrp47-zz fusion protein under the control of the GAL promoter (P957). The isogenic GAL-regulated *RRP6* and *rrp6Δ* strains were pre-grown in raffinose-based medium and galactose was added to induce Rrp47-zz expression to wild-type levels in the *rrp6Δ strain*. New protein synthesis was then inhibited by adding cycloheximide and the effect on Rrp47-zz levels was followed over a period of 40 minutes and visualised by western analysis. In the *rrp6Δ* strain, Rrp47 protein was effectively depleted within 20 minutes after addition of cycloheximide (lower panels) while Pgk1 levels appeared unaffected. In contrast, Rrp47 levels in the wild-type *RRP6* strain (upper panels) remained relatively constant for the duration of the time course (upper panels). The lower band on the Rrp47 westerns (marked with an asterisk) is a proteolytic degradation fragment of Rrp47 which is typically observed in native yeast cell extracts (but not in alkaline lysed cells). In conclusion, Rrp47 is rapidly depleted in *rrp6Δ* strains due to protein instability in the absence of Rrp6.

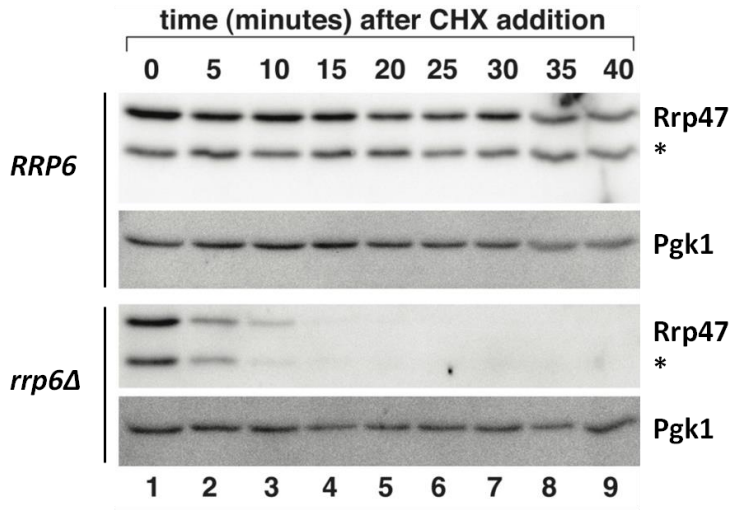


**Figure 4.4 Rrp47 protein is unstable in the absence of Rrp6.**
Rrp47 protein stability dependent on Rrp6 was assessed in a translation shut-off experiment. *GAL*-regulated Rrp47-zz *RRP6* (P957) and isogenic *rrp6Δ* strains were pre-grown in raffinose-based medium and Rrp47-zz expression was induced to "normal" levels in *rrp6Δ* by adding galactose. New protein synthesis was blocked by addition of cycloheximide and samples were taken at the time points indicated above from 0 to 40 minutes after addition of the inhibitor. Samples were resolved by 12 % SDS-PAGE and analysed by western blotting with a PAP antibody followed by anti-Pgk1 as internal control. The lower band (asterisk) on the Rrp47 panels is a proteolytic degradation product of Rrp47 typically observed in native cell extracts.

### 4.2.3 Proteasome inhibition recovers Rrp47 expression in the absence of Rrp6

The proposition that Rrp47-Rrp6 assembly and Rrp47 degradation in the absence of Rrp6 are spatially linked, led to the investigation of the mechanism by which Rrp47 is degraded. The two major eukaryotic protein degradation machineries are the cytoplasmic vacuole for mainly non-selective proteolysis and the proteasome for the majority of selective regulated proteolysis in nucleus and cytoplasm. Vacuolar degradation is typically blocked by the serine protease inhibitor phenylmethanesulfonylfluoride (PMSF), which inhibits the vacuolar proteinase A (Pep4 in yeast), or by deletion of the *PEP4* allele. The proteasome can be inhibited by short peptide aldehydes like Z-Leu-Leu-Leu-al (MG132) that block active sites of the proteasome (Lee and Goldberg 1996). Due to low drug permeability of the yeast cell wall, experiments with proteasome inhibitors are carried out in strains which are more permeable and therefore more sensitive to drugs like the *erg6*Δ mutant.

Accordingly, *erg6Δ* deletions were created in *RRP6* and isogenic *rrp6Δ* strains expressing the Rrp47-zz fusion protein. The *erg6Δ::kanMX4* deletion cassette (Euroscarf, Brachmann *et al*. 1998) was amplified by PCR as shown in the schematic (Fig. 4.5 A) with primers using *ERG6* ORF outlying sequences (o664/o665, ORF + 500b). Control PCRs were performed to confirm sizes of the PCR products from wild-type *ERG6* and donor *erg6Δ* strain (Fig. 4.5 B left panel) with the chosen primers. The gel-purified *erg6Δ* PCR fragment (2.5 kb) was then transformed into the target strains for homologous recombination with the *ERG6* allele. Cells were grown up on rich medium before selection of transformants on plates containing the drug geneticin (G418), which is tolerated upon expression of the kanamycin resistence gene. Using further outlying primers of the *ERG6* locus (o668/o669, ORF + 1kb), putative candidates were screened (Fig 4.5 B right panel) and confirmed by PCR to be 3.5 kb in size compared to the wild-type allele (3kb); growth of the mutant strains was checked to be unaffected compared to *RRP47* wild-type and *rrp47Δ strains* (Fig. 4.5 C).

**A**

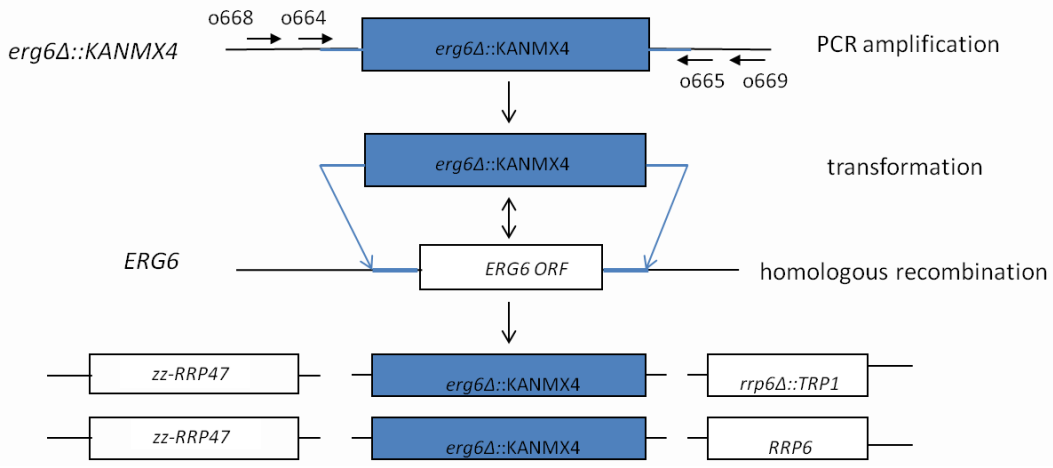

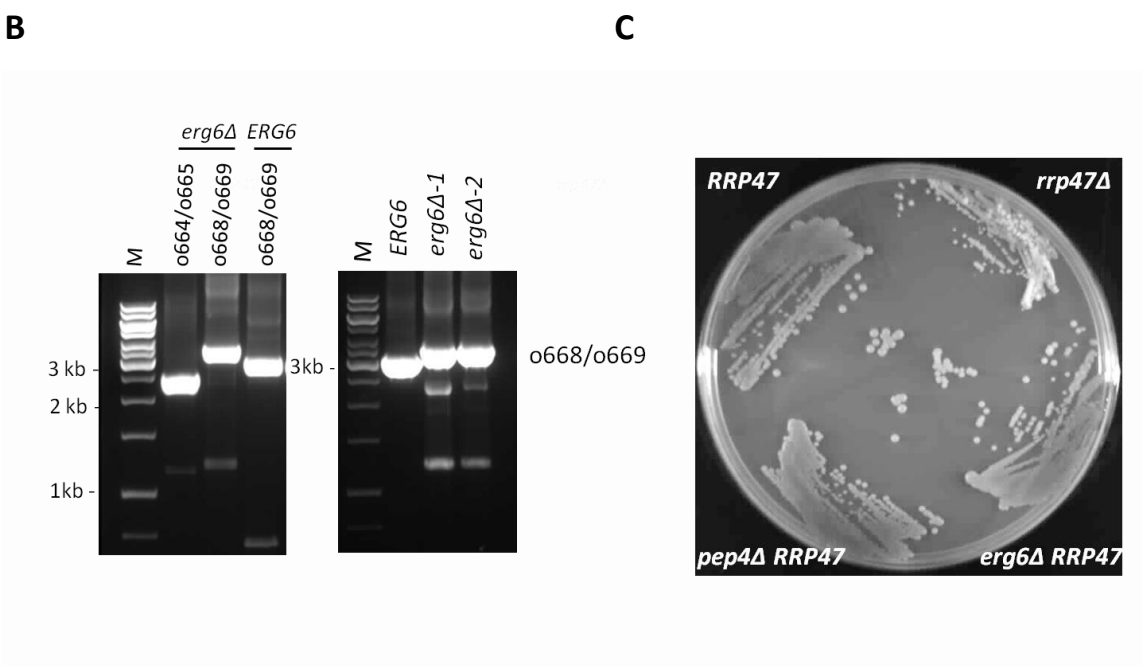


**Figure 4.5 Creating gene deletions by PCR-mediated gene disruption in *S. cerevisiae*.**
(A) Schematic of a typical gene disruption in *S. cerevisiae* using a *kanMX4* cassette (Wach *et al*. 1994) exemplified by the deletion of the *ERG6* allele. The deletion cassette *erg6Δ::kanMX4 (Euroscarf)* was amplified from genomic DNA by PCR using primers o664/o665 (+500b). The PCR product was transformed into the *RRP47-zz* (P414) and *RRP47-zz rrp6Δ* (P439) strains. Transformants were grown up on YPD and replica plated onto G418 to select for candidates expressing the kanamycin resistance gene**.** (B) PCR products for primer set 1 (o664/o665) on *erg6Δ* for transformation and primer set 2 (o668/o669) on *erg6Δ* and *ERG6* for screening (left) resolved on 1 % agarose. Putative candidates, *erg6Δ-1 and erg6Δ-2,* were screened by colony PCR using the primers o668/o669 (+1kb) against the *ERG6* wild-type strain (B, right panel). (C) Positive transformants, here *erg6Δ* and *pep4Δ,* were grown up on YPD for 2 days at 30˚C to check for normal growth compared to the *RRP47* wild-type and *rrp47Δ* strain.

***Inhibition of the proteasome, but not the vacuole, recovers Rrp47 expression in rrp6Δ***

The *RRP6* and *rrp6Δ* strains carrying the Rrp47-zz fusion protein and the *erg6Δ* deletion were cultured and treated with either PMSF or MG132 or the control solvents isopropanol and DMSO, respectively. The effect of the inhibitors on Rrp47 expression levels was followed over 90 minutes by western analysis of cell lysates (Fig. 4.6). Rrp47 expression levels in the *RRP6* strain (A and B, left panels) were not adversely affected by any of the inhibitors or control solvents, and stayed at a constant level comparable to the untreated control (0'). In the *rrp6Δ* strain, Rrp47 expression was reduced as expected pre-treatment (0', lane 1, right panel) and was not recovered during the time course by addition of PMSF or the control solvents. In contrast, treatment with the proteasome inhibitor MG132 (B, right panel) showed a considerable increase in Rrp47 expression in the *rrp6Δ* strain compared to the untreated or PMSF treated cells which showed no noticeable effects. Interestingly, the Rrp47 degradation

fragment typically observed in native cell extracts (compare Fig. 4.3) was observed in all *RRP6* cell extracts as a smaller fainter band (A and B left panels) except the MG132 treated sample. This confirms that proteasome inhibition clearly stabilises Rrp47 and prevents its degradation. In contrast, Pgk1 is a known substrate of the vacuolar autophagy pathway (Welter *et al*. 2010) and accumulates truncated proteolytic fragments in untreated cells which disappear when treated with the Pep4/vacuole inhibitor PMSF (data not shown). In conclusion, Rrp47 expression can be recovered by proteasome inhibition, but not by inhibition of the vacuole, therefore Rrp47 is most likely a substrate of proteasome-mediated degradation.

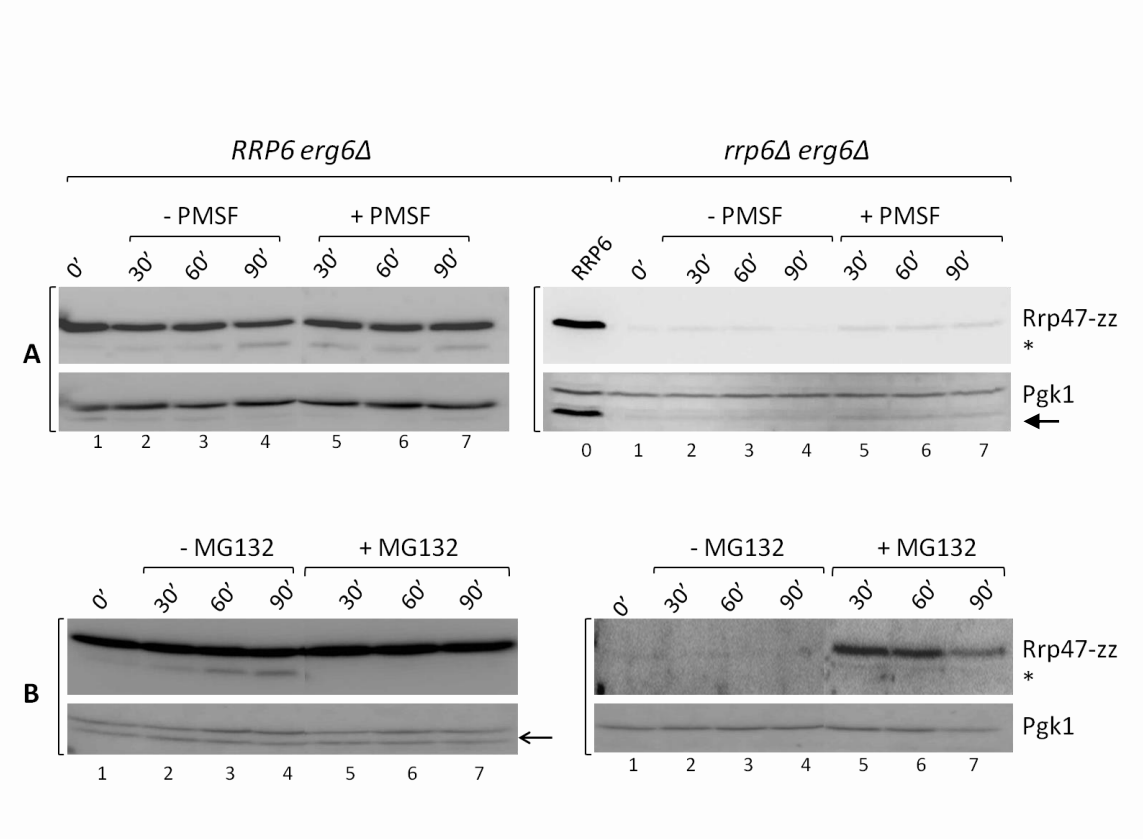


**Figure 4.6 Proteasome inhibition recovers Rrp47 expression in *rrp6Δ* mutants.**
Western analysis of Rrp47-zz expression in isogenic *RRP6 erg6Δ* and *rrp6Δ erg6Δ* strains after treatment with the protease inhibitor PMSF (A), the proteasome inhibitor MG132 (B) or the respective vehicle solvents isopropanol and DMSO. Cells of both strains were grown up at 30 ˚C to 1 $OD_{600}$ and 10 ml samples were harvested by centrifugation marking time point zero (0'). PMSF (A), MG132 (B) or the respective vehicle solvents were added, and 10 ml samples were harvested at 30, 60 and 90 minutes after addition. Cell extracts were resolved by SDS-PAGE and analysed by Western blotting with PAP followed by anti-Pgk1 antibodies to visualise Rrp47-zz protein levels compared to Pgk1 levels as internal reference. The arrows on the Pgk1 panels (B left, A right) point to Rrp47 bands retained from the PAP western. The asterisks below Rrp47-zz mark a proteolytic Rrp47 degradation fragment typically observed in native cell extracts.

***Blocking vacuolar degradation does not recover Rrp47 expression.***

Proteasomal, rather than vacuolar degradation of Rrp47 was further confirmed by deleting the *PEP4* wild-type allele in the *RRP6* and *rrp6Δ* strains by homologous recombination with the *pep4Δ* cassette (Euroscarf). Pep4 encodes the vacuolar proteinase A which is required for the maturation of numerous vacuolar proteases and is generally used as a marker for vacuolar degradation (*Charity et al. 2007*). Consistent with the inhibition experiments, blocking vacuolar degradation by deletion of *PEP4* could not recover Rrp47 expression in an *rrp6Δ* strain in two independent *pep4Δ* mutants (Fig. 4.7, lanes 4 and 5). There is no increase in Rrp47 expression compared to the *PEP4 rrp6Δ* strain (lane 3). The Rrp47 expression level in the *RRP6 pep4Δ* strain is not affected (lane 1 and 2).

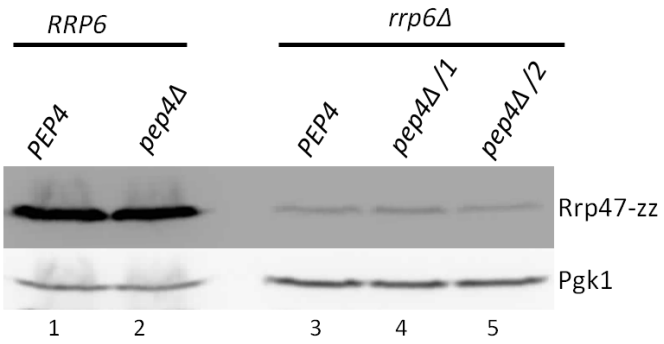


**Figure 4.7 Blocking vacuolar degradation does not recover Rrp47 expression.**
Western analysis of *pep4Δ* mutants created in isogenic *RRP6* wild-type (P414) and *rrp6Δ* (P439) strains by PCR-mediated replacement of the wild-type *PEP4* allele with the *pep4Δ-kanMX4* cassette. Strains were grown up alongside *PEP4* wild-type strains, subjected to alkaline lysis and resolved by 12.5 % SDS-PAGE for western analysis with PAP followed by anti-Pgk1 antibodies to detect Rrp47-zz (upper panel) and Pgk1 (loading control, lower panel).

In eukaryotes, control of protein stability is to a large extent mediated by the proteasome-ubiquitin system which targets proteins for proteolysis by conjugation with ubiquitin. According to the N-end rule for protein degradation (Varshavsky 1996), the N-terminal amino acid of a protein determines its half-life. As a consequence, shielding the N-terminus should avoid or interfere with proteasomal degradation. To test this hypothesis, a plasmid expressing an N-terminally zz-tagged Rrp47 fusion protein was transformed into an *RRP6* wild-type and an isogenic *rrp6Δ* strain. Rrp47 expression levels were analysed in three independent transformants for each strain (Fig. 4.8). Adding the N-terminally tagged zz-Rrp47 protein (in addition to the endogenous *RRP47* copy) clearly recovers Rrp47 expression in an *rrp6Δ* strain (lanes 4-6) to at least the same or slightly higher levels compared to the wild-type strain (lanes 1-3). This is in stark contrast to the depletion of Rrp47 seen in *rrp6Δ* strains expressing a C-terminally tagged Rrp47 fusion protein (compare Fig 4.1, 4.3B, 4.7). Taken together, these experiments are consistent with proteasome-mediated degradation of Rrp47 according to the N-end rule in the absence of Rrp6.

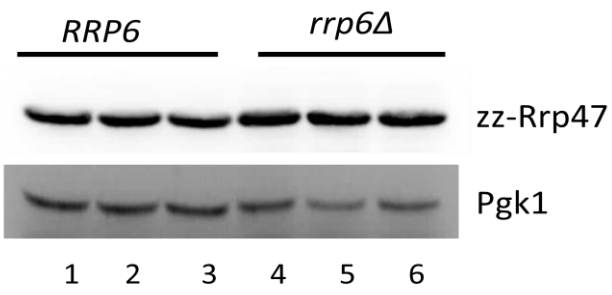


**Figure 4.8 Shielding the Rrp47 N-terminus recovers protein expression in *rrp6Δ* cells.**
Western analysis of *RRP6* (P414, lanes 1-3) and *rrp6Δ* strains (P439, lanes 4-6) transformed with a plasmid expressing an N-terminally tagged zz-Rrp47 fusion protein (p622). Alkaline lysed cell extracts were resolved by 12 % SDS PAGE and analysed by western blotting with PAP and Pgk1 antibodies. Triplicate samples are shown of each strain. Pgk1 serves as loading control. A comparison of zz-Rrp47 transformed and non-transformed wild-type (P364), *rrp47Δ* (P356) and *rrp6Δ* (P781) strains expressing endogenous Rrp47 is shown in Figure 5.12.

### 4.2.4 The Rrp6NT domain is sufficient to recover Rrp47 expression in an *rrp6Δ* strain

The lab has previously shown that Rrp47 directly interacts with the N-terminal PMC2NT domain of Rrp6, and deletion of the domain produces similar phenotypes to the loss of Rrp47 (Stead *et al.* 2007). Further, Rrp47 expression is significantly reduced in Rrp6ΔNT mutants, whereas the Rrp6NT domain is necessary and sufficient to recover Rrp47 expression. This indicates that Rrp47 interaction with the Rrp6NT domain directly stabilises Rrp47 to avoid degradation. Earlier experiments used GAL regulated fusion proteins to increase expression levels of the Rrp6NT mutant. Moreover, N-terminal zz-tagged Rrp6 mutants driven by a Rrp4 promoter (Allmang *et al*. 1999) were used in these studies due to a centromer (CEN) element in the Rrp6 promoter which causes problems during plasmid replication. However, the different promoter and protein-tag could potentially affect protein levels and stability and therefore give misleading results (compare Fig. 4.8).

Plasmids carrying a *RRP6* wild-type allele, but differing in promoter constitution (Fig. 4.9 A, Rrp6 promoter; B and C Rrp4 promoter) and epitope tag (A and B untagged, C zz-tagged) were compared for growth complementation in an *rrp6Δ* strain (P781) at 18 ˚C, 30 ˚C and 37 ˚C for the time indicated. Strains lacking Rrp6 are temperature sensitive (ts) at 37 °C and display slow growth at permissive temperature (30 °C) as demonstrated by the vector control (pRS416). All tested constructs carrying wild-type *RRP6* alleles complemented the *rrp6Δ* strain in a similar manner. Growth at 18 °C and 30 °C observed was similar to the wild-type strain (P364). Complementation of the *rrp6Δ* strain with the untagged *RRP6* wild-type allele was slightly worse at 37 °C.

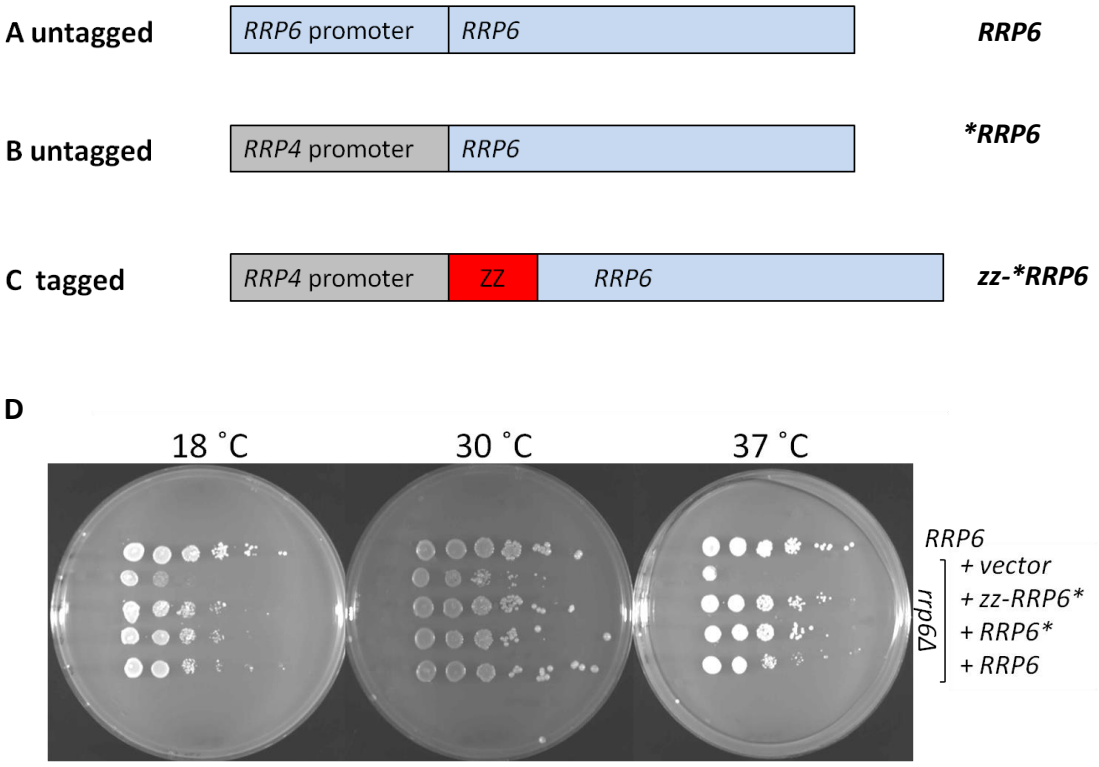


**Figure 4.9 Schematics and growth comparison of Rrp6 constructs.**

Rrp6 constructs commonly used in the lab were analysed for growth. All constructs carry a copy of the *RRP6* wild-type allele in the pRS416 vector. They differ with regard to promoter constitution and epitope tag. (A) *RRP6* is expressed under its endogenous promoter (p436), (B and C) *RRP6* is expressed under the *RRP4* promoter *(*RRP6, p390)*) and (C) the *RRP6* allele contains an N-terminal protein A-tag (zz-**RRP6, p263*). (D) Growth comparison of the three *RRP6* constructs transformed into the routinely used *rrp6Δ* deletion strain (P781) at 18 ˚C, 30 ˚C, and 37˚ C and spotted onto selective medium against a wild-type strain and vector controls.

To readdress and further investigate the requirements within Rrp6 for Rrp47 expression, Rrp6 mutants were analysed and a complementary set of untagged Rrp6 mutants driven by the *RRP6* promoter was created in addition to the zz-tagged fusion proteins expressed from the *RRP4* promoter. The centromer sequence (CEN) of the pRS416 plasmid encoding the *RRP6* wild-type allele was deleted for this purpose to avoid conflicts due to the additional CEN present in the Rrp6 promoter (Fig 4.10 A). A HpaI restriction site was introduced by SDM either side of the pRS416 CEN, the CEN sequence was removed by restriction digestion and the vector was religated. Mutant untagged *rrp6** sequences were subcloned into the polylinker of this construct, replacing the wild-type *RRP6* sequence.

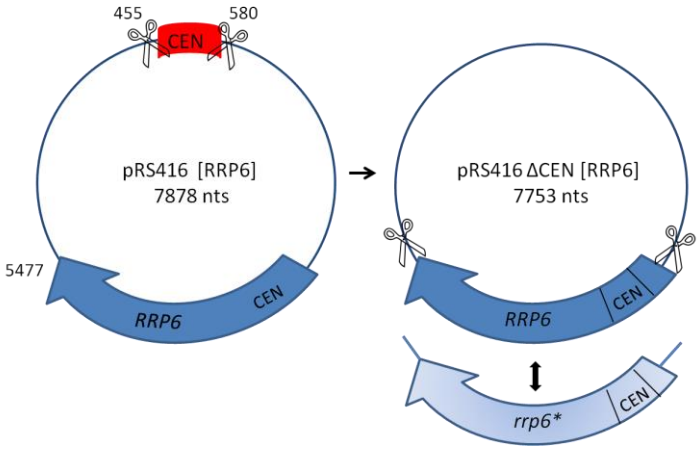


**Figure 4.10 (A) Removal of the pRS416 CEN sequence in dicentromeric *RRP6* constructs.**
In order to analyse the mutants under the endogenous *RRP6* promoter which harbours a CEN sequence, the essential CEN6 sequences (125 nts) from the pRS416 vector were removed by introducing a HpaI restriction site either side of the pRS416 CEN sequence by SDM. After restriction digestion with HpaI, the plasmid was religated. The mutant *rrp6** alleles were subcloned into this vector, replacing the wild-type *RRP6* sequence. The *RRP6* genomic sequence and mutant *rrp6** sequences are denoted as blue arrows; scissors represent restriction sites used for cloning.

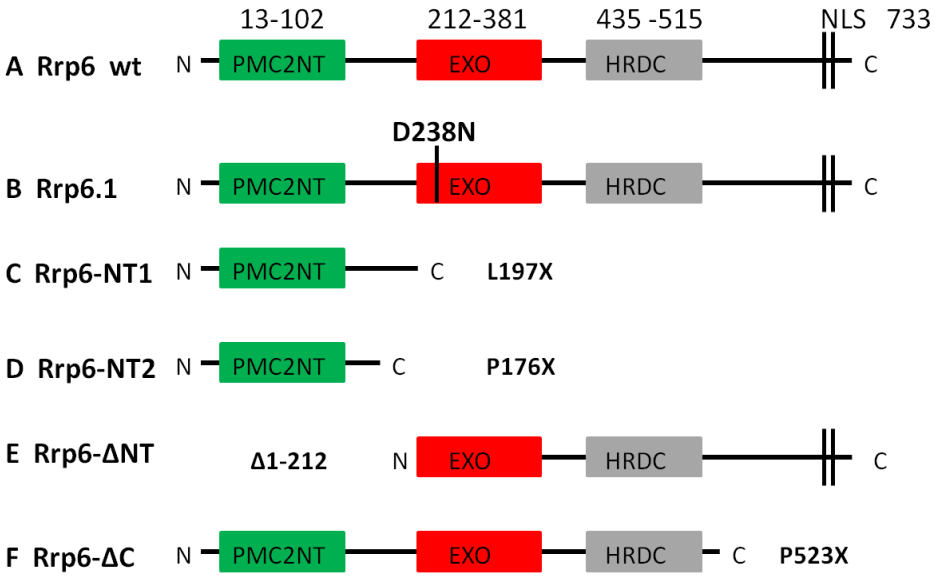


**Figure 4.10 (B) Schematic of Rrp6 domain structure and Rrp6 mutants analysed.**
Rrp6 wild-type protein architecture (top) and mutants investigated in this study. Rrp6 contains an N-terminal PMC2NT domain, a catalytic exonuclease domain, an HRDC domains and a consensus bipartite nuclear localisation signal (NLS) at its C-terminus. Rrp6.1 carries the D238N point mutation which renders the protein catalytically inactive (Burkard and Butler 2000); Rrp6NT1 and Rrp6NT2 are truncation mutants reduced to their N-terminal domain spanning residues 1-197 and 1-176, respectively; Rrp6ΔNT lacks the N-terminal domain including the PMC2NT domain crucial for Rrp47 interaction (Δ1-212); Rrp6ΔC lacks the C-terminal domain (523-733).

An overview of Rrp6 domain structure is shown (Fig. 4.9 B), as well as the Rrp6 mutants investigated. Rrp6 wild-type protein (top) consists of 733 amino acids with a molecular weight of 84 kDa. Rrp6 contains an N-terminal domain termed PMC2NT domain spanning residues 13-102 which is present in eukaryotes, but not in bacteria (Staub *et al*. 2004), an exonuclease domain (EXO 213-381) and an HRDC (helicase and RNase D C-terminal) domain (435-515). The C-terminus is required for association with the core exosome (Callahan and Butler 2008) and also contains a consensus bipartite nuclear localisation signal (NLS) (Briggs *et al*. 1998). The mutants depicted in Fig. 4.9 (B) were analysed as untagged proteins expressed from the *RRP6* promoter compared to the previously used zz-tagged proteins expressed from the *RRP4* promoter. The D238N mutant, termed *rrp6.1*, is a full-length, catalytically inactive protein with a single amino acid substitution in the exonuclease active site (Burkard and Butler 2000). The C-terminal 197X and 176X truncation mutants *rrp6NT1* and *rrp6NT2* reduce the protein to its N-terminal Rrp47 interaction domain with either 197 residues (L197X NT1) or 176 residues (P176X NT2). The *rrp6ΔNT* mutant lacks the N-terminal 211 residues of Rrp6 including the PMC2NT domain which is required for interaction with Rrp47. The C-terminal truncation P523X removes the NLS (Briggs *et al*. 1998) and a region which is thought to tether Rrp6 to the exosome (Makino *et al*. 2013a).

***The Rrp6NT domain is sufficient to recover Rrp47 expression in an rrp6Δ strain***

The tagged and untagged *RRP6* wild-type constructs (Fig. 4.9 A and C), as well as the mutant *rrp6* alleles (Fig. 4.10B) introduced into the tagged and untagged plasmids were transformed into an *rrp6Δ* strain expressing the Rrp47-zz fusion protein (P439) to assess the effect of the mutations on Rrp6 protein levels, Rrp47-zz expression (Fig. 4.11) and growth (Fig. 4.12). Denatured cell extracts of the Rrp6 mutant strains were resolved by 12 % SDS-PAGE and analysed for Rrp47-zz expression by western blotting using a PAP antibody (Fig. 4.11 upper panels A and B). Rrp6 expression was analysed in parallel (A and B middle panels) using an Rrp6 specific antibody raised against the Rrp6 N-terminus (Mitchell *et al*. 2003a).

Due to the zz-tag, which is recognised by the Rrp6 antibody, a direct comparison of expression levels in untagged and tagged mutants is difficult, since the combined signal for Rrp6 and zz-tag is stronger than for the Rrp6 protein by itself. However the *zz-rrp6ΔNT* mutant lacks the N-terminal domain recognised by the Rrp6 antibody, the signal in (A) therefore represents the sole contribution of the zz-tag to the western signal for tagged Rrp6 proteins (A, lane 5), therefore most of the signal seen for the other tagged mutants stems from Rrp6 protein and not the tag. For the untagged mutants (B, lane 5, right panel) Rrp6ΔNT is not detected by the Rrp6 antibody raised against the Rrp6 N-terminus. The analysis confirmed that Rrp6 protein

levels are higher in the zz-tagged Rrp4 promoter mutants compared to the wild-type *RRP6* strain (compare A, lane 1 to lane 3 tagged mutants and B, lane 1 to lane 3 untagged mutants). Expression of wild-type strain (P364, lane 1) and complemented wild-type (lane 3), as well as mutant proteins (B) are at similar levels in the untagged set and mirror physiological protein levels more accurately than the tagged Rrp4 promoter-driven constructs (A) which led to an overexpression of the *RRP6*/*rrp6* alleles.

Further analysis of the effects of the mutations on Rrp47-zz expression showed that Rrp47 is effectively depleted in the *rrp6Δ* strains transformed with the vector control (lanes 2) compared to the wild-type strain (lanes 1). All mutant Rrp6 proteins recover Rrp47-zz expression in the *rrp6Δ* strain apart from the Rrp6ΔNT mutant (lanes 5), which lacks the N-terminal Rrp47 interaction domain. Notably, in both tagged and untagged sets of proteins, the Rrp6NT interaction domain on its own is sufficient to recover Rrp47 expression to normal levels in the *rrp6Δ* strain (lanes 6). In conclusion, the direct interaction of Rrp47 with the Rrp6NT domain is required to prevent Rrp47 degradation.

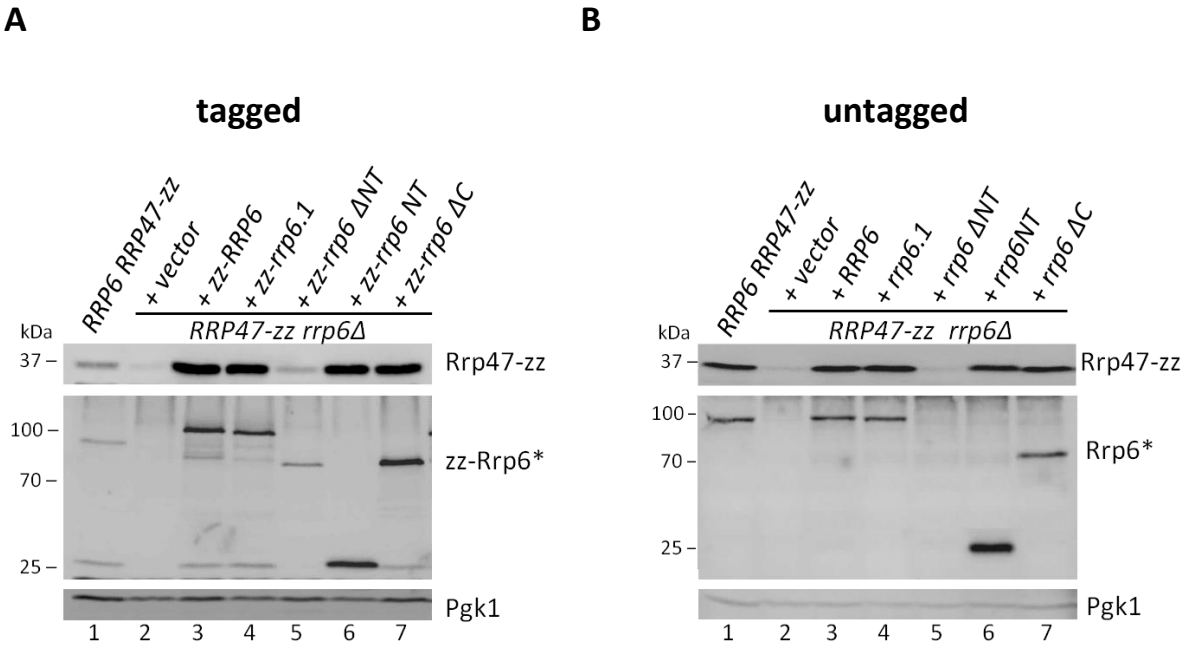


**Figure 4.11 The Rrp6NT domain is sufficient to recover Rrp47 levels in an *rrp6Δ* strain.**
Western complementation analysis of an *RRP47*-zz *rrp6Δ* deletion strain (P439) with (A) zz-tagged and (B) untagged Rrp6 mutants. Wild-type and mutant *rrp6* alleles were transformed into P439. Alkaline lysed cell extracts were resolved through 12 % SDS-PAGE and analysed for Rrp47-zz expression (upper panel) by PAP Western and for Rrp6 expression (middle panel) using an Rrp6 antibody raised against the Rrp6 N-terminus (Mitchell *et al*. 2003a). Pgk1 serves as internal control (bottom panel). (1) *RRP6* wild-type control (P414), (2) pRS416 vector control (3) *RRP6* (p263/p645), (4) *rrp6.1 (p389, p651)*, (5) *rrp6ΔNT* (p260/p652), (6) *rrp6 NT* (p287/p653), (7) *rrp6 ΔC* (p627/p654).

***Lack of the Rrp6 N-terminus affects growth worse than disconnecting Rrp6 from the exosome***

To investigate the effects of the Rrp6 mutants on growth, spot growth analyses were performed over 3 days at 37 °C and 30 °C and 5 days at 18 °C on minimal medium (Figure 4.12). Tagged and untagged sets of Rrp6 mutants were assayed separately with differing starting ODs and can therefore not be compared directly but only within their set. Strains lacking Rrp6 display slow growth at 30 °C and are known to be temperature sensitive at 37 °C (Burkard and Butler 2000). However, the effect of Rrp6 on growth is dependent on strain background and here the widely available BY4741 strain was used to assess Rrp6 mutants where the growth effect at 30 ˚C is only minor in the *rrp6Δ* strain compared to the W303-1A related strains used in the above cited study. The spot growth assays confirmed a slow growth phenotype at 37 °C (and 18 °C) for strains lacking Rrp6 and strains carrying the catalytically inactive *rrp6.1* allele were cold-sensitive as reported previously (Burkard and Butler 2000). Growth at the permissive temperature (30 °C) was very similar for all untagged mutants (B), whereas growth was slightly slower for strains expressing tagged Rrp6 mutants compared to tagged wild-type protein (A). In the tagged set (A), only the wild-type *RRP6* allele showed improved growth and complementation of the slow growth *rrp6Δ* phenotype whereas the other mutants displayed a similar slow growth phenotype to *rrp6Δ* strains expressing the vector control. This could be due to a beneficial effect of overexpressing or stabilising the fully functional wild-type protein as opposed to stabilising the compromised mutants.

In the untagged set, only the *rrp6.1* mutant showed slow growth at 18 °C whereas the other Rrp6 mutants were not significantly affected by the lower temperature. In contrast, growth of the tagged mutants except for Rrp6ΔC was generally worse compared to wild-type at 18 °C. Most striking is the difference in growth phenotypes at 37 °C, where only full length Rrp6 and Rrp6ΔC display normal growth, the Rrp6NT domain is clearly non-functional on its own to support growth at 37 °C and both the Rrp6ΔNT and Rrp6.1 proteins displayed slowed growth at 37 °C with good agreement in both sets. At the higher temperature, therefore, deletion of the Rrp47 interaction domain had significant effects on growth and survival. The differences between tagged and untagged sets can be explained by the overexpression or stabilisation of tagged proteins as observed in the western analyses. Overexpression of the tagged wild-type protein seemed beneficial as seen in the bigger differences between complemented wild-type versus mutant alleles in the tagged set. In contrast, overexpression of mutant proteins adversely affected growth at the non-permissive temperatures compared to the observations made in the untagged set.

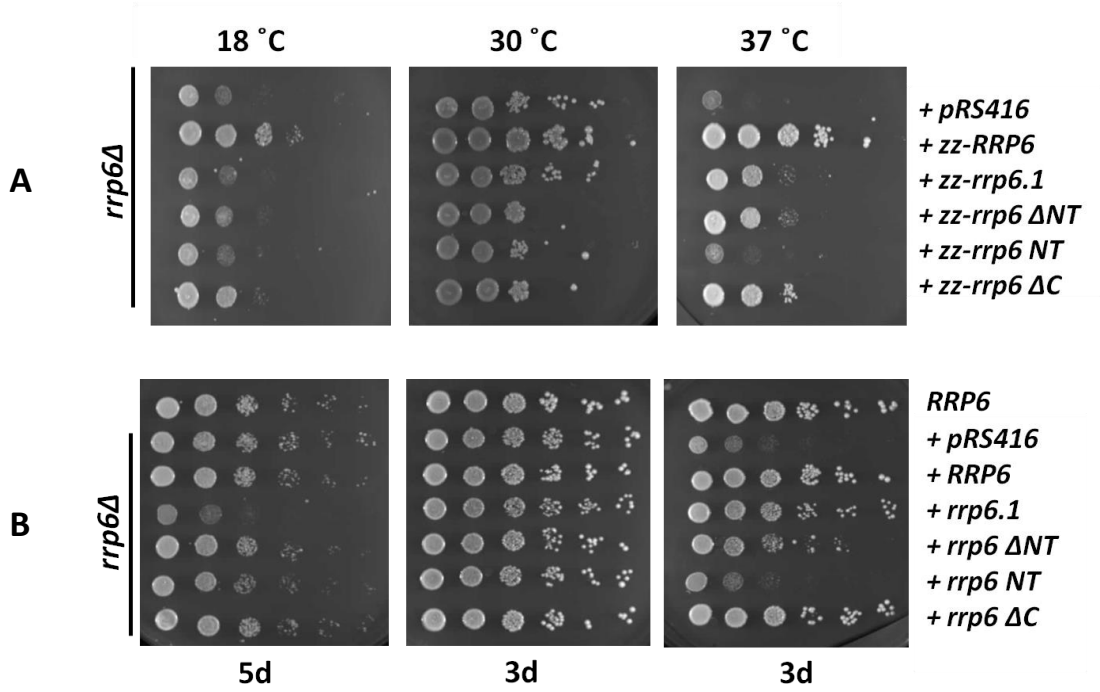


**Figure 4.12 Losing the Rrp6-Rrp47 interaction affects growth.**
Spot growth analysis of tagged (A) and untagged (B) *RRP6* wild-type and *rrp6* mutant alleles transformed into an *rrp6Δ* strain (P781) along with wild-type (P364) and vector controls (pRS416). Freshly grown liquid cultures adjusted for equal $OD_{600}$ were 10-fold serially diluted and 4 µl of each dilution was spotted onto selective medium (SD-ura). Growth was observed over 3 days at 30 °C and 37 °C and over 5 days on 18 °C. From top to bottom *RRP6* wild-type strain (B only, P364), (A and B) vector control (pRS416), full length *RRP6* (p263/p645), *rrp6.1* (p448/p651), *rrp6Δ*NT (p449/p652), *rrp6NT* (p287/p653), *rrp6 ΔC* (p627/p654).

In conclusion, growth effects of a *RRP6* deletion were milder in the BY4741 strain background at 30 ˚C than previously reported for the BMA38 strain. However, only the wild-type allele, but none of the Rrp6 mutant alleles complemented the *rrp6Δ* growth phenotype fully at the temperatures observed. Despite linking Rrp6 to the core exosome and containing an NLS for nuclear localisation, loss of the C-terminal domain Rrp6ΔC affected growth the least at any temperature. Lack of the Rrp6 catalytic activity showed the strongest effects on growth as seen for Rrp6.1 and the Rrp6NT truncation mutants at the non-permissive temperatures at 18 ˚C and 37 ˚C. Rrp6NT by itself did not complement slow or ts growth at the permissive and non-permissive temperatures. However, Rrp6ΔNT which lacks the N-terminal Rrp47 interaction domain clearly had an effect on growth, similar to losing the catalytic activity of Rrp6 at the non-permissive temperature.

***rrp6ΔNT mutants display a complete rrp6Δ RNA processing phenotype***

Parallel to the growth analyses, the strains carrying Rrp6 mutants were assessed for typical defects seen in *rrp6Δ* strains in pre-rRNA and sn/snoRNA processing by northern blot analyses. Cells were grown up to $OD_{600}$ < 0.5, total RNA was extracted and resolved through an 8 % denaturing polyacrylamide gel and transferred onto Hybond N+-membrane which was successively probed with oligonucleotides complementary to certain target RNA species (Fig. 4.13 A-C). A comparison of the *rrp6Δ* vector control (lane 2) with the isogenic wild-type strain (lane 1) shows the characteristic RNA processing defects of *rrp6Δ* strains. RNA processing intermediates which accumulate in the absence of Rrp6 include 3' extended polyadenylated precursors of snoRNAs and snRNAs (lane 1, A+B), cryptic unstable transcripts (CUTs, C), as well as aberrant species derived from rRNA processing, such as the 5'ETS fragment, the 5.8S +30 rRNA and the 5S degradation intermediate (D). Table 1 shows a summary of the results. CUTs are fairly short (median size 440 bases) non-coding transcripts produced by RNAPII and terminated by the Nrd1 pathway which are rapidly and efficiently degraded by the exosome and therefore not easily detectable in wild-type strains. However, they accumulate in *rrp6Δ* strains and other exosome mutants (Wyers *et al.* 2005, Arigo *et al.* 2006a). In order to test the Rrp6 mutants for a CUT accumulation phenotype a probe specific for the model CUT NEL025c (Thiebaut *et al*. 2006) was used (o809).

All the full-length *RRP6* alleles (lanes 3-5) expressed from plasmids complemented the *rrp6Δ* phenotype fully despite the tag or the difference in promoter constitution (asterisk in *RRP6** denotes *RRP4* promoter) compared to the *RRP6* wild-type strain (lane 1). In contrast, the catalytically inactive *rrp6.1* allele, the *rrp6NT* and the *rrp6ΔNT* allele lacking the Rrp47 interaction domain displayed *rrp6Δ* phenotypes for all RNA species tested (A-D, lanes 6, 7 and 8), except for the CUT NEL025c which accumulated in the *rrp6Δ* strain and to a lesser degree in the *rrp6NT* and the *rrp6ΔC* mutant, but not in the *rrp6.1* and *rrp6ΔNT* mutant. This is consistent with recent observations that Rrp6, independent of its catalytic activity, modulates the activity of the core exosome exo-/endonuclease Dis3/Rrp44 which is involved in the degradation of CUTs (Wasmuth *et al.* 2012).

Short (A2) and long (A1) exposures of the intron-encoded snR38 probe revealed the discrete '+3' nucleotide extended (snR38+3) and longer unprocessed 3' extensions (snR38-3' I-pA and II-pA) typically seen in *rrp6Δ* mutants (lane 2) which represent polyadenylated precursors of snoRNA transcript terminated at site I via the Nrd1 pathway and site II via the fail-safe terminator (Grzechnik and Kufel 2008). Other snoRNAs and snRNAs like snR13, U6 and U1 showed short, but more diffuse 3' extensions visible as a smear above the band of the mature RNA species (A and B, lane 2, lane 6, 7, 8) or longer 3' extended processing intermediates as seen for U14 (B2).

The snoRNA13 and U3 species also showed accumulation of a degradation intermediate, seen as a band below the mature species (A4 and B4). The *rrp6NT* domain by itself lacks the exonuclease and HRDC domains and is therefore not expected to be functional in RNA processing, however for some RNA species the phenotype was not as strong as a complete *rrp6Δ* null phenotype, e.g. and snR50 (A, lane 8), or was stronger than *rrp6Δ* as for the 5S and U3 degradation intermediates and the CUT (C). This could indicate independent functions of the *rrp6NT* domain possibly together with Rrp47, but separate from the Rrp6-Rrp47-exosome complex.

Surprisingly, the *rrp6ΔC* (Rrp6 P523X) mutant which has previously been reported not to affect RNA processing (Callahan and Butler 2008) clearly showed effects on certain RNA species tested here. The snR38 and snR50 snoRNAs (A, lane 9) showed half mature and half sn38+3 and snR50+3 species. The *rrp6ΔC* mutant clearly accumulated the 5'ETS by-product from the initial cleavage of the pre-rRNA (D, lane 9). A weak phenotype was also observed for U3 and 5S rRNA with a degradation intermediate visible as in the other mutants with null phenotypes (B, lane 9, and D, lane 9). Again, these phenotypes in mutants disrupting the association of Rrp6 with the exosome could be explained by the modulation of Rrp6 and core exosome Rrp44/Dis3 activities in each other's presence or absence (Wasmuth *et al.* 2012). Despite the zz-tag and expression of the *rrp6* alleles from the *RRP4* promoter, RNA analyses of zz-tagged and untagged Rrp6 mutants were identical, therefore only the set of data obtained from untagged Rrp6 constructs expressed from the *RRP6* promoter is shown in Fig 4.13.

**Table 4.1 RNA processing phenotypes of *RRP6/rrp6* mutants and growth at 37 ˚C**

| | snR38+3 | snR38-3' | U6 pA | 5'ETS | 5.S+30 | 5S | CUT | 37 ˚C |
|---|---|---|---|---|---|---|---|---|
| ***RRP6*** | - | - | - | - | - | - | - | ++++ |
| ***rrp6Δ*** | + | + | + | + | + | + | + | + |
| ***rrp6.1*** | + | + | + | + | + | + | - | ++ |
| ***rrp6ΔNT*** | + | + | + | + | + | + | - | ++ |
| ***rrp6NT*** | + | + | + | + | + | + | + | + |
| ***rrp6ΔC*** | + | - | - | + | - | +/- | + | +++ |

In conclusion, the lack of the Rrp47 interaction domain Rrp6ΔNT results in a complete *rrp6Δ* RNA processing phenotype, as does the lack of Rrp6 catalytic activity. This indicates an inhibition of the Rrp6-Rrp47 pathway due to either absence of Rrp47 or lack of Rrp6 catalytic activity.

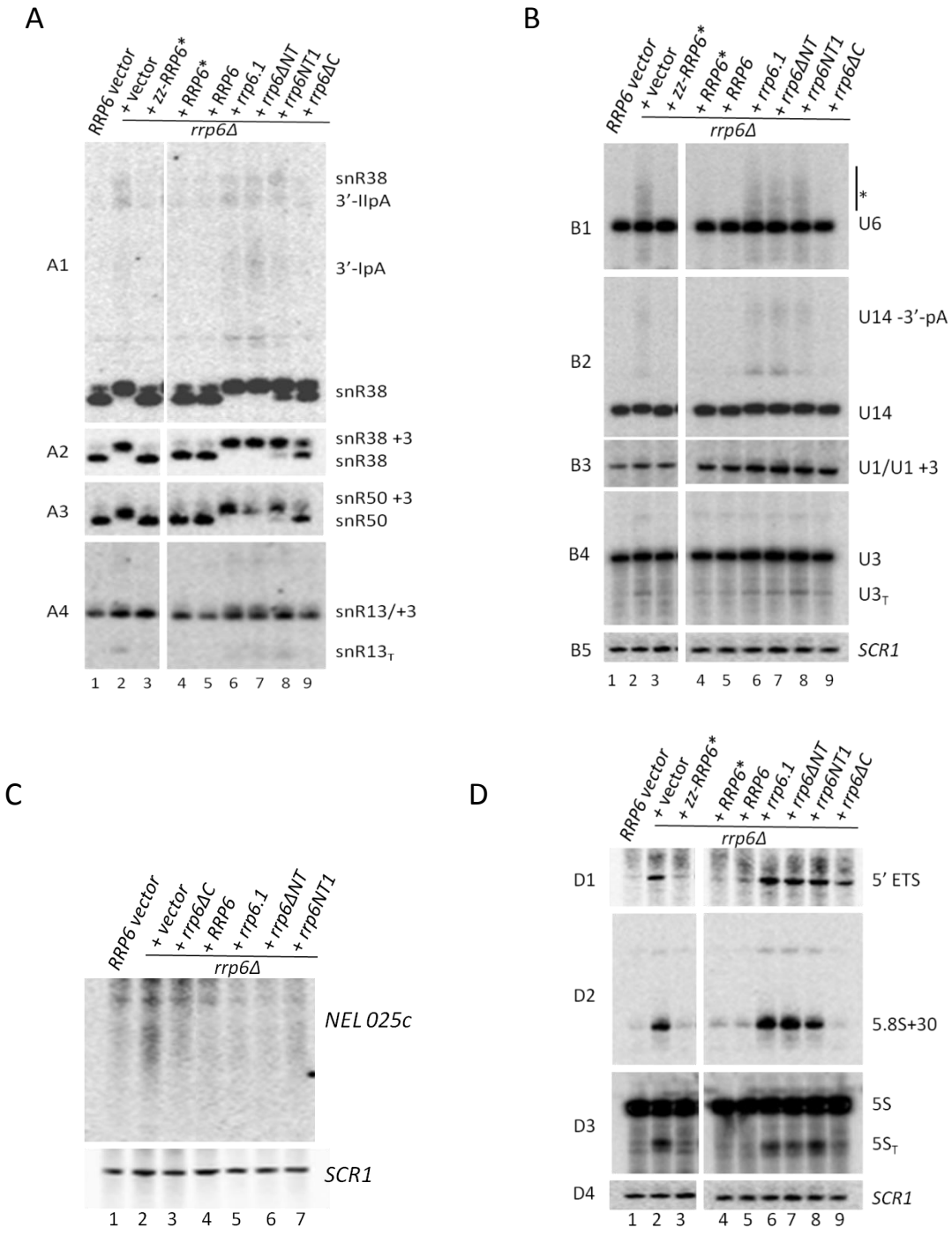


**Figure 4.13 *Rrp6ΔNT* mutants display a complete *rrp6Δ* RNA processing phenotype.**

Northern blot analyses of *rrp6Δ* strains expressing Rrp6 full length and mutant alleles as in Fig. 4.11. *RRP6* wild-type (P364) and *rrp6Δ* (P781) strains complemented with vector control and *rrp6* alleles were grown at 30 ˚C to 0.5 $OD_{600}$. Total RNA was extracted, resolved through an 8 % polyacrylamide gel and analysed by northern hybridisation with probes specific for the RNA species indicated to the right of the panels (A+B) snoRNAs and snRNAs (C) NEL025c CUT and (D) pre-rRNAs. *SCR1* (A-D, bottom panel) serves as loading control. Extended polyadenylated precursors are marked 3'-pA (A1, B2), I and II denote the termination sites (A1) for the longer snR38 exposure. Defined +3 (A, B) and +30 nucleotide extensions (D) are indicated. More diffuse 3' extensions seen for U6 are marked with an asterisk (B1). Degradation intermediates are denoted $snR13_T$ (A4), $U3_T$ (B4) and $5S_T$ (D3).

### 4.2.5 Overexpressing Rrp6NT titrates Rrp47 out of Rrp6-Rrp47 complexes

Rrp47 can be found in Rrp6-containing exosome complexes (Mitchell *et al.* 2003, Peng *et al.* 2003). Having established that Rrp6NT is sufficient for expression and interaction with Rrp47, it appeared feasible to remove Rrp47 out of Rrp47-Rrp6 complexes by overexpressing Rrp6NT. This would allow to investigate potential effects of Rrp47 independent of catalytic Rrp6 complexes. In order to address this, Rrp47 complexes were analysed using glycerol gradient density centrifugation. The procedure is presented in Figure 4.14. Gradients were prepared in lysis buffer with a glycerol concentration from 10 % at the top to 30 % at the bottom using a gradient mixer. Freshly prepared native cell extracts were loaded onto the gradients and sedimented for 24 hours in an ultracentrifuge. Then, 18 fractions were collected and analysed for protein concentration (Fig. 4.14 A, B) and protein distribution (Fig 4.14 C Coomassie gel) to ensure comparability of gradients run in parallel before western analysis. Protein concentration was determined using the Bradford Assay; for Coomassie stains, samples were resolved by 10 % SDS-PAGE and stained with Coomassie Instant Blue.

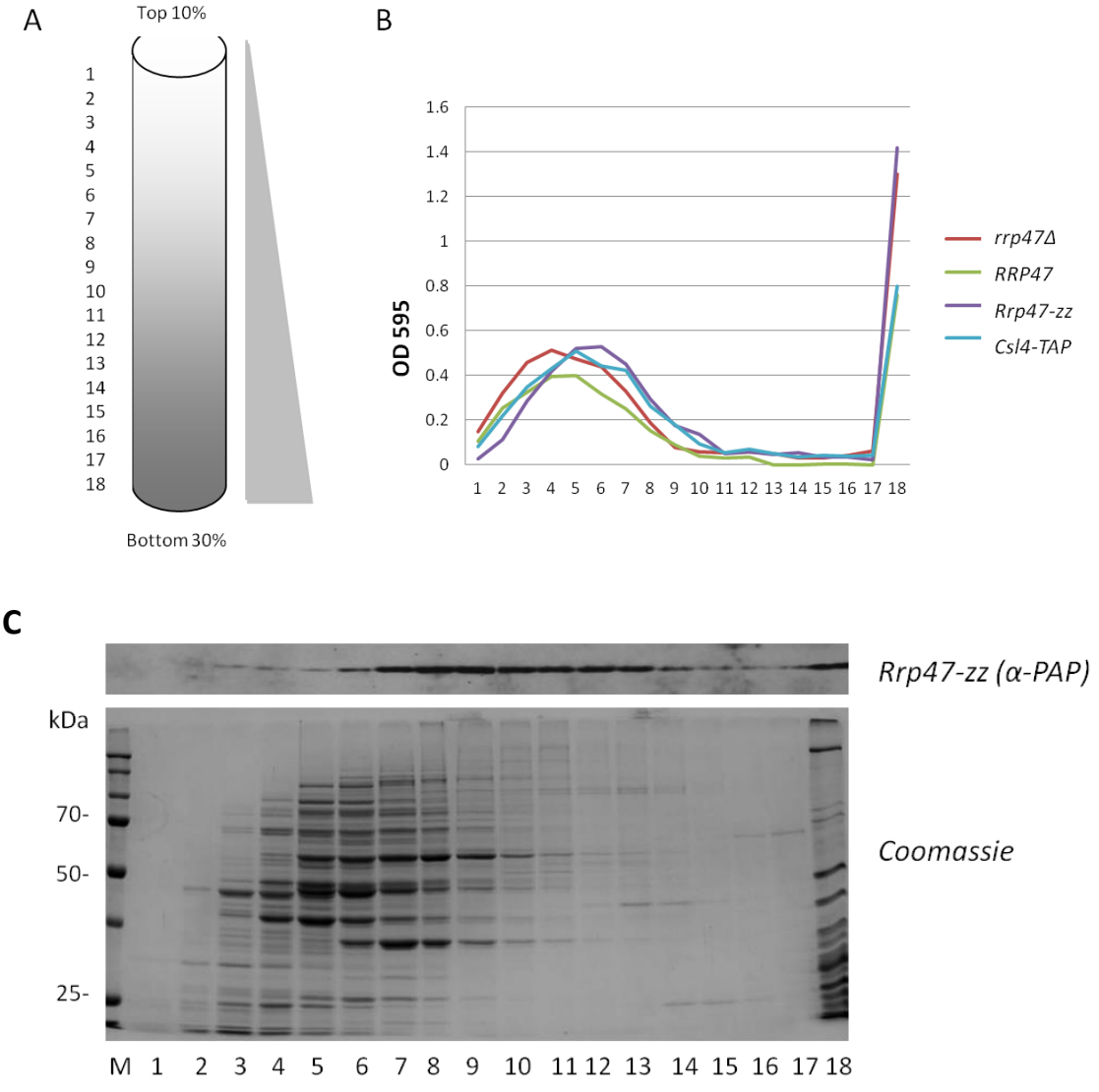

**Figure 4.14 Separation of protein complexes in glycerol gradients.**
(A) Schematic of a 10 to 30 % glycerol gradient prepared with yeast lysis buffer using a gradient mixer. The finished gradient has the highest concentration of glycerol at the bottom (30 %) with glycerol concentration gradually decreasing to 10 % at the top. Native yeast cell extracts were loaded and resolved in an SW41 rotor in a Beckmann ultracentrifuge at 36000 rpm, 4 ˚C for 24 hours. 18 fractions were collected from the top of each gradient and the protein concentration was determined using the Bradford assay. (B) Protein concentration curves of gradients run in parallel were plotted in a graph against the fraction number to ensure similar distribution of total protein for separate gradients. (C) Two sets of the fractionated samples were resolved by 10 % SDS-PAGE, one analysed by western blotting with a relevant specific antibody, here detection of the Rrp47-zz protein with the PAP antibody (C upper panel). The second gel was stained with Coomassie colloidal stain to further compare and confirm total protein distribution patterns (C, lower panel) with other gradients run in parallel.

In an initial experiment, it was established that the commonly used Rrp47-zz strain (P414) gives the same Rrp47 sedimentation profile as the wild-type strain (P575). Gradients of isogenic *rrp47Δ*, untagged *RRP47* wild-type and *RRP47*-zz strains were run in parallel with a strain expressing Csl4-TAP, one of the cap proteins of the yeast core exosome used here as marker for exosome complexes. Along with the yeast lysates, a mix of standard molecular weight markers with known sedimentation coefficients was fractionated containing BSA, ovalbumin and catalase as indicated (Fig. 4.15) to use as size markers.

Western analysis confirmed that Rrp47 and Rrp47-zz gradients result in the same sedimentation profile with a peak in fractions 9 and 10 (ranging from 8-12 and from 6-14, respectively). The signal from the PAP antibody is stronger and therefore observed over a wider range of the gradient than that obtained with an Rrp47-specific antibody for the wild-type protein. Also, results obtained with Rrp47 and Rrp47-zz were in good agreement which means the C-terminal tag does not affect inclusion of Rrp47 into higher molecular weight complexes. In conclusion, most of the Rrp47 protein is seen in larger complexes close to catalase (11.3 S, app. 250 kDa) and not as “free” protein. The higher molecular weight complexes are in good agreement with the profile seen for Csl4-TAP which displayed two peaks, one at around 11-13 which is representative of higher molecular weight complexes i.e. Csl4-TAP incorporated into exosome complexes with a sedimentation coefficient of 14S (Mitchell *et al.* 1997) and another peak around fraction 5 representing a fraction of Csl4-TAP protein not associated with the exosome (app. 70 kDa).

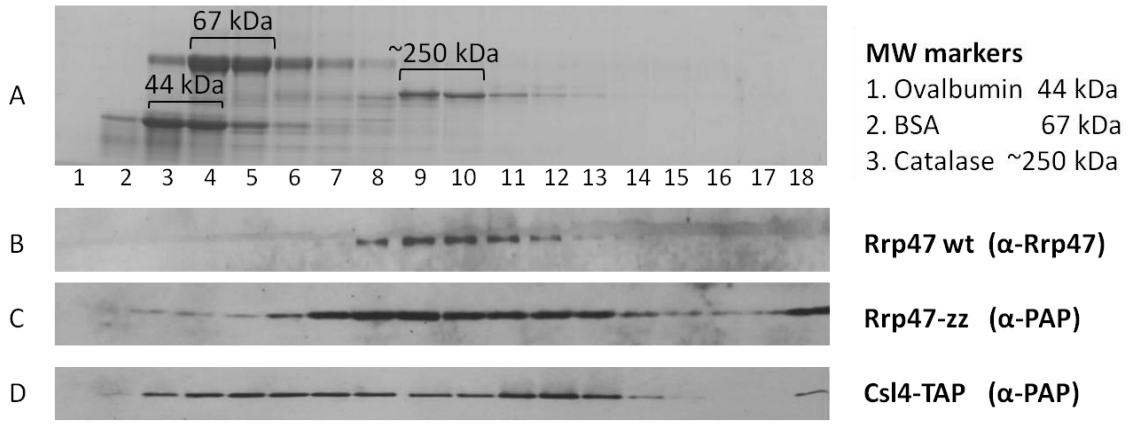


**Figure 4.15 Rrp47 wild-type and Rrp47-zz proteins sediment within the same range.**
Native yeast cell lysates of an *RRP47* wild-type strain (P575) and an *RRP47*-zz tagged strain (P414) were resolved through 10 to 30 % glycerol gradients along with an *rrp47Δ* strain, the *CSL4-TAP* strain and a mix of standard molecular weight markers (A, top panel) with sizes (in kDa) as indicated. 18 fractions with increasing glycerol concentration from left to right were resolved by 10 % SDS-PAGE and analysed for distribution and content of total protein by Coomassie stain and Bradford assay (as shown in Fig 4.13 B). Fractionated gradients were analysed by western blotting using an Rrp47-specific antibody (B) and a PAP antibody to detect Rrp47-zz (C) and Csl4-TAP (D).

***Overexpression of Rrp6NT shifts Rrp47 into Rrp6NT-Rrp47 complexes***

Due to the lack of Rrp47 expression in *rrp6Δ* mutants, it is difficult to investigate the function or contribution of Rrp47 in exosome- and Rrp6-mediated RNA processing independently of Rrp6. The lab has previously shown that Rrp6NT directly interacts with Rrp47 and can be stably overexpressed in yeast as a GST-tagged fusion protein driven by a galactose-inducible (GAL) promoter (Stead *et al*. 2007). To investigate whether overexpression of the Rrp6NT domain could segregate Rrp47 from Rrp47-Rrp6 complexes and to address functions of Rrp47 independently of catalytic Rrp6, multi-copy plasmids carrying the GST-Rrp6NT fusion protein or the GST control were transformed into an Rrp47-GFP strain (see 4.7). Cell lysates were fractionated as before. Shown are also gradients with lysates from Rrp47-zz strains grown in minimal medium based on either glucose or galactose as medium controls. Matching total cellular protein profiles were confirmed by SDS-PAGE and Coomassie stains of the fractionated samples. Parallel western analyses were performed to compare the sedimentation profiles of Rrp47-zz protein under the various growth conditions (Fig. 4.16).

As described above, cells expressing Rrp47-zz grown in rich medium (A, YPD) peaked in fraction 9 /10 as part of higher molecular weight complexes. In control cells grown in minimal medium based on either glucose (B, SD) or galactose (C, SGal), Rrp47-zz sedimented with a major peak in fraction 7 (range 6-9), which represents a clear shift into lower molecular weight complexes

for cells grown in minimal medium. In cells grown in galactose-based medium expressing GFP-tagged Rrp47 in addition to the GST domain (D, upper panel), a similar sedimentation profile for Rrp47-GFP was observed as for Rrp47-zz in minimal medium; GST peaked in fraction 3-4, similar to ovalbumin which was in good agreement with the size of the GST-dimer (D, lower panel). Both GST and GST-Rrp6NT form a GST dimer in the absence of Rrp47 and ran at the expected molecular weight for these dimers. The shift of Rrp47 with a peak in fraction 7 observed with the GST control (D upper panel) is due to growth in minimal medium (compare SD-Gal, SD minimal medium controls).

In cells where the GST-Rrp6NT domain was overexpressed (Fig. 4.16 E, upper panel), the profile of Rrp47 and GST-Rrp6NT proteins showed clearly overlapping peaks in fraction 5 and a similar sedimentation to that of BSA (4.3 S, 67 kDa). Here, Rrp47-GFP shifted into even smaller complexes which correspond to the size of a GST-Rrp6NT-Rrp47-GFP dimer. Pull-down assays by P. Mitchell confirmed that upon overexpression of the GST-Rrp6NT domain, Rrp47 was mainly associated with the Rrp6NT-GST fusion protein and the interaction between Rrp47 and Rrp6 was effectively disrupted and reduced to around 4 % (Garland *et al.* 2013).

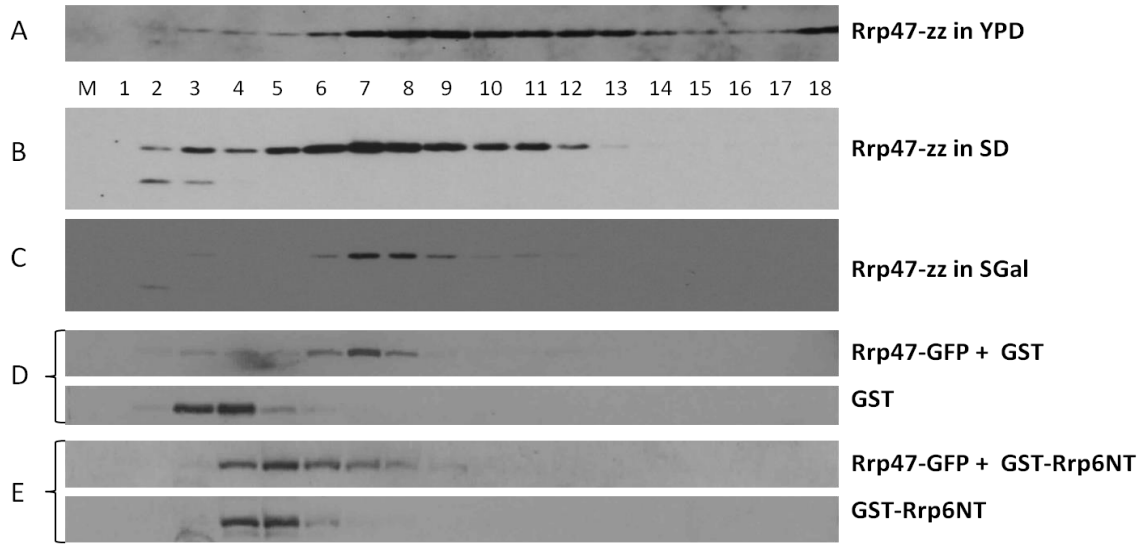


**Figure 4.16 Overexpression of Rrp6NT shifts Rrp47 into smaller complexes.**
Western analysis of native cell extracts from Rrp47-zz strains after fractionation through glycerol gradients. Extracts were prepared from Rrp47-zz strains grown in A complete medium (YPD), B glucose based minimal medium (SD), C galactose based minimal medium (SGal) and Rrp47-GFP strains transformed with a GST-tag (as control, D) or GST-Rrp6NT (E), an N-terminal GST fusion of Rrp6 that lacks residues 212 to 721 (Stead *et al.* 2007) on a multi copy plasmid grown in minimal medium (SD). Fractionated samples were resolved by 10 % SDS PAGE and analysed by western blotting using either PAP/GFP or anti-GST antibodies to detect zz-Rrp47 (A, B, C) /Rrp47-GFP (D, E upper panel) or GST (fusion) proteins (D, E lower panel), respectively.

Taken together, the data from glycerol gradient analyses and subsequent pull-down experiments demonstrate that Rrp47 is effectively titrated out of Rrp6-containing complexes upon overexpression of the Rrp6NT domain. Rrp47 is shifted from higher molecular weight complexes into smaller complexes which correspond to the expected size for an Rrp47-GST-Rrp6NT heterodimer. The segregation of Rrp47 from Rrp6 complexes by overexpression of GST-Rrp6NT was subsequently used as a tool to study functions of Rrp47 when uncoupled from the catalytic activity of Rrp6 (Garland *et al.* 2013).

### 4.2.6 Rrp47 does not require Rrp6 for nuclear import

Considering the dependency of Rrp47 on Rrp6 for expression and the fact that of the two proteins only Rrp6 is known to carry a nuclear localisation signal (NLS) (Briggs et al. 1998), it is likely that Rrp47 binding to Rrp6 might be required for Rrp47 to be imported into the nucleus. Proteins are synthesised in the cytoplasm and need to pass through nuclear pore complexes (NPCs) to reach the nucleus. Most macromolecules (> 60 kDa) require a nuclear localisation signal (NLS) for import (Mohr *et al.* 2009) which is recognised and bound by transport receptors, many of them belong to the karyopherin (importin and exportin) families. In yeast, Srp1 (karyopherin /importin-α, 60 kDa) binds the NLS of its protein substrates and forms a cargo-complex with Kap 95 (karyopherin β) to mediate translocation of the proteins through the NPC from cytoplasm to nucleus (Tabb *et al*. 2000, Gruenwald *et al.* 2011). Rrp6 carries two sequences similar to consensus NLS at its C-terminus (Briggs *et al*. 1998) which, if deleted, mislocalise a fraction of Rrp6 to the cytoplasm (Phillips and Butler 2003). Further, a stable association between TAP-tagged Rrp6 and the Srp1-Kap95 (importin α-β) complex has been reported from pull-down experiments (Peng *et al*. 2003, Synowsky *et al*. 2009). These observations suggest that Rrp6 uses the importin-$\alpha$/β pathway for nuclear import. Rrp47 and its human homologue C1D also localise to the nucleus (Nehls *et al.* 1998, Kumar *et al.* 2002), however, no nuclear localisation signal has been documented for Rrp47 and analogous pull-down experiments have not reported an association of Rrp47 with Srp1 (Peng *et al.* 2003). As a likely scenario, Rrp47 needs Rrp6 for nuclear import, therefore Rrp47-Rrp6 assembly could occur in the cytoplasm following translation for joint import and Rrp47 is degraded if Rrp6 is not available to facilitate import.

#### *Rrp47 is not part of the Rrp6-Srp1-import complex*

To test this hypothesis and investigate whether Rrp6 and Rrp47 can be found together in the Rrp6-Srp1-import complex, Rrp6 and Rrp47 proteins from yeast cell lysates were directly compared for Srp1 association. Yeast cell lysates expressing protein A-fusion proteins of Rrp47 and Rrp6 were bound to IgG-Sepharose beads and retained protein was eluted and resolved by

SDS-PAGE followed by western analyses using an Srp1-specific antibody (Fig. 4.17). Srp1 levels were comparable in input (lanes 1-3, upper panel) and supernatant fractions (lanes 4-6, upper panel). The eluate fractions represent the amount of Srp1 bound to the respective bait (lane 7 untagged control, lane 8 Rrp6-TAP, lane 9 Rrp47-zz, upper panel) and reproducibly showed increased levels of Srp1 associated with Rrp6 compared to the wild-type control strain, which accounts for non-specific background binding. The signal obtained for Srp1 binding to Rrp47 was close to background, despite the much greater amount of Rrp47 bound to IgG compared to Rrp6 (lane 6 vs. lane 5 and lane 9 vs. lane 8, lower panel). The efficiency of the Rrp6 pull-down on IgG was generally much lower than for Rrp47 as seen in the amounts of protein left in the supernatant (SN), as well as the amounts of protein recovered in the eluates (lower panel). Additional bands visible in the bound fractions result from traces of IgG heavy and light chains detected with the PAP antibody (lane 7, 8, 9, marked with asterisks), as well as proteolytic fragments of Rrp6 and Rrp47 typically observed in native cell extracts. These results suggest that a significant fraction of Rrp6, but not Rrp47, is stably associated with Srp1. Therefore, Rrp47 is not part of the Rrp6-Srp1-import complex and does not use this nuclear import pathway. As a consequence, unless Rrp6 uses additional import pathways, Rrp6 and Rrp47 are most likely imported into the nucleus separately.

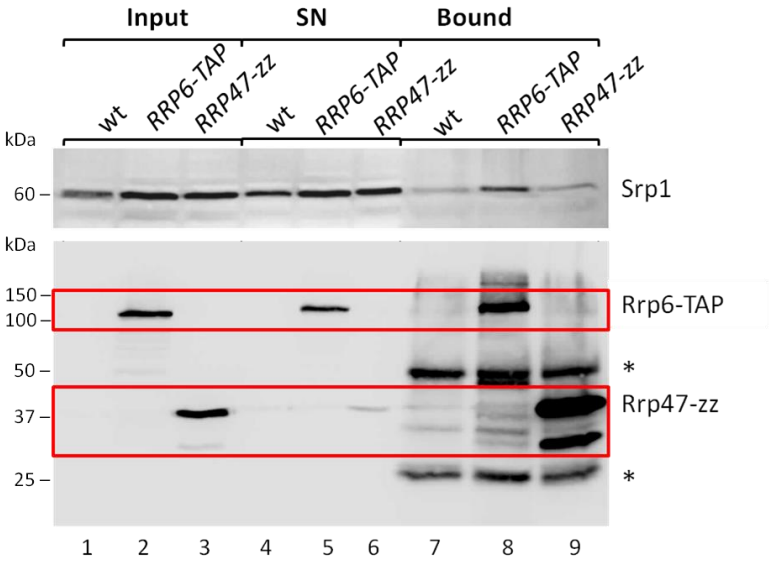


**Figure 4.17 Rrp47 is not associated with the Rrp6-Srp1-import complex.**
Western analysis of co-immunoprecipitation assays using yeast cell extracts from strains carrying tagged Rrp6-TAP (P539) and Rrp47-zz (P414) fusion proteins versus a wild-type strain (P575). The yeast cell extracts were incubated with IgG Sepharose and equal amounts of input, supernatant (SN) and eluate fractions were resolved by 12 % SDS-PAGE and analysed by western blotting with an Srp1-specific antibody (α-importin-α, upper panel) and a PAP antibody (lower panel) to detect bait protein. The PAP blot shows additional bands which are typical Rrp6 and Rrp47 proteolytic fragments in the respective lanes and IgG proteins (marked with an asterisk) in all eluate fractions which are detected by the PAP antibody.

***Rrp47-GFP and Rrp6-GFP localise to the nucleus independently of one another***

To further address the influence of Rrp6 on Rrp47 localisation, a C-terminally tagged Rrp47-GFP strain was created. The GFP tag was amplified from GFP (S65T) protein-tagging modules (Longtine *et al.* 1998) carrying either a HIS3MX6 or kanMX6 selectable marker. The GFP primers (o578/o579) were designed with homology sequences to the *RRP47* ORF and flanking sequences, which target the PCR product to the *RRP47* locus for homologous recombination. Transformants were screened by colony PCR for the appropriate size of the *RRP47*-GFP allele All candidates tested expressed the Rrp47-GFP protein as confirmed by western analysis using an anti-GFP antibody (Fig. 4.18 A). Plate assays confirmed that growth of the Rrp47-GFP strains was not affected by the GFP tag (Fig. 4.18 B). Cells were grown to $OD_{600} < 1$ in minimal medium for fluorescence microscopy along with a commercially available Rrp6-GFP strain and a wild-type strain (P364). Nuclei were stained with 4', 6-diamidino-2-phenylindole (DAPI) to confirm overlap of the nuclear and the Rrp47-GFP signal when merged. Live-images were taken using a Delta Vision microscope (GE Healthcare, Applied Precision) with a 100 x objective (Olympus). Both proteins, Rrp47-GFP and Rrp6-GFP, clearly localised to the nucleus as previously reported (Fig. 4.18 C). A GFP signal of similar strength is obtained for the Rrp47-GFP (P1160) strain as for the commercial Rrp6-GFP strain. On close inspection, the GFP signal in both strains is polarised and focused in a specific area of the nucleus consistent with nucleolar localisation (Fig. 4.18). The wild-type strain shows background signal only.

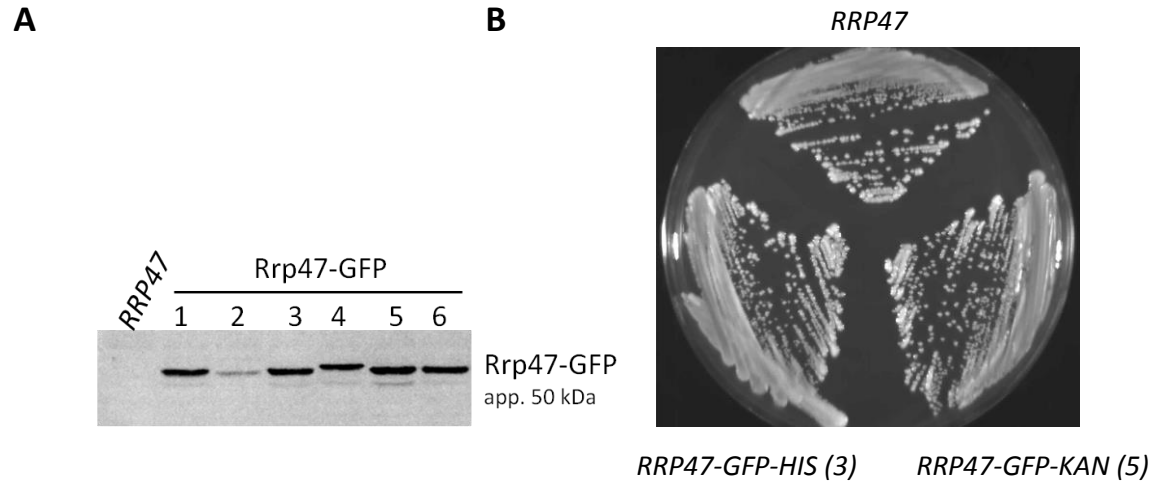


**Figure 4.18 The Rrp47-GFP fusion protein is localised to the nucleus.**
(A) Western analysis of Rrp47-GFP transformants for protein expression using a GFP-specific antibody. Cell lysates of candidates were resolved by 12 % SDS-PAGE (B) Growth assay to compare *RRP47* wild-type and GFP-tagged strains at 30˚ C for 3 days on complete medium.

**C**

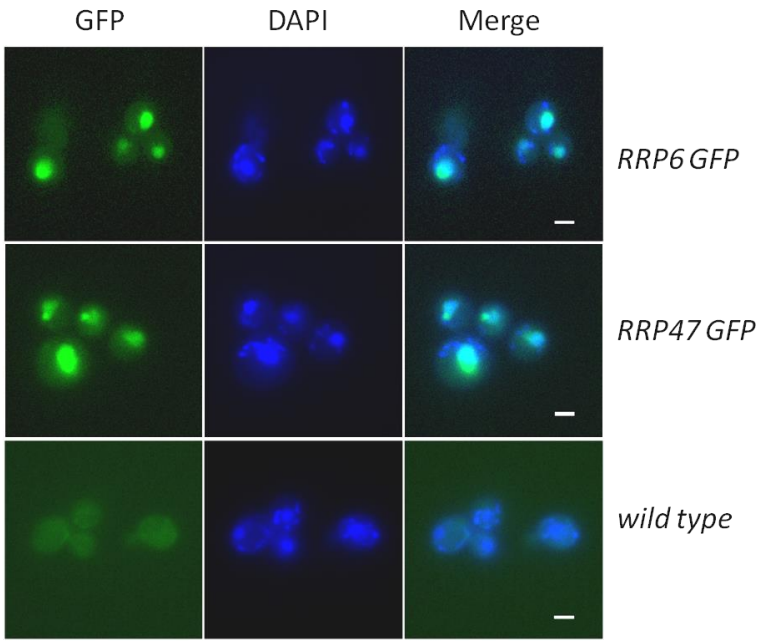


**Figure 4.18 The Rrp47-GFP fusion protein is localised to the nucleus.**
(C) Localisation of Rrp47-GFP vs. Rrp6-GFP and wild-type protein. Cells of the newly created *RRP47*-GFP strain (P1160) were grown up alongside a commercial *RRP6*-GFP strain (Roche) and a wild-type control (P364) in minimal medium to $OD_{600}$ < 1. Cells (1ml) were harvested, resuspended in 100 µl medium and stained with DAPI for 1 minute before analysis in a DeltaVision microscope using a 100 x Olympus objective. Representative images (stack projections) are shown from both strains for GFP, DAPI and merged signals. The bottom panel shows the isogenic wild-type strain (P364). The scale bar corresponds to 2 µm.

***RRP6 deletion leads to a decrease but not loss of the Rrp47-GFP signal in the nucleus***

In order to assess whether Rrp47 localisation is dependent on Rrp6, the *RRP6* wild-type allele in the *RRP47-GFP* strain was replaced with a *rrp6Δ::kanMX4* cassette by PCR-mediated homologous recombination using oligos o457/o458 (Rothstein 1983). Transformants were screened and confirmed by colony PCR for the *rrp6Δ::kanMX4* cassette, as well as the *RRP47-GFP* allele. Cells were prepared for live-imaging and localisation analysis as before. The loss of Rrp6 led to a decrease, but not to a complete loss of the Rrp47-GFP signal in the nucleus (Fig. 4.19 C). However, a clear nuclear signal was still observed in the *rrp6Δ* mutant compared to the wild-type control (A) which is surprisingly strong given the low expression levels of Rrp47 expected in an *rrp6Δ* strain. This strongly indicates that Rrp47-GFP is imported into the nucleus in the absence and thus independent of Rrp6. Adding any of the full length tagged and untagged *RRP6* expression constructs back to the *rrp6Δ* mutant, reinstated the fluorescence signal of the Rrp47-GFP fusion protein to wild-type levels (Fig. 4.19 D, E, F).

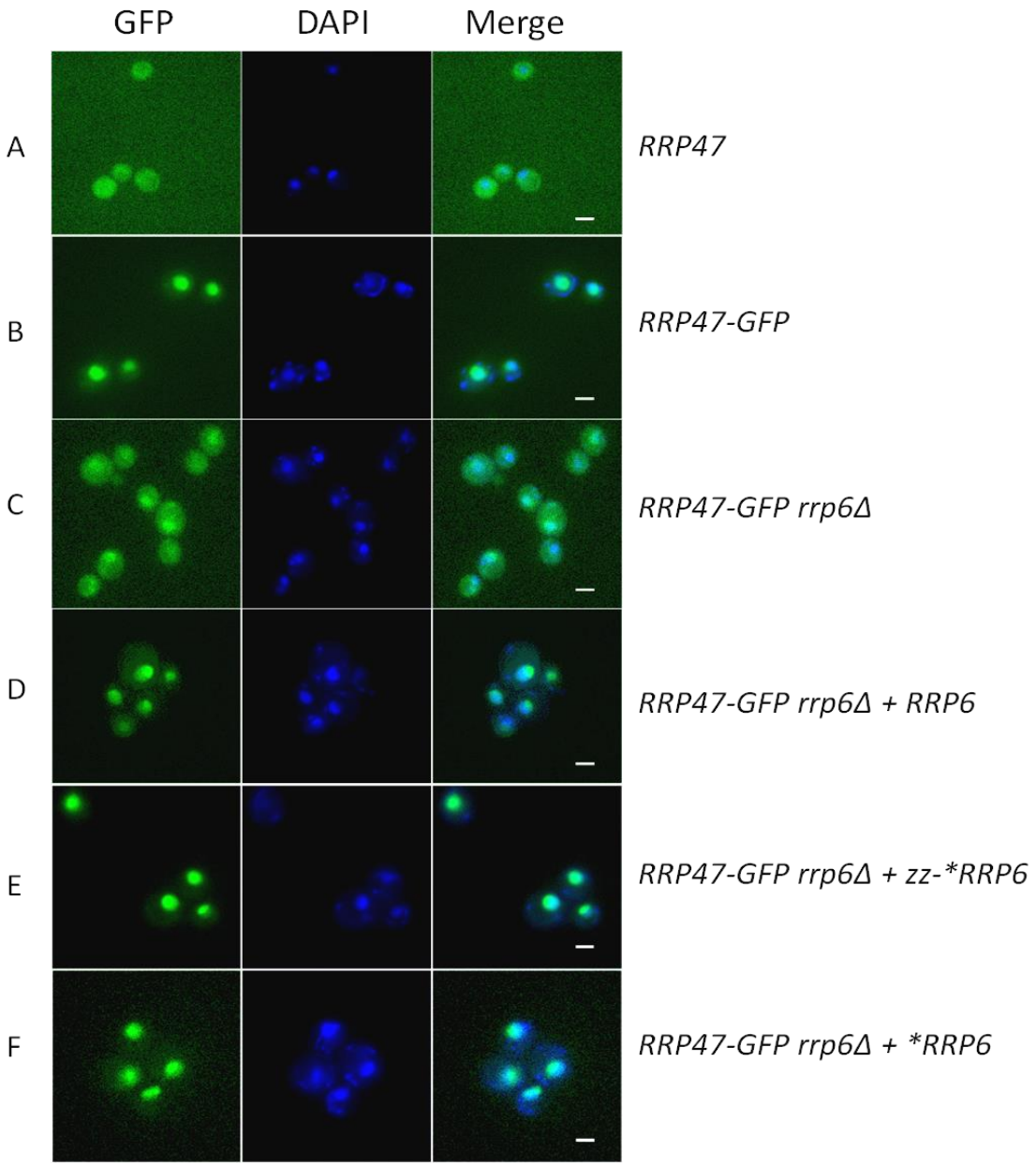


**Figure 4.19 The Rrp47-GFP signal in *rrp6Δ* mutants is reduced but not lost.**
Immunofluorescence of *RRP47-GFP* and *RRP47-GFP rrp6Δ* strains complemented with wild-type *RRP6* alleles to assess Rrp47 localisation in dependence of Rrp6. Representative GFP, DAPI and merged images (stack projections) are shown of A wild-type (P364), B *RRP47-GFP* (P1160) and C *RRP47-GFP rrp6Δ* strain (P1161), as well as *RRP47-GFP rrp6Δ* complemented with D untagged *RRP6* (p436) and the *pRRP4* promoter constructs E tagged *zz-RRP6** (p263) and F untagged *RRP6** (p390). The scale bar measures 2 µm.

***Rrp47-GFP rrp6Δ mutants accumulate a Rrp47-GFP degradation intermediate***

To further investigate a possible link between localisation of Rrp6 and Rrp47, the *RRP47-GFP rrp6Δ* strain was transformed with plasmids harbouring either full length zz-tagged Rrp6 proteins, Rrp6 mutants (*rrp6.1, rrp6ΔNT, rrp6NT1 and rrp6NT2*) or the vector control (pRS416). Western analyses were performed to assess recovery of Rrp47-zz expression using the anti-GFP antibody (Fig. 4.20 A). As expected, no GFP signal was detected for the wild-type control (lane 1), in contrast to the strong western signal obtained for the Rrp47-GFP strain (lane 2). Deletion of *RRP6* (lane 3) depleted the Rrp47-GFP signal, at the same time accumulating a smaller protein species the size of GFP (GFP*) detected by the GFP antibody. The GFP domain has a half-life of around 7 hours in yeast and is known to be resistant to proteolysis *in vivo* (Mateus and Avery 2000, Welter *et al*. 2010). The observed GFP* species is therefore most likely a Rrp47-GFP degradation intermediate since it is absent in the control (lane1), but also appears in the *rrp6ΔNT* mutant (lane 7) which does not stably express Rrp47 due to the lack of the Rrp6NT domain (see also Fig. 4.11). The full-length wild-type tagged and untagged Rrp6 constructs recovered Rrp47-GFP expression, as does the Rrp6.1 catalytically inactive protein. Notably, the Rrp6NT domain was sufficient to recover expression of the Rrp47-GFP protein, consistent with previous experiments using zz-tagged Rrp47 (Fig 4.11). A parallel western analysis of the zz-tagged Rrp6 proteins used in Fig. 4.20 A expressed in an *rrp6Δ* strain (P781) is shown in Figure 4.20 B showing sizes and expression levels of the mutant *rrp6* alleles. Notably, even the Rrp6NT2 mutant which is expressed at much lower levels compared to the other Rrp6 species fully recovered Rrp47 expression (compare Fig. 4.20 A lane 8 to B lane 5).

***The Rrp6NT domain recovers Rrp47-GFP expression in the nucleus fully***

Next, localisation of Rrp47-GFP was assessed in the *rrp6Δ* strains transformed with the mutant Rrp6 alleles (Fig. 4.21). The comparison of wild-type (panel 1) and Rrp47-GFP strain (panel 2) showed again a clear nuclear signal for Rrp47 which is depleted but not completely lost in the *Rrp47-GFP rrp6Δ* strain (vector control, panel 3). The Rrp47-GFP signal in the *rrp6Δ* strain could be recovered by expressing wild-type Rrp6 (panel 4) or Rrp6.1 (panel 5), but not with Rrp6ΔNT which lacks the Rrp47 interaction domain and therefore Rrp47-GFP expression and shows a reduced nuclear signal like *rrp6Δ*. Also, consistent with the western data, the Rrp6NT heterodimerisation domain is sufficient to recover Rrp47-GFP expression in the nucleus with a signal comparable in strength to the full-length Rrp6 protein. Thus, recovery of Rrp47 expression through interaction with Rrp6 or the Rrp6NT domain (Fig. 4.20) correlates with an increase in the nuclear GFP signal (Fig. 4.21 panel 4 and 7).

**A**

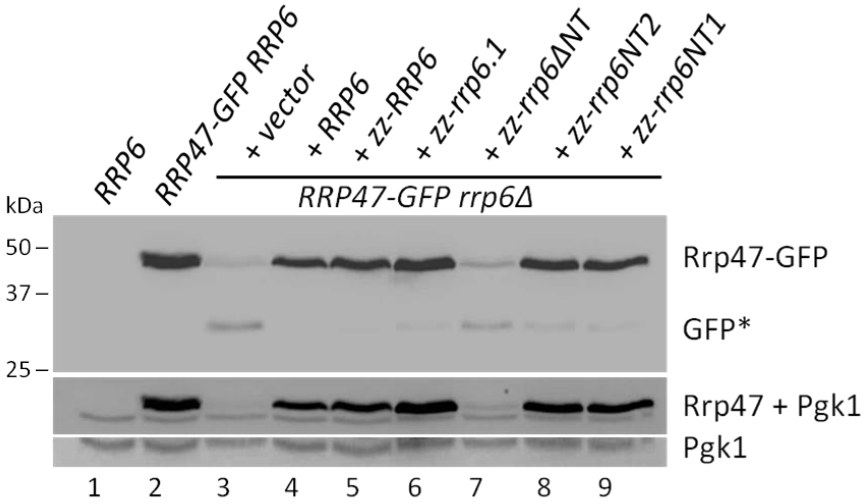


**B**

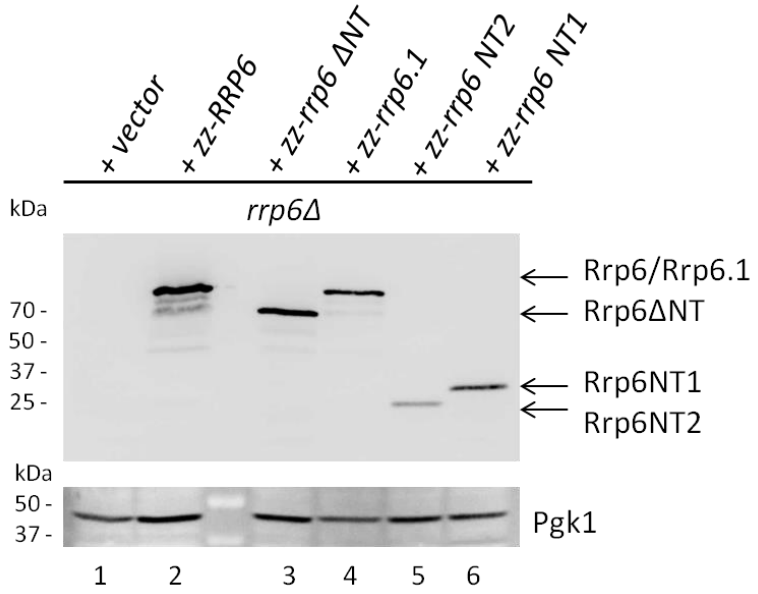


**Figure 4.20 A Rrp47-GFP degradation intermediate accumulates in *rrp6Δ* mutants.**
(A) Western analysis of Rrp47-GFP expression in wild-type (P364), *RRP47-GFP* (1160) and *RRP47-GFP rrp6Δ* strains (P1161) transformed with vector control (pRS416, lane 3) and plasmids encoding zz-tagged Rrp6 alleles (lanes 4-9, *zz-RRP6* p263, *zz-rrp6.1* p389, *zz-rrp6ΔNT* p260, *zz-rrp6NT1* p287, *zz-rrp6NT2* p285). Alkaline lysed cell extracts were resolved by 12 % SDS-PAGE and analysed by western blotting with anti-GFP (upper panel) and anti-Pgk1 antibodies. An Rrp47-GFP degradation intermediate (lane 3, 7 and weaker in lanes 6, 8, 9) is marked GFP*. The middle panel (A) shows both antibody signals on the same blot, as they were too difficult to separate. A separate panel for Pgk1 is shown at the bottom. (B) Western analysis of the same zz-tagged Rrp6 mutants as in (A) transformed into an *rrp6Δ* strain (P781) and probed with PAP followed by anti-Pgk1 antibodies. Rrp6NT1=Rrp6 197X, Rrp6NT2=Rrp6 285X (compare Fig. 4.10B and 4.11).

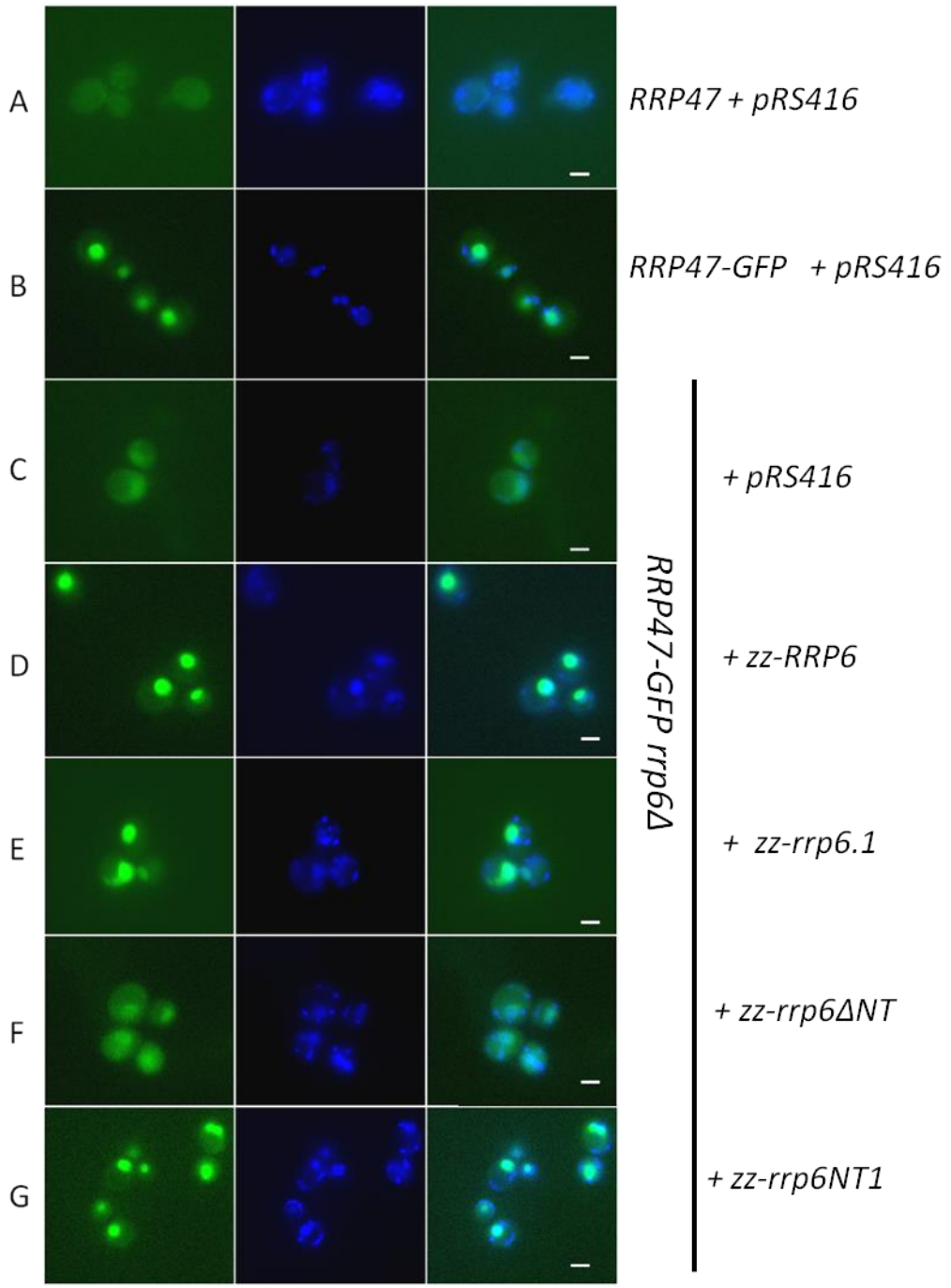


**Figure 4.21 Rrp6NT is sufficient to recover Rrp47-GFP signal in the nucleus.**
Localisation of the Rrp47-GFP fusion protein using fluorescence microscopy. *RRP47-GFP rrp6Δ* strains were transformed with either vector control or zz-Rrp6 alleles as indicated. Cell nuclei were stained with DAPI before live-imaging. Stack projections of GFP, DAPI and merged images are shown representative for cells of the tested strains; wild-type (no GFP fusion, P364); *RRP47-GFP (P1160)*; *RRP47-GFP rrp6Δ (1161)* complemented with vector (pRS416), full-length zz-*RRP6 (p263)*, zz-*rrp6.1 (p389)*, zz-*rrp6ΔNT (p260)*, and zz-*rrp6NT1 (p287)*.

In summary, the western and fluorescence microscopy analyses indicate that Rrp47-GFP is imported into the nucleus independently of Rrp6. If after import of Rrp47, Rrp6 is not available for interaction, Rrp47-GFP is degraded, as confirmed by the appearance of an Rrp47-GFP degradation intermediate detected in western analyses of both, the *rrp6Δ* strain and the *rrp6NT strain (Fig. 4.20 A GFP*).* Given the strength of the GFP signal in the nucleus of *rrp6Δ* cells, it is likely that the GFP degradation intermediate accumulates in the nucleus and contributes to the nuclear signal. GFP itself does not localise to the nucleus (Niedenthal *et al.* 1996). Therefore, the nuclear signal observed in the *rrp6Δ* mutant can only originate from imported Rrp47-GFP and/or its degradation intermediates.

### 4.2.7 Rrp47-GFP is degraded in the nucleus in *rrp6Δ* strains.

Assuming that Rrp47-GFP is degraded in the nucleus, and a GFP* degradation intermediate is stabilised in the nucleus, this intermediate should be more abundant than the full length Rrp47-GFP protein. In order to determine the amount of both species, six independent biological samples from *rrp47-GFP rrp6Δ* strains (Fig. 4.22) were quantified by GFP western using GeneTools software. Values were adjusted against the internal loading control (Pgk1). From these data, the average ratio of truncated protein to full-length protein was calculated to be 1.8:1 confirming that the amount of truncated protein was consistently more abundant than the full-length Rrp47-GFP fusion protein. All signals were within the linear range.

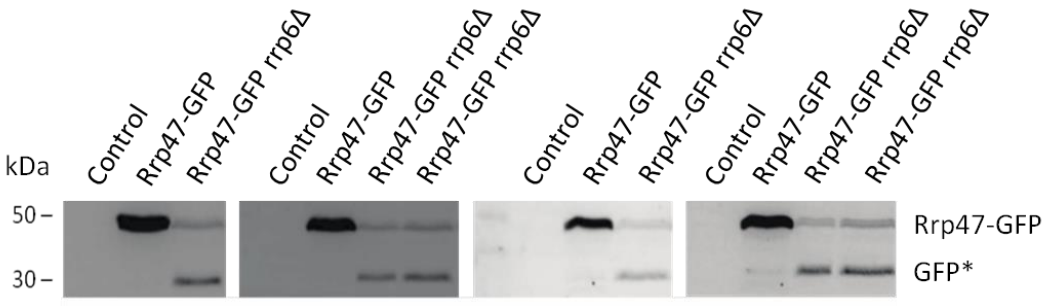


**Figure 4.22 The GFP* fragment is more abundant than Rrp47-GFP in *rrp6Δ* strains.**
Quantitative western analyses of six independent biological samples from *RRP47-GFP rrp6Δ* strains (P1161) alongside the *RRP47 GFP RRP6* (P1160) and the wild-type control strain (P364). Bands for the full-length Rrp47-GFP protein and the truncated degradation product (denoted GFP*) were quantified using GeneTools software and adjusted with Pgk1 (not shown). The ratios of GFP*:Rrp47-GFP for the 6 independent biological extracts from the *rrp47-GFP rrp6Δ* strain (calculated using GeneTools software) are 1.79, 1.47, 1.54, 1.89, 2.50 and 1.75 to 1 (average = 1.8 : 1, SEM = 0.15).

***Fluorescence of the Rrp47-GFP rrp6Δ strain is predominantly nuclear***

Moreover, trace quantification data was obtained from the microscopy images and Figure 4.23 shows plot profiles from traces obtained for strains shown in Figure 4.20. The position of the lines and traces obtained for each image are shown and the minimum and maximum pixel values are given with the strain name. Traces were compared from lines drawn (i) through the background, through (ii) the cell avoiding the nucleus (=cytoplasm) and (iii) through the nucleus. Results are summarised in Table 4.2. Peak values for the nucleus were obtained by subtracting peak values of the cytoplasmic trace from the peak value of the nuclear trace. Cells from an additional Rrp47-GFP *rrp6Δ* image were included (C2) to confirm consistency of data. Cytoplasmic trace lines were placed close to the nucleus to minimise any distance effects.

Trace quantification data of the microscopy images (Fig. 4.23) further confirmed that the *rrp6Δ* mutant displays around 30 % of the nuclear GFP signal seen in wild-type cells, which is considerably higher than the level of full-length Rrp47-GFP protein in this strain (approximately 6 %). Also, the strength of the cytoplasmic signal in the *rrp6Δ* strain is only slightly above the background fluorescence seen in the cytoplasm of wild-type cells, and is not clearly different to that seen in the *RRP6* wild-type strain (Fig. 4.23 B) or in the *rrp6Δ* strains complemented with either zz-tagged full-length Rrp6 or Rrp6NT domain (Fig. 4.23 D, E). In summary, these observations strongly indicate that the Rrp6-Rrp47-GFP is assembled in the nucleus after independent import of both proteins and that Rrp47 is degraded in the nucleus in the absence of Rrp6.

**Table 4.2 Summary of trace quantification data of microscopic images**

| | | Back-ground | Cyto-plasm | Cyt -bkg (Δ peak) | Nucleus | Nuc -cyt (Δ peak) |
|---|---|---|---|---|---|---|
| A | *RRP47* wt control | 125-129 | 126-134.5 | 5.5 | 125-134.5 | 0 |
| B | Rrp47-GFP | 133-136 | 135-145<br>134-145 | 9<br>9 | 135-177 | 32 |
| C1 | Rrp47- GFP *rrp6Δ* vector | 128-133 | 130-141<br>130-139.5 | 8<br>6.5 | 130-151 | 10-11.5 |
| C2 | Rrp47- GFP *rrp6Δ* vector | 130-134 | 135-142.5<br>137-142.5 | 8.5<br>8.5 | 130-151 | 8.5 |
| D | Rrp47-GFP *rrp6Δ RRP6* | 125-129 | 126-134<br>127-134 | 5 | 133-168 | 34 |
| E | Rrp47-GFP *rrp6Δ rrp6NT* | 127-130 | 128-137<br>128-135 | 5-7 | 135-168<br>135-168 | 31<br>33 |

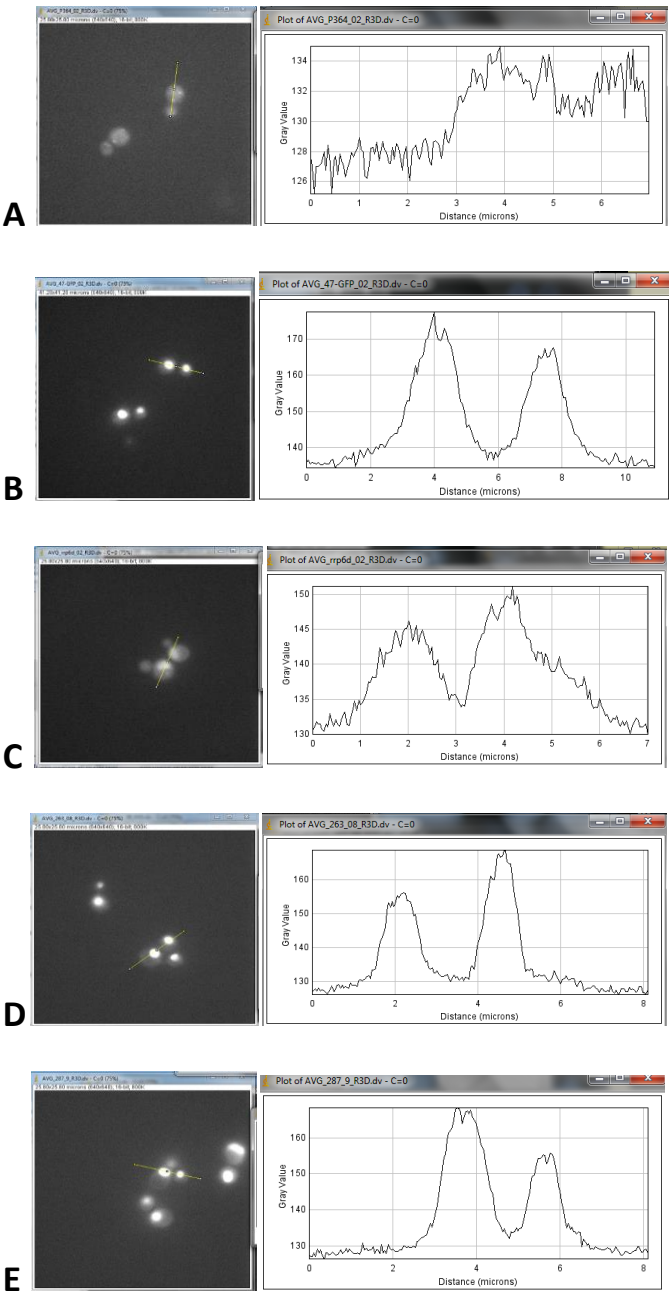


**Figure 4.23 The *rrp6Δ* mutant still displays 30 % of the nuclear signal of *RRP6.***
Trace quantification of micrographs and plot profiles obtained for the Rrp47-GFP strains analysed in Figure 4.20. Traces were drawn through average intensity projections of the micrographs and plots with pixel values were obtained using the ImageJ MacBiophotonics software package. Shown are images and plot profiles from traces starting in the background through the cytoplasm and cutting through the centre of the nuclei and giving the minimum to maximum values obtained.

### 4.2.8 Deletion of Rrp47 does not affect nuclear import of Rrp6

To confirm independent import of Rrp47 and Rrp6, corresponding localisation experiments were performed with Rrp6-GFP in an *RRP47* wild-type versus an *rrp47Δ* strain. An *rrp47* deletion was generated in the commercial Rrp6-GFP strain by homologous recombination with the *rrp47Δ::kanMX4* cassette (Euroscarf). Mutants were checked for effects on expression and localisation of Rrp6-GFP compared to the strain wild-type for *RRP47* using western analyses and fluorescence microscopy as before. Denatured cell extracts of three independent *rrp47Δ* mutants along with the *RRP47* strain were analysed by western blotting using the anti-GFP antibody (Figure 4.24). Levels of Rrp6-GFP were not drastically reduced but were consistently lower in the *rrp47Δ* mutants (lanes 2-4) being reduced to around 70 % of the signal in the strain with the wild-type *RRP47* allele (lane 1 and 5). Notably, the *rrp47* deletion strains also accumulated degradation intermediates which were detected by the GFP antibody (marked with asterisks), the smaller one of these was just only detectable in the *RRP47* control. This indicates that Rrp47 also plays a role in Rrp6 stability, albeit to a minor extent and is not as critical as Rrp6 is for Rrp47 stability. Localisation studies showed that the absence of Rrp47 does not impede Rrp6 localisation to the nucleus, since a strong polarisation is still observed in the nuclear Rrp6-GFP signal in the *rrp47Δ* mutant (Fig. 4.24 B lower panel).

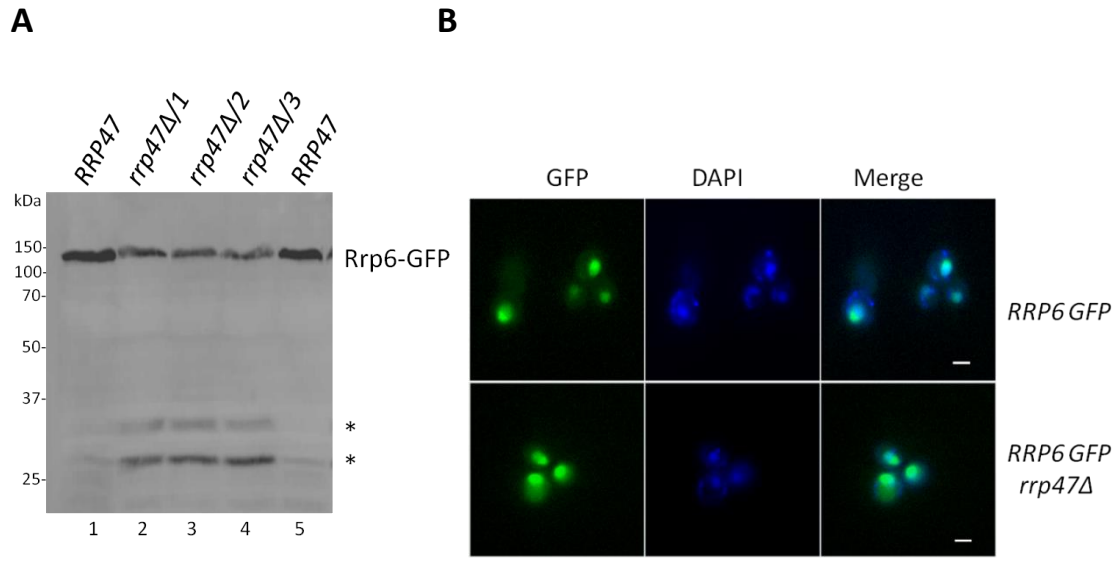


**Figure 4.24 Nuclear localisation of Rrp6 is independent of Rrp47.**
(A) Western analysis of three independent *rrp47Δ* deletion mutants (lane 2, 3, 4) created in the *RRP6-GFP* strain (lane 1 and 5) by PCR-mediated integration of an *rrp47Δ::hphMX4* cassette into the *RRP47* locus. Alkaline lysed cell extracts were resolved by 12 % SDS-PAGE and western analysis was performed with anti-GFP. Rrp6-GFP degradation products are marked with an asterisk. (B) Immunofluorescence of yeast cells expressing an Rrp6-GFP fusion protein that are either wild-type for the *RRP47* gene or carry an *rrp47Δ* deletion. Stack projections of GFP, DAPI and merged images are shown for representative cells of each strain. The scale bar denotes a length of 2 µm.

To further address whether the absence of Rrp47 affects the rate of Rrp6 import into the nucleus, a Fluorescence Recovery After Photobleaching (FRAP) experiment was attempted. However, despite keeping cells under optimal conditions by immobilising on 1 % agarose containing minimal medium and keeping the microscope environment at 30 ˚C, recovery of the Rrp6-GFP signal in the nucleus after photobleaching took more than 1 hour in the wild-type strain and suggested that there is no dynamic exchange between cytoplasmic and nuclear Rrp6 pools.

***The absence of Rrp47 has no effect on Rrp6 complexes***

The effects of the Rrp47 deletion on the Rrp6 sedimentation profile and its association with other proteins or complexes were analysed using glycerol gradients, as before for Rrp47 (Fig. 4.25). Cell lysates from strains grown in complete medium were fractionated as described (see Fig. 4.14). Western analyses of the *RRP47* and *rrp47Δ* gradients using a PAP antibody to detect Rrp6-TAP showed no significant difference between the sedimentation profiles of the two strains. Rrp6-TAP gives a peak in fraction 9-10 as previously observed for Rrp47-zz. In conclusion, the absence of Rrp47 has no significant effect on the Rrp6-TAP sedimentation profile or more specifically, the inclusion of Rrp6 into exosome complexes. Taken together, the studies on import and localisation give strong evidence that Rrp47 and Rrp6 are imported into the nucleus independently of one another. The nuclear Rrp47-GFP signal in strains lacking Rrp6 indicates that Rrp47 is most likely degraded in the nucleus in the absence of Rrp6.

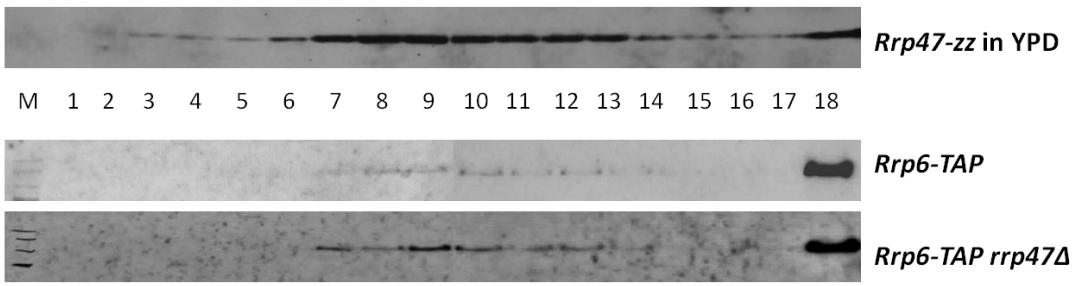


**Figure 4.25 Rrp47 deletion has no effect on Rrp6 complexes.**
Separation of Rrp6-TAP complexes in 10-30 % glycerol gradients in an *RRP47* wild-type (middle panel, P539) and the isogenic *rrp47Δ* strain (bottom panel, P540) compared to an *RRP47-zz* strain (top panel, P414). Gradient fractions (lane 1-18) were resolved by 10 % SDS-PAGE and analysed by western blotting with a PAP antibody detecting Rrp47-zz and Rrp6-TAP as indicated.

## 4.3 Discussion

Rrp47 forms a stable heterodimer with Rrp6 and is required for both exosome-mediated RNA degradation, as well as exosome-independent RNA 3' end processing functions of Rrp6 (Callahan and Butler 2008, Butler and Mitchell 2010). Rrp47 and Rrp6 are specifically required for the maturation of 5.8S rRNA and snoRNAs, and for the degradation of RNA processing intermediates and cryptic unstable transcripts (Arigo *et al.* 2006a, Wyers et al. 2005). In this study, the dependency of Rrp47 on Rrp6 has been addressed, and more specifically, the assembly of the Rrp47-Rrp6 complex. Quantitative western and RT-qPCR analyses, as well as protein synthesis inhibition experiments have revealed that Rrp47 is rapidly degraded in cells lacking Rrp6. Co-expression of the two proteins which have been shown to form a heterodimer (Feigenbutz *et al*. 2013a) is therefore not primarily regulated on the transcriptional level, as for example seen for ribosomal proteins, but determined by the presumably more important partner in the complex, the exonuclease Rrp6, and its direct effect on Rrp47 stability.

Expression of Rrp47 in the absence of its exonuclease partner Rrp6 is most likely not only unnecessary, but could have detrimental effects due to interference with redundant pathways e.g. by blocking access to RNA substrates for 3' end processing. Protein capture experiments have previously revealed that Rrp47 can interact with other proteins associated with snoRNA processing and Nrd1 termination e.g. Nop56, Nop58 and Nrd1 (Arigo *et al.* 2006b, Costello *et al.* 2011 and our unpublished data). In the absence of Rrp6, Rrp47 expression could potentially lead to the depletion of these associated proteins from active complexes or to a block in snoRNP assembly and maturation. Rrp47 has also been shown to function in the Nrd1 termination pathway (Arigo *et al.* 2006b) and without Rrp6 could have negative effects on the efficiency of termination. Notably, overexpression of the human Rrp47 homologue C1D in human tumour cell lines leads to an increased incidence of apoptosis and is prevented by proteasome-mediated degradation (Rothbarth *et al*. 1999 and 2002).

The data presented here strongly indicates that Rrp47 degradation in the absence of Rrp6 also occurs by a vacuole-independent, proteasome-mediated pathway. At steady state, after cleavage of the N-terminal methionine residue, Rrp47 is left with a destabilising N-terminal glutamate (Synowsky 2006) and is therefore a target for degradation according to the N-end rule pathway (Varshavsky 1996 and 2011). Inhibition of vacuolar proteases either using a chemical inhibitor or through gene deletion did not show an effect on Rrp47 expression levels in *rrp6Δ* strains. In contrast, recovery of Rrp47 expression in the absence of Rrp6 could be observed upon inhibition of the proteasome and also by shielding the destabilising N-terminus of Rrp47 with a protein-A tag. This latter discovery could be indeed of general importance when interpreting data where N-terminally tagged proteins are used, since other proteasome substrates could be stabilised by N-terminal tagging in a similar manner in the absence of a

binding partner. The zz-Rrp47 fusion will also provide a useful tool for future experiments, since it allows stable expression of Rrp47 in the absence of Rrp6 and therefore the investigation of Rrp47 functions independently of Rrp6.

To address the requirements within Rrp6 for Rrp47 expression, complementation studies were performed with various Rrp6 mutants expressed in an *rrp6Δ* strain. These studies show that the N-terminal Rrp47 interaction domain of Rrp6 is not only required, but also sufficient to maintain normal Rrp47 expression levels. This strongly suggests that the direct interaction with Rrp6 is required for stable expression of Rrp47 protein in yeast and protects the protein from degradation. Availability of Rrp6 thus provides a simple regulatory mechanism to ensure matching adequate levels of Rrp47 protein. Consequently, when Rrp6 levels are down-regulated as observed during meiosis (Lardenois *et al.* 2011) Rrp47 levels will be adjusted accordingly. Furthermore, RNA processing profiles of the Rrp6 mutants confirm that deletion of the Rrp47 interaction domain has a similar effect on RNA processing to rendering Rrp6 catalytically inactive. In contrast, deletion of the C-terminus which disrupts the interaction of Rrp6 with the core exosome clearly has very little effect on stable RNA processing consistent with previously published data (Callahan and Butler 2008). In conclusion, for RNA 3' end maturation the interaction of Rrp6 with Rrp47 seems more important than the interaction of Rrp6 with the core exosome. The C-terminal deletion also removes the Rrp6 NLS which has been reported to cause its mislocalisation to the cytoplasm, but does not impact on the role of Rrp6 in nuclear RNA processing and degradation (Briggs *et al.* 1998, Phillips and Butler 2003, Callahan and Butler 2008).

Analysis of Rrp47 complexes in glycerol density gradients confirmed a matching sedimentation profile for C-terminally protein A-tagged and untagged Rrp47 from cells grown in complete medium (YPD). Consistent with previous reports, both Rrp47 proteins were observed in larger complexes and co-sedimented with the exosome core subunit Csl4. However, a clear shift of Rrp47 into smaller complexes was observed in cells grown in glucose- or galactose-based minimal medium. This suggests that the association of the Rrp6-Rrp47 complex with the exosome may be influenced by cell growth conditions or nutrient availability. Crucially, overexpression of the GST-Rrp6NT heterodimerisation domain shifted Rrp47 into smaller molecular weight fractions. Moreover, clearly overlapping sedimentation profiles were obtained for GST-Rrp6NT and Rrp47 indicating the formation of a Rrp6NT-Rrp47 heterodimer and consequently segregation of Rrp47 from Rrp6 complexes. Further proof for titration of Rrp47 out of Rrp6 complexes by overexpression of Rrp6NT was obtained in pull down-experiments. Rrp6NT overexpression was subsequently used as a tool to investigate Rrp47 functions and contributions to RNA processing independently of catalytic Rrp6 and presented as the DECOID method (Decreased expression of complexes by overexpression of interaction

domains) with general application to investigate independent functions of proteins segregated from their complexes (Garland *et al.* 2013).

Further studies on Rrp6-Rrp47 assembly addressing nuclear import of Rrp6 and Rrp47 indicate that the proteins are imported into the nucleus independently of each other. A fraction of Rrp6 is associated with Srp1 presumably in a complex primed for translocation across the membrane or ready to be released within the nucleus. However, Rrp47 could not be detected in the Rrp6-Srp1-import-complex. Independent import routes were further confirmed by localisation studies using fluorescent GFP-fusions of Rrp47 and Rrp6. Both GFP-tagged Rrp47 and Rrp6 were imported into the nucleus in the absence of their respective partner. Rrp47-GFP still gave a clear, albeit weaker nuclear signal in the absence of Rrp6 compared to wild-type cells and was expressed mainly as a degradation fragment the size of GFP as determined in western analyses with GFP-specific antibodies. GFP by itself is known not to accumulate in the nucleus; therefore, the nuclear GFP-signal in the *rrp6Δ* strain can only be the result of Rrp47-GFP degradation in the nucleus which was confirmed by quantification of western analyses and GFP traces. Interestingly, the interaction between Rrp6 and Rrp47 might be important for their nucleolar localisation as indicated by observations in human cells and plants. In *Arabidopsis thaliana,* Rrp6 homologues with an N-terminal PMC2NT domain are localised to the nucleolus, as opposed to Rrp6 proteins lacking a PMC2NT domain which are localised to the nucleoplasm (Lange *et al*. 2008). Also, the human Rrp47 homologue C1D no longer localises to the nucleolus of human HEp-2 cells upon depletion of PM/Scl100 (Schilders *et al.* 2007).

In summary, the data presented here strongly supports the model that assembly of the Rrp6-Rrp47 complex occurs after independent import of Rrp6 and Rrp47 into the yeast cell nucleus (Fig. 4.24). Since Rrp47 is shown to be expressed as a homodimer, structural rearrangement and interaction of Rrp47 with Rrp6 are required to form active heterodimers thereby avoiding Rrp47 degradation. In the absence of its associated exonuclease Rrp6, Rrp47 degradation provides a simple form of Rrp47 regulation preventing inappropriate expression and potential detrimental effects to the cell due to independent expression of Rrp47. Independent import pathways could spatially limit RNA degradation competent complexes and ensure that assembly of such activated complexes only occurs in the nucleus where they function. How the proteins are prevented from association in the cytoplasm is unclear. The use of separate importins is a possibility. The association of Rrp6 with Srp1 in the cytoplasm may serve to block the interaction and prevent premature assembly of the Rrp47-Rrp6 heterodimer. Notably, some importins are thought to also function as chaperone proteins for highly basic RNA-binding proteins such as Rrp47 (Jäkel *et al.* 2002). However, Rrp47 might not need an importin due to its small size and import might be facilitated by its homodimeric conformation.

Other chaperone proteins, conformational changes due to interactions or chemical modifications that only occur after or during import could be necessary to enable complex formation. Rrp6 can be phosphorylated at multiple sites (Albuquerque 2008) and nuclear translocation is often regulated by phosphorylation, but it is also feasible that such modifications suppress the ability of Rrp6 to interact with Rrp47. The zz-Rrp47 N-terminal fusion which is stably expressed in the absence of Rrp6 will provide a useful tool for more detailed future studies on the Rrp6-independent nuclear import and functions of Rrp47.

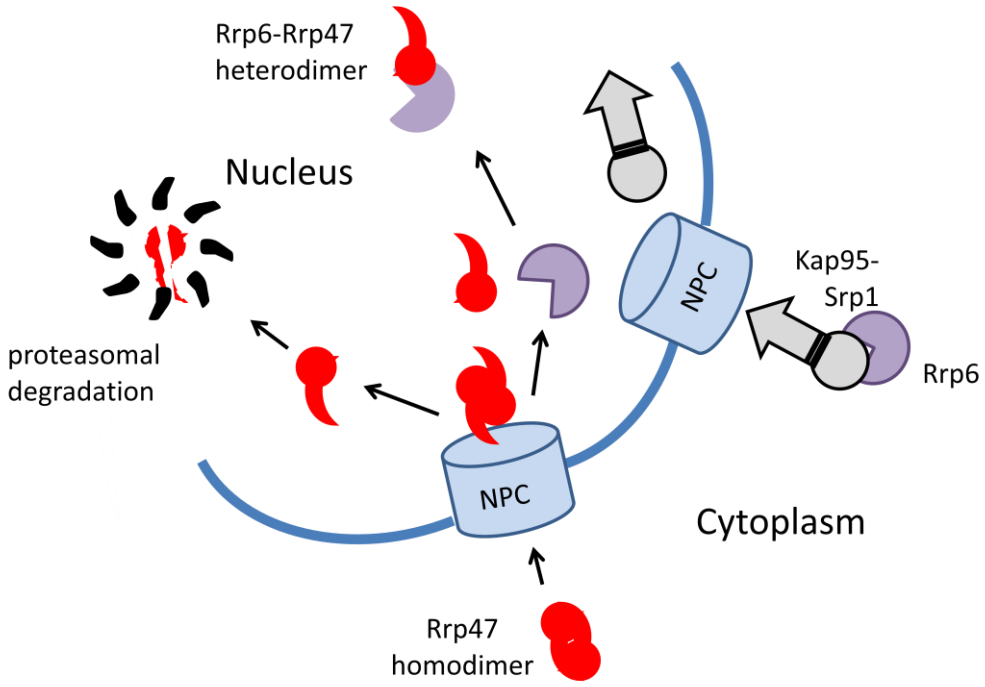


**Figure 4.26 Model for the assembly of the Rrp47-Rrp6 heterodimer.**
Rrp47 is expressed as a homodimer and can be imported into the nucleus independently of Rrp6. Rrp6 uses at least partly the Srp1-Kap95 importin adaptors for nuclear import through the nuclear pore complex (NPC). If Rrp6 is not available in the nucleus to form a Rrp47-Rrp6 heterodimer, Rrp47 is degraded by the nuclear proteasome.

# Chapter Five

# Dependency of Rrp6 expression on its co-factor Rrp47

**Figures 5.1 – 5.13**

# Chapter 5

# Dependency of Rrp6 expression on its co-factor Rrp47

## 5.1 Introduction

Unlike the core exosome subunits and Rrp44/Dis3, the exonuclease Rrp6 is not essential for viability, however it is required for optimal mitotic growth (Briggs *et al*. 1998). Deletion of Rrp6 or loss of catalytic activity not only leads to slowed 3' maturation of small stable RNAs and affects RNA maturation and turnover (Briggs *et al*. 1998, Allmang *et al*. 1999, van Hoof *et al.* 2000), but also, most likely as a result, leads to slowed growth at the permissive temperature of 30 ˚C and temperature sensitivity at 37 ˚C. As reported, functions of Rrp6 in pre-rRNA processing, 3' maturation of stable RNAs, degradation of cryptic unstable transcripts (CUTs) and RNA surveillance depend on its co-factor Rrp47 (Mitchell *et al.* 2003, Peng *et al.* 2003, Arigo *et al.* 2006a).

Again, the direct interaction of Rrp47 with Rrp6 which is critical for Rrp47 stability appears critical for Rrp6 functions, since deletion of the PMC2NT domain elicits similar phenotypes to the loss of Rrp47 (Stead *et al.* 2007). The partial structure obtained for yeast Rrp6 suggests that the PMC2NT domain folds over the Rrp6 catalytic exonuclease domain (Midtgaard *et al.* 2006) and could thus have an effect on Rrp6 activity or block the catalytic centre from uncontrolled RNA digestion providing substrate specificity mediated by Rrp47. It has been previously reported that Rrp47 does not appear to significantly affect Rrp6 expression levels (Mitchell *et al.* 2003, Stead *et al*. 2007). Therefore, the observed growth and RNA processing phenotypes in *rrp47Δ* mutants were not attributed to changes in Rrp6 levels or stability. However, in a number of experiments in this study (chapter 4 see Fig. 4.1, 4.3 B, 4.23) and previous investigations by Martin Turner in our lab, Rrp6 protein levels were observed to be decreased in the absence of Rrp47. Since previous studies were non-quantitative and used native yeast cell extracts for analysis, we re-addressed the influence of Rrp47 on Rrp6 steady state expression levels with more sensitive methods.

Described here are quantitative western and RT-qPCR analyses to address the effect of Rrp47 on Rrp6 protein and mRNA expression levels. As previously reported, Rrp6 levels are mildly decreased in the absence of Rrp47 in cells grown in complete medium. However, this decrease in Rrp6 protein levels is exacerbated in minimal medium, strongly indicating a link between Rrp6 expression and nutrient availability. Moreover, Rrp6 stability is clearly reduced in the absence of Rrp47 as demonstrated in 'translation shut-off' experiments.

The significance of this finding was further strengthened by raising Rrp6 levels in *rrp47Δ* mutants which led to the suppression of snoRNA processing defects and CUTS accumulation in *rrp47Δ* mutants.

Overexpression of Rrp6 could also suppress synthetic lethality in an *rex1Δ rrp47Δ* strain and, as observed in the single *rrp47Δ* mutant, specifically alleviated 3' snoRNA processing defects. Termination of snoRNAs and CUTs is dependent on Nrd1 and an investigation of Nrd1 levels showed that the around 5-fold increased Nrd1 protein levels in *rrp47Δ* mutants could also be normalised by Rrp6 overexpression indicating that a disruption of this pathway could be the reason for *rex1Δ rrp47Δ* synthetic lethality. In summary, this data shows that Rrp47 is critical for Rrp6 expression levels and that at least some effects seen in *rrp47Δ* mutants are due to reduced Rrp6 stability and reduced expression levels in the absence of Rrp47. Moreover, nutrient availability has a significant effect on Rrp6 expression and thus on levels of Nrd1-terminated RNAs like snoRNAs needed for ribosome biosynthesis, as well as CUTs and other ncRNAs with potentially significant and wide ranging effects on gene regulation. The main results of this study have been accepted for publishing (Feigenbutz *et al.* 2013b).

## 5.2 Results

In order to obtain quantifiable data from western analysis, cell extracts were prepared using an alkaline lysis protocol which due to immediate complete denaturation minimises degradation of the samples during preparation (Motley *et al.* 2012). For chemiluminescence imaging the Syngene G:BOX iChemi XL gel doc system was used to obtain data from western analyses, as opposed to the previously used chemiluminescent film which is unsuitable for quantification. Images were analysed using the associated GeneTools software. In addition to the commonly used tagged Rrp6 constructs, analyses were performed on a wild-type *RRP6* (P364) strain and its isogenic *rrp47Δ* strain (P356) to avoid misleading results due to potential effects of a tag on protein stability.

### 5.2.1 Rrp6 levels are significantly decreased in *rrp47Δ* strains in minimal medium

As a first point of reference, expression levels of either Rrp47-zz (Fig. 5.1 A) or Rrp6-TAP (Fig. 5.1 B) in the absence of their respective partner were compared when grown in minimal (MM) or complete medium (YPD) at 30 ˚C to 1 $OD_{600}$. Western analysis showed that Rrp6 affects Rrp47 expression levels much more drastically than vice versa; Rrp47-zz is effectively depleted in the absence of Rrp6, as shown before (Fig. 4.1).

Furthermore, this depletion occurs to a similar extent when grown in minimal (MM) or rich medium (YPD). In contrast, the absence of Rrp47 has only a small effect on Rrp6 expression in cells grown in rich medium, reducing Rrp6 expression levels to approximately 80 % of wild-type levels. However, cells grown in minimal medium show a much greater decrease in Rrp6 levels in an *rrp47Δ* strain. Only 30 % of Rrp6 protein is present at steady state in cells grown in minimal medium as compared to wild-type cells grown in rich medium. It should be noted however that both wild-type strains showed an approximately 20 % reduction of Rrp47 or Rrp6 expression levels in minimal medium compared to rich medium. In summary, Rrp6-TAP levels are affected by the absence of Rrp47, however to a milder extent when cells are grown in rich medium. A much stronger depletion of Rrp6-TAP levels was observed in *rrp47Δ* strains grown in minimal medium.

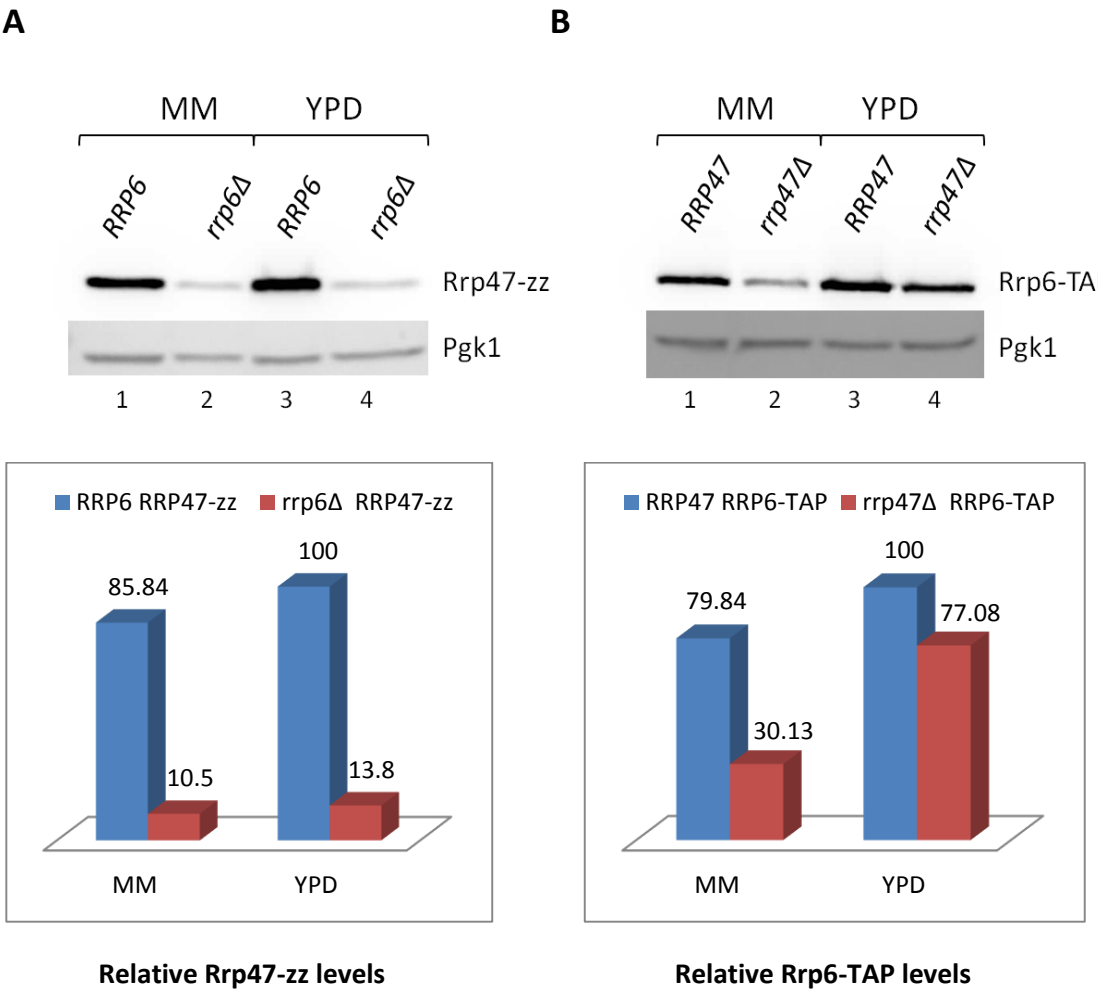


**Figure 5.1 Rrp6-TAP levels are greatly reduced in *rrp47Δ* cells grown in minimal medium.** Quantitative western analysis of A *RRP47-zz* (P414) and B *RRP6-TAP* strains (P539) and their isogenic *rrp6Δ* (P439) and *rrp47Δ* strains (P540), respectively, in minimal (MM) versus complete (YPD) medium. Upper panels show primary western data using PAP and Pgk1 antibodies. Corresponding graphs are shown below with the quantification of Rrp47-zz and Rrp6-TAP levels from 2 experiments adjusted against Pgk1 as internal control.

Next, to exclude effects of the TAP-tag on protein stability, Rrp6 expression levels and changes in the absence of Rrp47 were confirmed in an untagged *RRP6* wild-type strain (P364) and its isogenic *rrp47Δ* strain (P356). Three independent samples each were quantified by western analysis using an Rrp6-specific antibody (Fig. 5.2 A). The Rrp6 protein levels showed a very similar pattern to that observed before with TAP-tagged Rrp6, confirming a striking reduction of Rrp6 protein levels in the absence of Rrp47 in minimal medium against a much milder decrease in rich medium.

To further investigate the effect of Rrp47 on Rrp6 expression, steady-state levels of *RRP6* mRNA were determined by quantitative Real-Time PCR (Fig.5.2 B), as described in chapter 4. *RRP6* mRNA levels were determined relative to the internal control *SCR1* using comparative quantitation ($\Delta\Delta C_T$ method, Schmittgen *et al.* 2008). Comparison of the *RRP47* and *rrp47Δ* strains revealed that *RRP6* mRNA levels are not much altered in the absence of Rrp47 in rich medium (bottom graph); if at all, they appeared slightly increased (113 %, n=4, SEM=8.7). In contrast, mRNA levels were reduced to around 60 % of wild-type levels in *rrp47Δ* in minimal medium (62.5 %, SEM=3.6, n=4). To assess the effect of the culture medium, the data was re-plotted to compare *RRP6* mRNA levels in the same strains in minimal versus rich medium (Fig. 5.2 B, top graph). This showed that the reduction in mRNA levels is partly due to the growth conditions and not only due to the lack of Rrp47. In the wild-type strain *RRP6* mRNA levels were down to 65 % of levels when cells were grown in complete medium (SEM=1.4, n=4) and further reduced in the *rrp47Δ* strain to 36.3 % (SEM=1.3, n=4). The minimal medium effect on *RRP6* mRNA levels in the *rrp47Δ* strain is exacerbated since *RRP6* mRNA levels are increased in *rrp47Δ* cells in rich medium, but reduced in *rrp47Δ* cells in minimal medium compared to cells expressing wild-type *RRP47*.

In conclusion, results from quantification of tagged and untagged Rrp6 levels were consistent with regard to ratios of protein levels in the presence and absence of Rrp47, as well as growth in minimal or rich medium. The greatly reduced Rrp6 protein levels observed in *rrp47Δ* cells grown in minimal medium are partly due to decreased *RRP6* mRNA levels in minimal medium as compared to rich medium. However, the decrease in steady-state mRNA levels cannot account solely for the reduction seen in Rrp47 protein levels, therefore protein or mRNA stability is most likely affected, too.

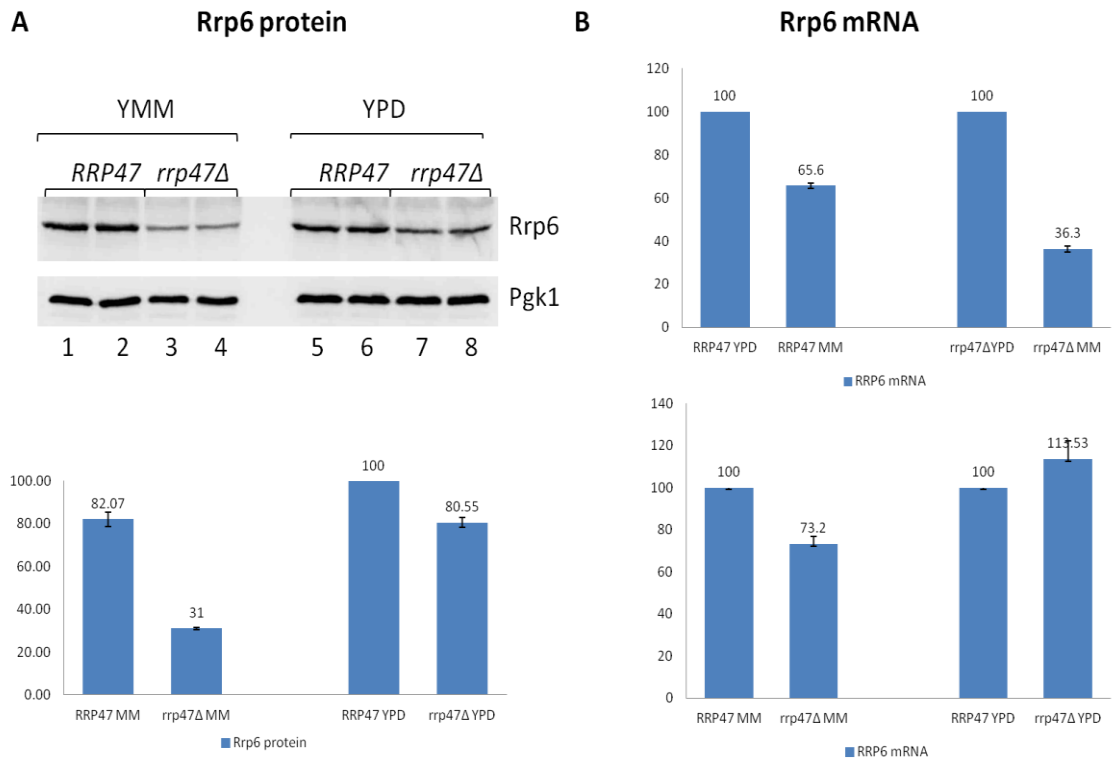


**Figure 5.2 Rrp6 expression is reduced in the absence of Rrp47 in minimal medium.**
Quantitative western (A) and RT-qPCR (B) analyses of Rrp6 protein (84 kDa) and *RRP6* mRNA steady state levels in an untagged wild-type strain (P364) and an isogenic *rrp47Δ* strain (P356) grown in minimal medium (MM, left) or complete medium (YPD, right). Data from 4 experiments with triplicate samples was collected for quantification. (A top) Representative western images of Rrp6 protein expression in denatured yeast cell extracts of strains indicated using an Rrp6-specific antibody and showing duplicate samples only. (A bottom) Quantification of western data adjusted against Pgk1 and displayed in the graph below. (B) RT-qPCR analysis of *RRP6* mRNA levels using *SCR1* as internal reference for comparative quantitation ($\Delta\Delta C_T$). The top graph shows *RRP6* mRNA levels depending on growth conditions, the lower graph shows mRNA levels in the presence or absence of Rrp47 (B). Error bars indicate the standard error of the data set.

### 5.2.2 Rrp6 protein stability is decreased in the absence of Rrp47.

Having demonstrated that Rrp47 is unstable in the nucleus without its partner protein Rrp6, a similar effect of Rrp47 on Rrp6 stability seemed likely. Therefore, a translation-shut off experiment was performed, comparing Rrp6 protein stability in the *RRP47* and *rrp47Δ* strain. Cells were cultured in minimal or rich medium and treated with the protein synthesis inhibitor cycloheximide. Samples were taken at time points up to 80 minutes after drug addition and analysed by western blotting using an Rrp6-specific antibody (Fig. 5.3). Strikingly, Rrp6 protein levels decreased markedly within 30 minutes of drug addition in the absence of Rrp47. The Rrp6 depletion occurred to a similar degree when cultured in minimal or rich medium.

In contrast, Rrp6 levels remained fairly stable throughout the time course in the wild-type strain, comparable to the internal control Pgk1. The absence of Rrp47 clearly has a destabilising effect on Rrp6 protein levels reducing the half-life of the protein from over 90 minutes to around 20 to 30 minutes. However, the type of culture medium did not affect Rrp6 stability any further.

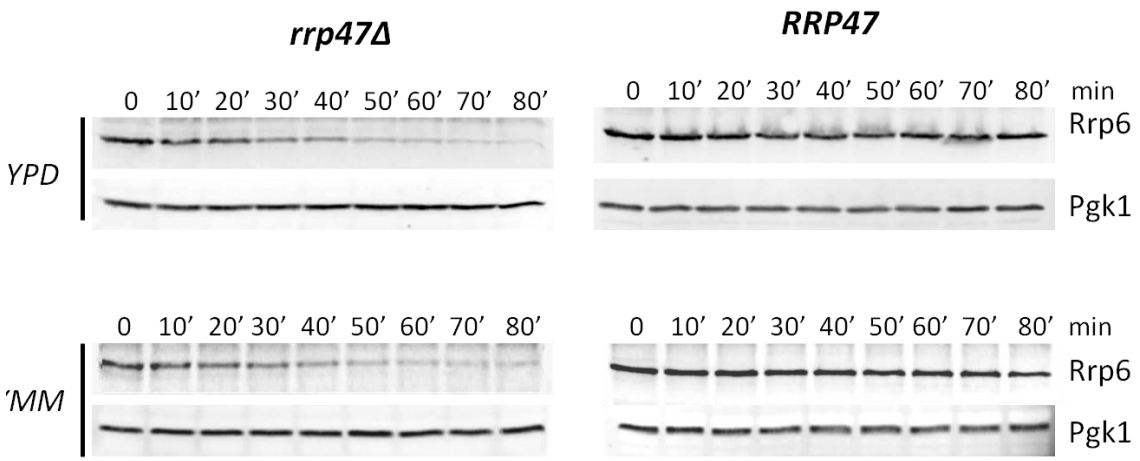


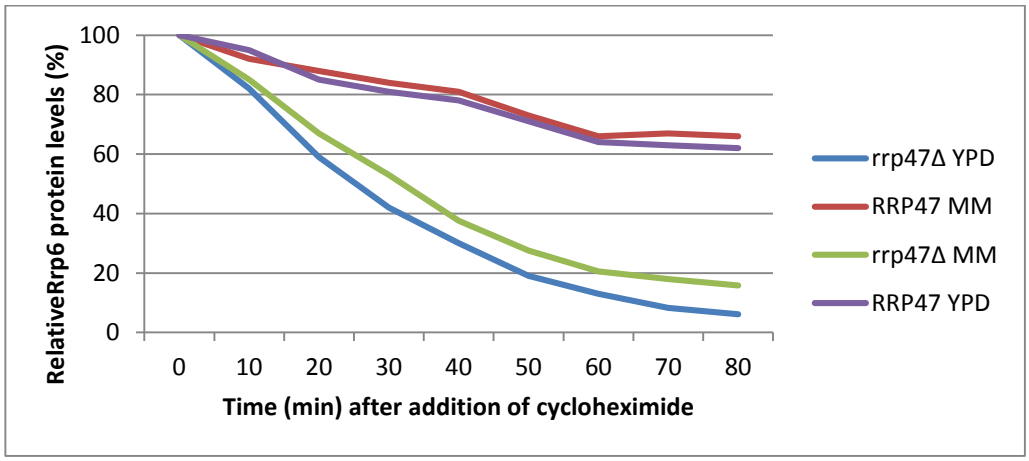


**Figure 5.3 Rrp6 is unstable in the absence of Rrp47.**
Western analysis of Rrp6 expression after translation shut-off induced by cycloheximide in an *RRP47* wild-type strain (P364, right panels) and an *rrp47Δ* strain (P356, left panels). Cells were grown in complete medium (YPD, top) or minimal medium (MM, bottom) at 30 ˚C to 1 $OD_{600}$. A 10 ml sample was taken marking the start (0') of the time course, cycloheximide was added and 10 ml samples were harvested every 10 minutes as indicated above the panels. Samples were prepared by alkaline lysis and resolved by 10 % SDS PAGE for western analysis with an Rrp6-specific antibody, followed by analysis with anti-Pgk1 as internal control. Results from two datasets were averaged and are displayed in the graph below

In order to directly compare and quantify Rrp6 expression levels before and after translation shut-off under the different conditions applied, samples taken before and 1 hour after cycloheximide addition were analysed side-by-side on the same gel (Fig. 5.4). Again, Rrp6 protein levels observed at steady state in minimal medium were lower compared to rich medium in the *RRP47* control strain (compare lane 1 to lane 5). After 60 minutes around a third of the protein was lost in the wild-type strain (compare lane 1 to 2 and lane 5 to 6). The absence of Rrp47 had a clear effect on Rrp6 stability, with an already reduced steady state level of Rrp6 at the start of the time course (compare lane 1 to 3 and lane 5 to lane 7). This effect was exacerbated in minimal medium, where Rrp6 protein levels were already depleted by more than half at the start of the time course. In both complete and minimal medium, Rrp6 levels were effectively depleted in the absence of Rrp47 after 60 minutes to below 10 %. Rrp6 expression followed a similar pattern for 0' and 60' minute time points in minimal and complete medium, indicating that nutrient availability had no effect on Rrp6 stability.

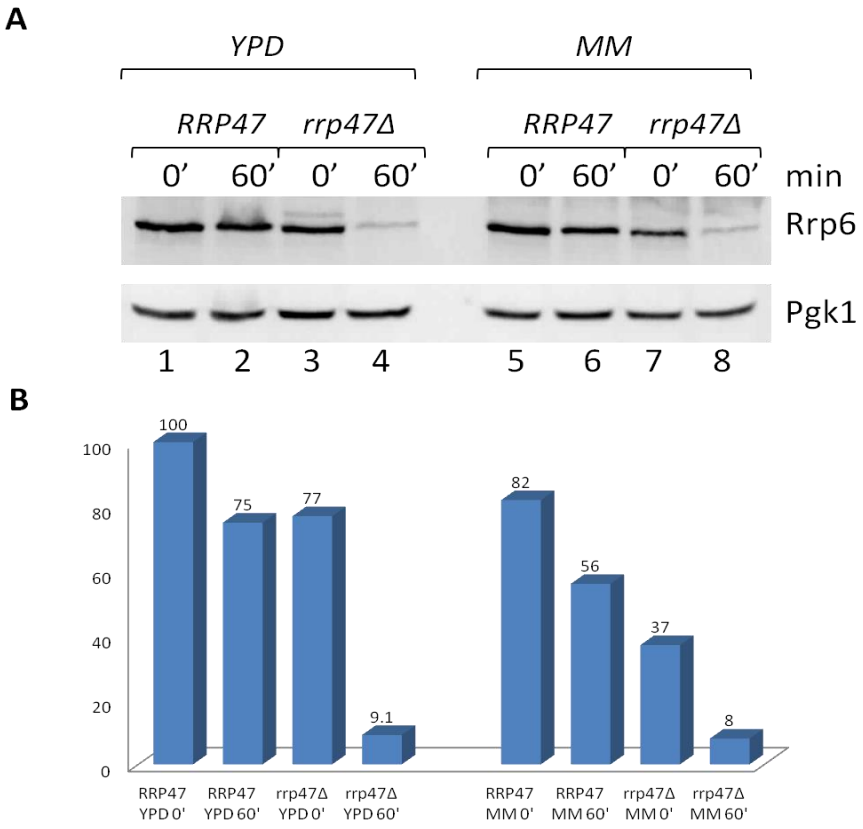


**Figure 5.4 Rrp6 protein levels are depleted in the absence of Rrp47.**
Western analysis and quantification of Rrp6 expression before (0') and 60 minutes after translation shut-off with cycloheximide in *RRP47* and *rrp47Δ* strains in YPD (lanes/columns 1-4) and minimal medium (MM, lanes/columns 5-8). The 0' and 60' minute time points of the time course in Fig. 5.3 were analysed side by side for comparison and quantification by western blotting with the anti-Rrp6NT antibody adjusted against the internal standard Pgk1. Relative Rrp6 expression levels from 2 experiments were plotted on the graph (below).

Taken together, the steady state protein and mRNA quantification, as well as the protein stability assay showed that Rrp6 is unstable in the absence of Rrp47. However, Rrp6 expression is also sensitive to nutrient availability which led to a decrease in *RRP6* mRNA levels in minimal medium. The exacerbated effect in *rrp47Δ* cells cultured in restrictive conditions is therefore due to an additive effect of reduced mRNA levels and decreased Rrp6 protein stability in the absence of Rrp47. Thus, the influence of Rrp47 on Rrp6 expression could represent a major function of Rrp47 in ensuring adequate amounts of Rrp6 in the nucleus.

### 5.2.3 Rrp6 can readily be overexpressed in wild-type and *rrp47Δ* cells.

Considering that Rrp6 levels are reduced in the absence of Rrp47, the effects observed on RNA processing in *rrp47Δ* strains could be due to the reduced amounts and availability of the exosome exonuclease Rrp6. To determine whether Rrp6 levels could be increased in wild-type strains and expressed to "normal levels" in *rrp47Δ* strains, additional copies of Rrp6 were introduced into these strains on single copy (sc) and multi copy (mc) *2μ* plasmids which add one or more copies of Rrp6 to the endogenously expressed Rrp6. Isogenic *RRP47 (P575)* and *rrp47Δ* (P368) strains were transformed with single and multi-copy plasmids carrying either the wild-type *RRP6* allele or the zz-tagged *RRP6* fusion protein (Allmang *et al*. 1999). Cell extracts were analysed by western blotting using an Rrp6-specific antibody (Fig. 5.5). Western analyses revealed a clear correlation between the type of plasmid and Rrp6 levels detected, with a clear increase of Rrp6 protein in cells transformed with the multi-copy plasmids compared to the single-copy. However, signals obtained for untagged Rrp6 and zz-tagged Rrp6 need to be interpreted independently since the protein-A zz-domain recognises IgG molecules non-specifically and thus leads to an additive signal for tagged proteins. Similar expression profiles were obtained in both *RRP47* and *rrp47Δ* strains confirming that Rrp6 can readily be overexpressed in both strains. Exogenous expression of *RRP6* from the multi-copy vector increased the Rrp6 protein levels in the *rrp47Δ* strain around 5-fold reaching expression levels at least as high as in wild-type cells (compare lanes 1-4). This shows that Rrp6 expression is clearly not limited by Rrp47.

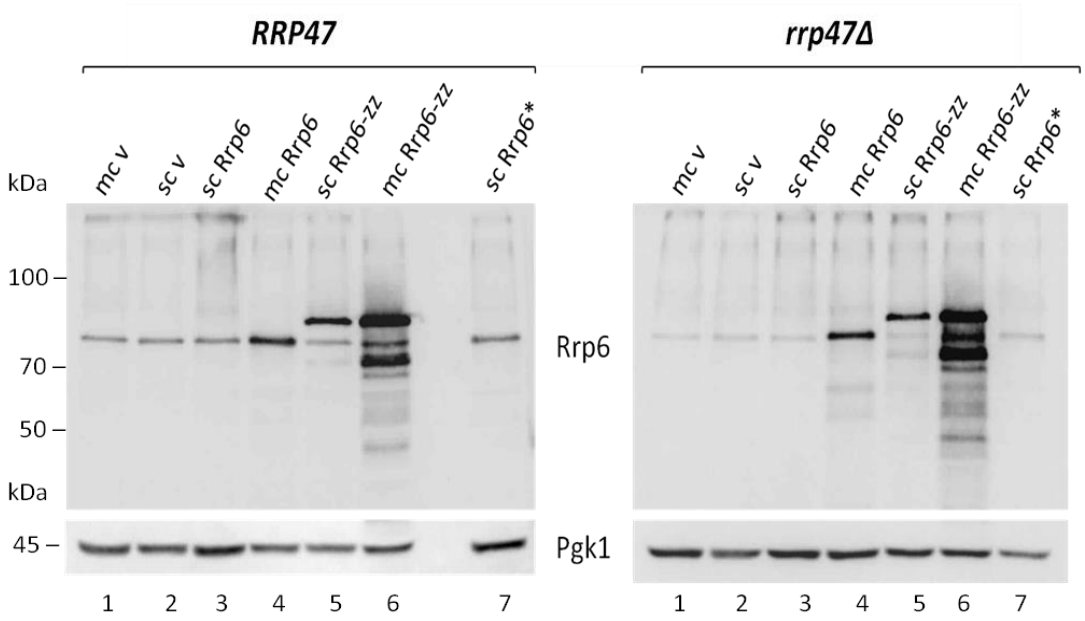


**Figure 5.5 Overexpression of Rrp6 in an *RRP47* and an isogenic *rrp47Δ* strain.**
Western analysis of an *RRP47* wild-type (left panel) and isogenic *rrp47Δ* strain (right panel) transformed with vector controls (lane 1 pRS416, lane 2 pRS426) and single copy (lane 3 p645, lane 5 p263) and multi-copy (lane 4 p503, lane 6 p322) plasmids bearing untagged (lanes 3,4) and zz-tagged (lanes 5,6) *RRP6* wild-type alleles. Cells were grown at 30 ˚C, subjected to alkaline lysis and resolved by 10 % SDS-PAGE. Western analysis was performed using an Rrp6 antibody (upper panels) followed by anti-Pgk1 (lower panels) as loading control.

### 5.2.4 Overexpression of Rrp6 does not adversely affect RNA processing

In order to assess any effects of Rrp6 overexpression on RNA processing and degradation, total RNA extracted from the strains (from Fig. 5.5) overexpressing Rrp6 was analysed along with controls. As before, RNA species which show characteristic defects in *rrp6* and *rrp47* mutants were tested to see whether RNA processing defects are due to Rrp6 protein levels rather than lack of Rrp47. As shown here, overexpression of Rrp6 had no significant effect on RNA processing or degradation in the wild-type strain as revealed by northern blot analyses and ethidium staining of the total RNA resolved on an 8 % denaturing polyacrylamide gel (Fig. 5.6, A-E lane 1-7). Only mature, correctly 3’ processed species of the snR38, U6, 5S and 5.8S RNAs were observed and there was no accumulation of the 5’ ETS degradation fragment. In contrast, the transformed *rrp47Δ* strains (lane 8 -14) showed typical RNA processing defects for *rrp47* mutants such as accumulation of 5’ ETS fragments (A) and 3’ extended snoRNA species (B and C), as well as 5.8 S processing intermediates (E). In conclusion, Rrp6 overexpression has no detrimental effect on RNA processing in the wild-type strain. On close inspection, there was a decrease in the 3’ extended snR38 species when Rrp6 was overexpressed from the multi-copy vector (lane 11). This led to further investigation of this suppression effect in other snoRNAs with a direct comparison to an *RRP47*-complemented strain (Fig. 5.7).

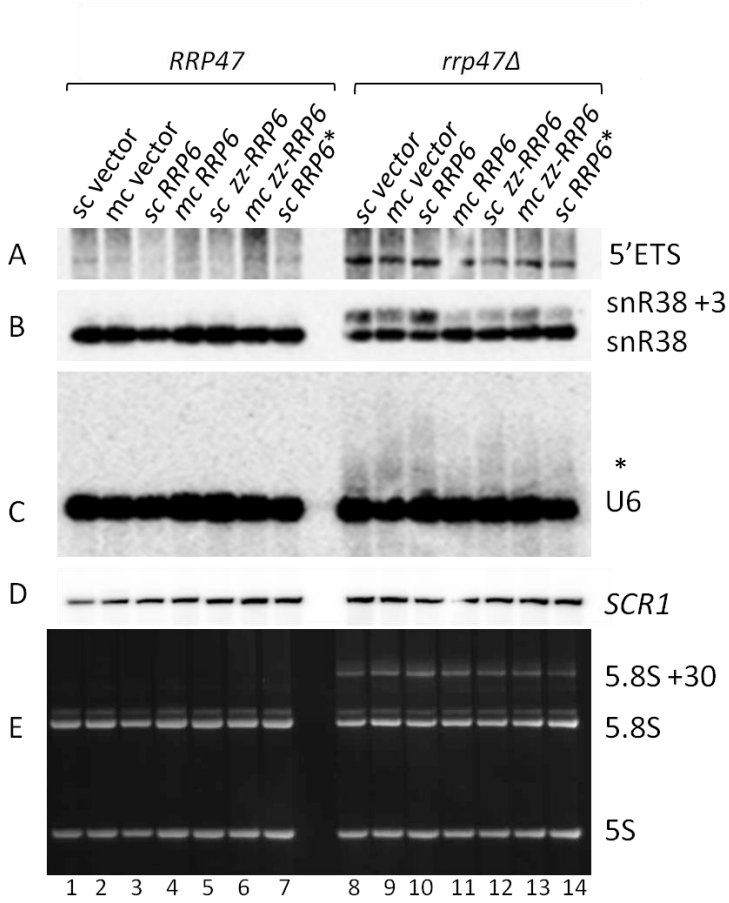


**Figure 5.6 Rrp6 overexpression has no effect on RNA processing in a wild-type strain.**
Total RNA analysis of an *RRP47* wild-type (P575) and an *rrp47Δ* strain (P368) expressing additional single and multiple copies of untagged (p436, p503) and zz-tagged Rrp6 (p263, p322) as indicated or single and multi-copy vector controls (pRS416, pRS426 lanes 1, 2, 8, 9). 5 µg RNA of each strain was resolved through a denaturing 8 % polyacrylamide gel and analysed by northern hybridisation with probes specific for (A) the 5' ETS fragment, (B) snR38, (C) U6 snRNA and (D) *SCR1* which serves as loading control. (E) Section of the ethidium bromide stained RNA gel with the 5S rRNA at the bottom and the 5.8S rRNA above, as well as the 5.8S +30 3' extended species in the *rrp47Δ* strain background. An asterisk points to the U6 3' extended species in the *rrp47Δ* mutant.

### 5.2.5 Rrp6 overexpression in *rrp47Δ* cells suppresses defects in snoRNA processing

To further investigate the mild suppression of snoRNA processing defects when overexpressing Rrp6 in the *rrp47Δ* strain, additional snoRNAs and the model cryptic unstable transcript (CUT) NEL025c (Wyers *et al*. 2005, Thiebaut *et al*. 2006) were probed in the same way. For a direct comparison, an *rrp47Δ* strain complemented with an *RRP47* wild-type allele was included in the northern analysis. As observed for snR38 in Fig. 5.6, additional copies of Rrp6 clearly reduced defects in snoRNA and CUT processing in *rrp47Δ* mutants (Fig. 5.7 A, B, D), whilst the amount of mature RNA (C) seemed unaffected.

The longer 3' extended species seen in the *rrp47Δ* vector controls (lanes 2 and 3), but not in the wild-type strain (lane 1), represent 3' extended polyadenylated snoRNA precursors terminated at site I using the Nrd1 pathway (3' I) or site II using a fail-safe terminator (3' II) in conjunction with the canonical 3'end mRNA termination/polyadenylation machinery (Mitchell *et al.* 2003, Grzechnik and Kufel 2008). Oligo- or polyadenylated (pA) pre-RNA species appear as a smear rather than a discrete band due to the varying length of the poly A tails. Besides the 3' extended precursors, *rrp47Δ* strains also accumulate truncated degradation intermediates (T) of snR13 and U3 snoRNAs (Mitchell *et al.* 2003). In *rrp47Δ* cells overexpressing Rrp6 (A-C, lanes 4 and 5) levels of all 3' extended species of the snR38, snR13, U14 snoRNAs (+3, 3'I and 3'II) decreased substantially, as did truncated degradation fragments observed for snR13 (A) and U3 (B) indicated below the mature RNA species ($U3_T$, $snR13_T$). The observed suppression effect was most prominent in cells expressing the multi-copy *RRP6* plasmid (lane 5) where 3' extensions decreased to almost the same levels as in *rrp47Δ* cells complemented with an *RRP47* allele (A, B lane 6).

Moreover, a decrease in the amount of accumulated NEL025c CUT (D) could be observed (-pNEL025c). In *rrp6Δ* and exosome mutants CUTs accumulate as short (300–600 nt) transcripts generally with a defined 5' end and heterogeneous 3' ends resulting from Trf4 dependent polyadenylation. The here used model CUT NEL025c has been well characterised (Wyers *et al.* 2005, Thiebaut *et al.* 2006). For better resolution of the CUTs accumulation phenotype, the genomic sequence of the CUT (coordinates 15,638–16,048 of chromosome V obtained by PCR using oligos o636/o637) was cloned into a multi-copy vector (pRS425) and expressed exogenously (+pNEL025C, upper panel). The *rrp47Δ* strain transformed with the vector control and the NEL025c CUT plasmid showed a very strong accumulation of the heterogeneous polyadenylated CUT providing a much clearer result compared to the strain without the NEL025c plasmid. This CUT signal was greatly reduced in the strains overexpressing Rrp6 (lanes 3 and 4) and was not detectable in the wild-type strain or the *rrp47Δ* mutant complemented with wild-type *RRP47*.

In contrast to the suppression of RNA processing defects observed for snoRNAs and CUTS, Rrp6 overexpression did not affect rRNA processing (Fig. 5.7 C). The accumulation of the 5' ETS fragment or the 3' extended 5.8 S rRNA precursors 7S and 58S +30 observed in *rrp47Δ* strains was not suppressed by increasing Rrp6 levels and is therefore clearly dependent on an activity/function provided by or in concert with Rrp47. In conclusion, these results suggest that expression of additional copies of Rrp6 specifically alleviates snoRNA processing defects and CUTs accumulation observed in *rrp47Δ* strains, particularly affecting site I transcripts that are generally terminated via the Nrd1 pathway. Thus, overexpression of Rrp6 can partly overcome the requirement for Rrp47 in snoRNA processing and CUTs degradation.

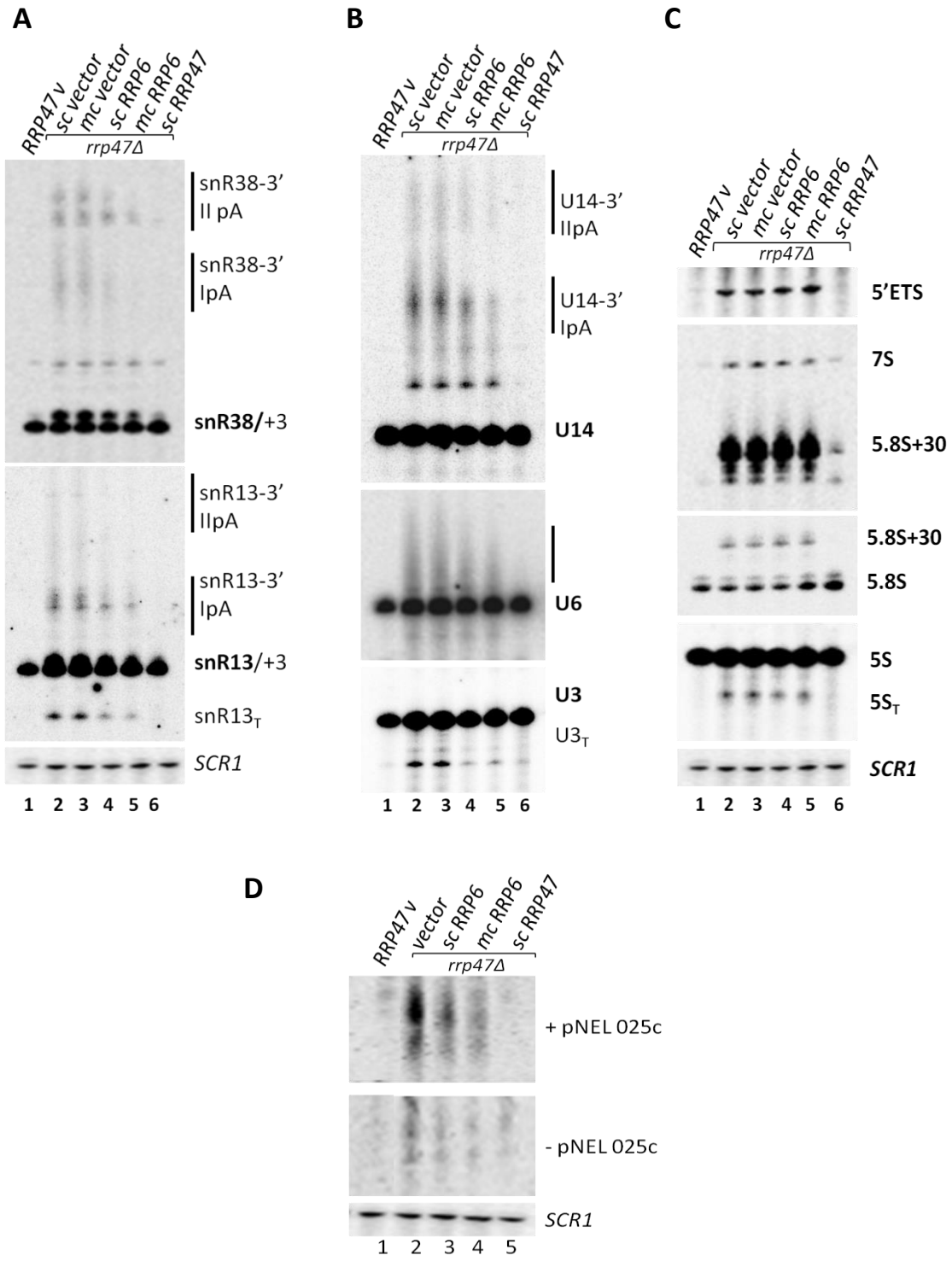


**Figure 5.7 Rrp6 overexpression in *rrp47Δ* strains restores snoRNA 3' and CUTs processing**.
Northern analysis of an *rrp47Δ* strain (P368) carrying single and multiple copies of the *RRP6* wild-type allele (lane 4 and 5) along with vector and wild-type *RRP47* controls (lanes 2, 3, 6). Total RNA (5 µg) of each strain was resolved through an 8 % polyacrylamide gel and analysed by successive northern hybridisations with probes specific for (A) snR38 and snR13, (B) U14, U6 and U3 snoRNAs, (C) rRNA processing intermediates 5' ETS, ITS2 (detecting 5.8S+30 and 7S), 5.8S, 5S. (D) The same strains were probed for the model cryptic unstable transcript (CUT) NEL025c (Thiebaut *et al*. 2006) with (+pNEL025c) or without (-pNEL025c, lower panel) the CUT expressed from a multi-copy plasmid (pRS425). *SCR1* serves as loading control. Black vertical bars denote 3' polyadenylated (pA) precursors of varying length terminated at site I (IpA) or II (IIpA), T denotes truncated RNAs.

### 5.2.6 Overexpression of Rrp6 suppresses *rex1Δ rrp47Δ* synthetic lethality

To investigate whether overexpression of Rrp6 could also overcome synthetic lethality of the *rex1Δ rrp47Δ* double mutant, the previously employed plasmid shuffle assay was used (see Fig. 4.13). Single and multi-copy plasmids carrying wild-type and mutant *RRP6* alleles were transformed into the *rex1Δ rrp47Δ* double mutant carrying a *RRP47* allele and a counter-selectable *URA3* marker. Transformants were assessed for growth on medium containing 5' FOA which is toxic to cells expressing *URA3* and thus selective for transformants that can grow without the original complementing *RRP47/*URA3 plasmid (Fig. 5.8). Strikingly, growth was observed for all mutants expressing additional copies of the tagged or untagged *RRP6* wild-type allele*,* thus adding just one additional copy of *RRP6* to a *rex1Δ rrp47Δ* double mutant suppresses synthetic lethality (A, B, C). No growth was observed for the vector control. Growth complementation was also investigated for an *rrp6.1* catalytically inactive mutant (B) which did not suppress *rex1Δ rrp47Δ* synthetic lethality even when expressed from a multi-copy plasmid; neither did expression of the Rrp6NT domain (C). To further analyse whether differences in growth observed on 5' FOA correlate with Rrp6 expression levels, spot growth assays on minimal medium and YPD were performed on cells selected via 5'FOA (D). However, there was no obvious difference in growth for cells expressing *RRP6* from single or multi-copy plasmids when grown on minimal or complete medium.

In conclusion, overexpression of just one additional copy of catalytically active Rrp6 can overcome *rex1Δ rrp47Δ* synthetic lethality without the need for Rrp47. Thus, the suppression of *rex1Δ rrp47Δ* synthetic lethality is dependent on sufficient amounts of the active exonuclease Rrp6. This indicates an important function of Rrp47 in controlling adequate Rrp6 expression, availability or activity at the subnuclear location where it is needed.

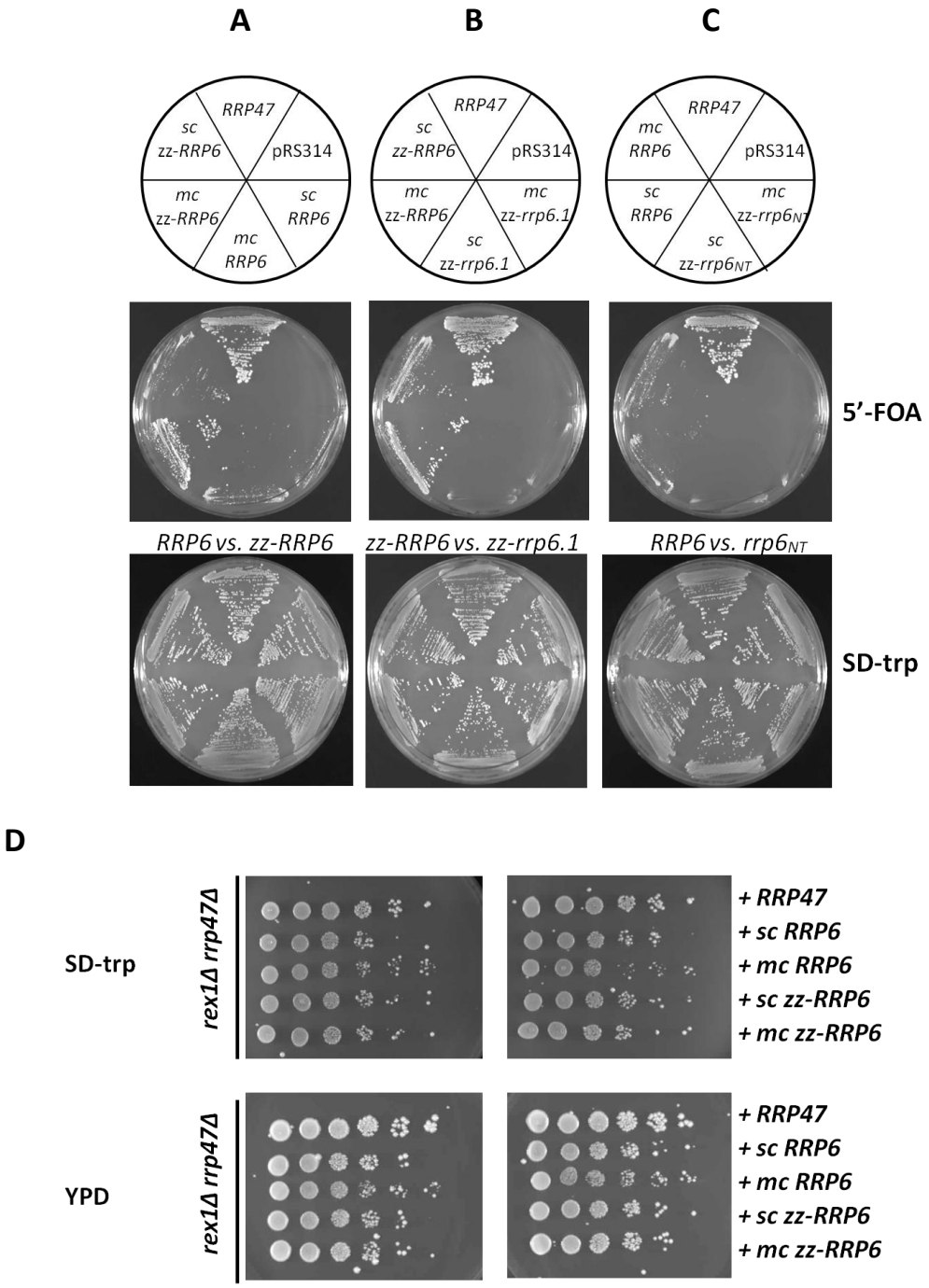


**Figure 5.8 Overexpression of Rrp6 recovers growth in an *rex1Δ rrp47Δ* strain.**
Growth analysis of *RRP6* wild-type and mutant alleles on single copy (sc, pRS314) and multi copy (mc, pRS425) plasmids transformed into a synthetic lethal (sl) *rrp47Δ rex1Δ* (P596) plasmid shuffle strain. Schematics at the top show the order of the strains analysed below. Strains were grown at 30 ˚C on 5'FOA (upper panel) to select for viable mutants without the *URA3*/*RRP47* alleles, and on SD-trp (lower panel) as a control. Complementation of the sl strain was assayed using (A) zz-tagged (sc p427, mc p494) and untagged (sc p552, mc p553) *RRP6* wild-type alleles, (B) zz-tagged wild-type *RRP6* and catalytically inactive *rrp6.1* alleles (sc p429, mc p495) and (C) wild-type *RRP6* or zz-tagged *rrp6N*T domain (sc p513, mc p496). (D) Spot growth assay of cells selected over 5'FOA and grown on SD-trp and YPD at 30 ˚C for 3 days.

### 5.2.7 Overexpression of Rrp6 alleviates RNA defects in *rex1Δ rrp47Δ* mutants

To assess the effect of Rrp6 overexpression on RNA processing in the *rrp47Δ rex1Δ* mutants, northern blot analyses were performed on total RNA extracts from the strains assessed for growth in Fig. 5.8. RNA processing phenotypes of *rrp47Δ rex1Δ rrp6(+)* mutants expressing additional copies of Rrp6 were compared to wild-type, *rex1Δ* and *rrp47Δ* single mutants and the *RRP47* complemented double mutant (Fig. 5.9). Mild to moderate overexpression of Rrp6 from untagged single and multi-copy plasmids (A, B lanes 5 and 6) resulted in an exacerbated accumulation (relative to the *rrp47Δ* single mutant) of heterogeneous adenylated 3' extended snoRNA species terminated at site I (3' I), and mature snoRNA species for snR38, snR13, U14 and snR50 were considerably depleted. Moreover, no "+3" species and less "3' II" species were observed as compared to the single *rrp47Δ* mutant (compare lane 3 to lanes 5-8). Interestingly, the extent of the snoRNA processing phenotypes correlated roughly with the amount of Rrp6 expressed (A, B, lanes 5-8). With increased Rrp6 expression from the zz-tagged constructs (lanes 7 and 8), snoRNA processing defects decreased and mature snoRNA levels were restored to near wild-type levels (A, B lanes 7 and 8). Overexpression of Rrp6 thus restores final maturation of snoRNAs in an *rrp47Δ rex1Δ* strain without the requirement for Rrp47.

As seen for the *rrp47Δ* single mutant, Rrp6 overexpression had no effect on pre-rRNA processing (C, D), the *rrp47Δ rex1Δ rrp6(+)* mutants showed the same defects in 5.8 S rRNA processing as the *rrp47Δ* single mutant with accumulated 5'ETS and 5S degradation fragments, as well as 7S and 5.8S +30 processing intermediates. The differences observed in the strength of the 5'ETS signal is most likely due to the different strain background of the *rrp47Δ* and the *rex1Δ rrp47Δ* strain, since no effect was observed in the single *rrp47Δ* mutant (Fig 5.7 C).

Some snoRNAs are required for the synthesis of 18S rRNA and are essential for mitotic growth (Venema and Tollervey 1999). These include U14 snoRNA which showed a strong accumulation of 3' extended precursors in the Rrp6 supplemented *rrp47Δ rex1Δ* strain (Fig. 5.9 A lanes 5-8). The reason for the synthetic lethality of *rrp47Δ rex1Δ* mutants could therefore lie in the reduced production of 18S rRNA in these mutants. The northern analysis of 25S and 18S rRNA levels (Fig. 5.9 D), however showed no significant difference in the ratios of 25S to 18S rRNA and therefore no specific depletion of 18S rRNA in the *rrp47Δ rex1Δ* strains overexpressing Rrp6. Notably, both stable rRNAs were reduced in these mutants (lanes 5-8) when compared to wild-type or single mutants (lanes 1-4).

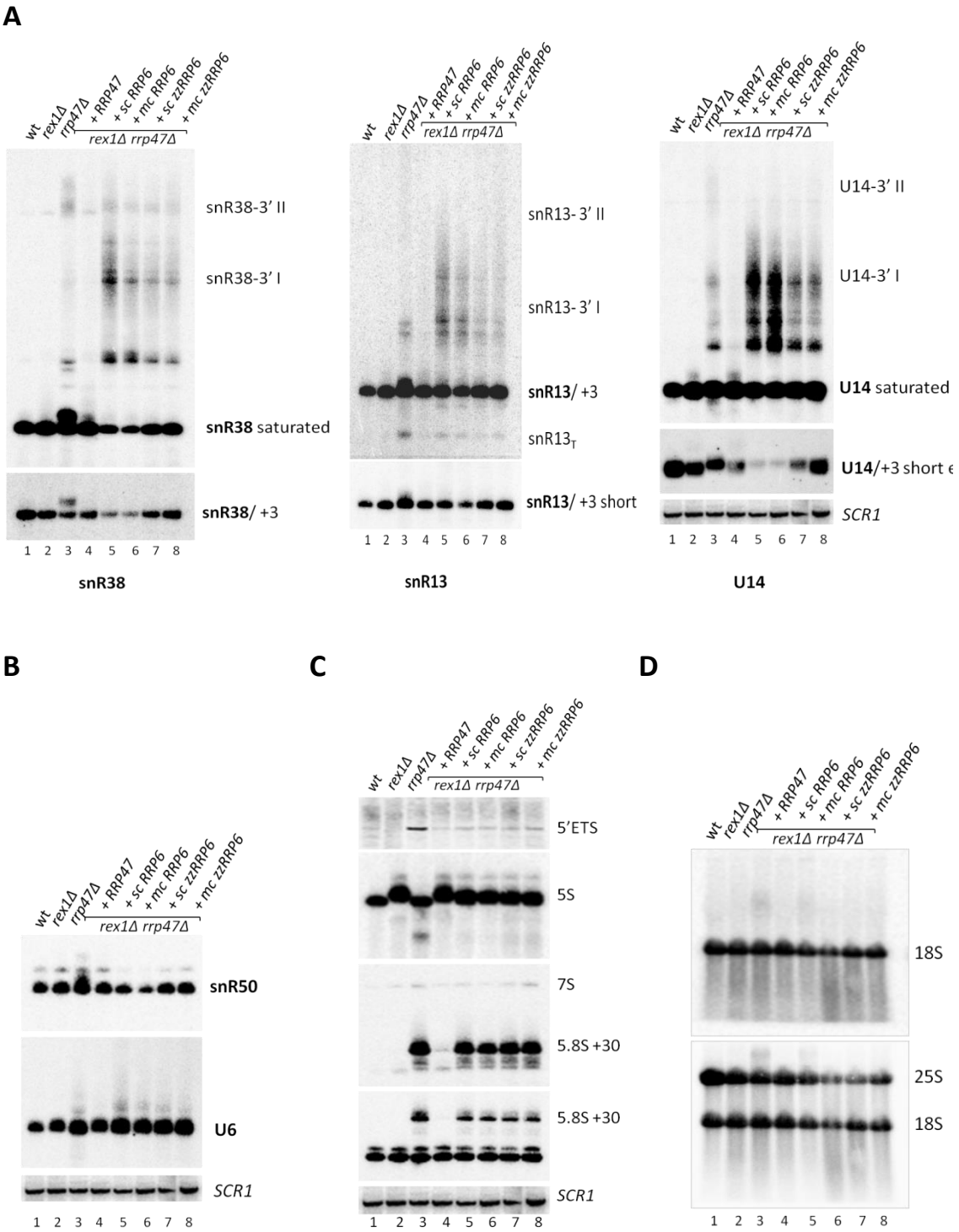


**Figure 5.9 Rrp6 overexpression in *rex1Δ rrp47Δ* alleviates snoRNA 3' processing defects.**
Northern analyses of an *rex1Δ rrp47Δ* strain carrying single and multiple copies of untagged *RRP6*, zz-tagged *RRP6,* and *RRP47* (p262, lane 4) alleles. 5 µg total RNA of each strain was resolved through a denaturing 8 % polyacrylamide gel (A-C) or 1.5 % agarose gel (D) along with wild-type (P575, lane 1), *rex1Δ* (P550, lane 2) and *rrp47Δ* (P368, lane 3) controls. Successive northern hybridisations were performed with probes against (A) snR38, snR13 and U14; short and long exposures are shown for either mature/+3 or 3'extended species 3'I and 3'II, (B) snR50 snoRNA and U6 snRNA, (C) pre-rRNA species 5'ETS, 5S rRNA and ITS2/5.8S rRNA (*SCR1* serves as loading control in panels A-C). (D) 18S and 25S rRNA.

In summary, growth and northern analyses of *rex1Δ rrp47Δ* strains supplemented with increasing amounts of Rrp6 showed that the synthetic lethality of this double mutant can be overcome by overexpression of Rrp6. Exacerbated RNA processing defects observed in those strains were restricted to the processing of snRNA/snoRNA transcripts terminated via the Nrd1 pathway and could be alleviated by expression of Rrp6 in a concentration-dependent manner. The mutants accumulated snoRNA species whose size is consistent with adenylation after termination at site I (Grzechnik and Kufel 2008). This strongly indicates that the observed defects in snRNA and snoRNA processing and possibly CUTs degradation or more generally the accumulation of Nrd1 terminated transcripts could be the basis for the *rex1Δ rrp47Δ* synthetic lethality.

### 5.2.8 Overexpression of Rrp6 in an *rrp47Δ* strains restores wild-type Nrd1 levels

As seen in experiments so far, Rrp6 overexpression in the absence of Rrp47 appeared to affect mainly transcripts produced via the Nrd1 termination pathway (Fig. 5.7-5.9). The exosome co-purifies with Nrd1 (Vasiljeva and Buratowski 2006), therefore it was interesting to assess whether the exosome needs Rrp47 or Rrp6 to associate with Nrd1 and to process Nrd1 transcripts. To this end, a yeast co-immunoprecipitation experiment was performed with Rrp4-TAP as exosome marker expressed in isogenic wild-type, *rrp47Δ* and *rrp6Δ* strains. Native yeast cell extracts of the three strains were incubated with IgG Sepharose and proteins associated with Rrp4-TAP were eluted with 0.5 M acetic acid (Fig. 5.10). Western analysis of input, non-bound and bound fractions using an Nrd1-specific antibody showed a similar 4-5 fold enrichment of Nrd1 in the *rrp47Δ and rrp6Δ* mutants. This suggests that Nrd1 associates with Rrp4-TAP and exosome complexes independently of Rrp47 and Rrp6. However, Nrd1 levels appear generally increased in the *rrp47Δ and rrp6Δ* mutants as seen in the input fractions (compare lane 2, 3 to lane 1).

It was previously reported that Nrd1 auto-regulates its own mRNA levels via Nrd1 termination and Rrp6-exosome mediated degradation (Arigo *et al.* 2006b). Nrd1 mRNA levels were reported to be significantly increased in Rrp47 mutants, but not Rrp6 mutants. Also, several studies working with TAP-tagged Nrd1 have reported similar Nrd1-TAP protein levels in wild-type and *rrp47Δ/rrp6Δ* strains (Grzechnik and Kufel 2008, Castelnuovo *et al.* 2013, Coy *et al.* 2013). To address and clarify the effect of Rrp47 and Rrp6 on Nrd1 protein levels, steady state levels of untagged wild-type Nrd1 protein were assessed by quantitative western analysis using an Nrd1-specific antibody to compare a wild-type strain to *rrp47Δ* and *rrp6Δ* single mutants. Nrd1 protein levels proved to be reproducibly 4-5 fold increased in both *rrp47Δ* and *rrp6Δ* mutants compared to the wild-type Rrp4-TAP strain (Fig 5.11). Relative Nrd1 levels in *rrp6Δ* and *rrp47Δ* strains were *at* 23 % of the wild-type strain set at 100 % (n=3, SEM = 1.1).

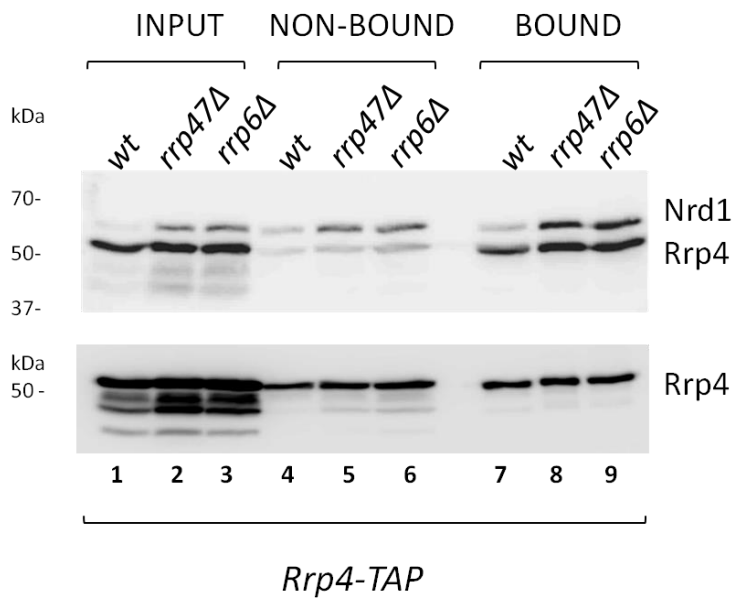


**Figure 5.10 Nrd1 associates with exosome complexes independently of Rrp6 and Rrp47.**
Western analysis of Nrd1 levels after co-immunoprecipitation of Nrd1 protein (64 kDa) with the exosome cap protein Rrp4-TAP (60 kDa) in a wild-type (P246), *rrp47Δ* (P369) and *rrp6Δ* (P589) strain. Native yeast cell extracts of the three strains were incubated with IgG sepharose. Bound Rrp4-TAP and associated proteins were eluted with 0.5 M acetic acid. Equal amounts of input, non-bound and eluted bound fractions were resolved by 10 % SDS-PAGE and analysed by western blotting using anti Nrd1 (upper panel) and PAP antibodies (lower panel).

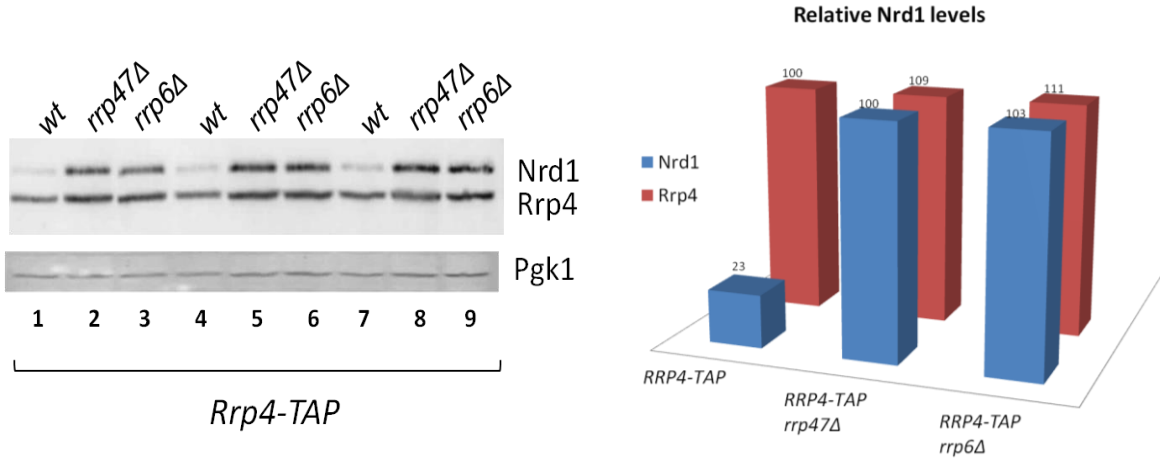


**Figure 5.11 Nrd1 protein levels are 4- to 5-fold increased in *rrp47Δ* and *rrp6Δ* strains.**
Quantitative western analysis of Nrd1 levels from triplicate samples of 1 $OD_{600}$ of alkaline lysed samples of the strains shown in (Fig. 5.10) resolved by 10 % SDS-PAGE. Nrd1 levels were analysed by western blotting with an Nrd1-specific antibody followed by a Pgk1 antibody. Bands were measured and adjusted against the internal control Pgk1. Relative Nrd1 levels are displayed in the graph (right).

To further address the contribution of Rrp47 or Rrp6 to the change in Nrd1 protein expression, a wild-type strain, isogenic *rrp47Δ* an *rrp6Δ* single mutants and an *rrp47Δ rrp6Δ* double mutant were transformed with a vector control or N-terminally tagged zz-Rrp47 which restores Rrp47 expression in an *rrp6Δ* mutant otherwise devoid of Rrp47 (Fig. 5.12). Again, levels of Nrd1 protein were 4 to 5-fold lower in the wild-type strain as compared to the *rrp47Δ* and *rrp6Δ* single and double mutants. Additionally expressing zz-Rrp47 did not affect Nrd1 levels in the wild-type strain, however, zz-Rrp47 expression restored Nrd1 levels close to wild-type levels in the *rrp47Δ* mutant (lane 4). In contrast, zz-Rrp47 expression had no effect on Nrd1 levels in the *rrp6Δ* single and *rrp47Δ rrp6Δ* double mutant (lane 6 and 8), which is not surprising since Rrp6 provides the actual catalytic activity for the degradation of Nrd1 terminated transcripts including Nrd1 mRNA. This indicates that Rrp47 has a connective function in Nrd1 termination or Rrp6-mediated processing of Nrd1 terminated mRNA transcripts. Contrary to previous reports, these transcripts which most likely accumulate in both mutants (not just in Rrp47 as reported), are translated and result in elevated protein levels as observed here for Nrd1 itself.

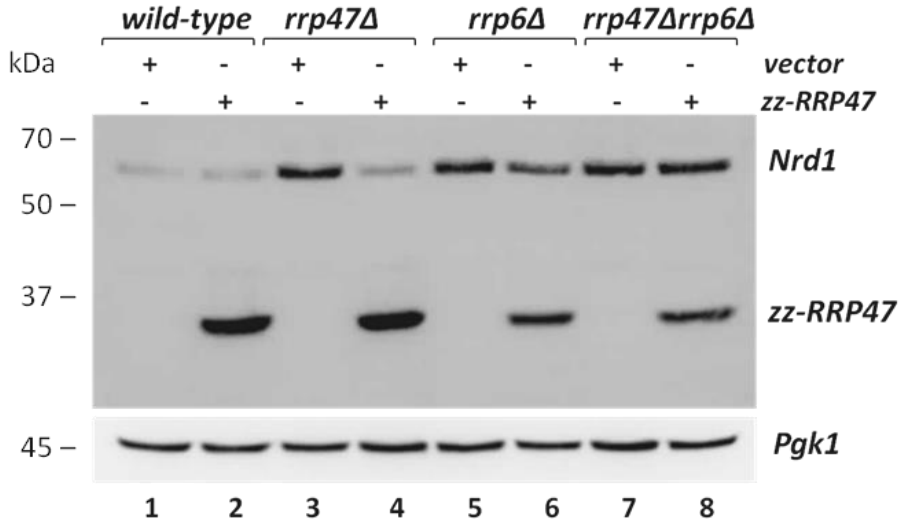


**Figure 5.12 Rrp47 interrupts Rrp6 processing of Nrd1 terminated transcripts.**
Western analysis of Nrd1 levels in wild-type (P364*), rrp47Δ* (P356), *rrp6Δ* (P1528) and *rrp47Δ rrp6Δ* double mutants (P1599) transformed with either vector control (pRS416) or N-terminally tagged zz-Rrp47 allele (p622) which is stably expressed in *rrp6Δ* cells. Pgk1 serves as loading control. Samples were prepared by alkaline lysis and western analysis was performed as described above.

To investigate whether overexpression of Rrp6 can overcome the *rrp47Δ* effect on Nrd1 levels and thus the requirement for Rrp47 in the Nrd1 pathway, denatured cell extracts of *rrp47Δ* mutants and an isogenic wild-type strain carrying single and/or multi-copy Rrp6 plasmids were probed with an Nrd1-specific antibody (Fig. 5.13). Overexpressing Rrp6 in the P575 wild-type strain had no effect on Nrd1 protein levels as compared to the vector control (lanes 1-3). As before in the P364 strain background (Fig. 5.11), elevated Nrd1 levels were observed in the *rrp47Δ* vector control and in the strain carrying an *RRP6* single copy plasmid. Strikingly, Nrd1 levels decreased correlating with increasing Rrp6 expression (lanes 5-8) and were similar to wild-type levels in the strain expressing multi-copy zz-Rrp6 (lane 8). Results from both strain backgrounds were consistent and showed that Nrd1 levels are up to 5-fold increased in *rrp47Δ* and *rrp6Δ* strains. In contrast, only mildly increased levels could be observed when using TAP-tagged Nrd1 (data not shown) which might explain why previous studies by other labs failed to observe an effect on Nrd1 levels. Taken together, overexpression of Rrp6 can alleviate the requirement for Rrp47 in the regulation of Nrd1 levels and more generally in the Nrd1 pathway.

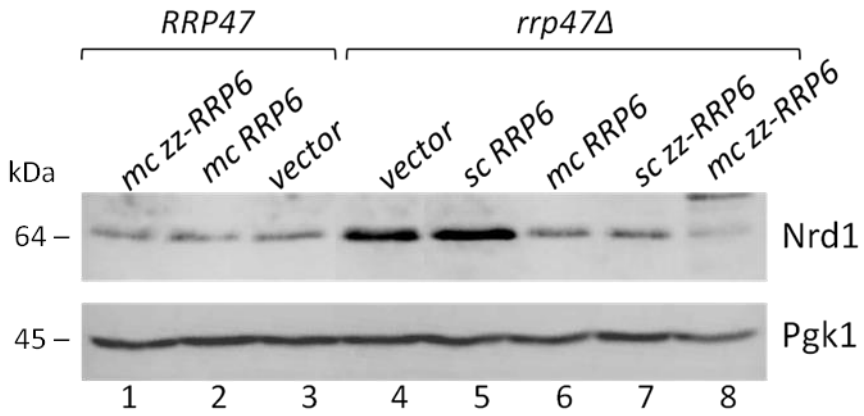


**Figure 5.13 Nrd1 protein levels are restored in *rrp47Δ* strains by Rrp6 overexpression.**
Western analysis of Nrd1 levels in an *RRP47* wild-type (P575) and isogenic *rrp47Δ* strain (P368) carrying tagged and untagged single and multi-copy Rrp6 expression plasmids (compare Fig. 5.5-7). Alkaline lysed cells were resolved by 10 % SDS-PAGE followed by successive western analysis with anti-Nrd1 antibody and anti-Pgk1 as internal control.

## 5.3 Discussion

The data presented here shows a clear and significant effect of Rrp47 on Rrp6 protein expression levels and stability. This effect has escaped previous investigations since it is only minor in cells grown in complete medium. However, the reduction of Rrp6 expression levels in the absence of Rrp47 is exacerbated when cells are cultured in minimal medium due to an additive effect of Rrp6 instability and reduced *RRP6* mRNA levels. Consistent with these observations, transcriptional activity of both genes is regulated by factors in response to nutrient availability (Lee *et al.* 2002, Nishizawa *et al.* 2008, Sattleger *et al.* 2011, Zaman *et al*. 2008 and 2009). Overexpression of Rrp6 in wild-type cells showed no detrimental effects and appears to allow optimal growth.

As observed in this study, overexpression of Rrp6 in *rrp47Δ* strains could recover Rrp6 protein levels to wild-type levels and above and strikingly, the defects in snoRNA processing or CUTs degradation observed in the *rrp47Δ* strain could at least partially be overcome by additional copies of Rrp6. Therefore, the defects seen in *rrp47Δ* mutants are at least partially due to reduced Rrp6 expression, availability or affinity. Assuming a role for Rrp47 in substrate recognition or recruitment, increasing the affinity and/or effective concentration of Rrp6 could make contact with substrates more likely in the absence of a mediator/adaptor like Rrp47. The role of Rrp47 in the 3' processing of 5.8S rRNA and 5'ETS degradation seems more direct, since overexpression of Rrp6 cannot alleviate these processing defects in the *rrp47Δ* strain. Both substrates are known to have extensive secondary structures at their 3' ends (Yeh *et al.* 1990) and the defects seen in the absence of Rrp47 are consistent with its assumed role in the processing of structured RNA substrates (Stead *et al.* 2007).

Surprisingly, overexpression of catalytically active Rrp6 in the *rex1Δ rrp47Δ* strain could suppress the synthetic lethality of the mutations and recover growth. The effects on RNA processing were again restricted to substrates terminated via the Nrd1-pathway. The Rrp6 supplemented double mutants showed an accumulation of 3' extended snoRNA precursors of varying length and notably, depletion of the mature snoRNAs. The RNA processing defects decreased with increasing amounts of Rrp6 expressed in the *rex1Δ rrp47Δ* strain. These observations are consistent with a functional redundancy between Rex1 and Rrp6 in snoRNA processing and the proposed model by Grzechnik and Kufel (2008) whereby snoRNA termination at site I is followed by multiple rounds of polyadenylation and 3' exonucleolytic processing in a kinetic proofreading competition (Grzechnik and Kufel 2008). Suppression of the specific snoRNA processing defect in *rrp47Δ rex1Δ* mutants by overexpression of Rrp6 indicates that the synthetic lethality could be due to a block in snoRNA maturation or CUTs degradation. This is supported by analyses of conditional *rex1 rrp6* mutants (Garland *et al.*

2013) where overexpression of Rrp6 also led to a suppression of synthetic lethality of the *rrp47Δ mpp6Δ* double mutant. In this case, however, complementation was independent of Rrp6 catalytic activity (W. Garland, personal communication). This is consistent with a non-catalytical function of Rrp6 proposed in mRNA surveillance (Milligan *et al.* 2005) which could result from the postulated allosteric effects of Rrp6 on Rrp44 activity (Wasmuth and Lima 2012, Makino *et al.* 2013a).

Finally, overexpression of Rrp6 in an *rrp47Δ* strain restored Nrd1 protein to levels observed in the wild-type strain. Since the effects of Rrp6 overexpression were restricted to snoRNAs and CUTs terminated via Nrd1, it was interesting to see how Nrd1 expression is affected. If Nrd1 is available in excess, it binds to its own mRNA resulting in premature transcription termination and the mRNA is degraded by the Rrp6-exosome thus auto-regulating its own levels (Arigo *et al.* 2006b). In *rrp47Δ* strains, the Nrd1 pathway and thus Nrd1 auto-regulation is disrupted and Nrd1 levels are 4- to 5-fold increased implying a critical role for Rrp47 in Nrd1-dependent termination. However, as for the Nrd1 substrates, overexpression of Rrp6 could compensate for the lack of Rrp47. Notably, Nrd1 has also been implied in regulating the cellular response to nutrient availability with a number of new mRNA targets of the Nrd1-Nab3 pathway that are rapidly repressed in response to nutrient availability (Thiebaut *et al*. 2008, Darby *et al*. 2012). Considering more recent studies, the transcriptional repression is most likely due to Rrp6-dependent processing of shortened transcripts which then function as transcriptional repressors. Recent reports indicate that Rrp6 is involved in RNAPII pausing and transcriptional repression of the HIV TAR RNA by producing such a regulatory transcript (Wagschal *et al.* 2012). Such selective degradation of RNAs to regulate gene expression, physiology and ultimately cellular phenotypes is widely exploited in bacteria (Gripenland *et al.* 2010, Mackie 2013). Rrp6 is also known to degrade distinct classes of ncRNAs during vegetative growth which are induced at the onset of meiosis when Rrp6 is depleted and the cell is reprogrammed for its new task (Lardenois *et al.* 2011). This indicates a critical role for Rrp6 in differential ncRNA expression and explains the requirement for tight control of Rrp6 levels and activity to modulate the cellular response to changing growth conditions.

Taken together, Rrp6 has critical roles in transcription termination, stable and ncRNA processing and surveillance, and as a result a multitude of secondary effects on other pathways by affecting expression levels of mRNA targets like Nrd1 and Nab2 (Arigo *et al.* 2006b, Roth *et al.* 2005) or by modulating the activity of the core exosome (Wasmuth *and Lima* 2012, Makino *et al.* 2013a). In the absence of Rrp6 or reduced Rrp6 levels, stable RNA processing and turnover is slowed most likely due to the use of redundant, less efficient processing pathways. Moreover, CUTs with potential regulatory functions in gene expression and other processes accumulate which could lead to a comprehensive change in the pattern of gene expression of the affected cells. Rrp6 can therefore be regarded as a molecular switch

that quickly adapts cells to changing conditions. The lack of Rrp6 shifts cells into economy mode, whereas sufficient levels of Rrp6 provide conditions for optimum growth.

Given that RNA is now widely regarded as the ancestral molecule, preceding DNA and proteins, ribozymes and later RNases would have been at the centre of all regulatory processes with RNA fragments, structures or non-coding RNAs as the main regulators of gene expression. Over time these have been replaced or supplemented by increasingly specific proteins acting as transcription factors and modulators. However, the importance of regulatory non-coding RNAs and the significance of RNases in their production and regulation are now re-emerging. Notably, higher organisms have evolved mechanisms to shield and modulate RNase activities with adaptor and modulator proteins, the exosome being a prime example for its substrates have to be channelled through a catalytically inactive core to reach the enzymatic activity of the complex (Bonneau *et al.* 2009, Wasmuth and Lima 2012). In this respect, the most likely function for Rrp47 and other exosome co-factors can be seen in conferring substrate specificity and act as adaptors and modulators of RNase efficiency or expression to keep a crucial activity in the cell and specifically in the nucleus under tight control.

On a final and general note, *rrp6Δ* mutants have long been used as a marker for nuclear exosome function. However, care must be taken when interpreting data from *rrp6Δ* mutants, not only because Rrp6 has core exosome-independent targets and functions (Callahan and Butler 2008, Graham *et al.* 2009, Gudipati *et al.* 2008, 2012, Schneider *et al.* 2012). As importantly, Rrp6 mutants cause a wide range of secondary effects such as Rrp47 depletion, decrease in core exosome/Rrp44 activity (Wasmuth and Lima 2012), differential ncRNA expression (Lardenois *et al.* 2011), as well as effects on levels of other proteins like Nrd1, Nab2 and other mRNAs targeted and regulated via Rrp47-Rrp6 and Nrd1 (Arigo *et al.* 2006b, Roth *et al.* 2005, Castelnuovo *et al.* 2013).

# Chapter Six

# Conclusions and Future Studies

# Chapter 6

# Conclusions and future studies

We successfully used a mutagenesis approach to reveal regions within Rrp47 critical for binding to Rrp6 and RNA. More specifically, we empirically determined the Sas10/C1D domain which so far had only been defined by bioinformatics and we demonstrated its importance for the main functions of Rrp47 in Rrp6 binding, RNA processing as well as normal growth. We could also show that the Sas10 domain and the C-terminus of Rrp47 cooperate in stable RNA binding. However, whilst the basic C terminus is required for stable RNA binding *in vitro*, it appears to be dispensable for RNA-processing functions *in vivo* suggesting the existence of alternative agents in this pathway. Residues in the C-terminal domain of Rrp47 have been found to be specifically required for the final step of box C/D snoRNA maturation and possibly snoRNP assembly. Protein capture experiments in our lab by J. Costello using recombinant Rrp47 and yeast cell lysates demonstrated interactions between Rrp47 and the yeast snoRNP proteins Nop56 and Nop58 suggesting a function for Rrp47 as sensor and checkpoint for snoRNP assembly (Costello *et al*. 2011). Moreover, titrating Rrp47 out of catalytically active Rrp6 complexes also recently confirmed a critical function for the Rrp47 C-terminus in snoRNA and CUTs processing (Garland *et al*. 2013).

In addition to snoRNP proteins, protein capture assays also revealed weak interactions of Rrp47 with the Nrd1-Nab3 heterodimer responsible for termination of sn/snoRNAs and CUTs (J. Costello, personal communication). Further investigation of Rrp47 function in this pathway is of great interest due to its links to exosome-mediated degradation of pervasive transcripts with potential roles in regulation of gene expression and silencing. Mutations within Nrd1 and Nab3 have so far not led to the satisfactory mapping of Rrp47 binding to either Nrd1 or Nab3 (my unpublished data). However, the effects of Rrp47 depletion on Nrd1 levels presented in this study show a clear and important function of Rrp47 in this termination pathway. We have shown that Nrd1 termination is disrupted in the absence of Rrp47 alone, suggesting that Rrp47 makes the critical connection or guarantees localised accumulation of Rrp6 necessary for Nrd1 termination (seeing it can be overcome by overexpression of Rrp6). Contrary to previous reports using TAP-tagged Nrd1, we have found around 4 to 5-fold elevated Nrd1 protein levels in *rrp6Δ* and *rrp47Δ* strains. This is consistent with Nrd1 transcription being auto-regulated by surplus Nrd1 binding to Nrd1 mRNA causing pre-mature termination and degradation of Nrd1 mRNA by Rrp6 (Arigo *et al.* 2006b). Again it would be interesting to confirm these findings with data on Nrd1 mRNA levels in wild-type versus *rrp6Δ* and *rrp47Δ* strains which could be produced by RT-qPCR and the same could be investigated for Nab3 and Sen1, the partner proteins of Nrd1 in the complex.

Over the course of this study, the association of Rrp47 with Rrp6 has been more closely characterised in a cooperation with the Harding lab, revealing that recombinant Rrp47 forms a homodimer, however in the presence of Rrp6 is found as a stable Rrp47-Rrp6 heterodimer (Feigenbutz *et al.* 2013). This implies a structural reconfiguration of Rrp47 to join its partner protein. The interdependency of expression of the protein partners has been demonstrated with almost complete depletion of Rrp47 in the absence of Rrp6 and a weaker but significant effect of Rrp47 on Rrp6 expression and stability. The discovery that an N-terminally tagged zz-Rrp47 construct is protected from degradation in the absence of Rrp6 opens up a number of possibilities to further investigate Rrp47 functions independently of its exonuclease Rrp6. Initially confirmation is needed that zz-Rrp47 sediments within the same range and forms the same complexes as its untagged wild-type counterpart. This could be done by fractionation of native cell extracts from wild-type strains and *rrp6Δ* mutants expressing zz-Rrp47, as described. Further, the effects of zz-Rrp47 on RNA processing and localisation could be established. Attempts to reveal *in vivo* RNA substrates of Rrp47 by UV cross-linking using "CRAC" in cooperation with D. Tollervey and S. Grannemann have so far been unsuccessful (my unpublished data) and might be worth revisiting using zz-Rrp47 protein as bait in an *rrp6Δ* mutant and a catalytically inactive *rrp6.1* strain.

Furthermore, critical effects of Rrp47 on Rrp6 expression have been established which are exacerbated in minimal medium. A more comprehensive analysis of Rrp6 protein expression levels and RNA processing phenotypes under various growth conditions could give crucial insights into gene expression reprogramming through changes in Rrp6 levels and the resulting effects on CUTs and ncRNA expression dependent on nutrient status. A parallel analysis of sedimentation profiles of Rrp6 and the identification of associated proteins could also give clues to changes in complex formations under different growth conditions. Rrp6 overexpression has been shown to alleviate certain *rrp47Δ* phenotypes connected to Nrd1 terminated transcripts like snoRNAs and CUTs implying that Rrp47 is not necessarily required for these functions if enough Rrp6 is available. However, this indicates a role for Rrp47 in maintaining appropriate Rrp6 levels, be it due to simply maintaining Rrp6 stability or increasing substrate affinity. Another possibility is that Rrp47 is involved in the subnuclear accumulation of Rrp6 in the nucleolus as seen for C1D. This could be investigated by co-localisation experiments of Rrp6-GFP with a nucleolar protein like Nop56 or Nop1 in the presence or absence of Rrp47. Taken together, despite crucial new insights into Rrp47 interactions with Rrp6 and RNA and assembly of the Rrp47-Rrp6 heterodimer, it is still unclear how exactly Rrp47 functions. However, this study has provided a number of promising new leads to follow and particularly the recently obtained Rrp47-Rrp6NT crystal structure obtained in Elena Conti's lab and analysis of mutants in our lab will add new momentum to unravelling how Rrp47 regulates the activity and functions of its associated exonuclease Rrp6.

# References


Albuquerque, C. P., Smolka, M. B., Payne, S. H., Bafna, V., Eng, J., and Zhou, H. (2008) A multidimensional chromatography technology for indepth phosphoproteome analysis. *Mol Cell Proteomics* 7: 1389-1396.

Allmang, C., Kufel, J., Chanfreau, G., Mitchell, P., Petfalski, E. and Tollervey, D. (1999) Functions of the exosome in rRNA, snoRNA and snRNA synthesis. *EMBO J* 18: 5399-410.

Allmang, C., Mitchell, P., Petfalski, E. and Tollervey, D. (2000) Degradation of ribosomal RNA precursors by the exosome. *Nucleic Acids Res* 28: 1684-91.

Altschul, S. F., Gish, W., Miller, W., Myers, E. W. and Lipman, D. J. (1990) Basic local alignment search tool. *J Mol Biol* 215: 403-10.

Alwine, J. C., Kemp, D. J. and Stark, G. R. (1977) Method for detection of specific RNAs in agarose gels by transfer to diazobenzyloxymethyl-paper and hybridization with DNA probes. *Proc Natl Acad Sci USA* 74: 5350-4.

Anderson, J. and Parker, R. (1998) The 3' to 5' degradation of yeast mRNAs is a general mechanism for mRNA turnover that requires the SKI2 DEVH box protein and 3' to 5' \exonucleases of the exosome complex. *EMBO J* 17: 1497-1506.

Anderson, J. T. (2005) RNA turnover: unexpected consequences of being tailed. *Curr Biol* 15: R635-R638.

Anderson, J. T. and Wang, X. (2009) Nuclear RNA surveillance: no sign of substrates tailing off. *Crit Rev Biochem Mol Biol* 44:16-24.

Arigo, J. T., Eyler, D. E., Carroll, K. L. and Corden, J. L. (2006a) Termination of cryptic unstable transcripts is directed by yeast RNA-binding proteins Nrd1 and Nab3. *Mol Cell* 23: 841-51.

Arigo, J. T., Carroll, K. L., Ames, J. M. and Corden, J. L. (2006b) Regulation of yeast NRD1 expression by premature transcription termination. *Mol Cell* 21: 641-51.

Askree, S.H., Yehuda, T., Smolikov, S., Gurevich, R., Hawk, J., Coker, C., Krauskopf, A., Kupiec, M., McEachern, M.J. (2004) A genome-wide screen for *Saccharomyces cerevisiae* deletion mutants that affect telomere length. *Proc Natl Acad Sci USA* 101:8658-63.

Baudin, A., Ozier-Kalogeropoulos, O., Denouel, A., Lacroute, F. and Cullin, C. (1993) A simple and efficient method for direct gene deletion in *Saccharomyces cerevisiae.* *Nucleic Acids Res* 21: 3329-30.

Belostotsky, D. (2009) Exosome complex and pervasive transcription in eukaryotic genomes. *Curr Opin Cell Biol* 21: 352-358.

Bernstein, J., Patterson, D. N., Wilson, G. M. and Toth, E. A. (2008) Characterization of the essential activities of *Saccharomyces cerevisiae* Mtr4p, a 3'->5' helicase partner of the nuclear exosome. *J Biol Chem* 283: 4930-42.

Bernstein, J. and Toth, E.A. (2012) Yeast nuclear RNA processing. *World J Biol Chem* 3:7-26.

Birnboim, H. C. and Doly, J. (1979) A rapid alkaline extraction procedure for screening recombinant plasmid DNA. *Nucleic Acids Res* 7: 1513-23.

Bonneau, F., Basquin, .J, Ebert, J., Lorentzen, E., Conti, E. (2009) The yeast exosome functions as a macromolecular cage to channel RNA substrates for degradation. *Cell 139:547-59.*

Bousquet-Antonelli, C., Presutti, C. And Tollervey, D. (2000) Identification of a regulated pathway for nuclear pre-mRNA turnover. *Cell* 102:765-75.

Brachmann, C.B., Davies, A., Cost, G.J., Caputo, E., Li, J., Hieter, P. and Boeke, J.D. (1998). Designer deletion strains derived from *Saccharomyces cerevisiae* S288C: a useful set of strains and plasmids for PCR-mediated gene disruption and other applications. *Yeast* 14:115-132.

Bradford, M. M. (1976) A rapid and sensitive method for the quantitation of microgram quantities of protein utilizing the principle of protein-dye binding. *Anal Biochem* 72: 248-54.

Briggs, M. W., Burkard, K. T. D. and Butler, J. S. (1998) Rrp6p, the yeast homologue of the human PM-Scl 100-kDa autoantigen, is essential for efficient 5.8 S rRNA 3 ' end formation. *J Biol Chem* 273: 13255-13263.

Brody, E. and Abelson, J. (1985) The "spliceosome": yeast pre-messenger RNA associates with a 40S complex in a splicing-dependent reaction. *Science* 228: 963-7.

Buratowski, S. (2005) Connections between mRNA 3' end processing and transcription termination. *Curr Opin Cell Biol* 17: 257-61.

Buratowski, S. (2009) Progression through the RNA polymerase II CTD cycle. *Mol Cell* 36:541-546.

Burkard, K. T. and Butler, J. S. (2000) A nuclear 3'-5' exonuclease involved in mRNA degradation interacts with Poly(A) polymerase and the hnRNA protein Npl3p. *Mol Cell Biol* 20: 604-16.

Butler, J. S. and Mitchell, P. (2010) Rrp6, Rrp47 and cofactors of the nuclear exosome. *Adv Exp Med Biol* 702: 91-104.

Callahan, K. P. and Butler, J. S. (2008) Evidence for core exosome independent function of the nuclear exoribonuclease Rrp6p. *Nucleic Acids Res* 36: 6645-55.

Callahan, K. P. and Butler, J. S. (2010) TRAMP complex enhances RNA degradation by the nuclear exosome component Rrp6. *J Biol Chem* 285: 3540-3547.

Carneiro, T., Carvalho, C., Braga, J., Rino, J., Milligan, L., Tollervey, D., Carmo-Fonseca, M. (2008) Inactivation of cleavage factor I components Rna14p and Rna15p induces sequestration of small nucleolar ribonucleoproteins at discrete sites in the nucleus. *Mol Biol Cell* 19:1499-1508.

Carroll, K. L., and Pradhan, D. A. and Granek, J. A. and Clarke, N. D. and Corden, J. L. (2004) Identification of cis elements directing termination of yeast nonpolyadenylated snoRNA transcripts. *Mol Cell Biol* 24: 6241-6252.

Carroll, K. L., Ghirlando, R., Ames, J. M. and Corden, J. L. (2007) Interaction of yeast RNA-binding proteins Nrd1 and Nab3 with RNA polymerase II terminator elements. *RNA* 13: 361-73.

Castelnuovo M., Rahman S., Guffanti E., Infantino V., Stutz F., Zenklusen D. (2013) Bimodal expression of PHO84 is modulated by early termination of antisense transcription. *Nat Struct Mol Biol* 20:851-8.

Chen, C. Y., Gherzi, R., Ong, S. E., Chan, E. L., Raijmakers, R., Pruijn, G. J., Stoecklin, G., Moroni, C., Mann, M. and Karin, M. (2001) AU binding proteins recruit the exosome to degrade ARE-containing mRNAs. *Cell* 107: 451-64.

Chen, E. S., Sutani, T. and Yanagida, M. (2004) Cti1/C1D interacts with condensin SMC hinge and supports the DNA repair function of condensin. *Proc Natl Acad Sci USA* 101: 8078-83.

Chen, Y. and Varani, G. (2005) Protein families and RNA recognition. *FEBS J* 272: 2088-97.

Chlebowski, A., Lubas, M., Jensen, T.-H., Dziembowski, A. (2013) RNA decay machines: The exosome. *Biochim et Biophys Acta* 1829:552-550.

Clamp, M., Cuff, J., Searle, S. M., Barton, G. J. (2004) The Jalview Java alignment editor. *Bioinformatics* 20:426-427.

Coy, S., Volanakis, A., Shah, S., Vasiljeva, L. (2013) The Sm complex is required for the processing of non-coding RNAs by the exosome. *PLoS One* 8:e65606.

Coppola, J. A., Field, A. S. and Luse, D. S. (1983) Promoter-proximal pausing by RNA polymerase II in vitro: transcripts shorter than 20 nucleotides are not capped. *Proc Natl Acad Sci USA* 80: 1251-5.

Costello, J. L. and Stead, J. A. and Feigenbutz, M. and Jones, R. M. and Mitchell, P. (2011) The C-terminal region of the exosome-associated protein Rrp47 is specifically required for box C/D small nucleolar RNA 3'-maturation. *J Biol Chem* 286: 4535-4543.

Cryer, D. R., Eccleshall, R. and Marmur, J. (1975) Isolation of yeast DNA. *Methods Cell Biol* 12: 39-44.

Darby, M.M., Serebrini, L., Pan, X., Boeke, J.D., Corden J.L. (2012) The *Saccharomyces cerevisiae* Nrd1-Nab3 Transcription Termination Pathway Acts in Opposition to Ras Signaling and Mediates Response to Nutrient Depletion. *Mol Cell Biol* 32:1762-1775.

Davis, C. A., and Ares, M. (2006) Accumulation of unstable promoterassociated transcripts upon loss of the nuclear exosome subunit Rrp6p in *Saccharomyces cerevisiae*. *Proc Natl Acad Sci USA* 103: 3262-3267.

Dinger, M.E., Gascoigne, D.K., Mattick, J.S. (2011) The evolution of RNAs with multiple functions. *Biochimie* 93:2013.

Doma, M. K., Parker, R. (2007) RNA quality control in eukaryotes. *Cell* 16; 131(4):660-668

Dragon, F., Gallagher, J. E., Compagnone-Post, P. A., Mitchell, B. M., Porwancher, K. A., Wehner, K. A., Wormsley, S., Settlage, R. E., Shabanowitz, J., Osheim, Y., Beyer, A. L., Hunt, D. F., Baserga, S. J. (2002) A large nucleolar U3 ribonucleoprotein required for 18S ribosomal RNA biogenesis. *Nature* 417: 967-970.

Drazkowska, K., Tomecki, R., Stodus, K., Kowalska, K., Czarnocki-Cieciura, M., Dziembowski, A. (2013) The RNA exosome complex central channel controls both exonuclease and endonuclease Dis3 activities *in vivo* and *in vitro*. *Nucleic Acids Res*. 41:3845-58.

Dziembowski, A., Lorentzen, E., Conti, E. and Seraphin, B. (2007) A single subunit, Dis3, is essentially responsible for yeast exosome core activity. *Nat Struct Mol Biol* 14: 15-22.

Edelhoch, H. (1967) Spectroscopic determination of tryptophan and tyrosine in proteins. *Biochemistry* 6: 1948-54.

Egecioglu, D. E., Henras, A. K., Chanfreau, G. F. (2006) Contributions of Trf4p- and Trf5p-dependent polyadenylation to the processing and degradative functions of the yeast nuclear exosome. *RNA* 12: 26-32.

Egloff, S. and Murphy, S. (2008) Cracking the RNA polymerase II CTD code. *Trends Genet* 24: 280-8.

Egloff, S., Szczepaniak, S., Dienstbier, M., Taylor, A., Knight, S. and Murphy, S. (2010) The integrator complex recognizes a new double mark on the RNA polymerase II carboxyl-terminal domain. *J Biol Chem* 285:20564-69.

Erdemir, T., Bilican, B., Oncel, D., Goding, C. R. and Yavuzer, U. (2002a) DNA damage-dependent interaction of the nuclear matrix protein C1D with Translin-associated factor X (TRAX). *J Cell Sci* 115: 207-16.

Erdemir, T., Bilican, B., Cagatay, T., Goding, C. R. and Yavuzer, U. (2002b) *Saccharomyces cerevisiae* C1D is implicated in both non-homologous DNA end joining and homologous recombination. *Mol Microbiol* 46: 947-57.

Fang, F., Phillips, S. and Butler, J. S. (2005) Rat1p and Rai1p function with the nuclear exosome in the processing and degradation of rRNA precursors. *RNA* 11: 1571-8.

Fasken, M. B. and Corbett, A. H. (2009) Mechanisms of nuclear mRNA quality control. *RNA Biol* 6:237-241.

Feigenbutz, M., Jones, R., Besong, T.M., Harding S.E., Mitchell, P. (2013a) Assembly of the Yeast Exoribonuclease Rrp6 with its Associated Cofactor Rrp47 Occurs in the Nucleus and is Critical for the Controlled Expression of Rrp47. *J Biol Chem* 288:15959-70.

Feigenbutz, M., Garland, W., Turner, M., Mitchell, P. (2013b) The Exosome Cofactor Rrp47 Is Critical for the Stability and Normal Expression of Its Associated Exoribonuclease Rrp6 in *Saccharomyces cerevisiae. PLoS ONE* 8(11): e80752. doi:10.1371/journal.pone.0080752.

Finn, R.D., Tate, J., Mistry, J., Coggill, P.C., Sammut, J.S., Hotz, H.R., Ceric, G., Forslund, K., Eddy, S.R., Sonnhammer E.L. and Bateman, A. (2008) The Pfam protein families database. *Nucleic Acids Research* 36:D281-D288.

Garland, W., Feigenbutz, M., Turner, M., Mitchell, P. (2013) Rrp47 functions in RNA surveillance and stable RNA processing when divorced from the exoribonuclease and exosome-binding domains of Rrp6. *RNA* Oct 8 2013 epub.

Gautier, T., Bergès, T., Tollervey, D., Hurt, E. (1997) Nucleolar KKE/D repeat proteins Nop56p and Nop58p interact with Nop1p and are required for ribosome biogenesis. *Mol Cell Biol* 17: 7088-7098.

Gietz, D., St Jean, A., Woods, R. A. and Schiestl, R. H. (1992) Improved method for high efficiency transformation of intact yeast cells. *Nucleic Acids Res* 20: 1425.

Graham, A. C., Kiss, D. L., and Andrulis, E. D. (2006) Differential distribution of exosome subunits at the nuclear lamina and in cytoplasmic foci. *Mol Biol Cell* 17: 1399-1409.

Graham, A. C., Kiss, D. L., Andrulis, E. D. (2009) Core exosome-independent roles for Rrp6 in cell cycle progression. *Mol Biol Cell* 20:2242-53.

Gripenland, J., Netterling, S., Loh, E., Tiensuu, T., Toledo-Arana, A., Johansson, J. (2010) RNAs: regulators of bacterial virulence. *Nat Rev Microbiol* 8:857-66.

Grünwald, D., Singer, R. H., Rout, M. (2011) Nuclear export dynamics of RNA-protein complexes. *Nature* 2011 475:333-41.

Grzechnik, P. and Kufel, J. (2008) Polyadenylation linked to transcription termination directs the processing of snoRNA precursors in yeast. *Mol Cell* 32: 247-58.

Gudipati, R. K., Villa, T., Boulay, J., Libri, D. (2008) Phosphorylation of the RNA polymerase II C-terminal domain dictates transcription termination choice. *Nat Struct Mol Biol* 15: 786-94.

Hahn, S. and Young, E. T. (2011) Transcriptional Regulation in *Saccharomyces cerevisiae*: Transcription factor regulation and function, mechanisms of initiation, and roles of activators and coactivators. *Genetics* 189: 705-736.

Haile, S., Cristodero, M., Clayton, C. and Estevez, A. M. (2007) The subcellular localisation of trypanosome *RRP6* and its association with the exosome. *Mol Biochem Parasitol* 151: 52-58.

Hemmerich, P., Bosbach, S., von Mikecz, A. and Krawinkel, U. (1997) Human ribosomal protein L7 binds RNA with an alpha-helical arginine-rich and lysine-rich domain. *Eur J Biochem* 245: 549-556.

Henras, A. K., Dez, C. and Henry, Y. (2004) RNA structure and function in C/D and H/ACA s(no)RNPs. *Curr Opin Struct Biol* 14: 335-43.

Henras, A. K., Soudet, J., Gerus, M., Lebaron, S., Caizergues-Ferrer, M., Mougin, A. and Henry, Y. (2008) The post-transcriptional steps of eukaryotic ribosome biogenesis. *Cell Mol Life Sci* 65: 2334-59.

Hieronymus, H., Yu, M.C., Silver, P.A. (2004) Genome-wide mRNA surveillance is coupled to mRNA export. *Genes Dev* 18:2652-62.

Hilleren, P., McCarthy, T., Rosbash, M., Parker, R., Jensen, T.H. (2001) Quality control of mRNA 3'-end processing is linked to the nuclear exosome. *Nature* 413:538-42.

Honorine, R., Mosrin-Huaman, C., Hervouet-Coste, N., Libri, D., Rahmouni, A. R. (2011) Nuclear mRNA quality control in yeast is mediated by Nrd1 co-transcriptional recruitment, as revealed by the targeting of Rho-induced aberrant transcripts. *Nucleic Acids Res* 39: *2809-2820.*

Houmani, J.L., Ruf, I.K. (2009) Clusters of Basic Amino Acids Contribute to RNA Binding and Nucleolar Localization of Ribosomal Protein L22. *PLoS ONE* 4: e5306.

Houseley, J., LaCava, J. and Tollervey, D. (2006) RNA-quality control by the exosome. *Nat Rev Mol Cell Biol* 7: 529-39.

Houseley, J., Kotovic, K., El Hage, A., Tollervey, D. (2007) Trf4 targets ncRNAs from telomeric and rDNA spacer regions and functions in rDNA copy number control. *EMBO J* 26: 4996-5006.

Houseley, J., and Tollervey, D. (2008) The nuclear RNA surveillance machinery: the link between ncRNAs and genome structure in budding yeast? *Biochim Biophys Acta* 1779(4): 239-46.

Houseley, J. and Tollervey, D. (2009) The many pathways of RNA degradation. *Cell* 136:763-776.

Jackson, R. N., Klauer, A. A., Hintze, B.J., Robinson, H., van Hoof, A., Johnson, S.J. (2010) The crystal structure of Mtr4 reveals a novel arch domain required for rRNA processing. *EMBO J* 29:2205-16.

Jamonnak, N., Creamer, T.J., Darby, M.M., Schaughency, P., Wheelan, S.J., Corden, J.L. (2011) Yeast Nrd1, Nab3, and Sen1 transcriptome-wide binding maps suggest multiple roles in post-transcriptional RNA processing. *RNA* 17:2011-2025.

Jäkel, S., Mingot, J.-M., Schwarzmaier, P., Hartmann, E., and Görlich, D. (2002) Importins fulfil a dual function as nuclear import receptors and cytoplasmic chaperones for exposed basic domains. *EMBO J* 21, 377-386.

Januszyk, K. and Lima, C. D. (2010) Structural components and architectures of RNA exosomes. *Adv Exp Med Biol* 702: 9-28.

Januszyk, K. and Liu, Q. and Lima, C. D. (2011) Activities of human RRP6 and structure of the human RRP6 catalytic domain. *RNA* 17:1566-1577.

Jensen, T. H., Dower, K., Libri, D., Rosbash, M. (2003) Early formation of mRNP: license for export or quality control? *Mol Cell* 11(5):1129-38. Review.

Jia, H. and Wang, X. and Liu, F. and Guenther, U.-P. and Srinivasan, S. and Anderson, J. T. and Jankowsky, E. (2011) The RNA helicase Mtr4p modulates polyadenylation in the TRAMP complex. *Cell* 145: 890-901.

Jung, M. Y., Lorenz, L. and Richter, J. D. (2006) Translational control by neuroguidin, a eukaryotic initiation factor 4E and CPEB binding protein. *Mol Cell Biol* 26: 4277-87.

Jurica, M. S. and Moore, M. J. (2003) Pre-mRNA splicing: awash in a sea of proteins. *Mol Cell* 12: 5-14.

Kamakaka, R. T., Rine J. (1998) Sir- and silencer-independent disruption of silencing in *Saccharomyces* by Sas10p. *Genetics* 149:903-14.

Kelley, L. A., Sternberg, M. J. (2009) Protein structure prediction on the Web: a case study using the Phyre server. *Nat Protoc* 4: 363-371.

Kim, H., Erickson, B., Luo, W., Seward, D., Graber, J.H., Pollock, D.D., Megee, P.C., Bentley. D.L. (2010) Gene-specific RNA polymerase II phosphorylation and the CTD code. *Nat Struct Mol Biol* 17:1279-1286.

Kim, M., Vasiljeva, L., Rando, O. J., Zhelkovsky, A., Moore, C. and Buratowski, S. (2006) Distinct pathways for snoRNA and mRNA termination. *Mol Cell* 24: 723-34.

Kiss, D. L. and Andrulis, E. D. (2010) Genome-wide analysis reveals distinct substrate specificities of Rrp6, Dis3, and core exosome subunits. *RNA* 16: 781-791.

Kos, M. and Tollervey, D. (2010) Yeast pre-rRNA processing and modification occur cotranscriptionally. *Mol Cell* 37:809-820.

Kranz, J. E., Holm, C. (1990) Cloning by function: an alternative approach for identifying yeast homologs of genes from other organisms. *Proc Natl Acad Sci U S A* 87:6629-33.

Kuai, L., Fang, F., Butler, J. S., and Sherman, F. (2004) Polyadenylation of rRNA in Saccharomyces cerevisiae. *Proc Natl Acad Sci USA* 101: 8581-8586.

Kuehner, J. N. and Pearson, E. L. and Moore, C. (2011) Unravelling the means to an end: RNA polymerase II transcription termination. *Nat Rev Mol Cell Biol* 12: 283-294.

Kufel, J., Dichtl, B. and Tollervey, D. (1999) Yeast Rnt1p is required for cleavage of the pre-ribosomal RNA in the 3' ETS but not the 5' ETS. *RNA* 5: 909-17.

Kufel, J., Bousquet-Antonelli, C., Beggs, J. D., Tollervey, D. (2004) Nuclear pre-mRNA decapping and 5' degradation in yeast require the Lsm2-8p complex. *Mol Cell Biol* 24:9646-57.

Kumar, A., Agarwal, S., Heyman, J. A., Matson, S., Heidtman, M., Piccirillo, S., Umansky, L., Drawid, A., Jansen, R., Liu, Y., Cheung, K. H., Miller, P., Gerstein, M., Roeder, G. S. and Snyder, M. (2002) Subcellular localization of the yeast proteome. *Genes Dev* 16: 707-19.

LaCava, J., Houseley, J., Saveanu, C., Petfalski, E., Thompson, E., Jacquier, A. and Tollervey, D. (2005) RNA degradation by the exosome is promoted by a nuclear polyadenylation complex. *Cell* 121: 713-24.

Lafontaine, D. L. J. and Tollervey, D. (1999) Nop58p is a common component of the box C+D snoRNPs that is required for snoRNA stability. *RNA* 5: 455-467.

Lafontaine, D. L. and Tollervey, D. (2000) Synthesis and assembly of the box C+D small nucleolar RNPs. *Mol Cell Biol* 20: 2650-9.

Lange, H., Holec, S., Cognat, V., Pieuchot, L., Le Ret, M., Canaday, J., and Gagliardi, D. (2008) Degradation of a polyadenylated rRNA maturation by-product involves one of the three RRP6-like proteins in Arabidopsis thaliana. *Mol Cell Biol* 28 3038-3044.

Lardenois, A. and Liu, Y. and Walther, T. and Chalmel, F. and Evrard, B. and Granovskaia, M. and Chu, A. and Davis, R. W. and Steinmetz, L. M. and Primig, M. (2011) Execution of the meiotic noncoding RNA expression program and the onset of gametogenesis in yeast require the conserved exosome subunit Rrp6. *Proc Natl Acad Sci USA* 108: 1058-1063.

Larkin, M. A., Blackshields, G., Brown, N. P., Chenna, R., McGettigan, P. A., McWilliam, H., Valentin, F., Wallace, I. M., Wilm, A., Lopez, R., Thompson, J. D., Gibson, T. J. and Higgins, D. G. (2007) Clustal W and Clustal X version 2.0. *Bioinformatics* 23: 2947-8.

Lebreton, A., Tomecki, R., Dziembowski, A. and Seraphin, B. (2008) Endonucleolytic RNA cleavage by a eukaryotic exosome. *Nature* 456: 993-6.

Lee, D. H., and Goldberg, A. L. (1996) Selective inhibitors of the proteasome-dependent and vacuolar pathways of protein degradation in Saccharomyces cerevisiae. *J Biol Chem* 271: 27280-27284.

Lee, T.I., Rinaldi, N.J., Robert, F., Odom, D.T., Bar-Joseph, Z., Gerber, G.K., Hannett, N.M., Harbison, C.T., Thompson, C.M., Simon, I., Zeitlinger, J., Jennings, E.G,. Murray, H.L.,Gordon, D.B., Ren, B., Wyrick, J.J., Tagne, J.B., Volkert, T.L., Fraenkel, E., Gifford, K., Young, R.A. (2002) Transcriptional regulatory networks in Saccharomyces cerevisiae. *Science* 298:799-804.

Lejeune, F., Li, X., and Maquat, L. (2003) Nonsense-mediated mRNA decay in mammalian cells involves decapping, deadenylating, and exonucleolytic activities. *Mol Cell* 12: 675-687.

Licatalosi, D. D. and Darnell, R. B. (2010) RNA processing and its regulation: global insights into biological networks. *Nat Rev Genet* 11: 75-87.

Liu, Q., Greimann, J. C. and Lima, C. D. (2006) Reconstitution, activities, and structure of the eukaryotic RNA exosome. *Cell* 127: 1223-37.

Longtine, M.S., McKenzie, A. 3rd, Demarini, D.J., Shah, N.G., Wach, A., Brachat, A., Philippsen, P, Pringle, J.R. (1998) Additional modules for versatile and economical PCR-based gene deletion and modification in Saccharomyces cerevisiae. *Yeast* 14:953-61.

Lopez, R., Silventoinen, V., Robinson, S., Kibria, A., Gish, W. (2003) WU-Blast2 server at the European Bioinformatics Institute. *Nucleic Acids Res* 31:3795-3798.

Lorentzen, E. and Conti, E. (2006) The exosome and the proteasome: nano-compartments for degradation. *Cell* 125:651-4. Review.

Lorentzen, E., Basquin, J., Tomecki, R., Dziembowski, A. and Conti, E. (2008) Structure of the active subunit of the yeast exosome core, Rrp44: diverse modes of substrate recruitment in the RNase II nuclease family. *Mol Cell* 29: 717-28.

Luna, R. and Gaillard, H. and González-Aguilera, C. and Aguilera, A. (2008) Biogenesis of mRNPs: integrating different processes in the eukaryotic nucleus. *Chromosoma* 117: 319-331.

Lykke-Andersen, S. and Jensen, T. H. (2007) Overlapping pathways dictate termination of RNA polymerase II transcription. *Biochimie* 89: 1177-82.

Lykke-Andersen, S., Brodersen, D. E. and Jensen, T. H. (2009) Origins and activities of the eukaryotic exosome. *J Cell Sci* 122:1487-1494.

Lykke-Andersen, S., Tomecki R., Jensen, T. H. and Dziembowski, A. (2011) The eukaryotic exosome. *RNA Biology* 8: 61-66.

Lykke-Andersen, S. and Mapendano, C. K. and Jensen, T. H. (2011) An ending is a new beginning: transcription termination supports re-initiation. *Cell Cycle* 10: 863-865.

Mackie, G.A. (2013) Determinants in the rpsT mRNAs recognized by the 5'-sensor domain of RNase E. *Mol Microbiol* 89:388-402.

Makino, D.L,. Baumgärtner, M., Conti, E. (2013) Crystal structure of an RNA-bound 11-subunit eukaryotic exosome complex. Nature 495:70-5.

Makino, D.L., Halbach, F. and Conti, E. (2013) The RNA exosome and proteasome: common principles of degradation control.*Nat Rev Mol Cell Biol* 14:654-60.

Maniatis, T., Fritsch, E. F. and Sambrook, J. (1982).Methods in Molecular Cloning: A Laboratory Manual*. Cold Spring Harbor Lab Press,* Cold Spring Harbor, NY, USA.

Marquardt, S. and Hazelbaker, D. Z. and Buratowski, S. (2011) Distinct RNA degradation pathways and 3' extensions of yeast non-coding RNA species. *Transcription* 2:145-154.

Mateus, C., and Avery, S. V. (2000) Destabilized green fluorescent protein for monitoring dynamic changes in yeast gene expression with flow cytometry. *Yeast* 16: 1313-1323.

Matera, A.G., Terns, R.M., Terns, M.P. (2007) Non-coding RNAs: lessons from the small nuclear and small nucleolar RNAs. *Nat Rev Mol Cell Biol* 8:209-20.

Midtgaard, S. F., Assenholt, J., Jonstrup, A. T., Van, L. B., Jensen, T. H. and Brodersen, D. E. (2006) Structure of the nuclear exosome component Rrp6p reveals an interplay between the active site and the HRDC domain. *Proc Natl Acad Sci USA* 103: 11898-903.

Milligan, L., Torchet, C., Allmang, C., Shipman, T. and Tollervey, D. (2005) A nuclear surveillance pathway for mRNAs with defective polyadenylation. *Mol Cell Biol* 25: 9996-10004.

Milligan, L., Decourty, L., Saveanu, C., Rappsilber, J., Ceulemans, H., Jacquier, A. and Tollervey, D. (2008) A yeast exosome cofactor, Mpp6, functions in RNA surveillance and in the degradation of noncoding RNA transcripts. *Mol Cell Biol* 28: 5446-57.

Mitchell, P., Petfalski, E. and Tollervey, D. (1996) The 3' end of yeast 5.8S rRNA is generated by an exonuclease processing mechanism. *Genes Dev* 10: 502-13.

Mitchell, P., Petfalski, E., Shevchenko, A., Mann, M. and Tollervey, D. (1997) The exosome: a conserved eukaryotic RNA processing complex containing multiple 3'->5' exoribonucleases. *Cell* 91: 457-66.

Mitchell, P., Petfalski, E., Houalla, R., Podtelejnikov, A., Mann, M. and Tollervey, D. (2003a) Rrp47p is an exosome-associated protein required for the 3' processing of stable RNAs. *Mol Cell Biol* 23: 6982-92.

Mitchell, P. and Tollervey, D. (2003b) An NMD pathway in yeast involving accelerated deadenylation and exosome-mediated 3'-->5' degradation. *Mol Cell* 11:1405-1413.

Mitchell, P. (2010) Rrp47 and the function of the Sas10/C1D domain. *Biochem Soc Trans* 38: 1088-1092.

Mitchell, P. and Tollervey, D. (2010) Finding the exosome. *Adv Exp Med Biol* 702: 1-8.

Mohr, D., Frey, S., Fischer, T., Güttler, T., and Görlich, D. (2009) Characterisation of the passive permeability barrier of nuclear pore complexes. *EMBO J* 28:2541-2553.

Mortimer, R. K. and Johnston, J. R. (1986) Genealogy of principal strains of the yeast genetic stock center. *Genetics* 113: 35-43.

Motley, A. M., Nuttall, J. M., and Hettema, E. H. (2012) Pex3-anchored Atg36 tags peroxisomes for degradation in Saccharomyces cerevisiae. *EMBO J.* 31:2852-2868.

Nehls, P., Keck, T., Greferath, R., Spiess, E., Glaser, T., Rothbarth, K., Stammer, H., and Werner, D. (1998) cDNA cloning, recombinant expression and characterization of polypetides with exceptional DNA affinity. *Nucleic Acids Res* 26:1160-1166.

Neil, H., Malabat, C., d'Aubenton-Carafa, Y., Xu, Z. Y., Steinmetz, L. M. and Jacquier, A. (2009) Widespread bidirectional promoters are the major source of cryptic transcripts in yeast. *Nature* 457: 1038-42.

Neuhoff, V., Arold, N., Taube, D. and Ehrhardt, W. (1988) Improved staining of proteins in polyacrylamide gels including isoelectric focusing gels with clear background at nanogram sensitivity using Coomassie Brilliant Blue G-250 and R-250. *Electrophoresis* 9: 255-62.

Niedenthal, R. K., Riless, L., Johnston, M., and Hegemann, J. (1996) Green fluorescent protein as a marker for gene expression and subcellular localization in budding yeast. *Yeast* 12:773-786.

Nishizawa, M., Komai, T., Katou, Y., Shirahige, K., Ito, T., Toh-E, A. (2008) Nutrient-regulated antisense and intragenic RNAs modulate a signal transduction pathway in yeast. *PLoS Biol* 6:2817-30.

Pace, C. N., Vajdos, F., Fee, L., Grimsley, G. and Gray, T. (1995) How to measure and predict the molar absorption coefficient of a protein. *Protein Sci* 4: 2411-23.

Papworth, C., Bauer, J. C., Braman, J. and Wright, D. A. (1996) QuikChange site-directed mutagenesis**.** *Strategies* 9: 3-4.

Patel, R.C., Sen, G. C. (1998) Requirement of PKR dimerization mediated by specific hydrophobic residues for its activation by double-stranded RNA and its antigrowth effects in yeast. *Mol Cell Biol* 18:7009-19.

Patel, S. B. and Bellini, M. (2008) The assembly of a spliceosomal small nuclear ribonucleoprotein particle. *Nucleic Acids Res* 36:6482-6493.

Peculis, B. (2002) Ribosome biogenesis: ribosomal RNA synthesis as a package deal. *Curr Biol* 12: R623-R624.

Peng, W. T., Robinson, M. D., Mnaimneh, S., Krogan, N. J., Cagney, G., Morris, Q., Davierwala, A. P., Grigull, J., Yang, X., Zhang, W., Mitsakakis, N., Ryan, O. W., Datta, N., Jojic, V., Pal, C., Canadien, V., Richards, D., Beattie, B., Wu, L. F., Altschuler, S. J., Roweis, S., Frey, B. J., Emili, A., Greenblatt, J. F. and Hughes, T. R. (2003) A panoramic view of yeast noncoding RNA processing. *Cell* 113: 919-33.

Phillips, S. and Butler, J. S. (2003) Contribution of domain structure to the RNA 3' end processing and degradation functions of the nuclear exosome subunit Rrp6p. *RNA* 9:1098-1107.

Piper, P. W., Bellatin, J. A., Lockheart, A. (1983) Altered maturation of sequences at the 3' terminus of 5S gene transcripts in a *Saccharomyces cerevisiae* mutant that lacks a RNA processing endonuclease. *EMBO J* 2:353-359.

Preker, P., Nielsen, J., Kammler, S., Lykke-Andersen, S., Christensen, M. S., Mapendano, C. K., Schierup, M. H., and Jensen, T. H. (2008) RNA exosome depletion reveals transcription upstream of active human promoters. *Science* 322:1851-1854.

Preker, P., Almvig, K., Christensen, M. S., Valen, E., Mapendano, C. K., Sandelin, A., Jensen, T. H. (2011) PROMoter uPstream Transcripts share characteristics with mRNAs and are produced upstream of all three major types of mammalian promoters. *Nucleic Acids Res* 39:7179-7193.

Proudfoot, N.J. (2011) Ending the message: poly(A) signals then and now. *Genes Dev* 25: 1770-1782.

Puig, O., Caspary, F., Rigaut, G., Rutz, B., Bouveret, E., Bragado-Nilsson, E., Wilm, M., Séraphin, B. (2001) The Tandem Affinity Purification (TAP) Method: A General Procedure of Protein Complex Purification. *Methods* 24: 218-229.

Reichow, S. L. and Hamma, T. and Ferré-D'Amaré, A. R. and Varani, G. (2007) The structure and function of small nucleolar ribonucleoproteins. Nucleic Acids Res 35:1452-1464.

Reinisch, K. M., Wolin, S. L. (2007) Emerging themes in non-coding RNA quality control. *Curr Opin Struct Biol* 17:209-214.

Richard, P. and Kiss, T. (2006) Integrating snoRNP assembly with mRNA biogenesis. *EMBO Rep* 7: 590-2.

Richard, P. and Manley, J. L. (2009) Transcription termination by nuclear RNA polymerases. *Genes Dev* 23(11): 1247-1269.

Rigaut, G., Shevchenko, A., Rutz, B., Wilm, M., Mann, M. and Seraphin, B. (1999) A generic protein purification method for protein complex characterization and proteome exploration. *Nat Biotechnol* 17: 1030-2.

Rondon, A.G., Mischo, H.E., Kawauchi, J., Proudfoot, N.J. (2009) Fail-safe transcriptional termination for protein-coding genes in *S. cerevisiae*. *Mol Cell* 36:88-98.

Rosonina, E., Kaneko, S., Manley, J. L. (2006) Terminating the transcript: breaking up is hard to do. *Genes Dev* 20:1050-1056.

Roth, K., Wolf, M., Rossi, M., Butler, J.S. (2005) The nuclear exosome contributes to autogenous control of NAB2 mRNA levels. *Mol Cell Biol* 25:1577-85.

Rothbarth, K., Spiess, E., Juodka, B., Yavuzer, U., Nehls, P., Stammer, H. and Werner, D. (1999) Induction of apoptosis by overexpression of the DNA-binding and DNA-PK-activating protein C1D. *J Cell Sci* 112: 2223-32.

Rothbarth, K., Stammer, H., Werner, D. (2002) Proteasome-mediated degradation antagonizes critical levels of the apoptosis-inducing C1D protein. *Cancer Cell Int* 2:12.

Rothstein, R. J. (1983) One-step gene disruption in yeast. *Methods Enzymol* 101: 202-11.

Rougemaille, M., Gudipati, R. K., Olesen, J. R., Thomsen, R., Seraphin, B., Libri, D. and Jensen, T. H. (2007) Dissecting mechanisms of nuclear mRNA surveillance in THO/sub2 complex mutants. *EMBO J* 26: 2317-2326.

Rougemaille, M., Villa, T., Gudipati, R. K. and Libri, D. (2008) mRNA journey to the cytoplasm: attire required. *Biol Cell* 100: 327-42.

Rougemaille, M. and Libri, D. (2010) Control of cryptic transcription in eukaryotes. *Adv Exp Med Biol* 702: 122-131.

Rowe, A. J. and Khan, G. M. (1972) Determination of corrected sedimentation coefficient at different temperatures using the MSE analytical ultracentrifuge. *Anal Biochem* 45: 488-97.

Russell, J. and Zomerdijk, J. C. (2005) RNA-polymerase-I-directed rDNA transcription, life and works. *Trends Biochem Sci* 30: 87-96.

Sattlegger, E., Barbosa, J. A., Moraes, M. C., Martins, R. M., Hinnebusch, A. G., and Castilho, B. A. (2011) Gcn1 and actin binding to Yih1. Implications for activation of the eIF2 kinase GCN2. *J Biol Chem* 286:10341-10355.

Schaeffer, D., Tsanova, B., Barbas, A., Reis, F. P., Dastidar, E. G., Sanchez-Rotunno, M., Arraiano, C. M. and van Hoof, A. (2009) The exosome contains domains with specific endoribonuclease, exoribonuclease and cytoplasmic mRNA decay activities. *Nat Struct Mol Biol* 16: 56-62.

Schilders, G., Raijmakers, A., Raats, J., and Pruijn, G. J. (2005) MPP6 is an exosome-associated RNA-binding protein involved in 5.8S rRNA maturation. *Nucleic Acids Res 33: 6795-6804*.

Schilders, G., van Dijk, E. and Pruijn, G. J. (2007) C1D and hMtr4p associate with the human exosome subunit PM/Scl-100 and are involved in pre-rRNA processing. *Nucleic Acids Res* 35: 2564-72.

Schmid, M. and Jensen, T. H. (2008a) The exosome: a multipurpose RNA-decay machine. *Trends Biochem Sci* 33: 501-10.

Schmid, M. and Jensen, T. H. (2008b) Quality control of mRNP in the nucleus. *Chromosoma* 117: 419-429.

Schmittgen, T. D., and Livak, K. J. (2008) Analyzing real-time PCR data by the comparative CT method. *Nat Protoc* 3:1101–1108.

Schneider, C., Anderson, J. and Tollervey, D. (2007) The exosome subunit Rrp44 plays a direct role in RNA substrate recognition. *Mol Cell* 27:324-331.

Schneider, C., Leung, E., Brown, J. and Tollervey, D. (2009) The N-terminal PIN domain of the exosome subunit Rrp44 harbors endonuclease activity and tethers Rrp44 to the yeast core exosome. *Nucleic Acids Res* 37: 1127-40.

Schneider, C., Kudla, G., Wlotzka, W., Tuck, A., and Tollervey, D. (2012) Transcriptome-wide analysis of exosome targets. *Mol Cell* 48:422-433.

Schneider, D. A. (2011) RNA polymerase I activity is regulated at multiple steps in the transcription cycle: Recent insights into factors that influence transcription elongation. *Gene* 493:176-84.

Sharp, P.A. (2009) The centrality of RNA. *Cell* 136:577-580.

Shapiro, A.L., Viñuela, E., Maizel, J.V. Jr. (1967) Molecular weight estimation of polypeptide chains by electrophoresis in SDS-polyacrylamide gels. *Biochem Biophys Res Commun* 28:815-20.

Sikorski, R.S., and Hieter, P. (1989) A system of shuttle vectors and yeast host strains designed for efficient manipulation of DNA in *Saccharomyces cerevisiae*. *Genetics* 122:19-27.

Sikorski, T. W. and Buratowski, S. (2009) The basal initiation machinery: beyond the general transcription factors. *Curr Opin Cell Biol* 21: 344-51.

Smith, D. B. and Johnson, K. S. (1988) Single-step purification of polypeptides expressed in *Escherichia coli* as fusions with glutathione S-transferase. *Gene* 67: 31-40.

Southern, E. M. (1975) Detection of specific sequences among DNA fragments separated by gel electrophoresis. *J Mol Biol* 98: 503-17.

Staals, R. H. J. and Pruijn, G. J. M. (2010) The human exosome and disease. *Adv Exp Med Biol* 702: 132-42.

Staub, E., Fiziev, P., Rosenthal, A., and Hinzmann, B. (2004) Insights into the evolution of the nucleolus by an analysis of its protein domain repertoire. *BioEssays* 26:567-581.

Stead, J. A., Costello, J. L., Livingstone, M. J. and Mitchell, P. (2007) The PMC2NT domain of the catalytic exosome subunit Rrp6p provides the interface for binding with its cofactor Rrp47p, a nucleic acid-binding protein. *Nucleic Acids Res* 35: 5556-67.

Steinmetz, E. J., Conrad, N. K., Brow, D. A. and Corden, J. L. (2001) RNA-binding protein Nrd1 directs poly(A)-independent 3'-end formation of RNA polymerase II transcripts. *Nature* 413: 327-31.

Steinmetz, E. J., Ng, S. B., Cloute, J. P. and Brow, D. A. (2006) cis- and trans-acting determinants of transcription termination by yeast RNA polymerase II. *Mol Cell Biol* 26: 2688-96.

Svedberg (1934) Molecular weight analysis in centrifugal fields. *Science* 79:327-32.

Synowsky, S. A., van den Heuvel, R. H., Mohammed, S., Pijnappel, P. W., and Heck, A. J. (2006) Probing genuine strong interactions and post-translational modifications in the heterogeneous yeast exosome protein complex. *Mol Cell Proteomics* 5:1581-1592.

Synowsky, S. A., van Wijk, M., Raijmakers, R., and Heck, A. J. (2009) Comparative multiplexed mass spectrometric analyses of endogenously expressed yeast nuclear and cytoplasmic exosomes. *J Mol Biol* 385:1300-1313.

Tabb, M.M., Tongaonkar, P., Vu, L., Nomura, M. (2000) Evidence for separable functions of Srp1p, the yeast homolog of importin alpha (Karyopherin alpha): role for Srp1p and Sts1p in protein degradation. *Mol Cell Biol* 20:6062-73.

Teste, M.-A., Duquenne, M., Francois J.M. and Parrou J.L. ( 2009) Validation of reference genes for quantitative expression analysis by real-time RT-PCR in *Saccharomyces cerevisiae.* *BMC Mol Biol* 10:99:1471-2199.

Thiebaut, M., Kisseleva-Romanova, E., Rougemaille, M., Boulay, J. and Libri, D. (2006) Transcription termination and nuclear degradation of cryptic unstable transcripts: a role for the Nrd1-Nab3 pathway in genome surveillance. *Mol Cell* 23: 853-64.

Thiebaut, M., Colin, J., Nei,l. H., Jacquier, A., Séraphin B., Lacroute, F., Libri, D. (2008) Futile cycle of transcription initiation and termination modulates the response to nucleotide shortage in *S. cerevisiae*. *Mol Cell* 31:671-682.

Tollervey, D., and Mattaj, I. (1987) Fungal small nuclear ribonucleoproteins share properties with plant and vertebrate U-snRNPs. *EMBO J*. 6:469-476.

Torchet, C., Bousquet-Antonelli, C., Milligan, L., Thompson, E., Kufel, J. and Tollervey, D. (2002) Processing of 3'-extended read-through transcripts by the exosome can generate functional mRNAs. *Mol Cell* 9: 1285-96.

Tuck, A. C. and Tollervey, D. (2011) RNA in pieces. Trends Genet 27:422-32.

Untergasser, A., Nijveen, H., Rao, X., Bisseling, T., Geurts, R., and Leunissen, J. A. (2007) Primer3Plus, an enhanced web interface to Primer3. *Nucleic Acids Res* 35:W71-W74.

van Hoof, A., Lennertz, P., and Parker, R. (2000) Yeast exosome mutants accumulate 3-extended polyadenylated forms of U4 small nuclear RNA and small nucleolar RNAs. *Mol Cell Biol* 20:441-452.

van Hoof, A., Frischmeyer, P. A., Dietz, H. C. and Parker, R. (2002) Exosome-mediated recognition and degradation of mRNAs lacking a termination codon. *Science* 295: 2262-4.

Vanacova, S., Wolf, J., Martin, G., Blank, D., Dettwiler, S., Friedlein, A., Langen, H., Keith, G. and Keller, W. (2005) A new yeast poly(A) polymerase complex involved in RNA quality control. *Plos Biology* 3: 986-997.

Vanacova, S. and Stefl, R. (2007) The exosome and RNA quality control in the nucleus. *EMBO Rep* 8: 651-7.

Varshavsky, A. (1996) The N-end rule: functions, mysteries, uses. *Proc Natl Acad Sci U S A.* 93:12142-9. Review.

Varshavsky, A. (2011) The N-end rule pathway and regulation by proteolysis. *Protein Sci* 20: 1298-1345.

Vasiljeva, L. and Buratowski, S. (2006) Nrd1 interacts with the nuclear exosome for 3' processing of RNA polymerase II transcripts. *Mol Cell* 21: 239-48.

Vasiljeva, L., Kim, M., Mutschler, H., Buratowski, S. and Meinhart, A. (2008a) The Nrd1-Nab3-Sen1 termination complex interacts with the Ser5-phosphorylated RNA polymerase II C-terminal domain. *Nat Struct Mol Biol* 15: 795-804.

Vasiljeva, L., Kim, M., Terzi, N., Soares, L. and Buratowski, S. (2008b) Transcription termination and RNA degradation contribute to silencing of RNA polymerase II transcription within heterochromatin. *Mol Cell* 29:313-323.

Venema, J. and Tollervey, D. (1999) Ribosome synthesis in *Saccharomyces cerevisiae*. *Ann Rev Genet* 33: 261-311.

Villa, T., Ceradini, F., Bozzoni, .I (2000) Identification of a novel element required for processing of intron-encoded box C/D small nucleolar RNAs in *Saccharomyces cerevisiae*. *Mol Cell Biol* 20:1311-20.

Vinciguerra, P. and Stutz, F. (2004) mRNA export: an assembly line from genes to nuclear pores. *Curr Opin Cell Biol* 16: 285-92.

Wach, A., Brachat, A., Poehlmann, R. & Philippsen, P. (1994). New heterologous modules for classical or PCR-based gene disruptions in *Saccharomyces cerevisiae*. *Yeast* 10:1793-1808.

Wagschal, A., Rousset, E., Basavarajaiah, P., Contreras, X., Harwig, A., Laurent-Chabalier, S., Nakamura, M., Chen, X., Zhang, K., Meziane, O. (2012) Microprocessor, Setx, Xrn2, and Rrp6 co-operate to induce premature termination of transcription by RNAPII. *Cell 150:1147-57.*

Wang, L. and Brown, S.J. (2006) BindN: a web-based tool for efficient prediction of DNA and RNA binding sites in amino acid sequences. *Nucleic Acids Res* 34:W243-W248.

Warner, J.R. (1999) The economics of ribosome biosynthesis in yeast. *Trends Biochem Sci* 24:437-440.

Wasmuth, E. V., and Lima, C. D. (2012) Exo- and endoribonucleolytic activities of yeast cytoplasmic and nuclear RNA exosomes are dependent on the noncatalytic core and central channel. *Mol Cell* 48:133-144.

Waterhouse, A.M., Procter, J.B., Martin, D.M., Clamp M., Barton G.J. (2009) Jalview Version 2-a multiple sequence alignment editor and analysis workbench. *Bioinformatics* 25:1189-91.

Welter, E., Thumm, M., and Krick, R. (2010) Quantification of nonselective bulk autophagy in *S. cerevisiae* using Pgk1-GFP. *Autophagy* 6:794–797.

White, R. J. (2011) Transcription by RNA polymerase III: more complex than we thought. *Nat Rev Genet* 12: 459-463.

Wiederkehr, T., Prétôt, R. F., Minvielle-Sebastia, L. (1998) Synthetic lethal interactions with conditional poly(A) polymerase alleles identify LCP5, a gene involved in 18S rRNA maturation. *RNA* 4: 1357-1372.

Wierzbicki, A. T. and Haag, J. R. and Pikaard, C. S. (2008) Noncoding transcription by RNA polymerase Pol IVb/Pol V mediates transcriptional silencing of overlapping and adjacent genes. *Cell* 135:635-648.

Wolin, S. L., Sim, S., and Chen, X. (2012) Nuclear noncoding RNA surveillance. Is the end in sight? *Trends Genet* 28:306-313.

Wong, I. and Lohman, T. M. (1993) A double-filter method for nitrocellulose-filter binding: application to protein-nucleic acid interactions. *Proc Natl Acad Sci USA* 90: 5428-32.

Wyers, F., Rougemaille, M., Badis, G., Rousselle, J. C., Dufour, M. E., Boulay, J., Regnault, B., Devaux, F., Namane, A., Seraphin, B., Libri, D. and Jacquier, A. (2005) Cryptic Pol II transcripts are degraded by a nuclear quality control pathway involving a new poly(A) polymerase. *Cell* 121: 725-737.

Xu, Z. Y., Wei, W., Gagneur, J., Perocchi, F., Clauder-Munster, S., Camblong, J., Guffanti, E., Stutz, F., Huber, W. and Steinmetz, L. M. (2009) Bidirectional promoters generate pervasive transcription in yeast. *Nature* 457: 1033-U7.

Yavuzer, U., Smith, G. C., Bliss, T., Werner, D. and Jackson, S. P. (1998) DNA end-independent activation of DNA-PK mediated via association with the DNA-binding protein C1D. *Genes Dev* 12: 2188-99.

Yeh, L. C., Lee, J. C. (1990) Structural analysis of the internal transcribed spacer 2 of the precursor ribosomal RNA from *Saccharomyces cerevisiae*. *J Mol Biol* 211: 699-712.

Zaman, S, Lippman, S.I., Zhao, X., Broach, J.R. (2008). How S*accharomyces* responds to nutrients. *Annu Rev Genet* 42:27-81.

Zaman, S, Lippman, S.I., Schneper, L., Slonim, N., Broach, J.R. (2009). Glucose regulates transcription in yeast through a network of signaling pathways. *Mol Syst Biol* 5:245.

Zuker, M. (2003) Mfold web server for nucleic acid folding and hybridization prediction. *Nucleic Acids Res* 31: 3406-15.